

UNIVERSITY OF SOUTHAMPTON

Faculty of Engineering, Science & Mathematics

School of Chemistry

**Bis-Sulfonamide Macrocycles as
Receptors for Carboxylates**

by

Oscar Mammoliti

Doctor of Philosophy

February 2007

UNIVERSITY OF SOUTHAMPTON

ABSTRACT

FACULTY OF ENGINEERING, SCIENCE & MATHEMATICS

SCHOOL OF CHEMISTRY

Doctor of Philosophy

BIS-SULFONAMIDE MACROCYCLES AS RECEPTORS FOR CARBOXYLATES

by Oscar Mammoliti

This thesis is principally concerned with the synthesis of a range of bis-sulfonamide based macrocycles and their ability to bind carboxylates of amino acid derivatives. Chapter I provides a general introduction to the field of supramolecular chemistry and discusses in details carboxylate binding and its applications in chiral recognition of amino acids. Chapter II describes the synthesis of acyclic bis-sulfonamide receptors. Traditional NMR binding studies revealed their tendency to form complexes with a 1:2 host/guest stoichiometry. The use of macrocyclic receptors proved to limit the formation of ternary complexes. Cyclohexane based chiral macrocycles gave poor results in terms of carboxylate binding and showed no enantioselectivity with amino acids. Chapter III describes the synthesis of more flexible chiral macrocycles, built from valine. Macrocyclisation reactions were carried out under anion templating conditions, which provided critical yield improvements. Valine based macrocycles showed very strong affinity for the acetate anion and NMR titrations had to be conducted in MeCN- d_3 /H₂O mixtures in order to obtain measurable binding constants. Selectivity for acetate over other anions was found. No enantioselectivity was shown in titrations with amino acids. Chapter IV, finally, describes the synthesis of bis-sulfonamides macrocycles bearing additional polar groups. In one particular case, moderate but general enantioselectivity was observed with *N*-protected amino acids displaying non-polar side chains.

To my dear grandfather,

Cesare Petitjacques

Table of Contents

Preface	i
Acknowledgements	ii
Abbreviations	iii
Chapter I	1
1.1 Supramolecular chemistry	1
1.2 Molecular recognition	2
1.3 Applications of supramolecular chemistry	3
1.3.1 <i>Transport across membranes</i>	4
1.3.2 <i>Catalysis</i>	5
1.3.3 <i>Molecular machines</i>	7
1.4 Host-guest chemistry	9
1.5 Thermodynamics of host-guest complexation	9
1.6 Preorganisation and macrocyclic effect	11
1.7 Nature of supramolecular interactions	13
1.7.1 <i>Ion-ion interactions</i>	13
1.7.2 <i>Ion-dipole interactions</i>	14
1.7.3 <i>Dipole-dipole interactions</i>	14
1.7.4 <i>Hydrogen bonding</i>	15
1.7.5 <i>π-π stacking interactions</i>	17
1.7.6 <i>Cation-π interactions</i>	19
1.7.7 <i>Van der Waals forces</i>	19
1.7.8 <i>Hydrophobic effect</i>	20
1.8 Anion binding	21
1.9 Artificial receptors for carboxylates	22
1.9.1 <i>Ureas, thioureas and guanidiniums</i>	22
1.9.2 <i>Amides</i>	27
1.9.3 <i>Pyrroles and bis-pyrroles</i>	32
1.10 Enantioselective receptors for amino acids	33
1.11 Aims of this work	41
Chapter II	44

2.1 Synthesis of acyclic receptor 65	44
2.2 Binding studies	45
2.3 Synthesis of receptor 71	48
2.4 Binding studies	49
2.5 A possible explanation	50
2.6 Synthesis of receptor 64	52
2.7 Binding studies	53
2.8 Synthesis of macrocyclic receptors 73 and 74	53
2.9 Binding studies	54
2.10 Chiral macrocyclic receptors	56
2.11 Synthesis of macrocycle 79	57
2.12 Binding studies	58
2.13 Synthesis of macrocyclic receptors 84 and 85	58
2.14 Binding studies on macrocycle 84	60
2.15 Binding studies on macrocycle 85	63
2.16 Synthesis of macrocycle 86	68
2.17 Binding studies	68
2.18 Conclusions	72
Chapter III	74
3.1 Introduction	74
3.2 Synthesis of macrocycles 87 and 88	75
3.3 Synthesis of acyclic receptor 93	78
3.4 Binding studies on receptors 87 , 88 and 93 with acetate in MeCN- <i>d</i> ₃	79
3.5 Binding studies on receptor 88 with halides	81
3.6 Anion templated synthesis of bis-sulfonamide based macrocycles	83
3.7 Binding studies on receptor 88 with simple anions in MeCN- <i>d</i> ₃ /2% H ₂ O	87
3.8 Synthesis of macrocycle 102	88
3.9 Binding studies on receptor 102 in CDCl ₃	90
3.10 Binding studies on receptor 102 in wet MeCN- <i>d</i> ₃	91
3.11 Binding studies on receptor 88 in DMSO- <i>d</i> ₆	97
3.12 Binding studies with <i>N</i> -Boc-phenylalanine	99
3.13 Synthesis of macrocycle 108	101
3.14 Binding studies with acetate	102
3.15 Binding studies with halides	104

3.16 Conclusions	105
Chapter IV	107
4.1 Introduction	107
4.2 Synthesis of macrocycle 112	108
4.3 Binding studies	110
4.4 Synthesis of macrocycle 117	112
4.5 Binding studies with simple anions in MeCN- <i>d</i> ₃ /2% H ₂ O	115
4.6 Binding studies with various amino acids in MeCN- <i>d</i> ₃ /2% H ₂ O	116
4.7 Binding studies with TBA acetate in DMSO- <i>d</i> ₆	119
4.8 Binding studies with <i>N</i> -Ac-phenylalanine in DMSO- <i>d</i> ₆	120
4.9 Synthesis of receptor 118	121
4.10 Binding studies with <i>N</i> -Ac-phenylalanine in CDCl ₃	122
4.11 Binding studies with <i>N</i> -Boc-phenylalanine in MeCN- <i>d</i> ₃	124
4.12 Synthesis of macrocycles 119 and 120	125
4.13 Binding studies with <i>N</i> -Ac-phenylalanine in DMSO- <i>d</i> ₆	127
4.14 Conclusions	129
4.15 General conclusions and outlooks	130
Chapter V	133
5.1 General experimental	133
5.2 Instrumentation	133
5.3 Experimental for NMR binding studies	134
5.4 Method used for obtaining binding constants	135
5.5 Synthesis	135
5.6 Binding studies	177
Appendices	213
Appendix A	213
Appendix B	222
Appendix C	224
References	269

Preface

The research contained within this thesis was carried out under the supervision of Professor J. D. Kilburn at the University of Southampton between April 2003 and July 2006. No part of this thesis has previously been submitted to this or any other University.

Acknowledgements

In the first place, I would like to thank Professor Jeremy Kilburn for his help, advice and encouragement during all three years. His sharp knowledge in Supramolecular Chemistry and his consummate teaching during the problem sessions had been an invaluable boost to my passion for Chemistry. I would like to thank him as well for some occasional but quite salutary rebukes.

Many thanks to Dr Philip Gale, for his advice and for being a great promoter of Supramolecular Chemistry.

I would also like to thank all members of the Kilburn group, past and present, particularly the old guard, Richard, Nittaya, Sarah, Suvi, Andrea, Jon Shepherd, Srin, Allison and Suad. Among them, I would like to address special thanks to Sandra. Amidst the newcomers, I wish to thank Luke and Jon Powell, for Friday football.

Many thanks to all chemistry staff, especially to Karl, Julie, John, Neil and Joan.

I wish to thank my housemates, particularly Marco and all others who made extra-lab hours more pleasant, especially Rohan, Ilaria and Eugen.

I would like, then, to thank my family, for their distant but steady support, as well as my family in-law, for their efficacious blitzes.

Back in the years, I have to thank Dr Arnaud Gautier, Dr Marie-Agnès Hourdin and Silvia Gonella, who first encouraged me to undertake PhD studies.

And last, but not least, I would like to address very special thanks to the person I owe most for this work. She was not happy enough to help me with spiritual and material support in order to achieve the PhD, to make nicer my evenings and weekends, to be a good labmate and to organise flights and movings, but accepted to marry me becoming my beloved wife. Thank you Sara!

Abbreviations

Ac	acetyl
Ala	alanine
Ala	alanine
Anal.	elemental analysis
Ar	aryl
Asn	asparagine
Boc	<i>tert</i> -butyloxycarbonyl
Bn	benzyl
br	broad
Bu	butyl
Bz	benzoyl
C	concentration
cat.	catalytic
CBS	carboxylate binding site
CDI	1,1'-carbonyldiimidazole
Cy	cyclohexyl
δ	chemical shift (ppm)
d	doublet
DCC	<i>N,N'</i> -dicyclohexylcarbodiimide
DCM	dichloromethane
DEPT	distortionless enhancement by polarization transfer
DIPEA	<i>N,N'</i> -diisopropylethylamine
DMAP	4-(<i>N,N'</i> -dimethylamino)pyridine
DME	1,2-dimethoxyethane
DMF	<i>N,N'</i> -dimethylformamide
DMSO	dimethylsulphoxide
EA	ethyl acetate
EDC	<i>N</i> -(3-dimethylaminopropyl)- <i>N'</i> -ethylcarbodiimide hydrochloride
ESMS	electrospray mass spectroscopy
Et	ethyl
Flu	fluorenyl

Fmoc	9-fluorenylmethoxycarbonyl
FT-IR	Fourier transform infrared
Gln	glutamine
His	histidine
HOBt	1-hydroxybenzotriazole
HOSu	<i>N</i> -hydroxysuccinimide
HRMS	high resolution mass spectroscopy
<i>i</i> -Bu	isobutyl
<i>i</i> -Pr	isopropyl
ITC	isothermal titration calorimetry
lit.	literature
m	multiplet
Me	methyl
Met	methionine
MP	melting point
NMR	nuclear magnetic resonance
NOE	nuclear Overhauser effect
oct	octet
PE	petroleum ether
PFP	pentafluorophenol
Ph	phenyl
Phe	Phenylalanine
ppm	parts per million
Pr	propyl
PyBOP	benzotriazole-1-yl-oxy-tris-pyrrolidino-phosphonium hexafluorophosphate
q	quartet
quant.	quantitative
quin	quintet
s	singlet
<i>s</i> -Bu	<i>sec</i> -butyl
sat.	saturated
Ser	serine
sept	septet

sext	sextet
t	triplet
TBA	tetrabutylammonium
<i>t</i> -Bu	<i>tert</i> -butyl
TFA	trifluoroacetic acid
THF	tetrahydrofuran
TLC	thin layer chromatography
Trp	tryptophan
Trt	trityl
TsOH	<i>p</i> -toluenesulfonic acid
UV	ultra-violet
Val	valine

Chapter I

Introduction

1.1 Supramolecular chemistry^[1]

For many years, since the synthesis of urea by Friederich Wöhler,^[2] the efforts of the organic chemists focused almost exclusively on breaking and forming covalent bonds, in the attempt to generate new molecules, replicate natural products and enrich their collection of synthetic methodologies. This field, which has its ultimate goal in the mastery of the covalent bond in order to obtain molecules, can be defined as ‘molecular chemistry’. In an analogous manner it is possible to define ‘supramolecular chemistry’ as the science aiming to gain control over the non-covalent interactions in order to obtain structured molecular assemblies, which can be called ‘supermolecules’.^[3]

The concept of molecular association was introduced in the late 19th and the early 20th century, notably by Alfred Werner,^[4] who laid down the basis of the coordination chemistry, by Emil Fischer,^[5] with the ‘lock and key’ analogy for the description of enzymes behaviour and by Paul Ehrlich,^[6] who stated that ‘*corpora non agunt nisi fixata*’ (molecules do not act if they do not bind), introducing the concept of receptor. The term ‘*übermoleküle*’ then appeared in the 1930’s, in order to describe molecular associations such as the dimer of acetic acid.^[7] Despite these early conceptualisations, the dawn of supramolecular chemistry is traditionally ascribed to the findings made by Charles Pedersen in 1967. Pedersen synthesised a series of polyether macrocycles, called ‘crown ethers’, which displayed unprecedented binding affinity towards alkali cations.^[8] Contributions to the birth of the new science came also from the prior work of Donald Cram, who tried to isolate intercalated complexes formed by macrocycles containing phenyl units with *para*-junctions (thus called paracyclophanes) and tetracyanoethylene (1959).^[9] Although this pioneering attempt was unsuccessful, it pointed the attention for the first time on inclusion complexes. In this early stage, other contributions came from Jean-Marie Lehn, who synthesised the first cryptands (1969).^[10]

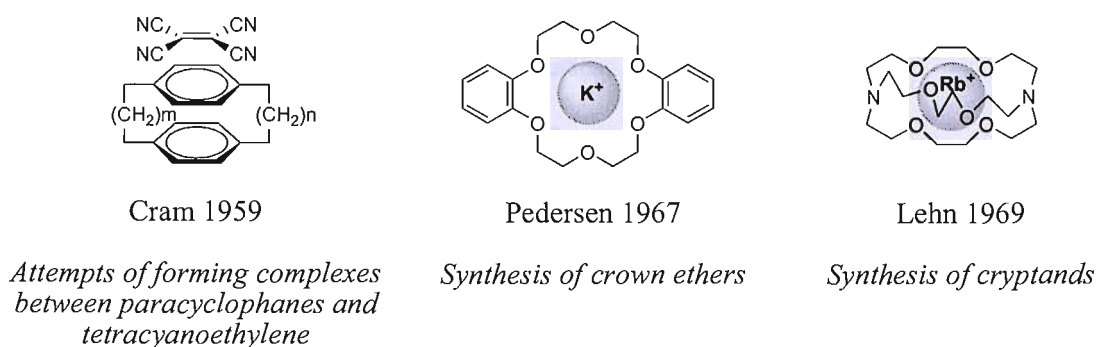


Figure 1.1 *The early stages of supramolecular chemistry.*

Lehn is undoubtedly one of the major contributors to the new branch of chemistry: he coined the name ‘Supramolecular Chemistry’ in 1978,^[11] he defined the central concepts of the field and today he is still giving great impulse to the supramolecular research area. For his fundamental support to the new science, he was awarded the Nobel Prize for Chemistry in 1987, along with Pedersen and Cram.

1.2 Molecular recognition

At the heart of supramolecular chemistry lies the concept of molecular recognition. Molecular recognition is not mere binding, but binding associated with information and it may involve a function. An enzyme, for example, can select the appropriate substrate among several others. The association in this case is selective, because the binding site of the enzyme is able to read the information contained in the particular arrangement of the substrate functionalities. The substrate, then, undergoes a particular reaction associated with the enzyme (function). The enzyme and the substrate in this case are complementary to each other. A representation of the concept of complementarity was given by Emil Fischer with the ‘lock and key’ principle (**Figure 1.2**).^[5,12]

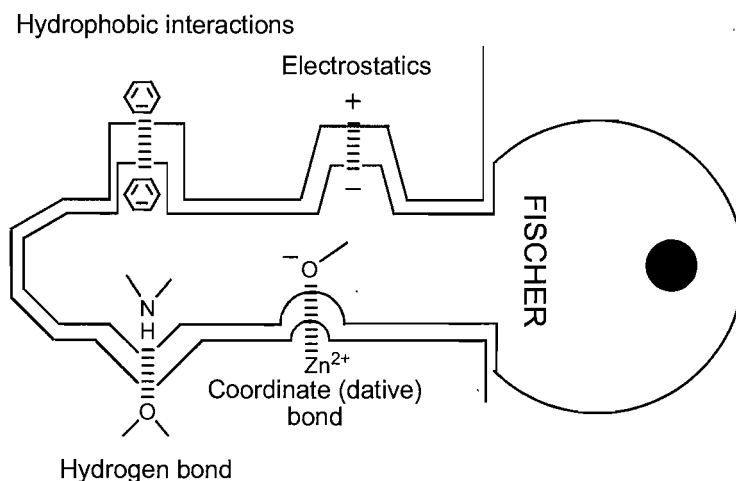


Figure 1.2 *The lock and key principle (with permission of Philip A. Gale).*

The ‘lock and key’ principle states that the selectivity of a receptor towards a particular substrate relies on the steric fit and on complementary interactions between the two components. The ‘lock and key’ model is still useful at the present time in the design of preorganised artificial receptors. For the interpretation of the behaviour of biological receptors, however, it does not take into account the existence of flexible species, able to reorganise themselves. For this reason, it has been nowadays substituted with the more modern principle of the ‘induced fit’,^[13] which considers the strong selective binding as a result of a conformational change induced by the recognition of the substrate by the enzyme.

1.3 Applications of supramolecular chemistry

Supramolecular chemistry has always been, since the outset, an interdisciplinary area of research. It lies at the intersection of the biological, chemical and physical science. The perfection of biological systems, based on the delicate balance of several non-covalent interactions, provides innumerable sources of inspiration for the supramolecular chemists. The plentiful collection of methodologies, attained by modern synthetic chemistry, supplies the powerful toolbox for the construction of the structured and diverse components for the supramolecular assemblies. The physical science, in the end, provides the necessary tools for measuring the properties of supramolecular systems. Herein are described some selected applications, in order to show the variety and the complexity of the aspects covered by current supramolecular chemistry.

1.3.1 Transport across membranes

Lipid bilayer membranes play a crucial role in living processes. They are a protective barrier maintaining functionality inside the cell. They provide, moreover, energy storage by creating a transmembrane gradient of Na^+ and K^+ ions. This and other pivotal functions are regulated by proteins which can act like carriers, simple pores or 'gated' channels (**Figure 1.3**).

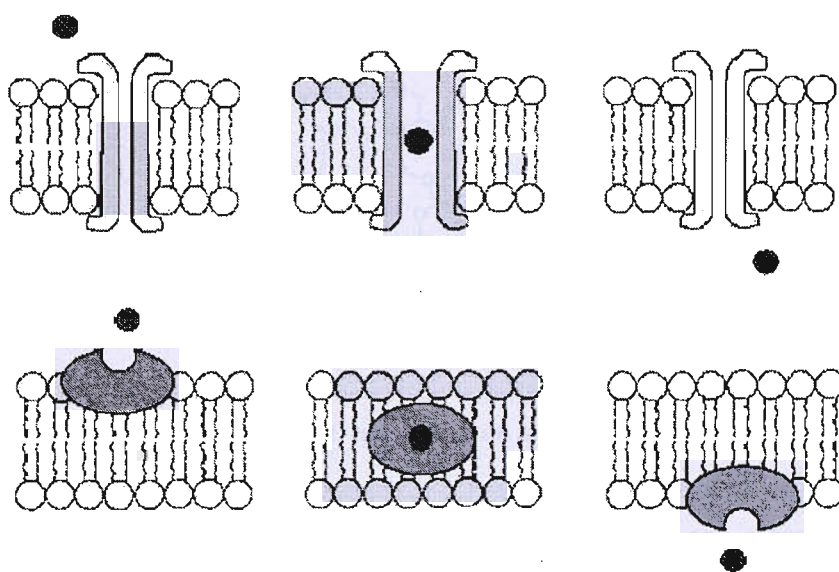


Figure 1.3 Transport across cell membrane regulated by a protein channel (above) and by a protein carrier (below).

Because of their importance and fascinating complexity, these systems have attracted the attention of supramolecular chemists. Much effort has been therefore devoted to the conception and realisation of artificial ion channels.^[1a]

Among the numerous works, Lehn and co-workers realised a series of ion channels based on crown ethers^[14,15] (**Figure 1.4**) and cyclodextrins.^[15]

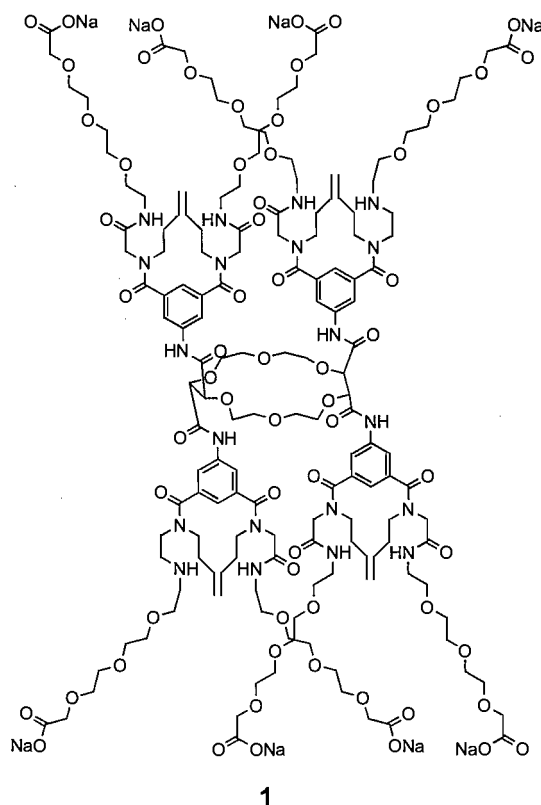


Figure 1.4 A 'bouquet' molecule, an artificial ion channel.

The ion channel **1**, defined as a 'bouquet' molecule for its shape, is constituted by a central annulus, based on a crown ether, which is the core of the structure and permits the transit of an alkali cation, two bundles of glycolic chains, which allow the molecule to intercalate amidst a lipophilic bilayer membrane, and terminal polar groups, which are anchored to the two aqueous interfaces, sustaining the correct conformation and functionality of the ion channel. When the 'bouquet molecule' **1** was incorporated in phospholipidic bilayer vesicles, it was found that the transport across the membrane of Na^+ and Li^+ ions was dramatically accelerated. The process was driven by the concentration gradient of the two solutes. Na^+ cations were present outside the vesicles and Li^+ inside. Because the rates of transport of the cations were equivalent, it was concluded that the ion transfer was proceeding by an antiport mechanism.^[16]

1.3.2 Catalysis

Since the first applications of their powerful properties^[17] and the first insights in their structure and mechanism,^[18] chemists and biologists have been fascinated by the

efficiency and selectivity of the enzymes, without whose activity no vital reaction can occur at the mild physiological temperatures. For example, carboxypeptidase A is a digestive enzyme that hydrolyses the carboxyl-terminal peptide bond in polypeptide chains. The mechanism of its active site is regulated by a delicate balance of intermolecular interactions with a very specific steric orientation (**Figure 1.5**).^[19]

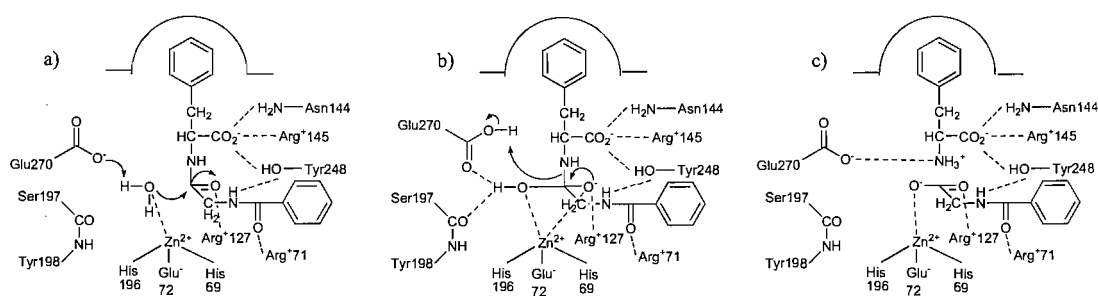


Figure 1.5 Mechanism of the proteolytic action of the carboxypeptidase A.

The central role of molecular recognition in enzymes activity and the practical benefits coming from making faster and more selective transformations have served as a great stimulus for supramolecular chemists. Lehn and co-workers^[20] synthesised an artificial enzyme with the intention to imitate the activity of acyltransferases (**Figure 1.6**).

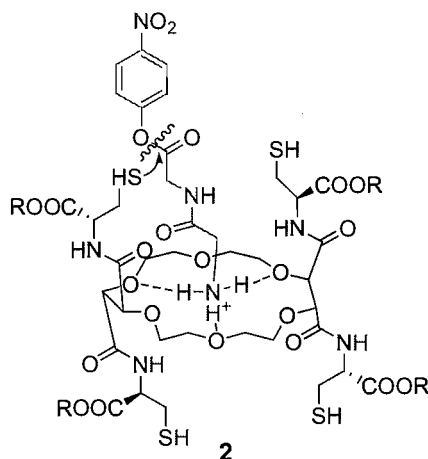


Figure 1.6 Artificial enzyme imitating the activity of the acyltransferases.

It was found that the artificial enzyme **2** was able to produce the thiolysis of dipeptide esters. The activity was measured following the rate of the production of *p*-nitrophenol in the solution. The evidence that the mechanism proceeds in fact as depicted in the **Figure**

1.6 was given by the inhibition caused by the presence of K^+ ions. The high affinity of the K^+ ions for the crown ether core excluded the ammonium moiety from the cavity, preventing the formation of the complex. The diminishing rate, therefore, proved that the thiolysis was associated with the formation of the complex.

In this domain, the studies made by Rebek and co-workers^[21] on Diels-Alder, and other cycloadditions, are particularly interesting. Only few naturally occurring enzymes are able to promote cycloadditions and they play usually a role in the secondary metabolism.^[22] Moreover, in some cases, it is not clear whether the mechanism follows a real cycloaddition pathway or a completely different one.^[23] Rebek and co-workers described recently a 1,3-dipolar cycloaddition accelerated by encapsulation in a resorcinarene based dimeric chamber (**Figure 1.7**).^[24]

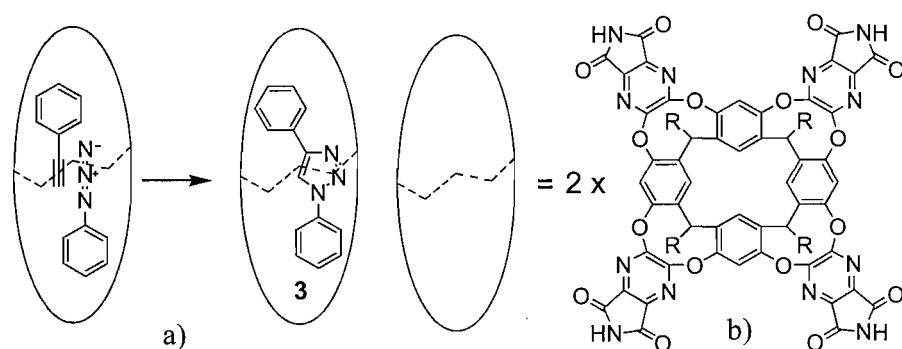


Figure 1.7 a) Cycloaddition accelerated by encapsulation. b) The resorcinarene based chamber.

In the absence of the molecular capsule the rate of the reaction shown in the **Figure 1.7** is not measurable. Conversely, in the presence of a catalytic amount of the resorcinarene macrocycle the reaction proceeded with a measurable rate ($1.3 \cdot 10^{-9} \text{ M s}^{-1}$). The reaction was completely regioselective and the existence of the encapsulated species was assessed by NMR analysis.

1.3.3 Molecular machines

A machine is a device able to perform some work powered by an energy source. The advent of machines at a molecular scale was forecast by Nobel Prize winner in physics Richard Feynman.^[25] In the last years, much effort has been put into this challenge by supramolecular chemists. As a result, different types of molecular switches, rotors,

shuttles and other devices had been conceived.^[26] At a molecular level, a machine can be defined as a system formed by a distinct number of molecular components, assembled in order to perform machinelike movements as a result of an appropriate external stimulation. The stimulation can be of photonic, electronic or ionic nature.^[1a] At this regard, particularly remarkable was the construction of a molecular elevator by Stoddart and co-workers^[27] (**Figure 1.8**).

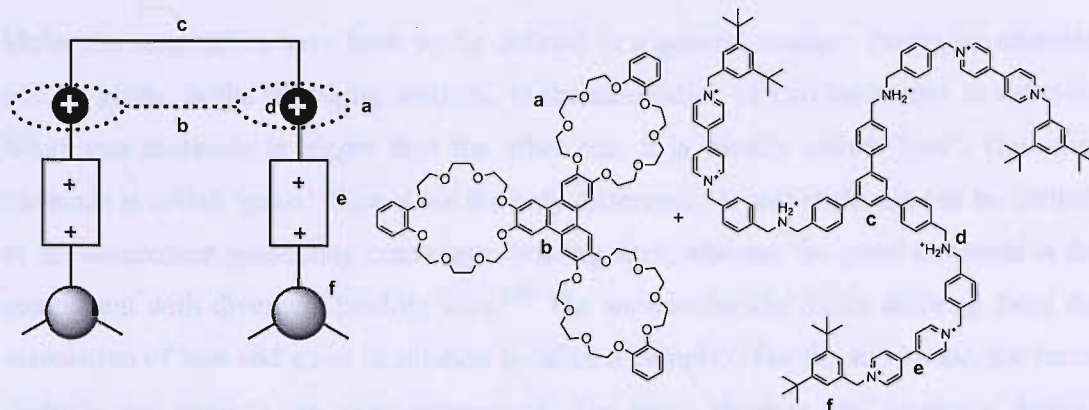


Figure 1.8 *The molecular elevator and its components.*

The elevator is constituted by a three-legged holder interlocked with a rigid platform. The platform is formed by a central rigid triphenylene core (**b**) and three crown ether macrocycles (**a**). The macrocyclic units are subjected to attractive interactions from the dialkylammonium (**d**) and bipyridinium (**e**) units on the holder. The bulky feet (**f**) at the bottom prevent the loss of the platform. In Stoddart's experiments, the 'up and down' movements were induced by changing the pH of the solution (**Figure 1.9**).

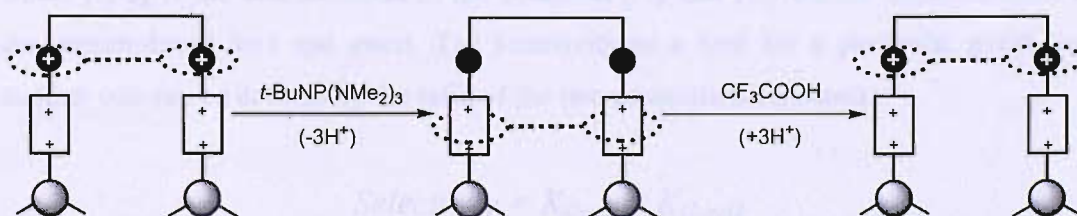


Figure 1.9 *The functioning of the molecular elevator.*

At acidic pH the dialkylammonium units were protonated and the crown ethers were binding preferentially to them thanks to a combination of ion-dipole and hydrogen

bonding interactions (§ 1.7). When a base was added, the dialkylammonium units were no longer protonated and the macrocycles were sliding down to interact with the bis-pyridinium units by ion-dipole interactions. When an acid was added, the initial situation was restored. Several cycles were repeated without loss of efficiency. The ‘up and down’ movements were assessed by NMR, UV and electrochemical methods.

1.4 Host-guest chemistry

Molecular assemblies have been so far defined in a general manner. Particular attention will be given, in the following sections, to the association of two molecules in solution. When one molecule is bigger than the other one, it is usually called ‘host’. The other molecule is called ‘guest’. Size is not the only difference. A host molecule can be defined as the component possessing convergent binding sites, whereas the guest molecule is the component with divergent binding sites.^[28] The supramolecular entity deriving from the association of host and guest in solution is called a complex. For the solid state, the terms clathrate and cavitare are more appropriate. The terms receptor and substrate, derived from enzymology, can be also used to describe the host and guest molecules.

1.5 Thermodynamics of host-guest complexation

The strength of the host-guest complex formation in solution can be assessed by measuring the thermodynamic association constant:

$$K_a = [HG] / [H] [G]$$

where $[HG]$ is the concentration of the complex, $[H]$ and $[G]$ are the concentrations of the uncomplexed host and guest. The selectivity of a host for a particular guest over another one can be defined by the ratio of the two association constants:

$$Selectivity = K_{Guest1} / K_{Guest2}$$

The association constant is related to the change in Gibbs free energy:

$$\Delta G^\circ = - RT \ln K$$

where ΔG° is the change in Gibbs free energy for a process under standard conditions, R is the gas constant and T the temperature measured in Kelvin degrees. For a spontaneous process the change in Gibbs free energy is negative. The change in Gibbs free energy can be divided into an enthalpic and an entropic term:

$$\Delta G^\circ = \Delta H^\circ - T\Delta S^\circ$$

where ΔH° and ΔS° are the change in enthalpy and in entropy under standard conditions. Strong binding will result from a decrease in enthalpy and from an increase of entropy, which is a measure of the disorder of the system. Sometimes molecular association is favoured on enthalpic grounds and disfavoured on entropic grounds or vice versa, but, if the free energy of the overall process is largely negative, strong binding occurs.

In aprotic non-competitive solvents the formation of a host-guest complex is favoured by negative enthalpy if strong intermolecular interactions are present between host and guest (the nature of such interactions will be extensively described in § 1.7). For the association between a polar host and a polar guest in a competitive solvent, such as methanol or DMSO, enthalpy acts favourably as long as the interactions between host and guest are stronger than those responsible for the solvation of the two species. If the interactions between the host and the solvent and between the guest and the solvent are stronger than the interactions between host and guest, the binding process is endothermic and can occur only in the presence of positive entropy. In the case of a non-polar host and a non-polar guest in a polar solvent, the association is favoured by the negative enthalpy deriving from the strong mutual interactions of the solvent molecules. Entropic factors also play an important role in this type of association (§ 1.7.8).

The formation of the host-guest complex involves an entropically unfavourable loss in the translational and rotational degrees of freedom of the system, due to the fact that two previously independent species are forced now to act as a whole. However, in the association process, an entropic gain derives from the release of solvent molecules to the bulk of the solvent. When the host and the guest are solvated, they are surrounded by cage-like structures of solvent molecules. In order to maximise the favourable interactions, these structures must be well organised, especially those in proximity of the host, which is normally a big sized molecule presenting cavities. When binding occurs,

numerous solvent molecules are released from their previously ordered and fixed architectures, resulting in an overall entropic gain for the system.

Some aspects of the thermodynamics of host-guest complexation were illustrated by Hamilton and co-workers^[29] by a series of experiments involving simple receptors for bis-carboxylate anions in solvents of different polarity (**Figure 1.10**).

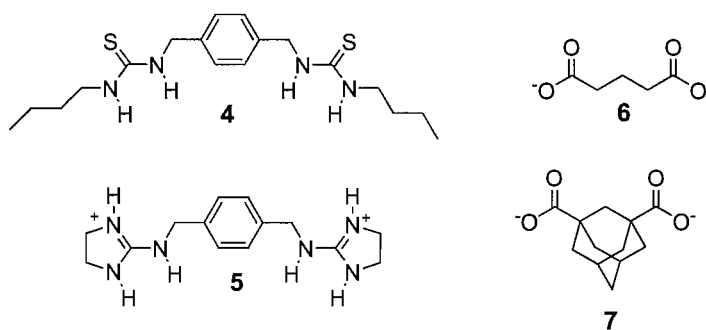


Figure 1.10 Hamilton's receptors for bis-carboxylates.

The binding constants were measured by isothermal titration calorimetry (ITC),^[30] which allows the direct evaluation of thermodynamic parameters. It was found that in DMSO the binding was essentially driven by enthalpy. In this case, the strength of the host-guest interactions was dominant over the solvation process. In the more competitive methanol, however, the binding was endothermic. Nonetheless strong association constants were obtained, due to the fact that the complex formation was driven by the large entropic contribution deriving from the desolvation of host and guest (**Table 1.1**).

Host	Guest	Solvent	K_a (M^{-1})	ΔH ($kcal\ mol^{-1}$)	ΔS ($cal\ mol^{-1}\ K^{-1}$)
4	6	DMSO	8400	-4.1	+4.3
4	7	DMSO	15000	-5.9	-0.6
5	6	MeOH	2700	+3.7	+28
5	7	MeOH	9500	+4.0	+32

Table 1.1

1.6 Preorganisation and macrocyclic effect

In order to bind, a host must be in a conformation which allows maximizing the favourable interactions with the guest. If the host is not in a conformation suitable for binding, reorganization must occur in order to form a complex. This change in conformation will result in a decreased binding strength, due to unfavourable entropy. If

the host is already fixed in a conformation that allows the most profitable interaction with the guest, it is said to be preorganised. In this case, the formation of the complex is more favourable, because no entropic penalty has to be paid. The preorganisation principle was well illustrated by Cram and co-workers, who synthesised a series of polyether receptors for alkali cations (**Figure 1.11**).^[31]

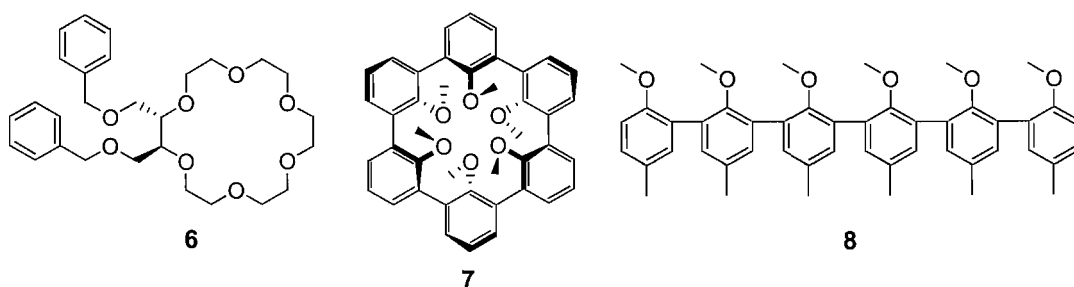


Figure 1.11 Cram's polyether receptors for alkali cations.

The binding free energies for the formation of the complexes between the corand **6**, the spherand **7** and the podand **8** and the picrate salts of the alkali cations were measured in CDCl_3 saturated with D_2O (**Table 1.2**).

Receptor	$-\Delta G^\circ$ (kcal mol ⁻¹)				
	Li ⁺	Na ⁺	K ⁺	Rb ⁺	Cs ⁺
6	6.3	8.4	11.4	9.9	8.5
7	> 23	19.2	< 6	—	—
8	< 6	< 6	< 6	< 6	< 6

Table 1.2

The rigid, preorganised spherand **7** showed a marked increase in binding energy towards Li^+ and Na^+ compared to the flexible corand **6**. The preorganisation of the receptor **7** resulted also in a significant selectivity.

The substantial difference in the binding energy between the receptors **6** and **7** and the acyclic podand **8** is due to the macrocyclic effect. This effect was first elucidated by Cabbiness and Margerum in 1969, with the synthesis of macrocyclic and acyclic ligands for Cu(II) (**Figure 1.12**).^[32]

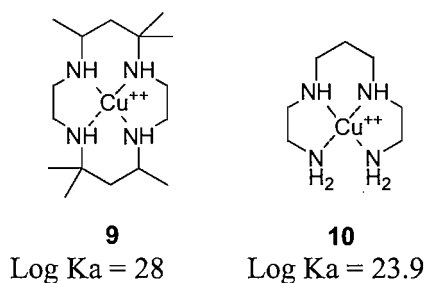


Figure 1.12 Macrocyclic effect shown by Cu(II) ligands.

Because of its macrocyclic nature, the complex **9** was about 10^4 times more stable than the complex **10**. The stabilisation arising from the macrocyclic effect has both enthalpic and entropic contributions. The enthalpic bonus arises from the fact that macrocyclic hosts are normally less strongly solvated than their acyclic analogues, because of the decreased solvent-accessible surface area. As a result, there will be less solvent-ligand bonds to break, compared to the case of elongated, solvent-accessible acyclic receptors. The entropic contribution arises from the fact that macrocycles are less conformationally flexible and thus they lose fewer degrees of freedom upon complexation. In fact the entropic penalty has been paid in advance during a more demanding synthetic process. The entropic contribution may be regarded as an extension of the preorganisation principle.

1.7 Nature of supramolecular interactions

Herein are described the major non-covalent interactions responsible for the formation of a host-guest complex. These interactions are diverse and comprised in a wide range of energies (from $< 5 \text{ kJ mol}^{-1}$ for the dispersion forces to 350 kJ mol^{-1} for a very stable ion-ion interaction). The energies involved are usually weaker than their covalent counterparts (from 350 kJ mol^{-1} to 942 kJ mol^{-1} for the triple bond in N_2). In order to obtain strong binding and high selectivity, host-guest complex design takes advantage of a combination of these interactions.

1.7.1 Ion-ion interactions ($100\text{-}350 \text{ kJ mol}^{-1}$)

The attraction between negatively and positively charged ions depends on their distance. Ion-ion bonding is often comparable in strength to covalent bonding and is typically

present in the lattice of ionic solids, such as NaCl. This interaction can be also exploited in solution for host-guest complex design (**Figure 1.13**).

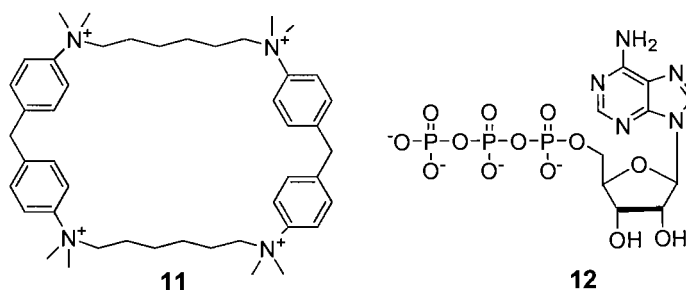


Figure 1.13 Schneider's receptor for ATP⁴⁻.

The cyclophane **11**, designed by Schneider and co-workers, was able to bind the ATP⁴⁻ **12** in H₂O with a high association constant ($K_a = 3.7 \cdot 10^4 \text{ M}^{-1}$).^[33]

1.7.2 Ion-dipole interactions (50–200 kJ mol⁻¹)

Ion-dipole interactions are the result of the mutual attraction between ionic and polarised species. A typical example is the stabilisation of alkali metal cations complexes with crown ethers (**Figure 1.14**).^[34]

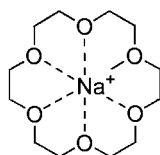


Figure 1.14 The Na⁺-18-crown-6 complex.

1.7.3 Dipole-dipole interactions (0–50 kJ mol⁻¹)

Dipole-dipole interactions are present among polarised species. Organic carbonyl compounds illustrate well this behaviour in the solid state (**Figure 1.15**).

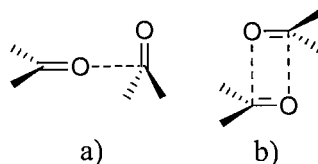


Figure 1.15 Dipole-dipole interactions in carbonyls.

Attractive interactions can result from the proximity of a single pair of poles on adjacent molecules (a) or from the opposite alignment of a dipole with another one (b). The low boiling point of ketones, such as acetone (56 °C), however, demonstrates that dipole-dipole interactions of this type are relatively weak in solution.

1.7.4 Hydrogen bonding (4-120 kJ mol⁻¹)

A hydrogen bond may be regarded as a particular kind of dipole-dipole interaction, in which a hydrogen atom attached to an electronegative atom is attracted from a neighbouring dipole. Because of its relatively strong and highly directional nature, hydrogen bonding is very important in host-guest complex design. The directional character of the hydrogen bond is well illustrated by the crystal packing of ice^[35] and by the structure of carboxylic acids dimers in the vapour state^[36] (**Figure 1.16**).

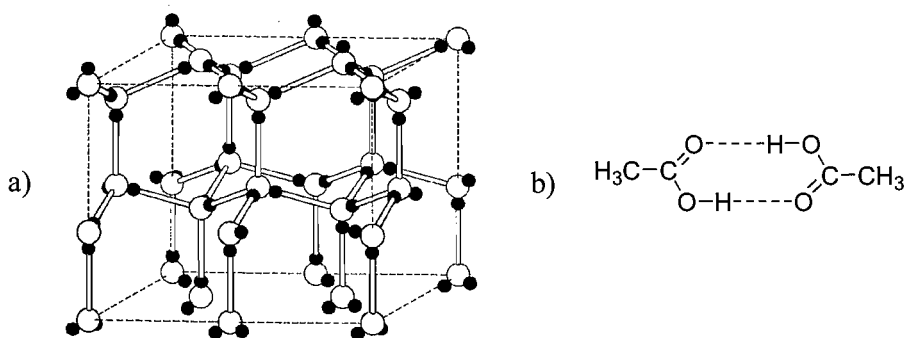


Figure 1.16 a) Crystal packing of ice. b) Structure of the dimer of the acetic acid.

The three centres involved in the hydrogen bonding (in this case [O-H····O]) display preferentially an axial orientation, although different arrangements are also effective (like, for example, the bifurcate hydrogen bond, present in the crystal structure of glycine).^[37] In order to obtain strong binding, a combination of multiple hydrogen bonds is often necessary. This concept was well illustrated by Hamilton and co-workers with the synthesis of a macrocyclic receptor for barbiturates (**Figure 1.17**).^[38]

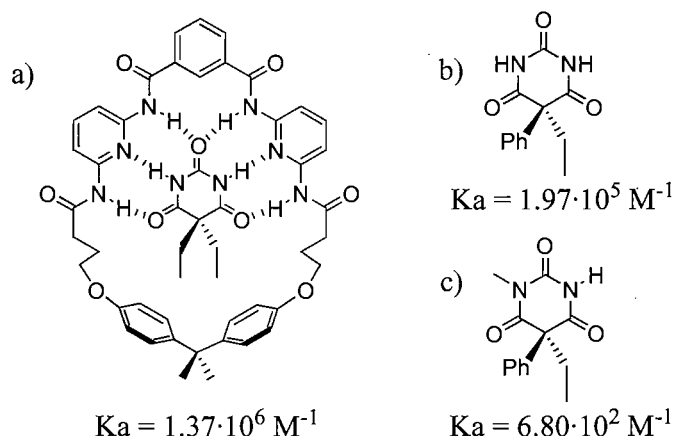


Figure 1.17 Hamilton's receptor for barbiturates. Constants measured in CDCl_3 .

When a methyl group (a) on the guest is substituted with a phenyl group (b) the binding is decreased by one order of magnitude, but when one hydrogen atom is substituted with a methyl group (c), with the loss of a hydrogen bond in the complex, the binding drops of almost three orders of magnitude. Although the strength of the hydrogen bond relies mostly on axial alignments, secondary interactions are also important. This fact becomes evident from the analysis of multiple hydrogen bond arrays.^[39] Among the numerous examples, Zimmerman and co-workers studied the binary complexes resulting from the association of molecules with different arrangements of hydrogen bonding donors (D) and acceptors (A) (**Figure 1.18**).^[40]

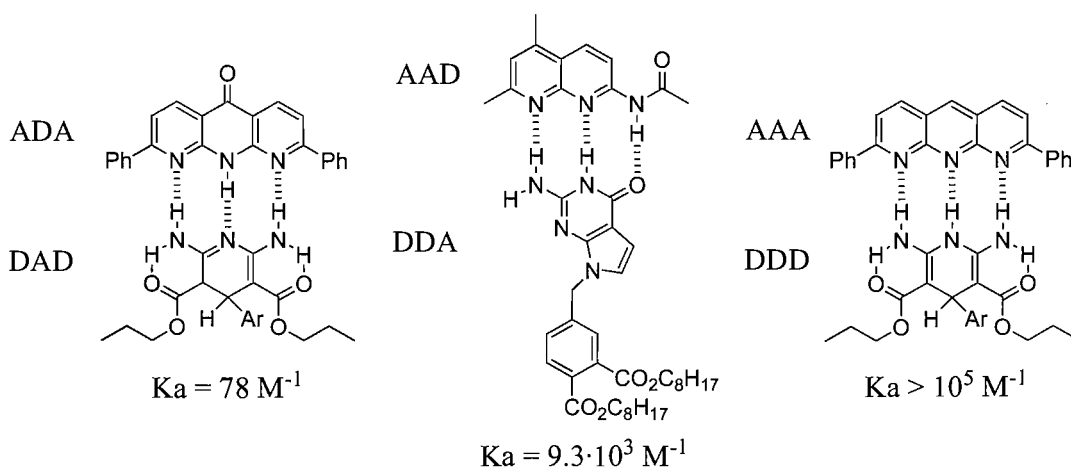


Figure 1.18 Triple hydrogen bond arrays. Constants measured in CDCl_3 .

The sheer difference in the association constants can be explained by secondary attractive ($\text{D} \cdots \text{A}$) and repulsive ($\text{D} \cdots \text{D}$, $\text{A} \cdots \text{A}$) forces (**Figure 1.19**).

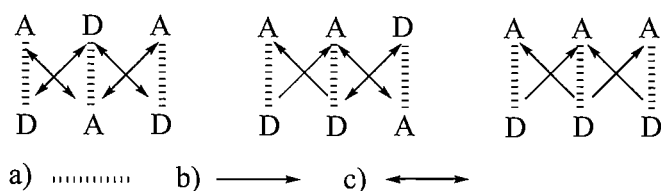


Figure 1.19 a) Hydrogen bonds. b) Attractive secondary interactions. c) Repulsive secondary interactions.

1.7.5 π - π stacking interactions (0-50 kJ mol⁻¹)

π - π stacking are weak electrostatic interactions occurring between aromatic rings. Such interactions control numerous and diverse phenomena, like the vertical base-base interactions which stabilise the double helical structure of DNA^[41] or the packing of aromatic molecules in crystals.^[42] There are two general types of π stacking: face-to-face and edge-to-face (**Figure 1.20**).

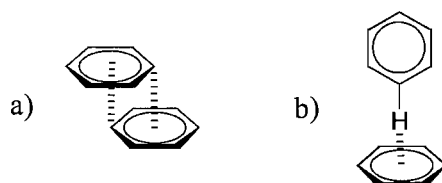


Figure 1.20 π - π stacking interactions. a) Face to face. b) Edge to face.

π stacking interactions may be regarded as an attraction between the negatively charged π -electron cloud of an aromatic ring and the positively charged σ -framework of an adjacent molecule (**Figure 1.21**).^[43]

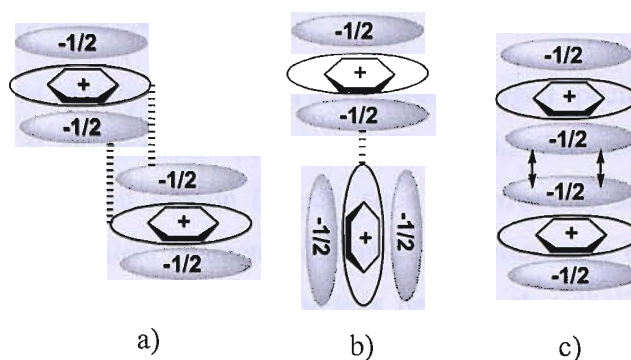


Figure 1.21 π - π stacking interactions. a) Offset face-to-face. b) Edge-to-face. c) Straight face-to-face.

This model accounts for the general preference for the offset face-to-face arrangement (a), compared to the less favoured straight face-to-face (c), due to the electrostatic repulsion between two adjacent electronic clouds. π - π stacking is more effective when the interaction occurs between electron-rich and electron-poor aromatic systems. This fact was illustrated by Zimmerman and co-workers with the synthesis of a series of aromatic cleft-type receptors (**Figure 1.22**).^[44]

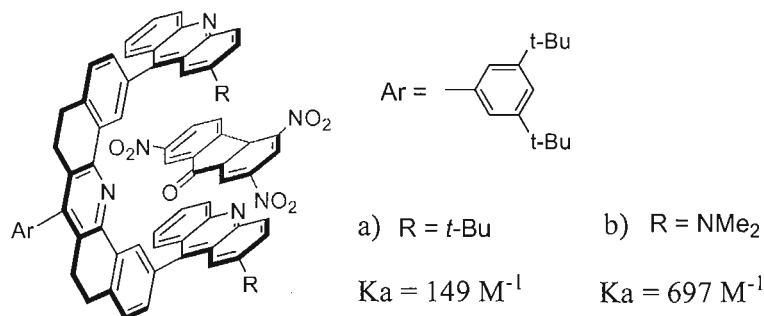


Figure 1.22 Zimmerman's receptors for 2,3,7-trinitrofluorenone. Constants calculated in $CDCl_3$.

Because of the enhanced π -basicity due to the presence of electron-donating groups (b), the affinity of the host for the electron-poor aromatic guest 2,4,7-trinitrofluorenone increased by almost five times.

1.7.6 Cation- π interactions (5-80 kJ mol⁻¹)

A cation- π interaction usually occurs when a positively charged species is in proximity of a π -electron cloud of an aromatic system or double bond. The complexes formed by transition metal cations and π -basic ligands, such as ferrocene, do not fall into this category, due to their covalent character. Cation- π interactions can be relatively strong. This fact is confirmed by the binding energies between the alkali metal cations and benzene molecules in the gas phase.^[45] The binding energy for the complex $[K^+ \cdots C_6H_6]$ is about 80 kJ mol⁻¹ (Figure 1.23).^[46]

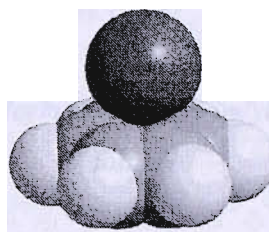


Figure 1.23 The complex between K^+ and C_6H_6 .

Cation- π interactions are also effective in solution. Mandolini and co-workers observed the formation of several complexes between quaternary ammonium and phosphonium salts and π -basic calixarenes, largely due to cation- π interactions (Figure 1.24).^[47]

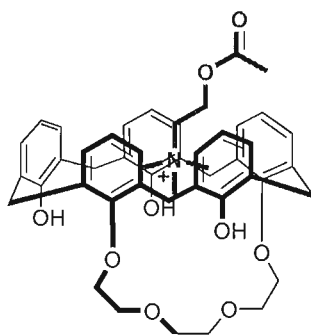


Figure 1.24 Mandolini's receptor for quaternary ammonium and phosphonium salts.

1.7.7 Van der Waals forces (< 5 kJ mol⁻¹)

Van der Waals interactions arise from the polarisation of an electron cloud by the proximity of an adjacent nucleus, resulting in a weak electrostatic attraction. They are non-directional and, for this reason, they possess only limited scope in the design of specific hosts for selective complexation of particular guests. In supramolecular

chemistry, their importance lies mostly in the formation of inclusion compounds, in which small, typically organic molecules are loosely incorporated within crystalline lattices or molecular cavities. An example is the incorporation of a molecule of toluene in the cavity of the *p*-*tert*-butylcalix[4]arene, obtained by Andreetti and co-workers (Figure 1.25).^[48]

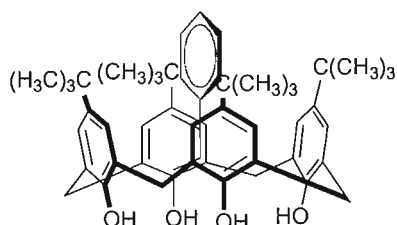


Figure 1.25 Inclusion complex formed by *p*-*tert*-butylcalix[4]arene and a molecule of toluene.

1.7.8 Hydrophobic effect

The hydrophobic effect is responsible for the formation of complexes or aggregates of non-polar molecules in polar solvents. There are two factors influencing this process. From an enthalpic point of view, the molecules of a polar solvent try to maximise their contact, in order to obtain the highest stabilisation energy deriving from their mutual, strong interactions. Molecules of solvent, in this manner, are driven away from hydrophobic host cavities, facilitating the formation of host-guest complexes. From an entropic point of view, the presence of non-polar molecules in a polar solvent causes a disruption in the bulk solvent by confining solvent molecules in hydrophobic cavities. When the non-polar molecules are associated, this disruption is decreased resulting in an entropic gain (Figure 1.26).

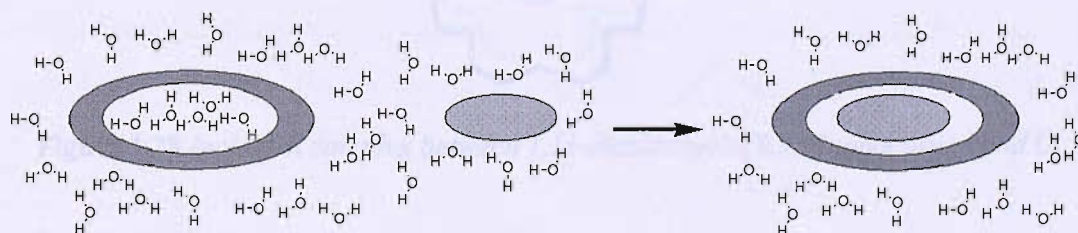


Figure 1.26 Entropic gain in the hydrophobic effect.

The hydrophobic effect was illustrated by Diederich and co-workers with the formation of a complex between a cyclophane host and *p*-dimethoxybenzene (**Figure 1.27**).^[49]

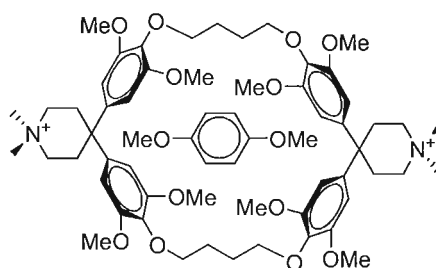


Figure 1.27 Diederich's receptor for small aromatic molecules.

The constant for the complex in water was $1.0 \cdot 10^4 \text{ M}^{-1}$, which is considerably high and cannot be explained exclusively on the basis of weak π - π stacking interactions and Van der Waals forces. In methanol the value of the constant dropped to 8 M^{-1} , proving that the formation of the complex was essentially driven by solvent-solvent interactions (weaker in methanol).

1.8 Anion binding

The first report of an artificial receptor for anions dates back to 1968. After only one year from the pivotal work on crown ethers by Pedersen, Simmons and Park reported the formation of an inclusion complex between a macrobicyclic diammonium and a Cl^- anion in 50% aqueous TFA (**Figure 1.28**).^[50]

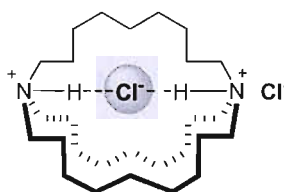


Figure 1.28 Inclusion complex between 1,11-diazabicyclo[9.9.9]nonacosane and Cl^- .

Receptors of this type were named katapinands (from the Greek *καταπίνω*, which means swallow up, engulf). Despite this early discovery, anion binding was developing slowly compared to the design of new hosts for cations and neutral molecules. The reason for this delay may lie in the fact that the design of receptors for anions is particularly

challenging. Anions are relatively large species and, therefore, they require receptors of greater size than those designed for cations. For example, one of the smallest anions, F^- , is comparable in size to K^+ . Anions, besides, present a plethora of geometries, stretching from spherical (halides), linear (SCN^- , N_3^-) and trigonal (NO_3^-) to tetrahedral (PO_4^{3-}) and octahedral (PF_6^-), without mentioning more complicated examples of biologically important species. In comparison to cations with similar size, moreover, anions have higher free energies of solvation and hence anion hosts must compete more effectively with the surrounding medium. Many anions, in the end, exist only in a relatively narrow pH window, limiting the design of anion hosts to those which are stable at the appropriate pH. Notwithstanding these challenges, since the late 1980's anion complexation has known a rapid and continuous growth, with the contribution of numerous research groups worldwide.^[51] This fact may be ascribed to the importance of the anions in biological systems. Between 70 and 75 per cent of enzyme substrates and cofactors are anions, the genetic information is expressed by DNA, which is a polyanion and chloride anion is widely involved in the transport across cell membrane. Other numerous examples are there to justify the growing attention given by supramolecular chemists to anion complexation.

1.9 Artificial receptors for carboxylates

Carboxylates are ubiquitous in biological systems and are involved in many crucial processes. Because of the extensive presence of carboxylates in oligopeptides and proteins, as well on the surface as at the C-terminus, the design of receptors able to bind them is particularly attractive due to the perspective of controlling critical phenomena such as enzyme inhibition or signal transduction.^[52] For such reason, the design of receptors for carboxylates is a flourishing field.^[53] A host for carboxylates usually incorporates a Carboxylate Binding Site (CBS), which is the moiety involved directly in carboxylate binding. Herein a brief description of some selected receptors for carboxylates is given on the basis of the different CBS's.

1.9.1 Ureas, thioureas and guanidiniums

Ureas, thioureas and guanidiniums present a bidentate hydrogen bonding donor motif which is a geometrical and steric match of the hydrogen bonding acceptor system of the carboxylate (**Figure 1.29**).

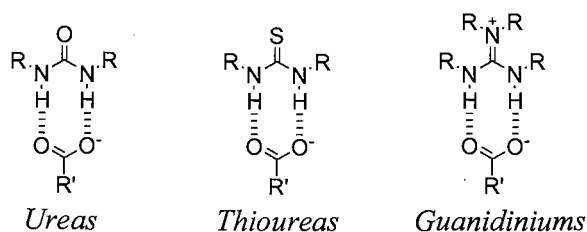


Figure 1.29 Ureas, thioureas and guanidinium as carboxylate binding sites.

One of the first examples of urea based receptor for carboxylates was synthesised by Wilcox and co-workers (**Figure 1.30**).^[54]

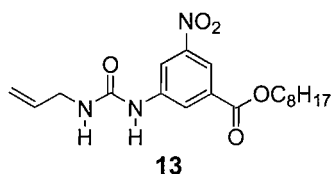


Figure 1.30 Wilcox's urea based receptor.

Urea **13** showed marked downfield shifts for the signals of the *NH* protons in the NMR spectrum in CDCl₃ upon addition of TBA benzoate, indicating that association occurred. The association constant was then measured by UV titrations in chloroform ($K_a = 2.7 \cdot 10^4 \text{ M}^{-1}$). Another example of a receptor based on urea moiety was provided by Moràn and co-workers (**Figure 1.31**).^[55]

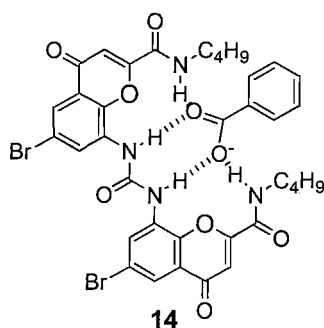


Figure 1.31 Moràn's urea based receptor.

The complex **14** presented a high association constant ($K_a = 1.5 \cdot 10^4 \text{ M}^{-1}$) in the competitive solvent DMSO-*d*₆, probably because of the preorganisation of the host

deriving from the rigidity of the chromenone rings. The two amidic groups provided additional hydrogen bonding.

Bis-ureas also proved to be effective. Recently Gale and co-workers synthesised a simple fully aromatic bis-urea receptor able to bind selectively TBA acetate ($K_a = 3210 \text{ M}^{-1}$) in the competitive solvent $\text{DMSO-}d_6/5\% \text{ H}_2\text{O}$ (**Figure 1.32**).^[56]

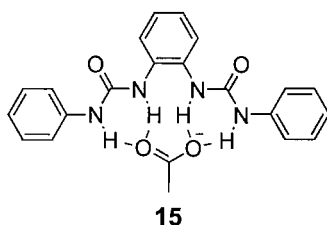


Figure 1.32 Gale's bis-urea based receptor.

Thiourea-based receptors are usually more soluble than their urea-based counterparts and in many cases they offer better binding. Comparison experiments were performed by Hamilton and co-workers, who confronted simple receptors for tetramethyl ammonium acetate as well as more complicate hosts for TBA glutarate (**Figure 1.33**).^[57]

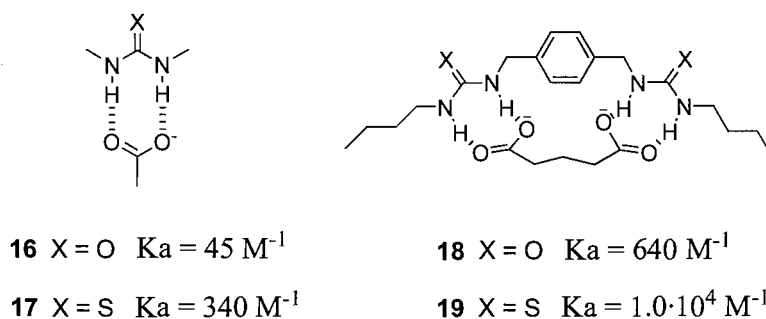


Figure 1.33 Hamilton's receptors for acetate and glutarate. Constants determined in $\text{DMSO-}d_6$.

From the binding studies carried out in $\text{DMSO-}d_6$, a ten-fold increase resulted when the CBS was switched from urea to thiourea.

An extensive study on macrocyclic effect, preorganisation and additional binding sites on thiourea based receptors was made by Tobe and co-workers (**Figure 1.34**).^[58]

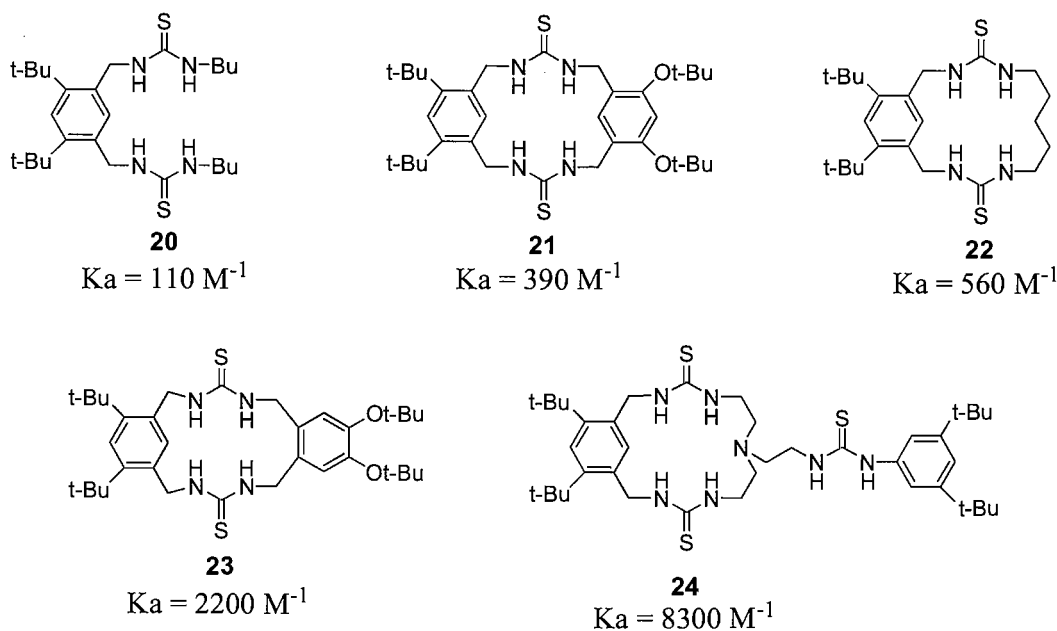


Figure 1.34 Tobe's thiourea-based receptors for acetate. Constants determined in $\text{DMSO-}d_6$.

Binding between receptor **20** and TBA acetate was poor. The increase of the binding shown by receptor **21** was due to its macrocyclic structure, although it was badly preorganised. This fact was proved by the increment in the binding constant resulted from the more flexible host **22**. An improvement in preorganisation was made with the rigid receptor **23**, which displayed a binding constant four times higher than the flexible **22**. Receptor **24**, in the end, took advantage from the additional thiourea moiety, resulting in a fifteen-fold increase compared to the parent macrocycle **22**.

Guanidinium is a popular CBS in carboxylate binding. Its success is due to the fact that it provides strong binding, resulting from the combined action of an ion-ion interaction between the positively charged host and the anion guest and a well preorganised hydrogen bonding. Moreover, guanidinium salts remain protonated over a wider pH window ($\text{p}K_a = 13.5$) compared to other charged receptors (e.g. ammonium salts). Schmidtchen was among the first supramolecular chemists to exploit the guanidinium moiety in carboxylate binding (**Figure 1.35**).^[59]

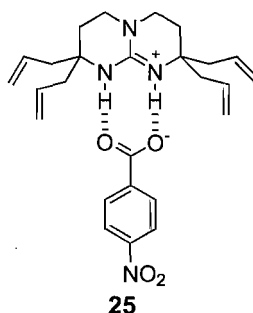


Figure 1.35 Schmidtchen's bicyclic guanidinium receptor (tetraphenyl borate salt) complexing *p*-nitrobenzoate (TBA salt).

Schmidtchen and co-workers measured a very high constant of association ($K_a > 10^4 \text{ M}^{-1}$) for the complex **25** in $\text{MeCN-}d_3$. The stability of complex **25** is also deriving from the preorganisation of the rigid bicyclic structure of the receptor. This effect was elucidated by Hamilton and co-workers, who made a direct comparison of simple cyclic and acyclic guanidinium receptors (**Figure 1.36**).^[60]

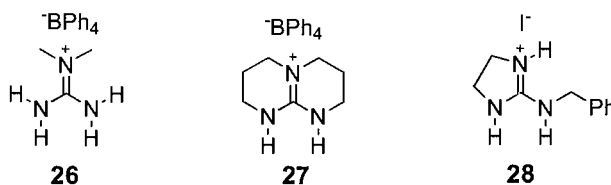


Figure 1.36 Hamilton's basic guanidinium receptors for acetate.

Calorimetric measurements in DMSO were carried out on receptors **26-28** with TBA acetate. The better affinity showed by cyclic receptors was due essentially to their preorganisation, as indicated by the entropy values (**Table 1.3**).

Receptor	$K_a (\text{M}^{-1})$	$\Delta H (\text{kcal mol}^{-1})$	$\Delta S (\text{cal mol}^{-1} \text{K}^{-1})$
26	3400	-3.8	+3.3
27	5600	-3.6	+5.0
28	7200	-2.8	+9.4

Table 1.3

The cyclic guanidinium **28** was incorporated by Anslyn and co-workers in a tripodal receptor for the tris-carboxylate citrate anion **30** (**Figure 1.37**).^[61]

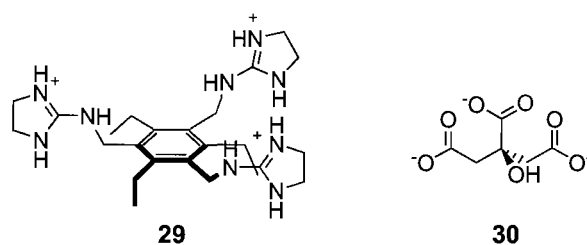


Figure 1.37 Anslyn's receptor for citrate.

Receptor **29** showed a tight binding with the citrate **30** in water ($K_a = 6.8 \cdot 10^3 \text{ M}^{-1}$) and was successfully employed in a fluorescent assay for citrate in beverages.^[62]

The bicyclic guanidinium **27** was extensively used as CBS because of the possibility to derivatise it with different moieties (see § 1.10) in order to bind a wide range of carboxylates. For example, Lehn, de Mendoza and co-workers designed a receptor able to extract quantitatively the *p*-nitrobenzoate anion in chloroform from an aqueous solution (**Figure 1.38**).^[63]

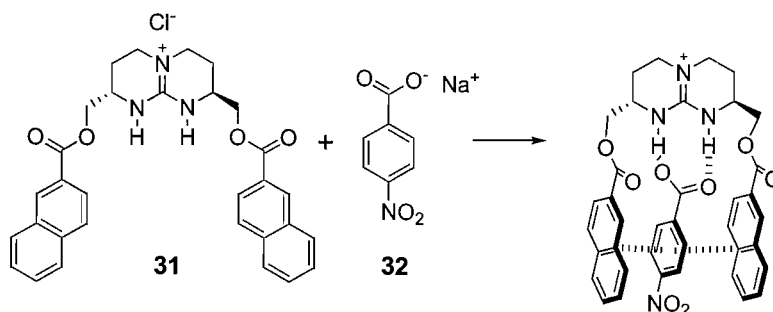


Figure 1.38 Lehn's and de Mendoza's receptor for *p*-nitrobenzoate.

The complex was stabilised by additional π - π stacking interactions, as proved by the change in the chemical shift of the aromatic protons. The binding constant between receptor **31** and TBA *p*-nitrobenzoate was measured in CDCl_3 ($K_a = 1609 \text{ M}^{-1}$).

1.9.2 Amides^[64]

The amide group itself provides far weaker binding in comparison with the groups so far described. For this reason, amides are often present as ancillary, yet important, sources of binding. Receptors based solely on amides, in order to obtain satisfactory complexation, must display many amidic groups acting synergistically. Moreover, molecules containing

more than one amide are prone to intramolecular hydrogen bonding,^[65] due to the marked amphiphilic donor-acceptor character of the amidic group. For this reason, in order to make *NH* bonds accessible to the carboxylate guest, a careful arrangement of the amide moieties is needed. On the other hand, amides are easy to make^[66] and they consent a great number of different architectures. The binding properties of basic bis-amides with different spacers was investigated by Schneider and co-workers (**Figure 1.39**).^[67]

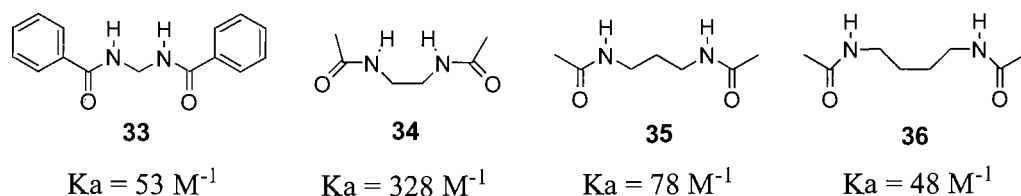


Figure 1.39 Schneider's bis-amide receptors for benzoate. Constants measured in CDCl_3 .

The best spacing of the two amide moieties was found for receptor **34**. Binding constants, however, were generally low because of the flexibility of such structures.

Better binding with more rigid receptors was achieved by Crabtree and co-workers with a series of cleft-type bis-amides and sulfonamides (**Figure 1.40**).^[68]

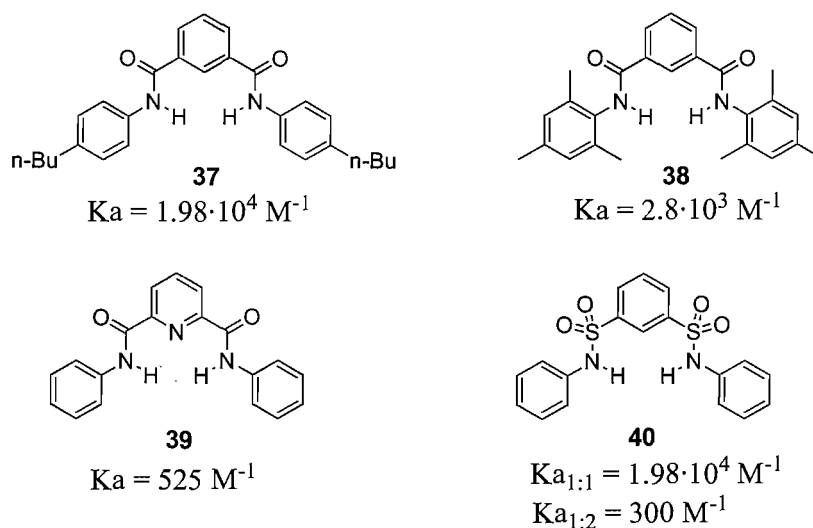


Figure 1.40 Crabtree's cleft-type receptors for acetate. Constants measured in CD_2Cl_2 .

NMR titrations were carried out on receptors **37-40** in CD_2Cl_2 with TBA acetate and the salts of other anions. Generally high constants were obtained with acetate, especially in

the case of receptor **37** and the bis-sulfonamide **40**, which was able to bind a second guest molecule with a weak interaction. The preference for the bis-amide **37** over **38** was due to both steric and electronic reasons, with three alkyl substituents reducing the acidity of the *NH* bonds. The low binding constant for the pyridyl host **39** can be ascribed to the electrostatic repulsion between the negative charge on the anion and the lone pair of the nitrogen atom.

Smith and co-workers improved the binding capability of bis-amide cleft-type receptors by internal Lewis acid coordination (**Figure 1.41**).^[69]

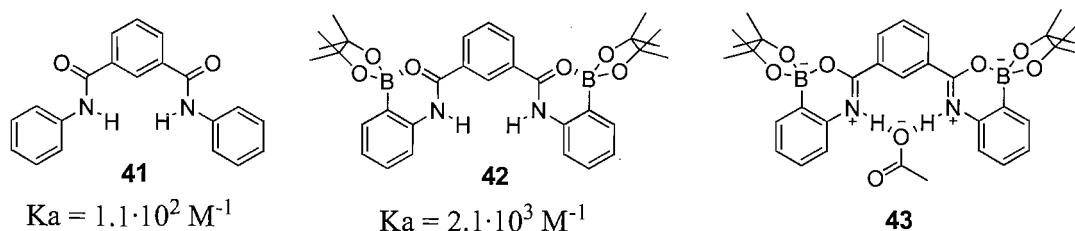


Figure 1.41 Smith's receptor for acetate with internal Lewis acid coordination.
 Constants measured in $\text{DMSO-}d_6$.

The incorporation of the electron-deficient boron moieties led to a twenty-fold increase in the binding constants with TBA acetate in $\text{DMSO-}d_6$. The nature of this effect is two-fold. From NOE measurements resulted that receptor **42** was assuming in $\text{DMSO-}d_6$ a well preorganised conformation with the *NH* bonds pointing in the same direction. ^{11}B NMR experiments, moreover, carried out on the neat host as well as on the complex, indicated that the resonance form **43** was the most plausible for the complex. In this structure, increased acidity of the *NH* bonds is provided by the polarisation effect induced by the boron moieties.

The receptors so far illustrated presented acyclic structures. The binding properties of macrocyclic tetralactams have been extensively studied by Jurczak and co-workers. The effect of the size was investigated. 20-membered macrocycle **45** displayed the best affinity for TBA acetate in $\text{DMSO-}d_6$ (**Figure 1.42**).^[70]

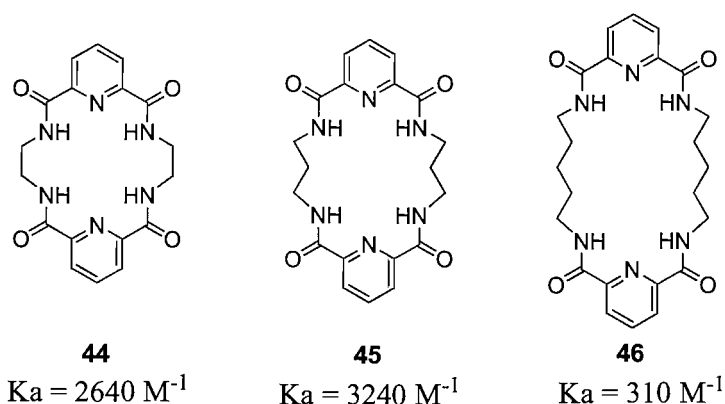


Figure 1.42 Effect of the size in Jurczak's tetralactam receptors for acetate. Constants measured in DMSO-d_6 .

All three receptors **44-46** incorporate two bis-amidopyridyl subunits. This moiety caused marked inhibition in the binding of the simple receptor **39** (**Figure 1.40**), due to the electrostatic repulsion between the anion and the nitrogen lone pair. In more complex structures, such as macrocycles **44-46**, however, the lone pair can favour the preorganisation of the entire system, by interacting with the two NH bonds (**Figure 1.43**). This effect can result in an overall increase of the binding.

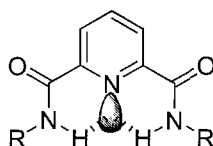


Figure 1.43 Preorganisation in bis-amidopyridyl subunits.

The improved preorganisation of structures containing bis-amidopyridines was demonstrated by Hunter and co-workers^[71] and corroborated by Kilburn.^[72] Further investigations were made by Jurczak and co-workers with a direct comparison of three tetralactam macrocycles, containing respectively two bis-amidopyridyl units, two bis-amidophenyl units and a combination of the two components (**Figure 1.44**).^[73]

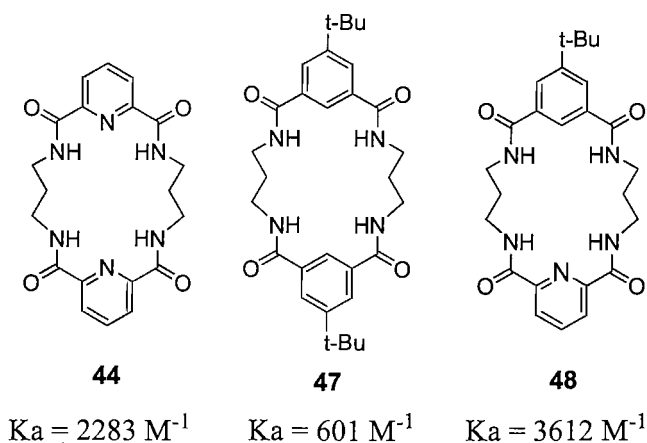


Figure 1.44 Effect of the nitrogen lone pair in Jurczak's tetralactam receptors for benzoate. Constants measured in $\text{DMSO-}d_6$.

The binding studies were carried out in $\text{DMSO-}d_6$ using TBA benzoate as guest. The low binding constant found for receptor **47** was due to a lack of preorganisation. In solution macrocycle **47** was adopting a conformation not suitable for binding, because of the stabilisation resulting from internal hydrogen bonding (**Figure 1.45**).

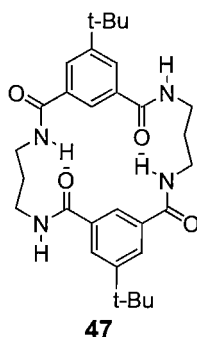


Figure 1.45 Internal hydrogen bonding of receptor **47**.

The binding constant found for receptor **48** indicated that the presence of one bisamido-pyridyl unit largely improved the preorganisation of the system, as confirmed by NOE experiments. Preorganisation was still present in receptor **44**. However, a lower binding constant compared to receptor **48** was found. This fact can be explained by an increased electrostatic repulsion due to the presence of an additional lone pair.

1.9.3 Pyrroles and bis-pyrroles

In the recent years, great impulse has been given to the use of the pyrrole moiety in anion binding, mostly by Sessler, Gale and Schmuck.^[74] The advantage of using pyrroles consists in the fact that they are ‘pure’ donor moieties, not featuring any hydrogen bonding acceptor side. The incorporation of a pyrrole unit in an amidic framework, as in 2-amidopyrroles, was a powerful idea, since a rigid binding site with a convergent bidentate hydrogen bonding system is created (**Figure 1.46**).

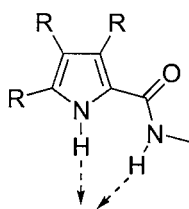


Figure 1.46 Convergent hydrogen bonding system in 2-amidopyrroles.

Gale’s and co-workers investigated the binding properties of simple 2-amidopyrroles towards benzoate and other anions (**Figure 1.47**).^[75]

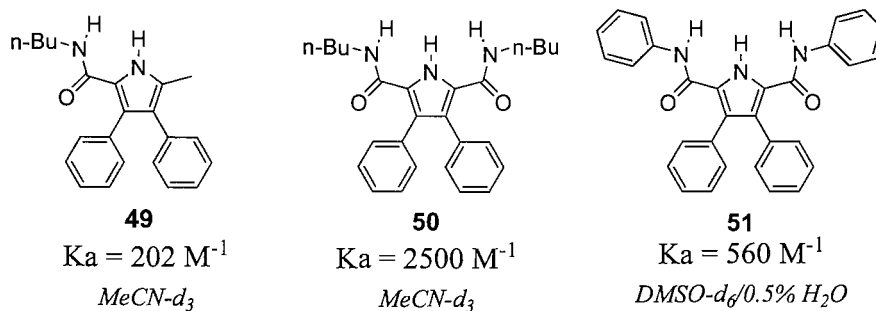


Figure 1.47 Gale’s 2-amidopyrrole receptors. Association constants with benzoate.

The introduction of an additional amidic group led to a twelve-fold increase in the binding constant of receptor **50** compared to receptor **49**. An indication of the effect of introducing the pyrrole moiety can be quantified by comparing receptor **51** with the similar receptor **41** (**Figure 1.41**). With the additional hydrogen bonding and the different geometry provided by the pyrrole group, a five-fold increase in the binding constant was obtained.

An interesting variant in the pyrrole host-guest chemistry is constituted by bis-pyrroles. Associated with amides, bispyrroles display a highly convergent binding site formed by four *NH* bonds. Gale and co-workers synthesised two simple bis-pyrrole based receptors and investigated their binding properties with benzoate and other anions (**Figure 1.48**).^[76]

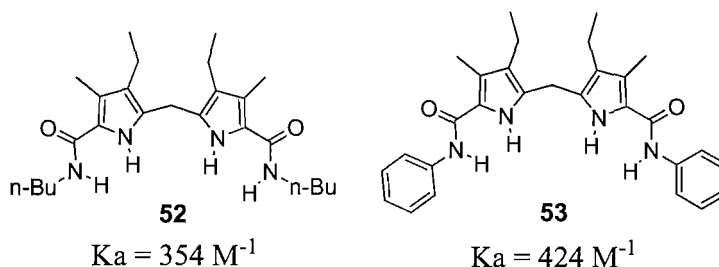


Figure 1.48 Gale's bis-pyrrole based receptors and binding constants with benzoate. All binding constants measured in $\text{DMSO-}d_6/5\% \text{ H}_2\text{O}$.

Reasonably high binding constants were obtained in the competitive solvent mixture $\text{DMSO-}d_6/5\% \text{ H}_2\text{O}$. Receptor **53** showed a stronger binding than receptor **52**. Even more marked prevalence was found in the case of the H_2PO_4^- anion, in the very competitive solvent mixture $\text{DMSO-}d_6/25\% \text{ H}_2\text{O}$ ($K_a = 20 \text{ M}^{-1}$ for **52** and $K_a = 234 \text{ M}^{-1}$ for **53**). These results confirm a general trend of higher binding constants for aromatic amides compared to the aliphatic ones (see § 1.9.2, receptors **33-36** and **37-40**). This tendency can be explained with two arguments. Aromatic groups are more rigid and thus they favour preorganisation. On the other hand, aromatic moieties usually display a negative inductive effect enhancing the acidity of the *NH* bond, whereas aliphatic groups display positive inductive effect reducing the acidity.^[77] However, the utilisation of aromatic amides has drawbacks. Aromatic groups leave limited space to derivatisation and their rigid nature consent only a restricted number of possible architectures. Moreover, aromatic amides are prepared from anilines, which are usually toxic and carcinogenic. Aliphatic amides, conversely, allow numerous structural motifs, facilitating, for example, the introduction of chirality.

1.10 Enantioselective receptors for amino acids^[78]

Amino acids are extremely important, for the manifold roles they play in biological systems as well as in the chemical and pharmaceutical industry. There is, therefore, a high

demand for receptors able to recognise them in biological systems and, on the other hand, there is a need for enantiopure amino acids at industrial level. For these reasons, chiral recognition of amino acids has been, in the last two decades, a constantly growing field.

The design of enantioselective receptors is particularly challenging. The discrimination of two guest enantiomers, which present the same functionalities, requires a very careful spatial arrangement of the binding sites in order to obtain the appropriate exclusive interaction. The receptor, obviously, must be chiral. Normally, more than one binding site is needed, along with rigid barriers deputed to create steric repulsion. All these components must be integrated in a subtle combination in order to obtain effective enantioselectivity. A remarkable embodiment of such principles was provided by de Mendoza and co-workers, who designed an enantioselective receptor for amino acids with aromatic residues in their zwitterionic form (Figure 1.49).^[79]

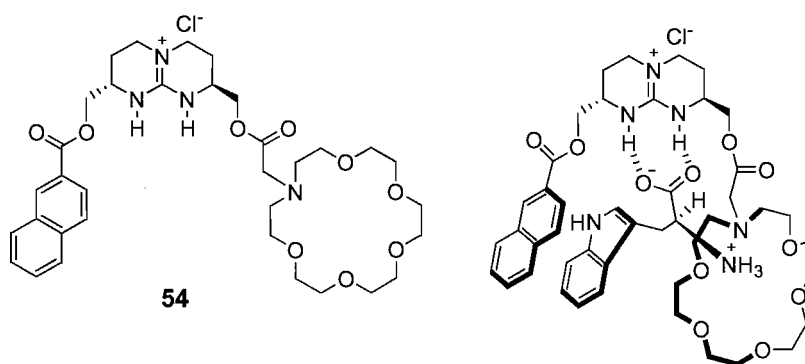


Figure 1.49 *de Mendoza's enantioselective receptor for amino acid with aromatic residues.*

Receptor **54** represents an evolution of receptor **31** (Figure 1.38). Single extraction experiments were carried out. It was found that receptor **54** was able to extract in DCM *L*-tryptophan and *L*-phenylalanine from an aqueous layer, whereas *L*-valine was not extracted. The extraction efficiencies (the fraction of host molecules occupied by the substrate) were ~ 40%. A competition experiment with the three amino acids furnished the ratios 100:97:6 for Phe/Trp/Val. Receptor **54**, moreover, showed great enantioselectivity, with only 0.5% of *D*-tryptophan and 2% of *D*-phenylalanine extracted from racemic aqueous solutions. The efficiency of receptor **54** derives from the presence of the coordinated effect of three components. The guanidinium group interacts directly with the carboxylate by hydrogen bonding and ion-ion electrostatic attraction, the crown

ether binds the ammonium group with hydrogen bonding and ion-dipole interaction and the naphthoyl moiety interacts with the aromatic side chain of the amino acid by π - π stacking. The importance of this latter interaction is proved by the fact that only amino acids with aromatic side chains were extracted by the receptor. The enantioselectivity, in the end, derived from the chirality associated with the rigid structure of the bicyclic guanidinium skeleton. Identical results were obtained with D amino acids using the (*R,R*) version of receptor **54**. The PF_6^- salt of the guanidinium **54**, moreover, revealed to be an efficient enantioselective transmembrane carrier for L-tryptophan.^[80] This type of transport experiment is usually carried out measuring the enantiomeric enrichment of an aqueous receiving phase separated from the racemic mother solution by a membrane constituted by an organic solvent containing the receptor carrier (**Figure 1.50**).

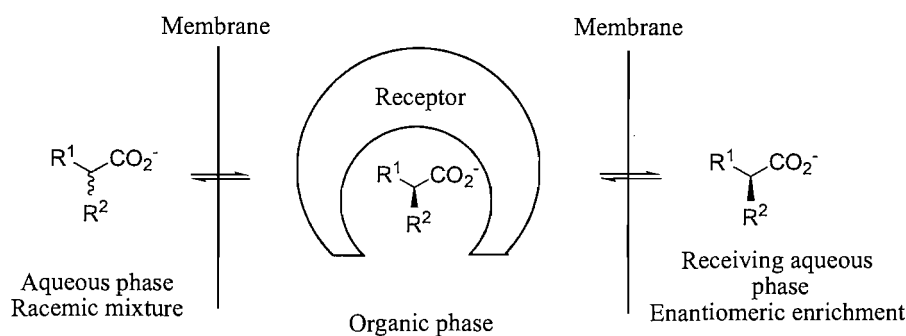


Figure 1.50 Enantiomeric enrichment achieved by transmembrane transport.

Apart from a method to assess enantioselective recognition, transmembrane transport can be used in order to achieve separation of racemates and is starting to become appealing in industrial milieus.^[81]

Other contributions to the development of enantioselective recognition were given by Kilburn and co-workers, who developed an acyclic thiourea based receptor for *N*-protected amino acids (**Figure 1.51**).^[72]

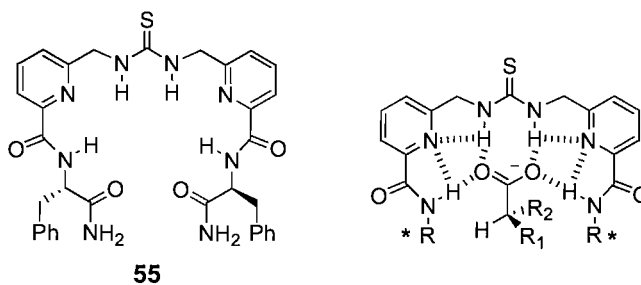


Figure 1.51 Kilburn acyclic receptor for *N*-protected amino acids.

The preorganisation of receptor **55** was insured by a hydrogen bonding network coordinated by the lone pairs of the nitrogen atoms in the pyridyl units. Receptor **55** showed moderate enantioselectivity towards the TBA salts of a series of *N*-protected amino acids in CDCl_3 . L amino acids were preferred (selected data are shown in **Table 1.4**).

<i>Amino acid</i>	Ka_L (M^{-1})	Ka_D (M^{-1})
<i>N</i> -Ac-Ala- CO_2^-	3450	2520
<i>N</i> -Ac-Phe- CO_2^-	4770	2990
<i>N</i> -Ac-Asn- CO_2^-	1690	800
<i>N</i> -Ac-Gln- CO_2^-	9000	4520
<i>N</i> -Boc-Gln- CO_2^-	1190	810
<i>N</i> -Boc-Trp- CO_2^-	3140	2225

Table 1.4

Kilburn and co-workers, then, building on the preorganised architecture of receptor **55**, designed a macrocyclic receptor bearing two binding sites, with the intention to obtain chiral recognition of *N*-protected bis-carboxylic amino acids (**Figure 1.52**).^[82]

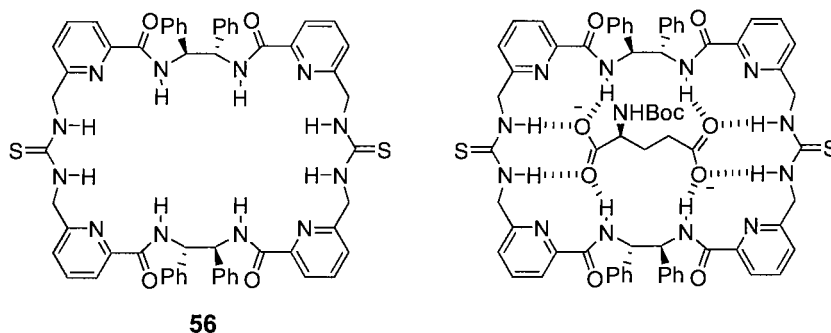


Figure 1.52 Kilburn's receptor for bis-carboxylic amino acids.

The macrocyclic receptor **56** formed a strong 1:1 complex with the bis-TBA salt of *N*-Boc-L-glutamate in MeCN ($K_a = 2.83 \cdot 10^4 \text{ M}^{-1}$, determined by ITC). In the same conditions, with *N*-Boc-D-glutamate, however, receptor **56** formed with the substrate both 1:1 and 1:2 complexes, with the 1:2 binding mode largely favoured ($K_{a_{1:1}} = 38.4 \text{ M}^{-1}$, $K_{a_{1:2}} = 4.92 \cdot 10^4 \text{ M}^{-1}$). Hence, for the 1:1 binding, the enantioselectivity for *N*-Boc-L-glutamate was $> 700:1$. Binding studies in DMSO gave a similar picture, although the binding constants for the 1:1 and the 1:2 complex with *N*-Boc-D-glutamate could not be reliably obtained. In the less competitive CDCl_3 , surprisingly, receptor **56** remained unperturbed upon addition of the bis-carboxylate guests. In such unpolar solvent, macrocycle **56** showed a wrapped conformation with a C_4 symmetry, instead of the expected D_2 , due to internal hydrogen bonding. The stabilisation coming from the formation of the complex was clearly not enough to overcome the energetic barrier necessary for the reorganisation. The wrapped conformation was confirmed by NOE experiments as well as computational studies.^[83]

An original and fruitful approach to enantioselective recognition was developed by Davis and co-workers. They derivatised the rigid scaffold of cholic acid with hydrogen bonding donor groups, such as carbamate and guanidinium (**Figure 1.53**).^[84]

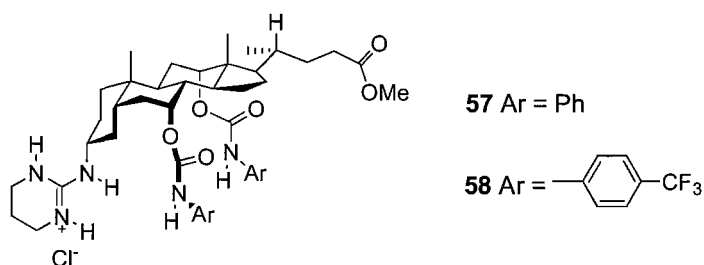


Figure 1.53 Davis' steroidal receptors for amino acids.

Single extraction experiments were carried out on receptors **57** and **58**. Several *N*-protected amino acids were extracted from an aqueous racemic solution into chloroform with good enantioselectivities (selected data are shown in **Table 1.5**).

Receptor	Substrate	Extraction efficiency (%)	Enantioselectivity (L:D)
57	<i>N</i> -Ac-DL-Ala-CO ₂ ⁻	52	7:1
57	<i>N</i> -Ac-DL-Phe-CO ₂ ⁻	87	7:1
57	<i>N</i> -Ac-DL-Val-CO ₂ ⁻	71	7:1
57	<i>N</i> -Ac-DL-Trp-CO ₂ ⁻	83	7:1
57	<i>N</i> -Boc-DL-Ser-CO ₂ ⁻	92	3:1
57	<i>N</i> -Boc-DL-His-CO ₂ ⁻	66	3.5:1
58	<i>N</i> -Ac-DL-Ala-CO ₂ ⁻	41	10:1
58	<i>N</i> -Ac-DL-Phe-CO ₂ ⁻	63	9:1
58	<i>N</i> -Ac-DL-Val-CO ₂ ⁻	90	9:1
58	<i>N</i> -Ac-DL-Trp-CO ₂ ⁻	83	9:1
58	<i>N</i> -Ac-DL-Met-CO ₂ ⁻	74	7:1

Table 1.5

The enantioselectivities were calculated by integrating the NMR signals of the two diastereoisomeric complexes. More acidic *NH* bonds in receptor **58** led to an improvement in enantioselectivity. NOE experiments and computational studies were consistent in indicating realistic binding models.

Enantioselective recognition in polar solvents such as DMSO, methanol and ultimately water is a demanding task. Schmuck made a substantial progress in this field with the design of a 2-(guanidiniocarbonyl)-pyrrole based receptor (**Figure 1.54**).^[85]

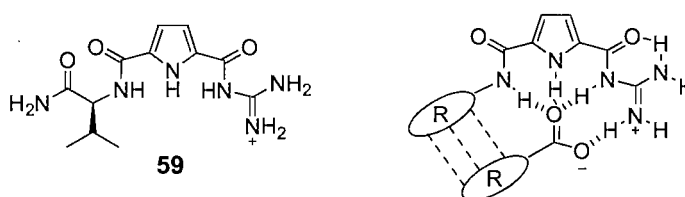


Figure 1.54 Schmuck's 2-(guanidiniocarbonyl)-pyrrole based receptor for amino acids.

The picrate salt of guanidinium **59** was able to discriminate between the tetramethylammonium salts of the two enantiomers of *N*-Ac-alanine in the very polar solvent mixture DMSO-*d*₆/40% H₂O ($K_a = 1610 \text{ M}^{-1}$ and $K_a = 930 \text{ M}^{-1}$ for L and D respectively). Computational studies confirmed the proposed geometry shown in **Figure 1.54**. According to the molecular modelling, the enantioselectivity arose from the steric clash present between the methyl group in *N*-Ac-D-Ala and the isopropyl group in receptor **59** (**Figure 1.55**).

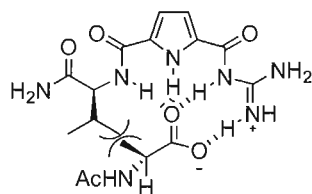


Figure 1.55 Steric repulsion in the complex between receptor **59** and *N*-Ac-*D*-Ala.

An important application of enantioselective recognition is the design of HPLC chiral columns. Enantioselective receptors, when immobilised on a stationary phase, can lead to different retention times for the two substrate enantiomers. Cram and co-workers accomplished one of the first chromatographic resolution immobilising a binaphthol based macrocycle on a polystyrene resin in order to obtain enantiomeric separation of ammonium salts of amino acids (**Figure 1.56**).^[86]

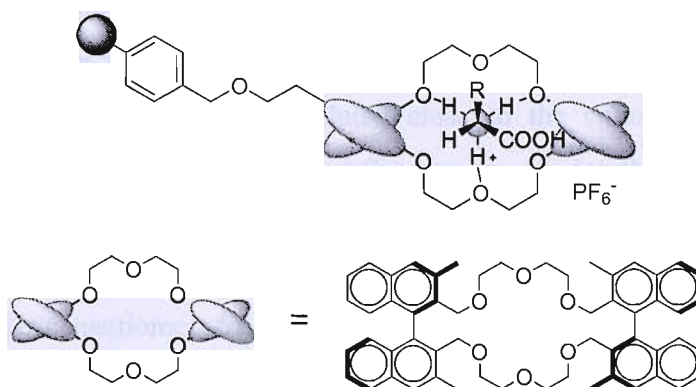


Figure 1.56 Cram's immobilised receptor for amino acids resolution.

More recently, Villani and co-workers synthesised a tetralactam receptor that was covalently attached to silica (**Figure 1.57**).^[87]

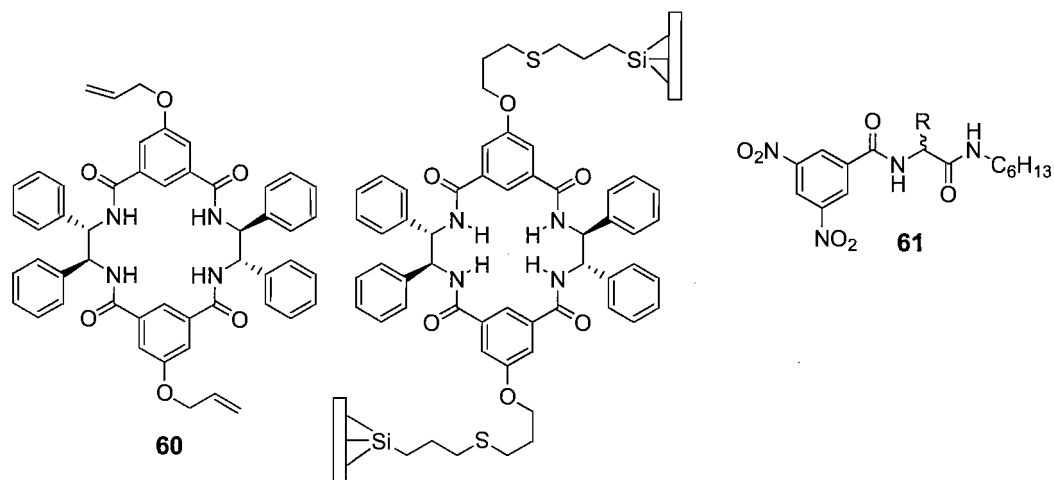


Figure 1.57 Villani's tetralactam receptor for derivatised amino acids.

The silica with the grafted receptor was then packed in a HPLC column in order to resolve racemic mixtures of derivatised amino acids **61**. Separation of several racemates was achieved with a DCM/2-propanol mixture as eluent. L derivatives were preferentially retained, whereas D derivatives were eluted close to the column void volume. In principle, it is possible to calculate the difference in ΔG for the interaction of two different elutes with a receptor immobilised in a stationary phase from their retention time.^[88] In such a way, Villani and co-workers calculated high $\Delta\Delta G$ values for the chiral recognition of guest enantiomers **61** (selected data are shown in **Table 1.6**).

<i>R</i>	$-\Delta\Delta G$ (kcal mol ⁻¹)
<i>Me</i>	1.5
<i>Et</i>	2.4
<i>Pr</i>	2.8
<i>Bu</i>	3.0
<i>i-Pr</i>	3.0
<i>s-Bu</i>	3.0
<i>i-Bu</i>	2.0
<i>t-Bu</i>	1.4
<i>Ph</i>	2.2
<i>Bn</i>	1.3
<i>MeSCH₂CH₂</i>	2.5

Table 1.6

1.11 Aims of this work

Amides are a recurring motif in carboxylate binding and many hosts are built on them (see § 1.9.2). Fewer and usually basic receptors,^[61,89] however, display sulfonamides as hydrogen bonding donors, despite the fact that they are more acidic than amides ($pK_a = 17.5$ for $\text{Me-SO}_2\text{-NH}_2$ and $pK_a = 25.5$ for Me-CO-NH_2)^[90] and generally more soluble. Moyer and Kavallieratos investigated the binding properties towards TBA acetate of simple mono- and bis-sulfonamide receptors in 1,2-dichloroethane- d_4 (**Figure 1.58**).^[89a]

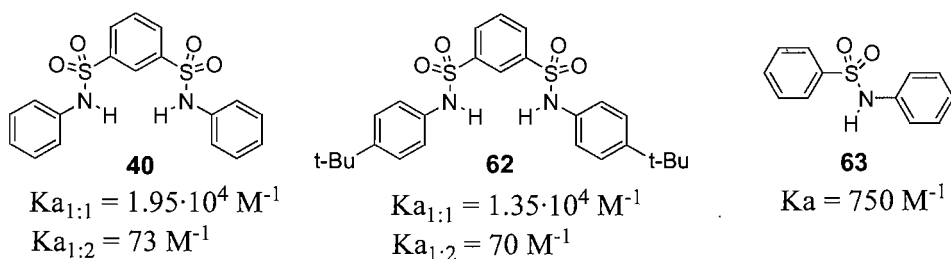


Figure 1.58 Moyer's sulfonamidic receptors for acetate. Constants calculated in 1,2-dichloroethane- d_4 .

Receptor **40** had already been investigated by Crabtree in CD_2Cl_2 and the data are in agreement (see § 1.9.2). A minor 1:2 complexation was confirmed for this type of receptors. Another conclusion of this work was that the synergistic action of two sulfonamidic groups is necessary in order to obtain strong binding (**40** and **62**), otherwise poor association occurs (**63**). Recently, Yano and co-workers synthesised a bis-sulfonamide receptor incorporating two hydroxyl groups (**Figure 1.59**).^[89d]

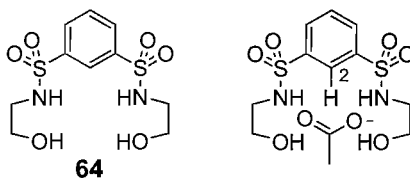


Figure 1.59 Yano's receptor for acetate.

After NMR titration, a considerably high binding constant ($K_a = 2.38 \cdot 10^4 \text{ M}^{-1}$) was reported for receptor **64** with TBA acetate in the rather competitive solvent $\text{MeCN-}d_3$, although the high value was calculated solely on the basis of the $\Delta\delta$ (the changes in

chemical shift induced by adding an aliquot of guest) of the C_2-H proton, not directly involved in hydrogen bonding.

Considering the encouraging examples of strong interaction between the bis-sulfonamide moiety and the carboxylate anion along with the scarcity, on the other hand, of more structured receptors built on this motif, the aim of this project was to incorporate the bis-sulfonamide unit into a more complex scaffold, in order to obtain strong and selective binding of carboxylates and eventually to achieve enantioselective recognition of amino acids (**Figure 1.60**).

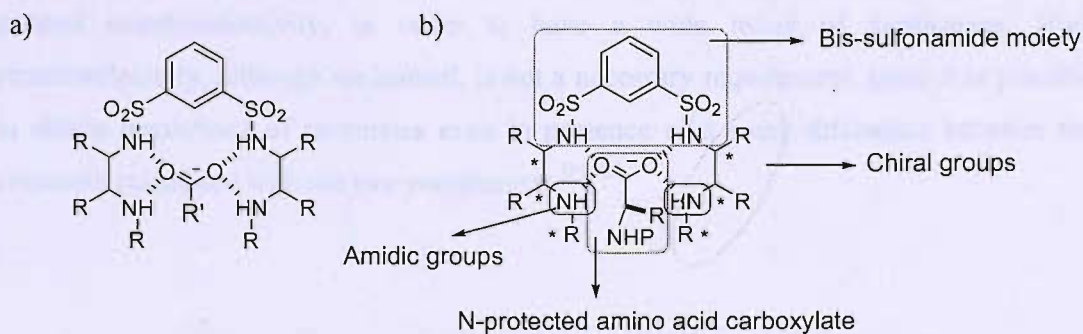


Figure 1.60 a) General scheme of bis-sulfonamide receptor for carboxylates. b) Enantioselective receptor for *N*-protected amino acids.

Two additional amide groups can contribute to strengthen the interaction with the carboxylate anion. For a better chance of preorganisation, macrocyclic structures were also to be investigated (**Figure 1.61**).

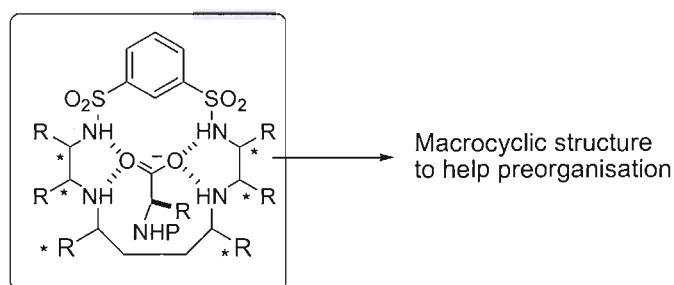


Figure 1.61 General scheme of a macrocyclic bis-sulfonamide receptor.

Enantioselectivity can be achieved with the introduction of chiral moieties able to give secondary interactions or to function as steric barriers. *N*-protected amino acids are ideal

candidate substrates due to their synthetic utility and they were to be tested in the form of their TBA salts in order to increase the solubility of the ionic couple in organic media and to minimise the effects of the counter anion.^[91] The stability constants for each host-guest complex were to be measured by traditional ¹H NMR titrations.

As part of an EU network involving companies and universities, this project ultimately aimed to develop receptors suitable for applications in resolution of racemates, such as chromatographic separations or transport across membrane, with particular attention to commercial aspects. At this regard, an ideal receptor has to be easy to make in few steps, possibly with high yields, to facilitate the necessary scale-up. It has to display, moreover, general enantioselectivity, in order to have a wide range of application. High enantioselectivity, although welcomed, is not a necessary requirement, since it is possible to obtain resolutions of racemates even in presence of a small difference between the constants calculated with the two enantiomers.^[81,92]

Chapter II

Bis-Sulfonamide Based Receptors for Carboxylates

2.1 Synthesis of acyclic receptor 65

In order to test the possibility of exploiting bis-sulfonamide based receptors in amino acid binding and chiral recognition, a simple acyclic receptor was conceived (**Figure 2.1**).

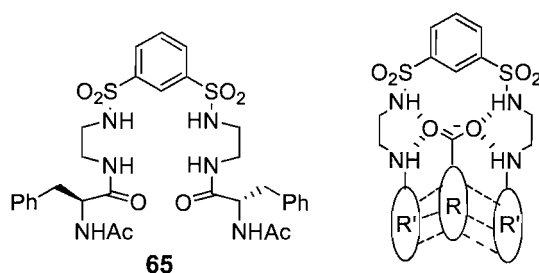
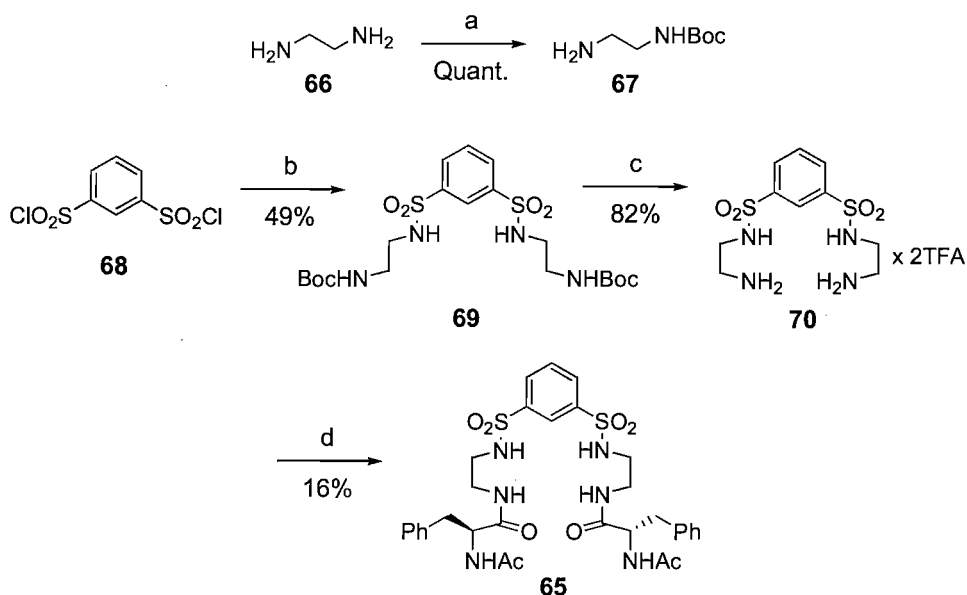


Figure 2.1 Bis-sulfonamide based receptor for amino acids.

The binding of the carboxylate group can be insured by the bis-sulfonamide bis-amide binding site, while chiral recognition can arise from secondary interactions between the substrate and the two amino acid moieties incorporated in the receptor in a pendant fashion. The synthesis was accomplished following well established standard procedures (**Scheme 2.1**).



Scheme 2.1 Reagents and conditions: a) Boc_2O , DCM; b) **67**, Et_3N , DCM; c) 80:20 DCM/TFA; d) $N\text{-Ac-L-Phe-OH}$, EDC, HOBt, DIPEA, DCM/DMF 50:50.

After mono-protection of bis-amine **66**,^[93] amine **67** was coupled to the commercially available bis-sulfonyl chloride **68** with acceptable yield.^[94] Bis-Boc intermediate **69** was deprotected to afford the bis-ammonium TFA salt **70**. The relatively low yield of the latter transformation was the consequence of several washes carried out on the product with the intent to isolate it with high purity standards. A typical coupling procedure^[66] led to the candidate receptor **65** with poor, unoptimised yield.

2.2 Binding studies

^1H NMR binding studies were carried out on receptor **65** by adding aliquots of a solution of the guest to a solution of the host and monitoring the change in the chemical shift ($\Delta\delta$) of the protons directly involved in hydrogen bonding. The data were then treated with a curve fitting program, kindly provided by Hunter (see § 5.4 and appendix B for additional information. For all the binding studies described in this work, the output of the treating program, for the 1:1 or 1:2 host/guest stoichiometry, is provided in § 5.6).^[95] The two enantiomers of $N\text{-Ac-phenylalanine}$ TBA salt were used as guests. This particular amino acid was chosen because of its relatively bulky side chain. The titrations were performed in $\text{MeCN-}d_3$, as receptor **65** was not soluble in CDCl_3 . Large $\Delta\delta_{\text{max}}$ resulted from the three NH protons monitored, indicating the presence of strong hydrogen bonding (**Figure 2.2**).

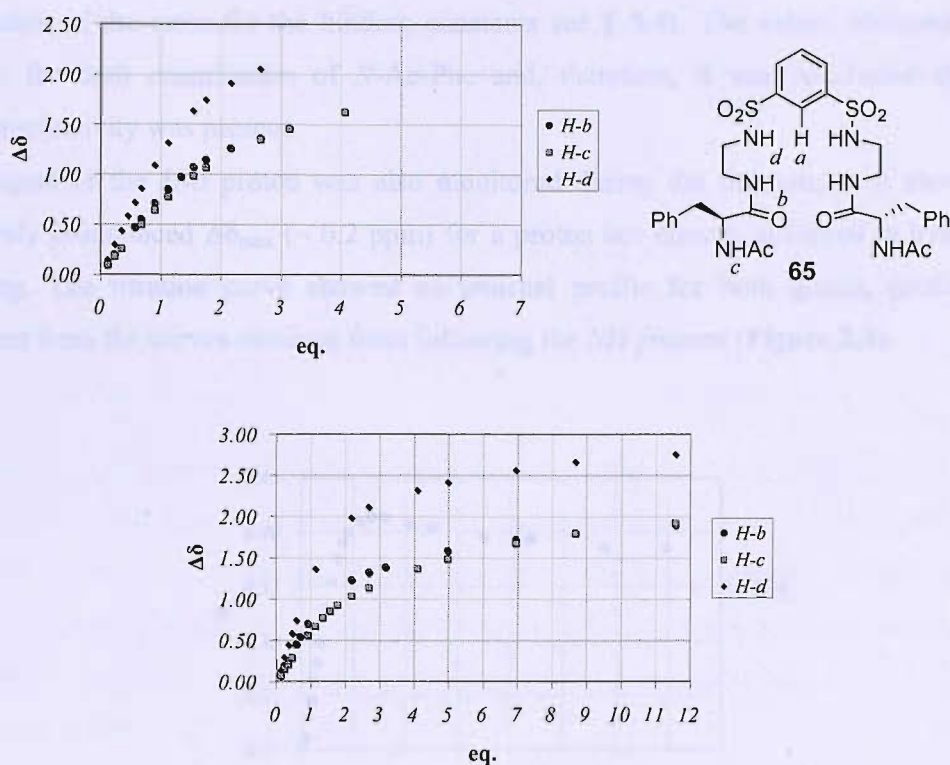


Figure 2.2 Binding titration curves of receptor **65** upon addition of *N*-Ac-L-Phe TBA salt (above) and *N*-Ac-D-Phe TBA salt (below) in MeCN-d_3 .

For the titration with *N*-Ac-L-Phe, proton signals could be followed only at low concentration of guest, due to a marked superimposition of the proton signals. Good fit, nevertheless, was obtained with the 1:1 curve fitting program.^[95] High discrepancies, however, were present among the values of the constants obtained from different protons, especially between *H*-*b* and *H*-*c*. Also the titration with *N*-Ac-D-Phe presented such differences (**Table 2.1**).

Host	Guest	K_a (M^{-1})			Solvent
		<i>H</i> - <i>b</i>	<i>H</i> - <i>c</i>	<i>H</i> - <i>d</i>	
65	<i>N</i> -Ac-L-Phe-OTBA	888	489	1000	MeCN-d_3
65	<i>N</i> -Ac-L-Phe-OTBA	718	400	1090	MeCN-d_3

Table 2.1

Because of the disagreement among the various constants, large errors (> 25% for *N*-Ac-L-Phe and > 35% for *N*-Ac-D-Phe) were calculated. Precise overall constants, thus, could

not be reliably expressed (for a detailed discussion on the criteria that apply to the estimation of the error for the binding constants see § 5.4). The values obtained were similar for both enantiomers of *N*-Ac-Phe and, therefore, it was concluded that no enantioselectivity was present.

The signal of the *H*-*a* proton was also monitored during the titration, as it showed a relatively pronounced $\Delta\delta_{\max}$ (~ 0.2 ppm) for a proton not directly involved in hydrogen bonding. The titration curve showed an unusual profile for both guests, profoundly different from the curves obtained from following the *NH* protons (**Figure 2.3**).

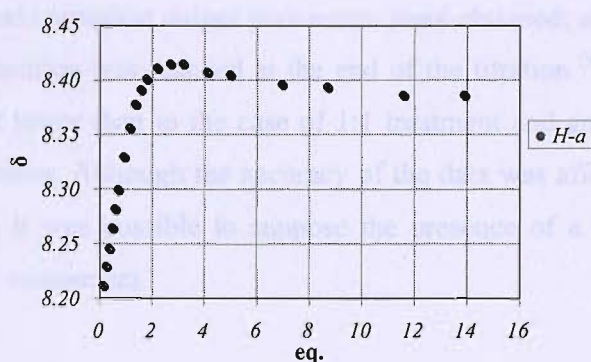


Figure 2.3 Titration curve for *H*-*a* of receptor 65 upon addition of *N*-Ac-*D*-Phe TBA salt in *MeCN*-*d*₃. A similar result was obtained with *N*-Ac-*L*-Phe.

A steep slope resulted from the early additions of the guest stock solution, until saturation was reached. Then the trend was reversed, and an upfield shift with a gentle gradient was induced by further addition of guest aliquots. The curve could not be fitted with the 1:1 treating program. Some fit could be obtained, instead, with the 1:2 treating program. However, the fit was markedly poor. Moreover, for a series of parameters associated with the data processing, such as the percentage of saturation of the host (*Min % bound* and *Max % bound* in the output) and the estimated chemical shift at 100% saturation (δ *bound*) (see § 5.6), nonsensical values were calculated. Negative percentages of saturation were found and the δ *bound* for the 1:2 complex was far lower than the chemical shift of the uncomplexed host. For this reason, the accuracy of the binding constants calculated resulted undermined and the values obtained could serve only as a rough indication of the binding. For the binding studies with *N*-Ac-*L*-Phe, $K_{a1:1}$ resulted $\sim 4.7 \cdot 10^3 \text{ M}^{-1}$ and $K_{a1:2} \sim 5 \text{ M}^{-1}$, whereas with *N*-Ac-*D*-Phe $K_{a1:1}$ resulted $\sim 3.4 \cdot 10^3 \text{ M}^{-1}$ and $K_{a1:2} \sim 4 \text{ M}^{-1}$. In order

to obtain further elucidations, the curves of the other protons obtained from the titration with *N*-Ac-D-Phe were also treated with the 1:2 fitting program (the level of saturation for the titration with *N*-Ac-L-Phe was too low in order to obtain an acceptable fit) (Table 2.2).

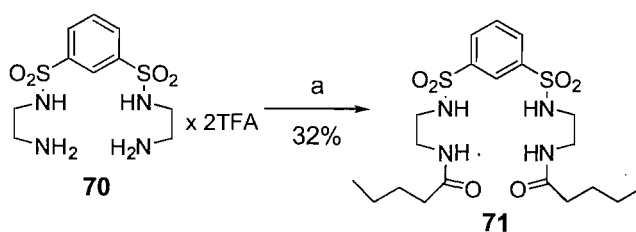
	$K_{1:1} (M^{-1})$	$K_{1:2} (M^{-1})$
<i>H</i> -a	~3400	~4
<i>H</i> -b	1088	5.5
<i>H</i> -c	706	4.6
<i>H</i> -d	1494	6.2

Table 2.2

In this case, good fit and consistent output parameters were obtained, although only a low percentage of host saturation was reached at the end of the titration.^[96,97] The error was still high (~ 30%), but lower than in the case of 1:1 treatment and good agreement was found for the 1:2 constants. Although the accuracy of the data was affected by the above mentioned limitations, it was possible to suppose the presence of a major 1:1 binding along with a minor 1:2 component.

2.3 Synthesis of receptor 71

In order to clarify the unusual curve profile found for the aromatic proton *H*-a in receptor 65, it was decided to carry out binding studies on simpler receptors. The already available bis-carbamate 69 and easily accessible bis-amide 71 were chosen as candidates. Receptor 71 was obtained by coupling diamine 70 with valeryl chloride (Scheme 2.2).



Scheme 2.2 Reagents and conditions: a) Valeryl chloride, Et_3N , MeCN.

The disappointing yield was probably due to the presence of side-products deriving from bis-acylation.

2.4 Binding studies

Binding studies were carried out on receptors **69** and **71** with TBA acetate in MeCN- d_3 . Again high $\Delta\delta_{\max}$ were shown by C_2 -H aromatic proton (~ 0.5 ppm for **69** and ~ 0.35 ppm for **71**) and the anomalous effect found for receptor **65** appeared to be general. Receptors **69** and **71** showed a similar behaviour, with the upfield shift even more pronounced, especially in the case of **71** (Figure 2.4).

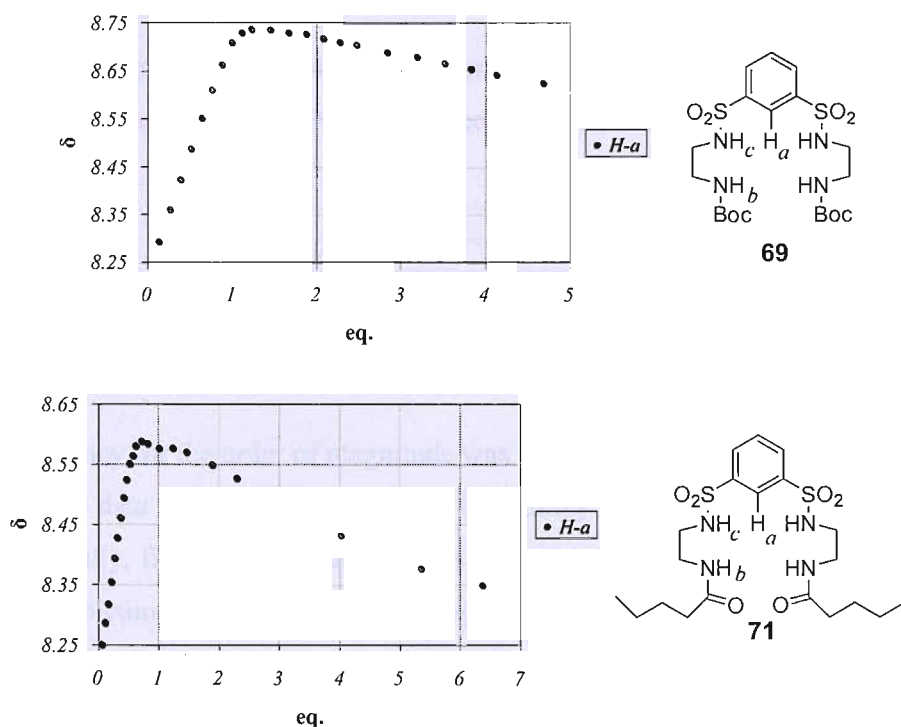


Figure 2.4 Titration curves for H -a proton of receptors **69** and **71** upon addition of acetate TBA salt in MeCN- d_3 .

In both cases, the steep slope of the titration curve was progressing downfield until about one equivalent of guest was added, then inversion occurred. The sulfonamidic H -c signals underwent intense broadening and could not be followed. The curves obtained from the $\Delta\delta$ of the amidic H -b signals did not present the unusual pattern found for H -a, but they could not be fitted with the 1:1 treating program. Therefore, the 1:2 treating program was used.

In the case of receptor **69**, good fit was found for H -a, although the constants obtained were undermined by nonsensical parameters (see § 2.2) and thus they have to be taken as

a rough indication. Good fit was also found for amidic *H-b*. The results are summarised in **Table 2.3**.

	$K_{1:1} (M^{-1})$	$K_{1:2} (M^{-1})$
<i>H-a</i>	12800	28
<i>H-b</i>	36000	26

Table 2.3

The data calculated were consistent for $K_{1:1}$, at least for the order of magnitude, and very similar values were found for $K_{1:2}$.

In the case of receptor **71**, for both proton signals *H-a* and *H-b* poor fit and nonsensical output parameters were found. The binding constants so obtained are showed in **Table 2.4**.

	$K_{1:1} (M^{-1})$	$K_{1:2} (M^{-1})$
<i>H-a</i>	~8000	~10
<i>H-b</i>	~11000	~4

Table 2.4

Again consistency for the order of magnitude was obtained.

Although some data were deeply affected by inaccuracy and, for this reason, they have to be taken carefully, from the combined results obtained with acyclic receptors **65**, **69** and **71**, a general picture of a strong 1:1 binding accompanied by a minor 1:2 component emerged clearly.

2.5 A possible explanation

A plausible model, capable to explain both the formation of a 1:2 complex and the unusual profile of the curves of the C_2-H aromatic proton in receptors **65**, **69** and **71**, is illustrated in **Figure 2.5**.

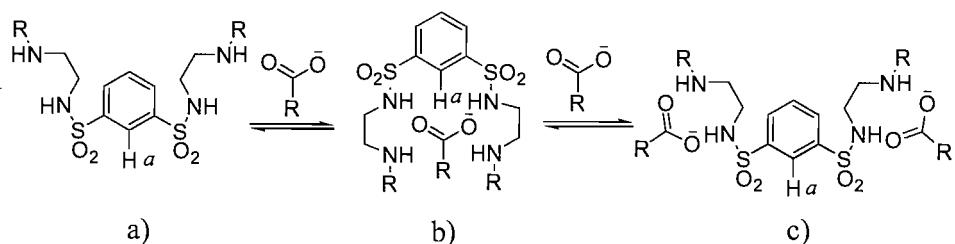


Figure 2.5 Formation of a 1:2 complex between a bis-sulfonamide bis-amide acyclic receptor and a carboxylate anion.

During the first additions of guest aliquots, the formation of the 1:1 complex is accompanied by significant conformational reorganisation, probably due to the stability of a non-preorganised conformation assumed by the neat host (in **Figure 2.5** is shown the *anti-anti* conformation, but the *syn-anti* may also be favoured).^[68] This should account for the large $\Delta\delta$'s registered for the *H-a* proton before one equivalent of guest is added. At higher concentrations of guest, a 1:2 complex can be formed and the receptor tends to return to its initial conformation, resulting in an inversion of the trend for the *H-a* titration curve. These findings seem to confirm a general tendency of bis-sulfonamide receptors towards 1:2 association. Crabtree and co-workers found that receptor **40** (see § 1.9.2) was able to complex a second molecule of TBA acetate with a weak constant and they utilised a model similar to the one depicted in **Figure 2.5** in order to explain the strong association between the bis-sulfonamide **40** and TBA fluoride.^[68] This model was used more recently by Yano and co-workers in order to describe the association between the phenolic bis-sulfonamide **72** and TBA chloride (**Figure 2.6**).^[98]

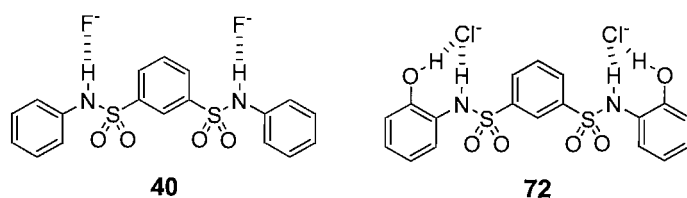


Figure 2.6 Crabtree's (**40**) and Yano's (**41**) bis-sulfonamides displaying a 1:2 binding mode.

In order to assess the stoichiometry of the association between receptor **69** and TBA acetate a Job Plot experiment was performed (**Figure 2.7**).^[96]

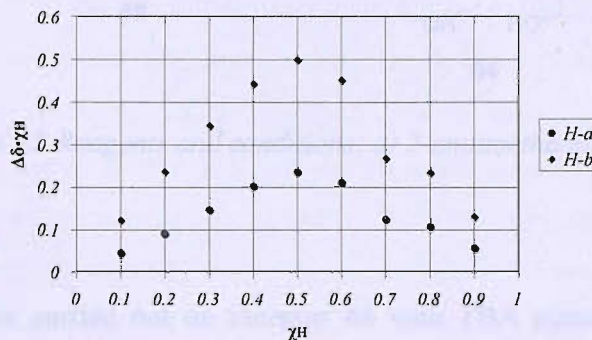


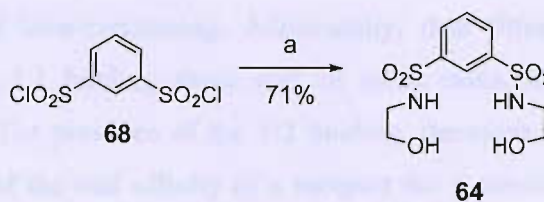
Figure 2.7 Job Plot experiment on receptor **69** with acetate TBA salt in MeCN- d_3 .

For the Job Plot curves the maximum was found to be around $\chi_H = 0.5$. This result is consistent with a binding mode which is predominantly 1:1. This latter result confirmed the overall picture of a predominant 1:1 binding with only a minor 1:2 component for the association between acyclic bis-sulfonamide receptors and carboxylate substrates.^[68,89a,98]

2.6 Synthesis of receptor **64**

In 2002 Yano and co-workers^[89d] synthesised a bis-sulfonamide based receptor with two pendant hydroxyl groups (see § 1.11). The constant reported for this receptor with TBA acetate in MeCN- d_3 was $> 2 \cdot 10^4 \text{ M}^{-1}$ with a 1:1 stoichiometry. This value, however, was calculated on the exclusive basis of a series of minor changes in chemical shift concerning the aromatic $C_2\text{-H}$ proton (**Figure 1.59**), because of the intense broadening of the protons directly involved in hydrogen bonding. Additionally, no more than two equivalents of guest were added to the host solution. With the intention to understand if the presence of hydroxyl groups can be really effective to obtain exclusively the 1:1 stoichiometry, receptor **64** was synthesised in order to investigate its behaviour when more equivalents of guest are added.

Bis-sulfonamide **64** was easily obtained with satisfactory yield from the coupling between the bis-sulfonyl chloride **68** and 2-aminoethanol (**Scheme 2.3**).



Scheme 2.3 Reagents and conditions: a) 2-aminoethanol, DCM.

2.7 Binding studies

Binding studies were carried out on receptor **64** with TBA acetate in MeCN-d_3 . As reported by Yano and co-workers the intense broadening of the *NH* and *OH* signals did not allow following these protons. The aromatic *H-a* was hence monitored (**Figure 2.8**).

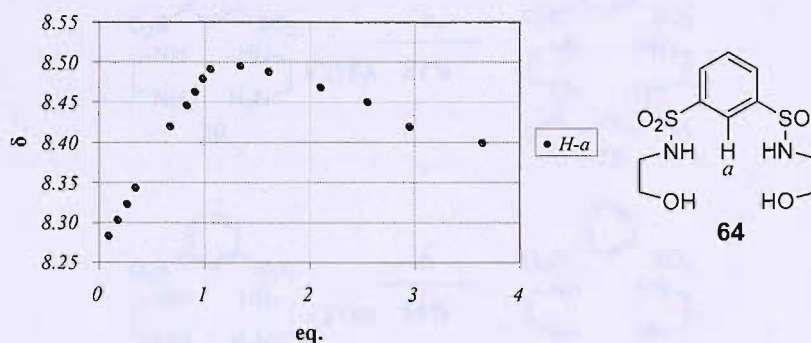


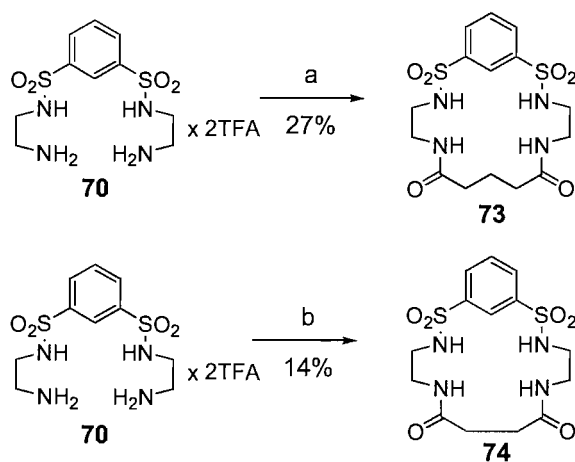
Figure 2.8 Titration curve for *H-a* proton of receptor **64** upon addition of acetate TBA salt in MeCN-d_3 .

The titration curve of the *H-a* proton in receptor **64** followed the general pattern found for receptors **65**, **69** and **71**, with the inversion of the trend clearly occurring at one equivalent of guest added. Therefore, also for the binding between receptor **64** and TBA acetate a 1:2 complex was formed. The data were treated with the 1:2 curve fitting program. Poor fit and nonsensical output parameters (see § 2.2) were found, but again, from the values of the binding constants so obtained ($K_{a1:1} \sim 6400 \text{ M}^{-1}$ and $K_{a1:2} \sim 7 \text{ M}^{-1}$) it was possible to assume a major 1:1 complex formation along with minor 1:2 component.

2.8 Synthesis of macrocyclic receptors 73 and 74

There are some drawbacks in dealing with 1:2 complexes. In fact, in order to obtain accurate constants for a 1:2 association model, several data points are needed, making ^1H

NMR titrations more time-consuming. Additionally, data fitting is more difficult in comparison with the 1:1 binding mode and, in some cases, the constants cannot be reliably obtained.^[83] The presence of the 1:2 binding, therefore, may interfere with the accurate assessment of the real affinity of a receptor for a substrate and a clear-cut 1:1 binding stoichiometry is thus desirable. In order to prevent the receptor from binding an additional guest molecule, it was decided to synthesise macrocyclic receptors. In a macrocyclic system, the bent conformation, plausibly assumed by acyclic receptors in the 1:2 complex (**Figure 2.5**) is less likely. For this reason, the 1:2 complex formation should be inhibited. In order to confirm this hypothesis, macrocycles **73** and **74** were synthesised from bis-amine precursor **70** modifying a procedure described by Picard and co-workers (**Scheme 2.4**).^[99]



Scheme 2.4 Reagents and conditions: a) $\text{ClCO}(\text{CH}_2)_3\text{COCl}$, Et_3N , MeCN ; b) $\text{ClCO}(\text{CH}_2)_2\text{COCl}$, Et_3N , MeCN .

For the synthesis of macrocycles **73** and **74** high dilution and slow addition were used. Macrocycle **73** was obtained with an acceptable yield, in line with other bimolecular macrocyclisation reactions described in the literature.^[73,99,100] Receptor **74** was obtained with lower yield, probably due to steric constraint.

2.9 Binding studies

Macrocycles **73** and **74** were soluble in DMSO only. Binding studies were hence carried out in this solvent. Surprisingly, receptor **74**, upon addition of acetate guest, showed the same behaviour found for acyclic receptors, with an inversion in the trend of the aromatic $C_2\text{-H}$ proton titration curve (**Figure 2.9**).

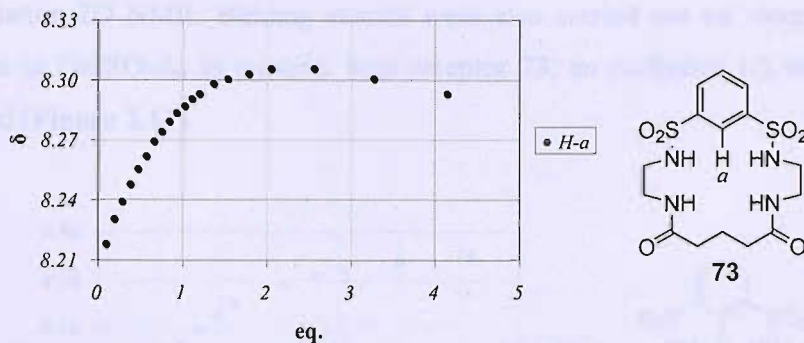


Figure 2.9 Titration curve for *H-a* proton of receptor **73** upon addition of acetate TBA salt in $\text{DMSO-}d_6$.

In this case, however, the phenomenon was less marked compared to the acyclic receptors tested with acetate. This fact seems to indicate that the macrocyclic scaffold effectively weakened the formation of the 1:2 complex, although a direct comparison with the other receptors in $\text{MeCN-}d_3$ was not possible. A 1:1 stoichiometry was found, instead, for receptor **73** with the less basic benzoate TBA salt (**Figure 2.10**).

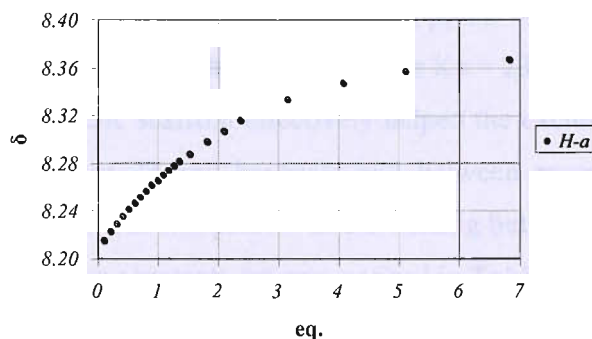


Figure 2.10 Titration curve for *H-a* proton of receptor **73** upon addition of benzoate TBA salt in $\text{DMSO-}d_6$.

In this case, the titration curve of the aromatic $\text{C}_2\text{-H}$ proton followed a typical 1:1 pattern. The association constant was determined from the binding titration curves of the sulfonamidic and amidic *NH* protons, which were directly involved in hydrogen bonding ($\Delta\delta_{\text{max}} \sim 1$ ppm and $\Delta\delta_{\text{max}} \sim 0.6$ ppm for sulfonamidic and amidic protons respectively). The average value was $K_a = 94 \text{ M}^{-1}$, with a error $< 1\%$. For this and other receptors with ambiguous proton signals, amidic and sulfonamidic peaks were assigned by C-H long

range correlation 2D NMR. Binding studies were also carried out on receptor **74** with TBA acetate in DMSO- d_6 . In contrast with receptor **73**, an exclusive 1:1 stoichiometry was obtained (Figure 2.11).

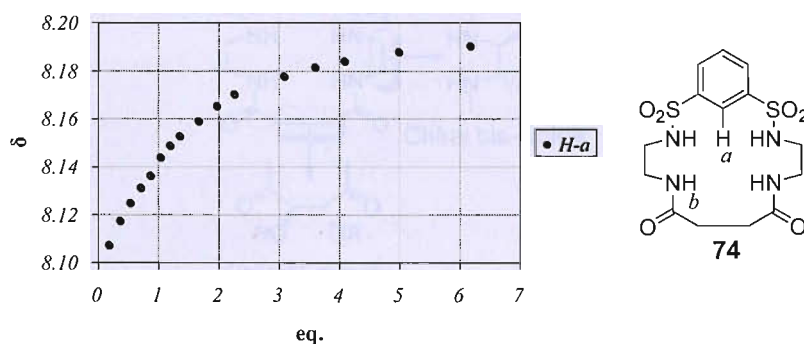


Figure 2.11 Titration curve for *H-a* proton of receptor **74** upon addition of acetate TBA salt in DMSO- d_6 .

The $\Delta\delta_{\max}$ was only ~ 0.1 ppm, less pronounced than in the other cases. Sulfonamidic protons showed intense broadening and could not be followed. The binding constant was thus calculated from amidic *H-b* protons ($\Delta\delta_{\max} \sim 0.6$ ppm). The titration curve showed an excellent fit (error $< 5\%$) and the value obtained was $K_a = 236 \text{ M}^{-1}$.

In conclusion, the macrocyclic scaffold effectively helped the exclusive formation of the 1:1 adduct between receptor **73** and benzoate and between receptor **74** and acetate, although some 1:2 character was still present in the binding between the more flexible **73** and acetate. The values of the constants are summarised in Table 2.5.

Host	Guest	$K_a \text{ (M}^{-1}\text{)}$	Error	Solvent
73	TBAOBz	94	$< 1\%$	DMSO- d_6
74	TBAOAc	236	$< 5\%$	DMSO- d_6

Table 2.5

2.10 Chiral macrocyclic receptors

Simple receptors **73** and **74** showed good binding towards carboxylates in competitive DMSO- d_6 . In order to investigate if this macrocyclic scaffold was suitable for enantioselective recognition, chiral groups had to be introduced. Moreover, better solubility in less competitive solvents was desirable, in order to amplify host-guest

interactions, increasing the chances of discrimination. With the intent to satisfy these conditions, modifications of receptors **73** and **74** were conceived (**Figure 2.12**).

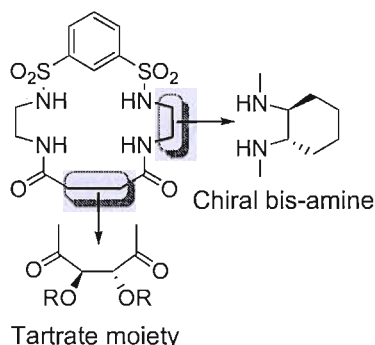
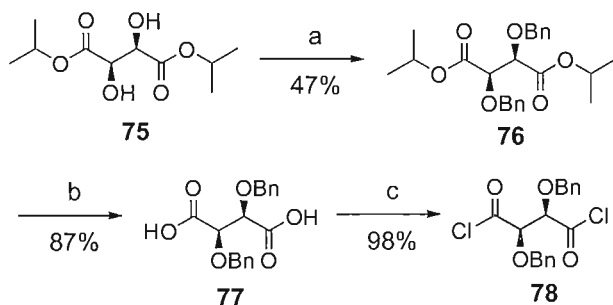


Figure 2.12 Introduction of chirality in a bis-sulfonamide macrocyclic scaffold.

The introduction of a chiral cyclohexane moiety on the side ‘arms’, by mean of the commercially available chiral 1,2-bis-aminocyclohexane, can greatly increase the solubility and help the preorganisation of the receptor reducing the number of possible conformations. Chirality can be introduced at the ‘southern’ end as well, by an opportunely protected tartrate moiety, derived from inexpensive starting materials.

2.11 Synthesis of macrocycle **79**

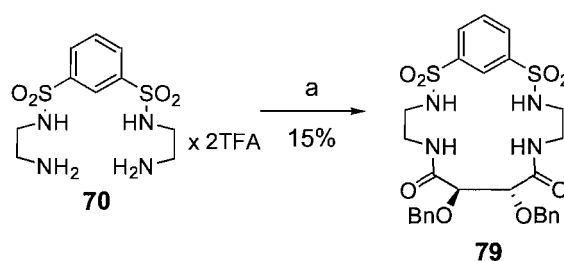
The introduction of a tartrate derived moiety was considered first. In order to follow the successful route which led to receptors **73** and **74**, tartaric acid bis-chloride **78** was prepared by standard methods (**Scheme 2.5**).



Scheme 2.5 Reagents and conditions: a) NaH, THF; *n*-Bu₄I cat., 18-crown-6 cat., BnBr;

b) 60:40 1,4-dioxane/1 M LiOH; c) (COCl)₂, DMF cat., DCM.

Commercially available ester **75** was benzylated with acceptable yield following a procedure by Yamamoto and co-workers.^[101] Bis-ether **76** was hydrolysed with a standard method.^[102] Reactive tartaric acid bis-chloride **78** was eventually obtained following a procedure by Marchese and co-workers.^[103] The benzyl group was chosen for three reasons. It displays, in fact, good lipophilicity, favouring solubility. It is bulky, and that may increase the chance of enantioselectivity by selective steric repulsion. Benzyl ethers, moreover, are relatively easy to prepare, compared, for example, with *t*-butyl ethers.^[104] Macrocycle **79** was synthesised by coupling bis-amine **70** with tartaric acyl bis-chloride **78** with a yield comparable to the one obtained for the parent macrocycle **74** (Scheme 2.6).



Scheme 2.6 Reagents and conditions: a) **78**, Et_3N , MeCN.

High dilution and slow addition were used also for this transformation.

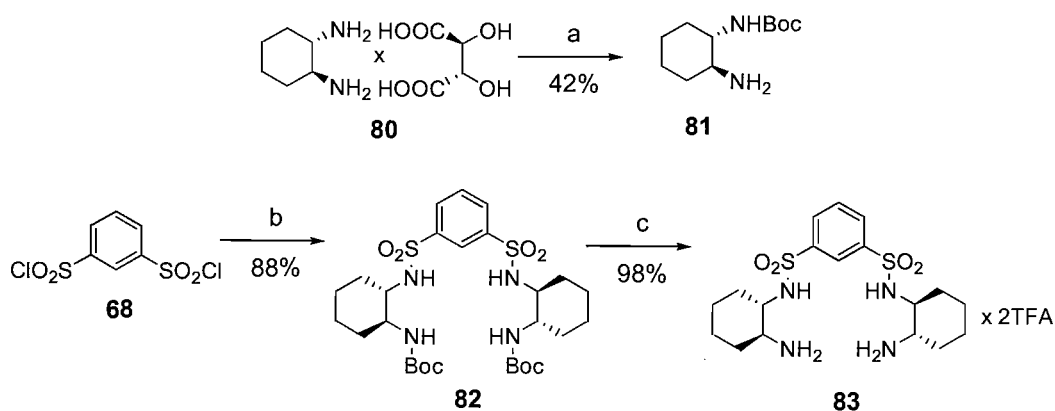
2.12 Binding studies

Unfortunately receptor **79** was neither soluble in $CDCl_3$ nor in $MeCN-d_3$. Binding studies were, therefore, carried out in $DMSO-d_6$. The two enantiomers *N*-Ac-Phe were used as guests. In both cases, all proton signals of macrocycle **79** remained essentially unperturbed upon addition of the guest solution, indicating that no association was occurring.

2.13 Synthesis of macrocyclic receptors **84** and **85**

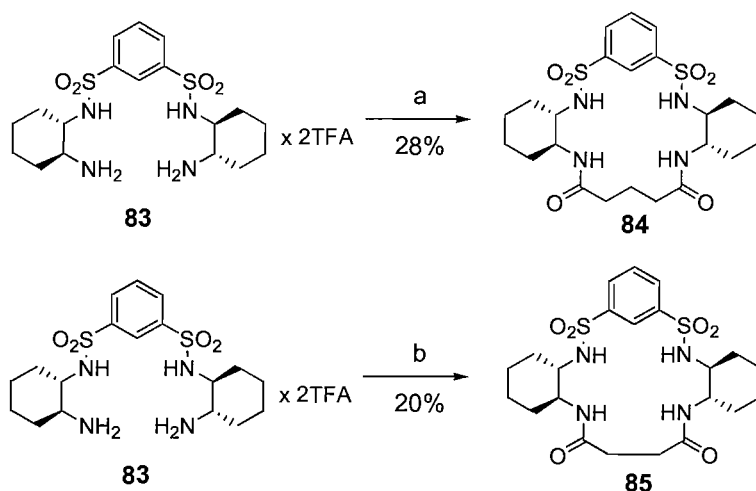
The incorporation of a tartrate based moiety failed to increase the solubility and did not produce chiral recognition. It was, therefore, decided to introduce two chiral cyclohexane rings on the side 'arms' to achieve these goals (Figure 2.12). Macrocycles **84** and **85** were, therefore, conceived. The synthesis was achieved by following the reliable route

established for the preparation of receptors **73** and **74**. The common precursor **83** was obtained easily in three steps (**Scheme 2.7**).



Scheme 2.7 Reagents and conditions: a) Boc_2O , K_2CO_3 , 90:10 $\text{EtOH}/\text{H}_2\text{O}$; b) **81**, Et_3N , DCM ; c) 80:20 DCM/TFA .

Mono-protected bis-amine **81** was obtained with acceptable yield from salt **80** modifying a literature procedure.^[105] Intermediate **82** was then prepared in high yield by coupling bis-sulfonyl chloride **68** with mono-Boc amine **81**. Deprotection was almost quantitative. Bis-amine **83** was finally coupled with the appropriate bis-chloride to yield macrocycles **84** and **85** (**Scheme 2.8**).



Scheme 2.8 Reagents and conditions: a) $\text{ClCO}(\text{CH}_2)_3\text{COCl}$, Et_3N , MeCN ; b) $\text{ClCO}(\text{CH}_2)_2\text{COCl}$, Et_3N , MeCN .

The same conditions used in the synthesis of macrocycles **73** and **74** were employed, with slightly improved yields. Both macrocycles were soluble in MeCN as well as in chloroform and DCM.

2.14 Binding studies on macrocycle **84**

Binding studies were carried out on macrocycle **84** with TBA acetate in CDCl₃ in order to assess its affinity towards carboxylates. In this case the $\Delta\delta_{\max}$ of the C₂-H aromatic proton was negligible (~ 0.05 ppm) and thus it was not taken into account. The signal of the sulfonamidic protons underwent intense broadening and could not be followed. The amidic protons signal, conversely, could be followed and showed a very large $\Delta\delta_{\max}$ (~ 2.5 ppm), consistent with hydrogen bonding (**Figure 2.13**).

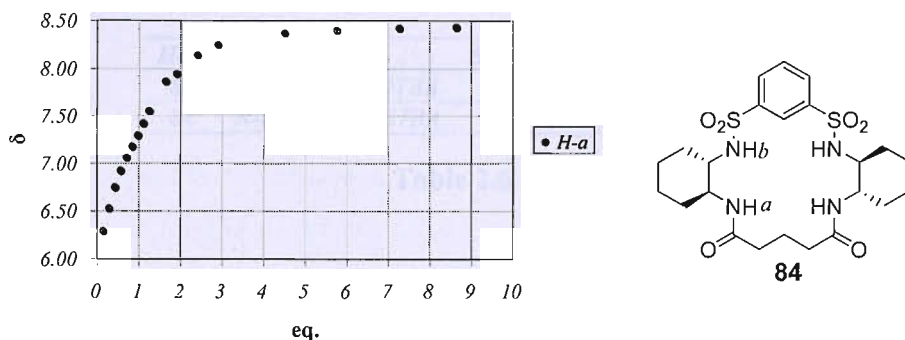


Figure 2.13 Binding titration curve of receptor **84** upon addition of acetate TBA salt in CDCl₃.

The titration curve showed an acceptable fit with the 1:1 treating program and the constant calculated was $K_a = 758 \text{ M}^{-1}$. The error was estimated with the computer program EQNMR^[106] and an error value of 9% was found. Despite the high $\Delta\delta_{\max}$, however, the binding constant was relatively low, considering that the titration was performed in the non-competitive solvent CDCl₃.

In order to test receptor **84** for enantioselectivity, binding studies were carried out with the two enantiomers of *N*-Boc-phenylalanine. Both amidic and sulfonamidic protons could be followed in this case. A large $\Delta\delta_{\max}$ was registered also for the sulfonamidic proton (~ 1.8 ppm). Disappointingly, the titration curves were very similar for the two enantiomers and poor fit resulted from the 1:1 treating program (**Figure 2.14**).

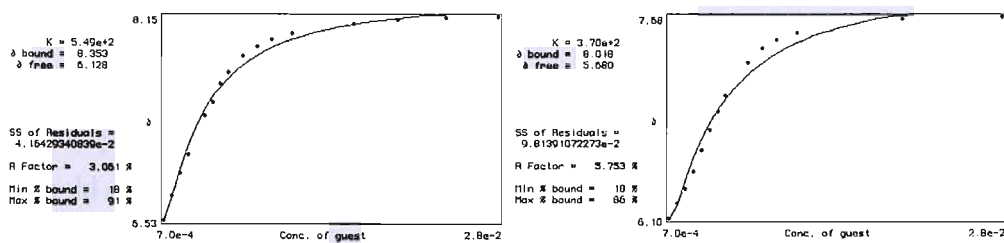


Figure 2.14 Binding titration curves of receptor **84** upon addition of *N*-Boc-*L*-Phe TBA salt. Curves referring to amidic (left) and sulfonamidic (right) protons.

In **Figure 2.14** are shown the curves relative to the titration with *N*-Boc-*L*-Phe. Almost identical profiles were obtained with the *L* enantiomer. Binding constants were calculated as the average between the two values, and, probably due to the poor fit, they were affected by large errors (**Table 2.6**).

Host	Guest	K_a (M^{-1})	Error	Solvent
84	<i>N</i> -Boc- <i>L</i> -Phe-OTBA	460	20%	$CDCl_3$
84	<i>N</i> -Boc- <i>D</i> -Phe-OTBA	406	17%	$CDCl_3$

Table 2.6

Because of the high errors calculated, the values obtained for the constants have to be taken as rough indications. Nevertheless, the very similar values obtained for the two enantiomers along with almost superimposable titration curves, suggested that no appreciable chiral recognition was present.

A possible explanation for the relatively poor affinity of receptor **84** towards carboxylates in $CDCl_3$ may be found in an 'alternate' conformation that macrocycle **84** can plausibly adopt (**Figure 2.15**).

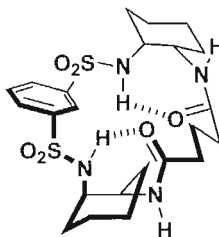


Figure 2.15 Possible 'alternate' conformation of receptor **84** in $CDCl_3$.

Internal hydrogen bonding, favoured in non-polar $CDCl_3$, can stabilise this badly preorganised conformation,^[65] in which the *NH* bonds are pointing alternatively 'up' and

'down', resulting in a lack of synergy of the hydrogen donor moieties. In this case, because of the rigidity of the cyclohexane rings, a significant energy penalty must be paid by the receptor in order to rearrange towards a conformation more suitable for binding. This would explain the low constants obtained in CDCl_3 .

Examples of this kind of conformation are known in the literature. An 'alternate' motif, built on the rigid 1,2-bis-aminocyclohexane moiety, was used by Still and co-workers^[107] and, more recently, by Fang and co-workers^[108] for the recognition of small peptides (Figure 2.16).

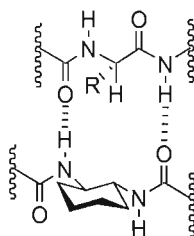


Figure 2.16 1,2-bis-aminocyclohexane moiety as building block for peptide receptors.

In order to investigate more this aspect, binding studies were carried out on receptor **84** with TBA acetate in $\text{MeCN-}d_3$. Sulfonamidic protons showed intense broadening and, thus, only amidic protons were followed (Figure 2.17).

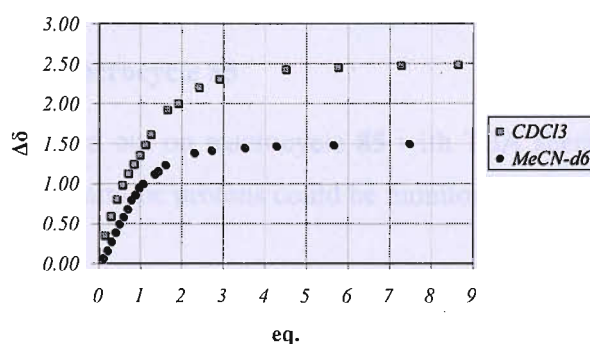


Figure 2.17 Binding titration curves of receptor **84** upon addition of acetate TBA salt in CDCl_3 and $\text{MeCN-}d_3$.

In comparison with the titration curve obtained in CDCl_3 , the $\Delta\delta_{\text{max}}$ was lower, but saturation was reached after fewer equivalents of guests. For this reason, a higher binding constant was found. The curve showed a good fit (error = 6%) with the 1:1 treating program, and the constant calculated was $K_a = 1.83 \cdot 10^3 \text{ M}^{-1}$.

In case of simple receptors, strong binding constants are obtained preferably in non-polar solvents, while a substantial depletion of the binding occurs in more competitive media.^[109] In a complex macrocyclic receptor, with multiple hydrogen bonding donors and acceptors, however, an internal hydrogen bonding network can stabilise conformations not suitable for binding, especially in non-polar media. The interaction with the guest may not be strong enough in order to break such network. Better binding can occur in more polar media. The interaction with the solvent molecules, in fact, can contribute to disrupt the internal hydrogen bonding, leaving the binding site more accessible to the substrate. These were the findings of Kilburn and co-workers when they studied a complex bis-thiourea macrocyclic receptor for bis-carboxylates (see § 1.10).^[82] According to the latter discussion, the fact that a higher binding constant was found in the more competitive MeCN-*d*₃ corroborates the hypothesis that macrocycle **84**, in CDCl₃, is assuming preferably a conformation poorly suitable for binding, due to stabilisation by internal hydrogen bonding.

The results of the binding studies on macrocycle **84** with TBA acetate are summarised in Table 2.7.

Host	Guest	K_a (M^{-1})	Error	Solvent
84	TBAOAc	758	9%	CDCl ₃
84	TBAOAc	1830	6%	MeCN- <i>d</i> ₃

Table 2.7

2.15 Binding studies on macrocycle **85**

Binding studies were carried out on macrocycle **85** with TBA acetate in CDCl₃. In this case both amidic and sulfonamidic protons could be monitored (Figure 2.18).

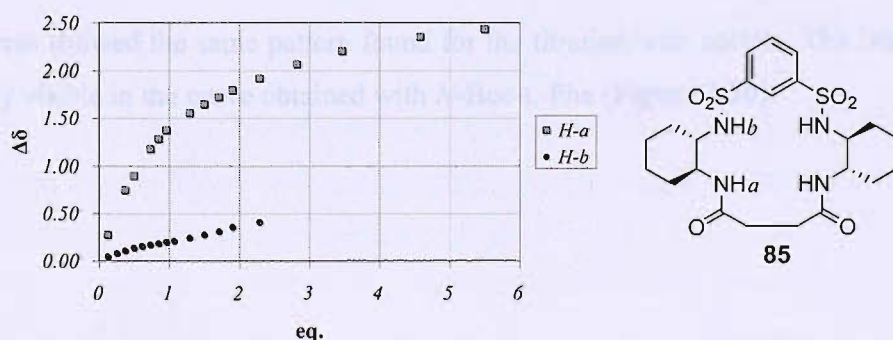


Figure 2.18 Binding titration curves of receptor **85** upon addition of acetate TBA salt in CDCl₃.

High $\Delta\delta_{\max}$ resulted from following amidic protons, while very low $\Delta\delta_{\max}$ was registered for sulfonamidic protons. This fact seems to indicate that sulfonamidic *NH* protons are less accessible for binding, contrary to the amidic *NH* protons. The curves could neither be fitted with the 1:1 nor with the 1:2 binding model. The shape of the profiles, however, seems to reveal the formation of a 1:2 complex. After the addition of ~ 1 equivalent of guest, a change in the slope for the curves was registered without reaching saturation. Further evidence was added by the presence of a revelatory ‘stall’ point in the titration curve of the sulfonamidic protons (**Figure 2.18 H-b**). Gale and co-workers showed that a ‘stall’ point may indicate the formation of a 1:1 complex which is suddenly followed by association of another molecule of guest resulting in a conformational change.^[110] Binding studies with the two enantiomers of *N*-Boc-Phe were carried out in order to see if some enantioselectivity was displayed by receptor **85**. Disappointingly, almost identical titration curves were obtained (**Figure 2.19**).

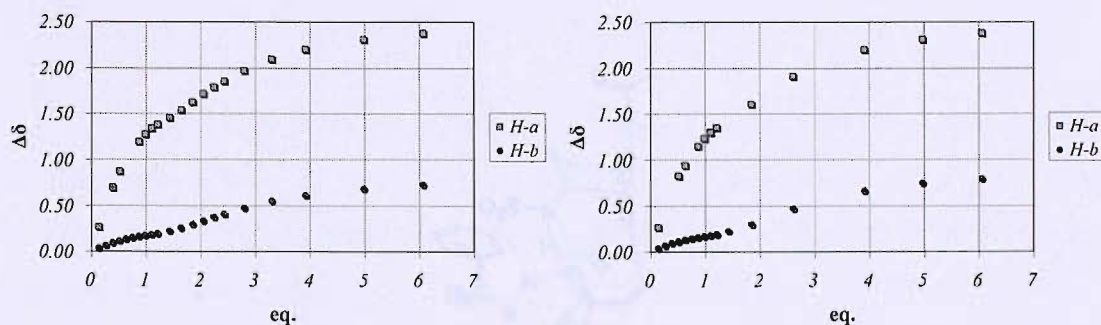


Figure 2.19 Binding titration curves of receptor **85** upon addition of *N*-Boc-*L*-Phe TBA salt (left) and *N*-Boc-*D*-Phe TBA salt (right).

The curves showed the same pattern found for the titration with acetate. The ‘stall’ point is clearly visible in the curve obtained with *N*-Boc-*L*-Phe (**Figure 2.20**).

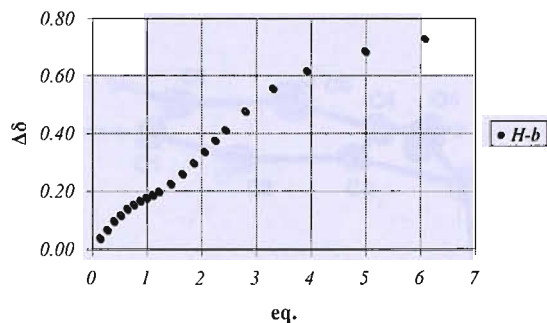


Figure 2.20 Titration curve for sulfonamidic protons of receptor **85** upon addition of *N*-Boc-*L*-Phe TBA salt.

The low $\Delta\delta_{\max}$ of the sulfonamidic protons and the formation of the 1:2 complex can be both explained by the presence of the ‘alternate’ conformation previously described. Moreover, receptor **85**, due to the smaller size, is likely more constrained than receptor **84**. For this reason, reorganisation can be more difficult and, therefore, the effects of this particular conformation may result accentuated (**Figure 2.21**).

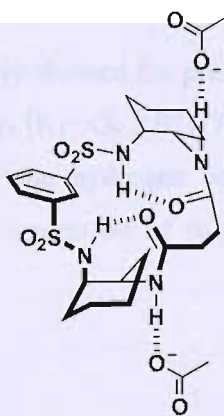


Figure 2.21 Possible ‘alternate’ conformation of receptor **85** in CDCl_3 .

According to this model, sulfonamidic *NH*'s are involved in strong internal hydrogen bonding, while amidic protons are pointing towards opposite directions, with the possibility of interaction with two molecules of guest.

Substantial evidence in favour of the ‘alternate’ conformation arose from the crystal structure of macrocycle **85**, which clearly showed that *NH* bonds are pointing alternatively ‘up’ and ‘down’.

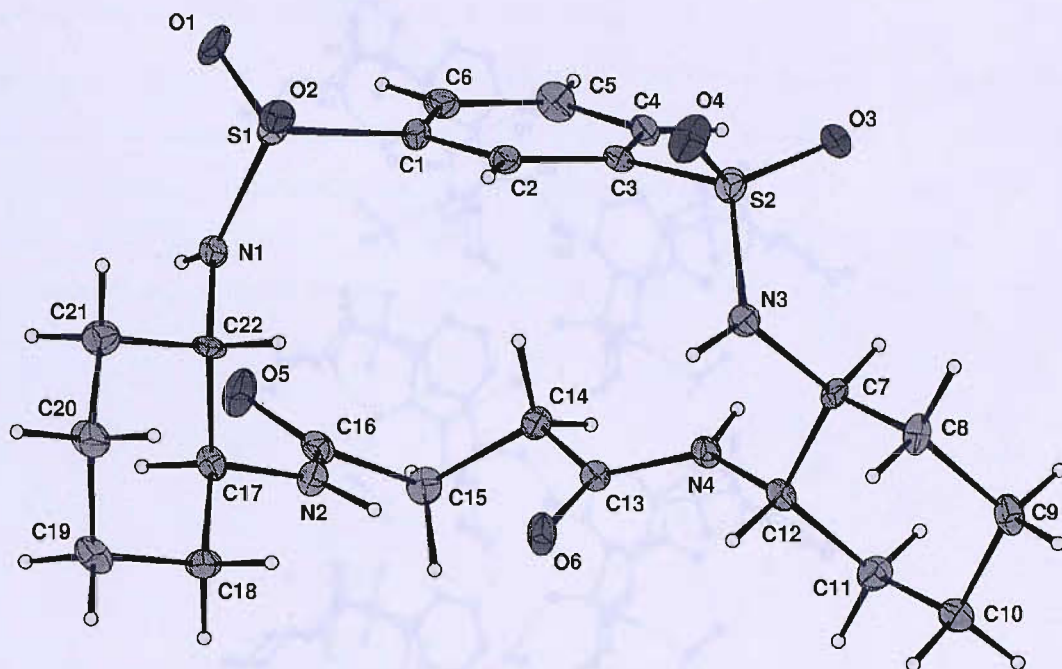


Figure 2.22 Crystal structure of macrocycle **85**. Thermal ellipsoids drawn at the 30% probability level, solvent not shown.

Besides, crystallographic data clearly showed the presence of internal hydrogen bonding, with the distances between $N_1H \cdots O_5$ [$N_1 \cdots O_5$ 2.971(7) Å] and $N_2H \cdots O_6$ [$N_2 \cdots O_6$ 2.777(6) Å] being in the typical range of the hydrogen bonding interactions. N_3H and N_4H displayed hydrogen bonding with molecules of solvent (MeOH) [$N_3 \cdots O_8$ 2.795(6) Å, $N_4 \cdots O_7$ 2.886(6) Å] (**Figure 2.23**).

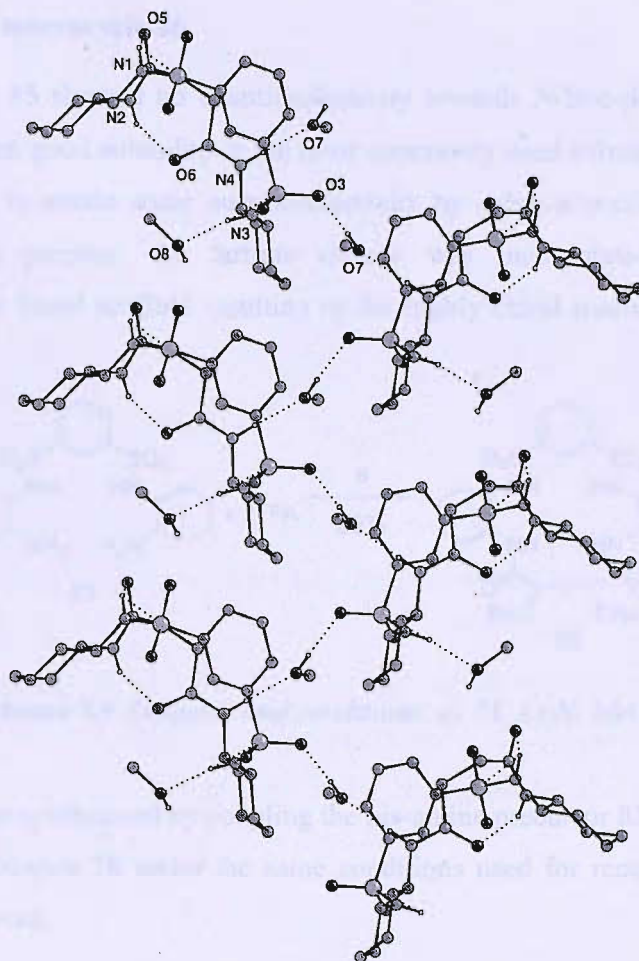


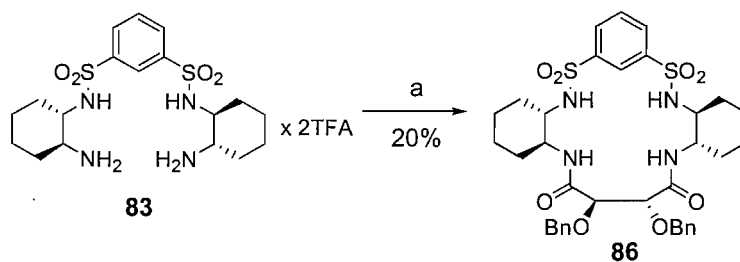
Figure 2.23 Extended structure of macrocycle **85** showing the hydrogen bonding network.

Although a conformation adopted by a particular molecule in the solid state can undergo dramatic changes upon solvation, the structure of receptor **85** seems to be quite rigid and, hence, the crystal structure showed in **Figure 2.22** might represent realistically the conformation assumed in a non-polar solvent, such as CDCl_3 .

Binding studies, finally, were carried out on receptor **85** with TBA acetate in $\text{MeCN-}d_3$. The profile of titration curve of the amidic protons seemed to indicate the presence of a 1:1 binding stoichiometry. The curve gave a reasonable fit (11% of error) with the 1:1 treating program. Again, as in the case of receptor **84**, some improvement was obtained performing the titration in $\text{MeCN-}d_3$. The binding constant ($K_a = 989 \text{ M}^{-1}$), however, resulted considerably lower than the one obtained with macrocycle **84**, probably because of the higher rigidity.

2.16 Synthesis of macrocycle **86**

Receptors **84** and **85** showed no enantioselectivity towards *N*-Boc-phenylalanine. They displayed, however, good solubility in the most commonly used solvents. For this reason, a further attempt to obtain some enantioselectivity by using a similar framework was made. With this purpose, the tartrate moiety was incorporated in the 1,2-bis-aminocyclohexane based scaffold resulting in the highly chiral macrocycle **86** (Scheme 2.9).



Scheme 2.9 Reagents and conditions: a) **78**, Et_3N , MeCN .

Macrocycle **86** was synthesised by coupling the bis-amine precursor **83** with the available tartaric acid bis-chloride **78** under the same conditions used for receptor **79**. The yield was slightly improved.

2.17 Binding studies

Binding studies were carried out in CDCl_3 with the two enantiomers of *N*-Boc-phenylalanine. During the titrations, amidic and sulfonamidic protons remained almost unperturbed upon addition of both guests. A ^1H NMR spectrum of the host was then recorded in presence of one equivalent of acetate, in order to check if the previous result was depending on the size of the guest. Again, no change was observed (Figure 2.24).

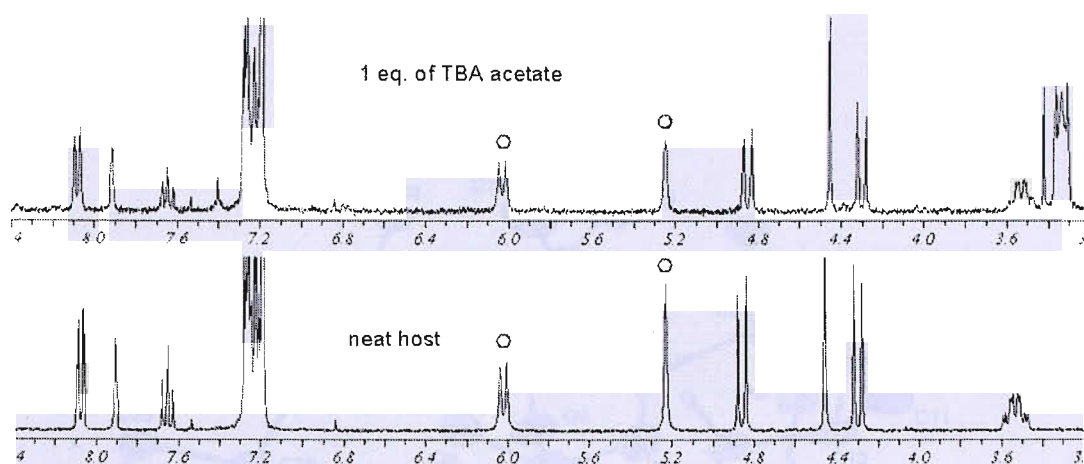


Figure 2.24 ^1H NMR spectrum of neat macrocycle **86** and after addition of one equivalent of acetate TBA salt. Spectra recorded in CDCl_3 .

The absence of binding can be explained again with an 'alternate' conformation assumed by the host, this time with additional unfavourable steric hindrance caused by two bulky benzyl groups. These suppositions seem to be confirmed by the crystal structure of macrocycle **86** (Figure 2.25).

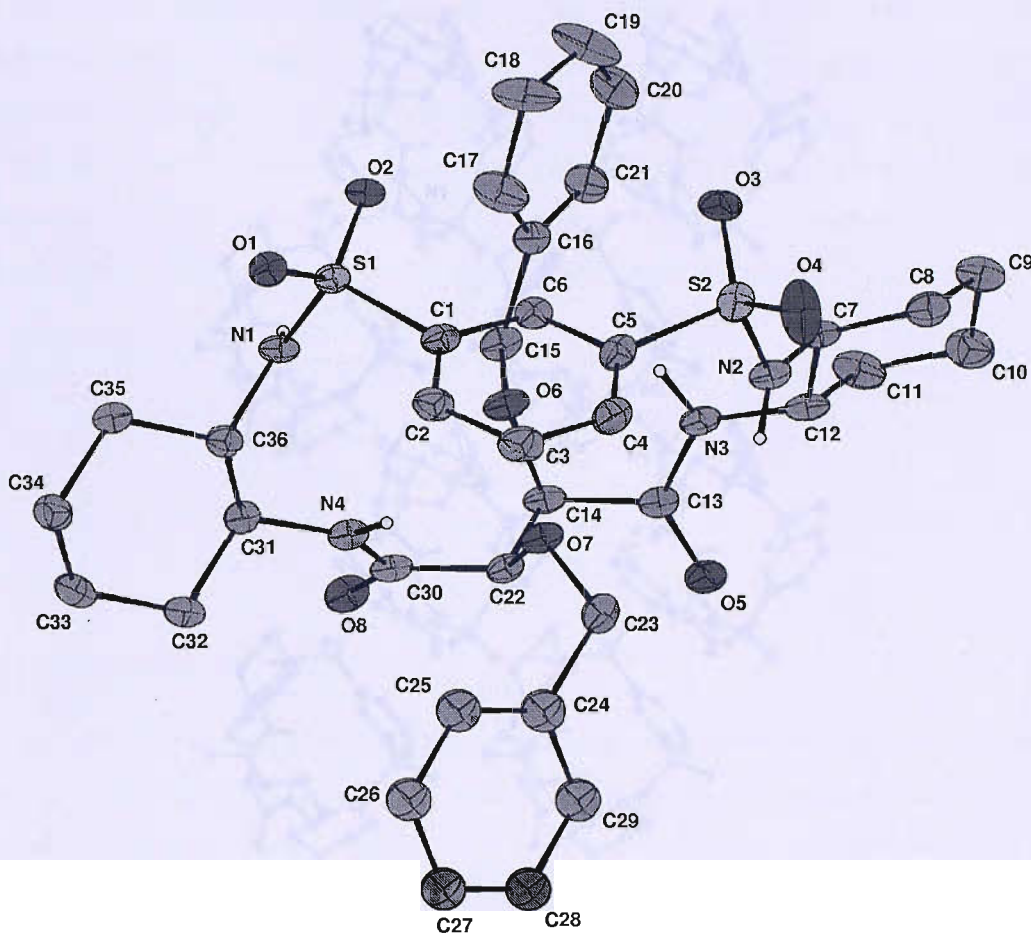


Figure 2.25 Crystal structure of macrocycle **86**. Thermal ellipsoids drawn at the 30% probability level, non acidic hydrogens omitted for clarity.

From the crystal structure emerged clearly that the *NH* bonds were pointing in opposite directions, causing a lack of synergy towards a possible anionic guest. The extended structure showed the presence of an intermolecular hydrogen bonding network based on the $N_1H \cdots O_1$ [$N_1 \cdots O_1$ 3.142(5) Å] and $N_2H \cdots O_5$ [$N_2 \cdots O_5$ 2.842(5) Å] interactions between adjacent molecules (**Figure 2.26**).

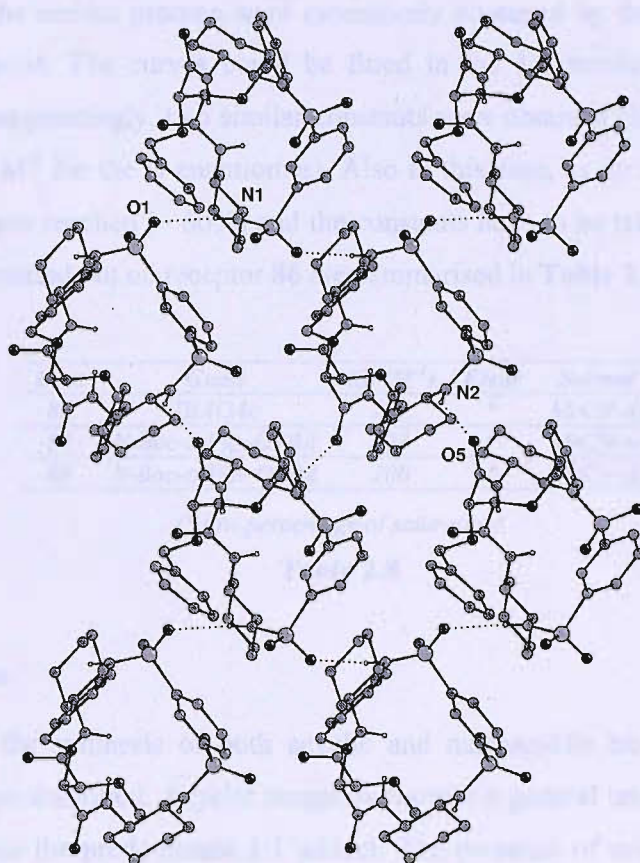


Figure 2.26 Extended structure of macrocycle **86** showing the hydrogen bonding network.

Binding studies were then performed with acetate in $\text{MeCN-}d_3$. In this case, broadening of the sulfonamidic protons was observed, while a significant $\Delta\delta_{\text{max}}$ resulted from following the amidic protons (~ 1.4 ppm). The curve showed an excellent fit with the 1:1 titrating program and the constant was $K_a = 255 \text{ M}^{-1}$, although at the end of this titration only $\sim 60\%$ of the host resulted bound in the complex. In order to obtain a reliable constant, the data should cover a range of about 20–75% of complexed host.^[96,97,111,112] The value obtained, hence, has to be taken only as an indication.

Although poor binding was showed, the binding was better than in CDCl_3 . Again, the affinity towards acetate was enhanced by a more competitive solvent. As for receptor **84**, this fact suggests that receptor **86** in the non-competitive CDCl_3 is assuming a conformation not suitable for binding, due to strong intramolecular hydrogen bonding.

Binding studies were then carried out in $\text{MeCN-}d_3$ with the two enantiomers of *N*-Boc-phenylalanine in order to see if the various chirophore moieties displayed by receptor **86** could induce some chiral recognition. Only sulfonamidic protons could be followed, due

to the fact that the amidic protons were extensively obscured by the aromatic peaks of both host and guest. The curves could be fitted in the 1:1 treating program with an excellent fit. Disappointingly, two similar constants were obtained ($K_a = 223 \text{ M}^{-1}$ for the L and $K_a = 200 \text{ M}^{-1}$ for the D enantiomer). Also in this case, as for acetate, only a poor saturation level was reached ($\sim 60\%$) and the constants have to be taken as an indication. Binding studies carried out on receptor **86** are summarised in **Table 2.8**.

<i>Host</i>	<i>Guest</i>	<i>K_a (M⁻¹)</i>	<i>Error</i>	<i>Solvent</i>
86	TBAOAc	225	*	MeCN- <i>d</i> ₃
86	<i>N</i> -Boc-L-Phe-OTBA	223	*	MeCN- <i>d</i> ₃
86	<i>N</i> -Boc-D-Phe-OTBA	200	*	MeCN- <i>d</i> ₃

(* low percentage of saturation)

Table 2.8

2.18 Conclusions

In this chapter, the synthesis of both acyclic and macrocyclic bis-sulfonamide based receptors has been described. Acyclic receptors showed a general tendency to form a 1:2 complex alongside the predominant 1:1 adduct. The presence of multiple equilibria did not allow the correct assessment of the affinity towards carboxylates. It was, therefore, decided to overcome this problem with the synthesis of macrocyclic receptors.

Macrocycle **73** still showed some 1:2 character in presence of acetate, although a clear 1:1 binding was obtained with benzoate. A clear-cut 1:1 behaviour was also showed by macrocycle **74** with acetate. Both macrocycles were poorly soluble and hence binding studies were limited to DMSO-*d*₆.

Chiral macrocycles **84**, **85** and **86**, built from 1,2-bis-aminocyclohexane, showed poor affinity for carboxylates, especially in CDCl₃, and no enantioselectivity was found. These results were explained with the hypothesis of an 'alternate' conformation preferably assumed by the receptor. Such conformation, unsuitable for binding, is likely stabilised by strong internal hydrogen bonding. The rigidity of the cyclohexane rings, moreover, can further penalise the reorganisation towards a conformation more favourable for binding. This hypothesis was corroborated by the crystal structure of macrocycles **85** and **86** and by the improved binding obtained in the more competitive MeCN-*d*₃.

The most relevant results obtained from the binding studies described in this chapter are summarised in **Table 2.9**.

Host	Guest	K_a (M^{-1})	Error	Solvent
73	TBAOBz	94	< 1%	DMSO- d_6
74	TBAOAc	236	< 5%	DMSO- d_6
84	TBAOAc	758	9%	$CDCl_3$
	TBAOAc	1830	6%	MeCN- d_3
	<i>N</i> -Boc- <i>L</i> -Phe-OTBA	460	20%	$CDCl_3$
	<i>N</i> -Boc- <i>D</i> -Phe-OTBA	406	17%	
85	TBAOAc	989	11%	MeCN- d_3
86	TBAOAc	225	*	MeCN- d_3
	<i>N</i> -Boc- <i>L</i> -Phe-OTBA	223	*	
	<i>N</i> -Boc- <i>D</i> -Phe-OTBA	200	*	

(* low percentage of saturation)

Table 2.9

Chapter III

A New Class of Bis-Sulfonamide Based Macrocycles

3.1 Introduction

For macrocycles **84**, **85** and **86** carboxylate binding was disfavoured by internal hydrogen bonding. The rigidity of the cyclohexane rings, moreover, was a serious impediment to a rearrangement towards a conformation more suitable for binding. In order to obtain better results, a new class of macrocycles, with increased flexibility, was conceived. With this aim, it was decided to build a scaffold incorporating amino acid residues on the side 'arms'. Apart from rendering the structure more flexible, this strategy consents the introduction of chirality from inexpensive starting materials and allows tunability of the substituents, depending on the amino acid side chain (**Figure 3.1**).

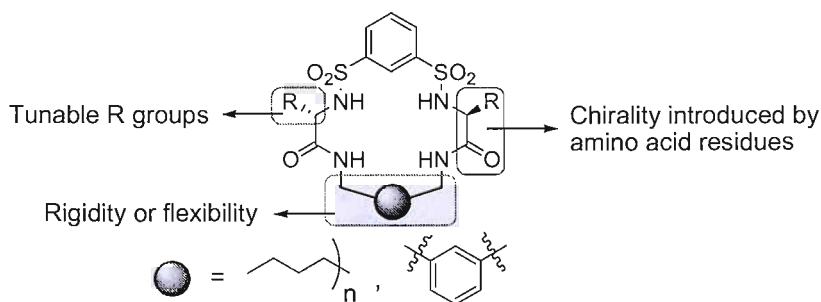


Figure 3.1 General scheme of a bis-sulfonamide based macrocycle incorporating amino acid residues.

The two side 'arms' can be tied up by a flexible or a rigid spacer, in order to study the effect on the preorganisation. The fact that hydrogen bonding donors and acceptors are arranged in a different set up, in comparison with the macrocycles previously described, can be seen as another advantage (**Figure 3.2**).

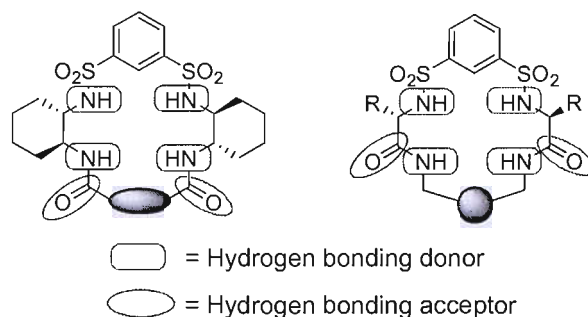


Figure 3.2 Disposition of hydrogen donors and acceptors for two different classes of bis-sulfonamide based macrocycles.

In this manner, the formation of potential intramolecular interactions might result disfavoured.

3.2 Synthesis of macrocycles **87** and **88**

In order to test whether the general scaffold shown in **Figure 3.1** could be suitable for carboxylate binding, two macrocycles were first conceived (**Figure 3.3**).

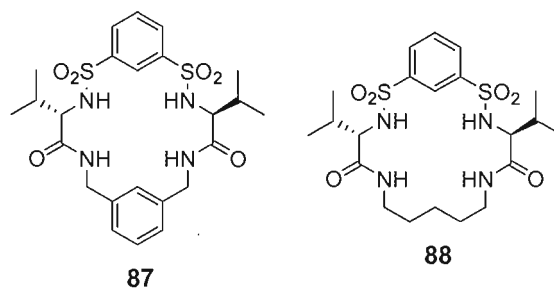
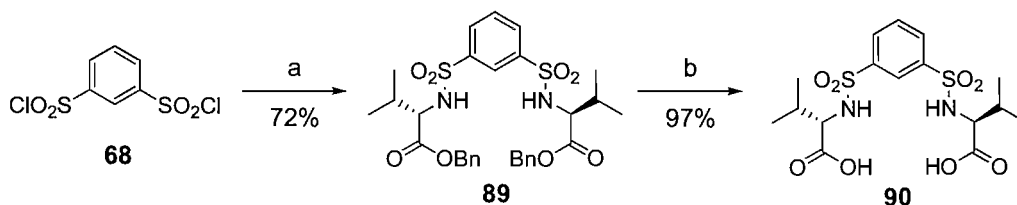


Figure 3.3 Bis-sulfonamide based receptors with side 'arms' derived from valine.

Macrocycle **87** differs from macrocycle **88** only for the more rigid spacer at the 'southern' end. Both receptors are built from valine; this particular amino acid was chosen for different reasons. The isopropyl groups can increase the solubility in less polar solvents. They are reasonably bulky and, for this reason, they might play an active role in enantioselective recognition as steric barriers. Furthermore, only a small interaction is likely to occur with small carboxylates, such as acetate or benzoate, giving the possibility of assessing the 'pure' interaction between the carboxylate anion and the general scaffold

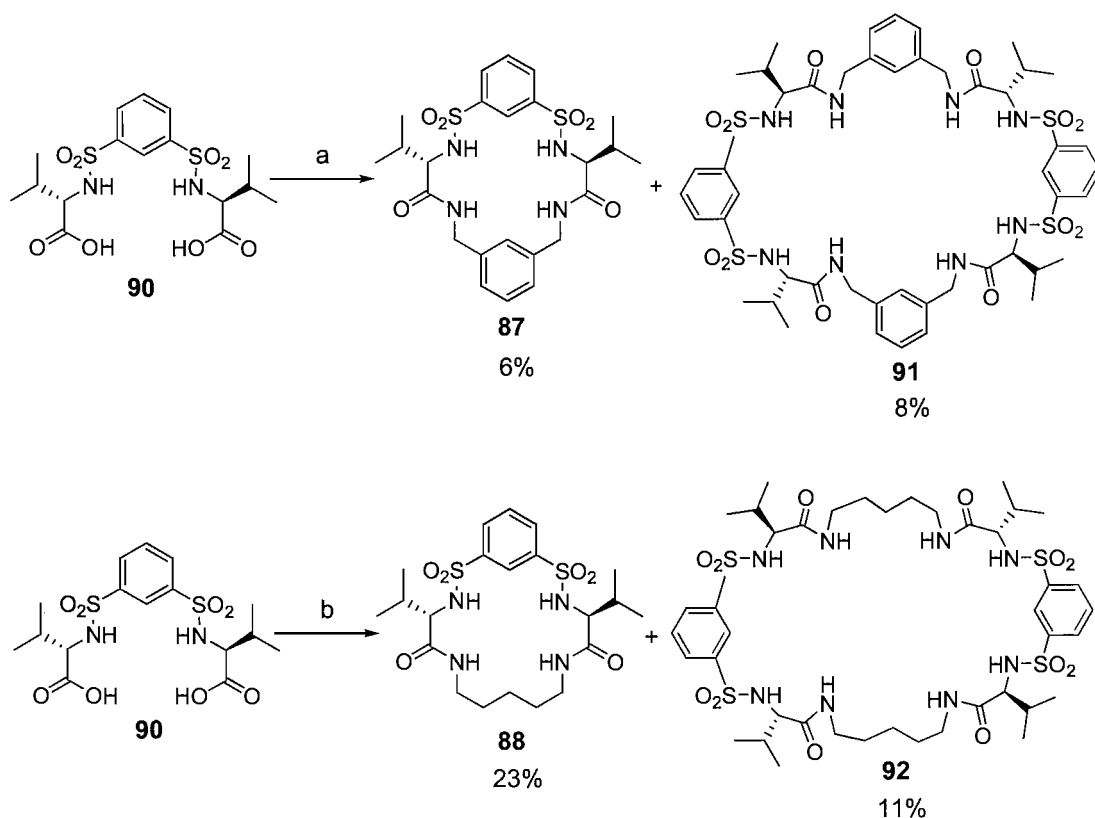
shown in **Figure 3.1**. The fact that the peaks of the isopropyl protons fall in a region well away from the amidic and sulfonamic signals, finally, was also considered positively. The synthesis of the common precursor bis-acid **90** was accomplished easily in two steps from bis-sulfonyl chloride **68** (**Scheme 3.1**).



Scheme 3.1 Reagents and conditions: a) *H*-Val-OBn-TsOH, Et₃N, DCM; b) Pd/C 10% cat., H₂, MeOH.

The bis-ester **89** was obtained in good yield by coupling bis-sulfonyl chloride **68** with the commercial L-valine benzyl ester.^[94] Deprotection by catalytic hydrogenolysis yielded bis-acid **90** almost quantitatively.^[113]

For the synthesis of receptors **87** and **88** the critical macrocyclisation step was carried out using CDI as coupling reagent. The choice of this activating agent was determined by the clean conditions associated with this kind of coupling, due to the absence of additives.^[114] In some cases macrocyclic products can be obtained only in traces and, for this reason, they are difficult to isolate. At this regard, clean conditions can be particularly advantageous. Moreover, an example of macrocyclisation with CDI was known from the literature.^[100c] Bis-acid **90** was thus coupled with *m*-xylylenediamine and with 1,5-diaminopentane (**Scheme 3.2**).



Scheme 3.2 Reagents and conditions: a) CDI, THF; 1,5-diaminopentane; b) CDI, THF; *m*-xylylenediamine, Et_3N .

Macrocycle **88** was obtained with an acceptable yield for this type of transformation, while macrocycle **87** was isolated with a very poor yield. Both reactions were accompanied by formation of [2+2] macrocycles (**91** and **92**, **Scheme 3.2**). The reactions were performed batchwise. High dilution and slow addition were also tested, but no yield improvement was found. The identification of macrocycles **87-88** and **91-92** was made by the analysis of the isotopic patterns in the ES-MS spectra.^[115] Subsequently, X-ray crystal structures of macrocycles **87**, **88** and **92** were obtained. Crystal structure of receptor **92** is shown in **Figure 3.4**. Crystal structures of macrocycles **87** and **88** will be discussed in § 3.10.

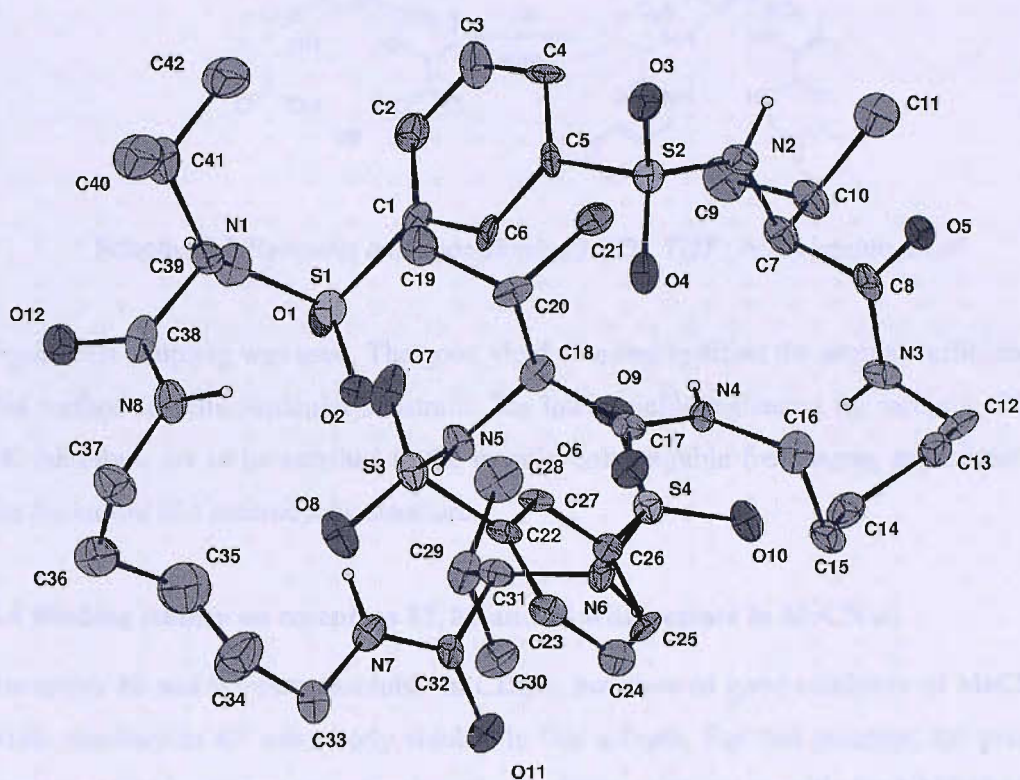
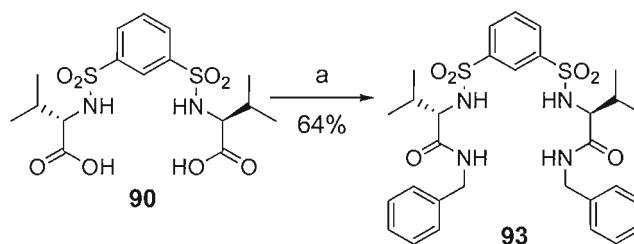


Figure 3.4 Crystal structure of macrocycle **92**. Thermal ellipsoids drawn at the 30% probability level, non acidic hydrogens omitted for clarity.

Crystallographic data showed extensive intramolecular hydrogen bonding [$N_3 \cdots O_{10}$ 3.014(11) Å, $N_4 \cdots O_4$ 3.410(11) Å, $N_7 \cdots O_2$ 3.424(11) Å, $N_8 \cdots O_7$ 3.113(12) Å], as expected from a large and flexible macrocycle containing multiple hydrogen bonding donors and acceptors.

3.3 Synthesis of acyclic receptor **93**

Before undertaking binding studies, acyclic receptor **93** was synthesised in order to make a direct comparison with macrocycles **87** and **88** (Scheme 3.3).



Scheme 3.3 Reagents and conditions: a) CDI, THF; benzylamine, Et_3N .

Again CDI coupling was used. The good yield obtained testified the intrinsic efficiency of this method for this particular substrate. The lower yields registered for receptors **87** and **88**, therefore, are to be ascribed to the usually unfavourable free energy associated with the formation of a macrocyclic structure.

3.4 Binding studies on receptors **87**, **88** and **93** with acetate in $MeCN-d_3$

Receptors **88** and **93** were insoluble in $CDCl_3$, but showed good solubility in $MeCN-d_3$, while macrocycle **87** was poorly soluble in this solvent. For this receptor, the problem was overcome by using sonication in order to obtain solutions suitable for NMR titrations (concentration $\sim 10^{-3}$ M). TBA acetate was used as guest. In all titrations, sulfonamidic protons underwent intense broadening and they could not be followed. Amidic signals, on the other hand, showed significantly high $\Delta\delta_{max}$. The titration curve for the amidic protons of receptor **88** is shown in **Figure 3.5**.

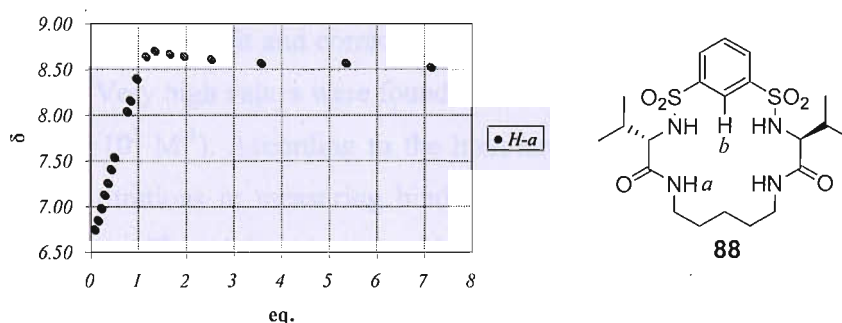


Figure 3.5 Titration curve for H-a proton of receptor **88** upon addition of acetate TBA salt in $MeCN-d_3$.

A steep slope associated with a large $\Delta\delta_{max}$ resulted from the early additions of guest solution aliquots. Saturation was then reached around the equivalency point, indicating

the presence of strong 1:1 association. Thereafter, a little inversion of the trend occurred. As extensively argued in the previous chapter, this phenomenon may be ascribed to a minor formation of the 1:2 complex. The data points were, hence, treated with the 1:2 curve fitting program. A large constant for the 1:1 complex was found ($K_{a1:1} \sim 5.7 \cdot 10^4 \text{ M}^{-1}$) accompanied by a considerably smaller value for the 1:2 complex ($K_{a1:2} \sim 6 \text{ M}^{-1}$). The accuracy of the calculation, however, was affected by an approximate fit and the presence of nonsensical parameters in the output (see § 2.2). Therefore, the result must be interpreted as a rough indication. The signal of the aromatic proton *H-b* (Figure 3.5) followed a continuous trend towards upfields, associated with a very small $\Delta\delta_{\text{max}}$. For this reason it was not taken into account in the analysis. A similar result was obtained for receptor **87** (Figure 3.6).

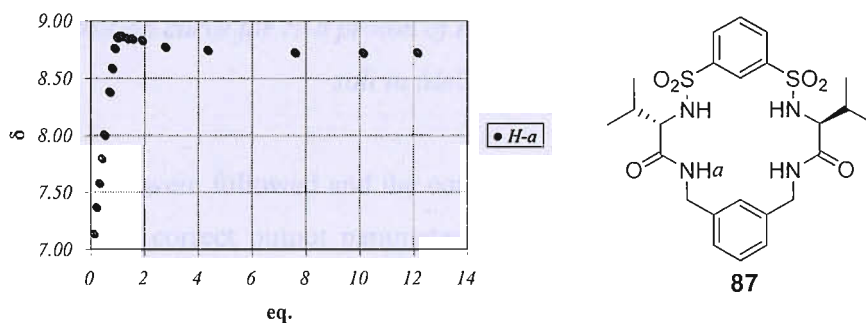


Figure 3.6 Titration curve profile of *H-a* proton of receptor **87** upon addition of acetate TBA salt in MeCN-d_3 .

In this case, however, good fit and correct output parameters were obtained with the 1:2 treating program. Very high values were found for the binding constants ($K_{a1:1} = 1.18 \cdot 10^7 \text{ M}^{-1}$, $K_{a1:2} = 2.55 \cdot 10^3 \text{ M}^{-1}$). According to the literature on the limits of applicability of traditional NMR titrations in measuring binding constants,^[96,97] $K_{a1:1}$ was beyond the limit of accuracy ($\sim 10^4$) and thus the value obtained could only be estimated to be $> 10^4 \text{ M}^{-1}$. Nevertheless, a picture of an extremely strong binding with acetate in MeCN-d_3 emerged from the last two experiments. Although the exact values for the association constants could not be determined, macrocycles **87** and **88** showed a far greater affinity towards acetate than 1,2-bis-aminocyclohexane based macrocycles **84**, **85** and **86** previously described.

Binding studies were then carried out on acyclic receptor **93** under the same conditions. As for the acyclic receptors described in the previous chapter, the aromatic C_2 -H proton showed a relatively high $\Delta\delta_{\max}$ associated with an anomalous trend inversion, this time even more pronounced (**Figure 3.7**).

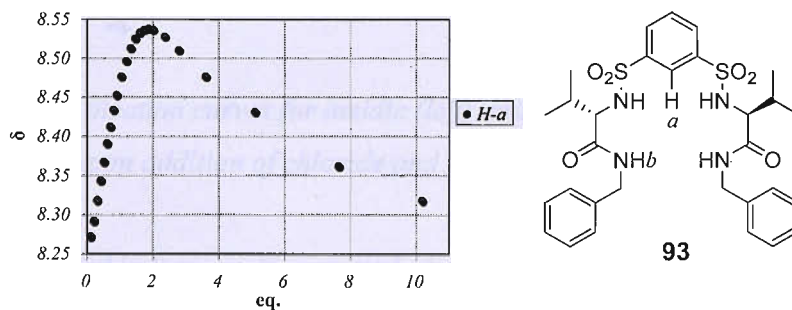


Figure 3.7 Titration curve for *H-a* proton of receptor **93** upon addition of acetate TBA salt in MeCN-d_3 .

Amidic protons *H-b* were followed and the curve showed a good fit with the 1:2 titrating program along with correct output parameters. The calculated binding constants were $K_{a1:1} = 3.64 \cdot 10^3 \text{ M}^{-1}$ and $K_{a1:2} = 32 \text{ M}^{-1}$ and the errors were estimated to be $\sim 10\%$ for $K_{a1:1}$ and $\sim 5\%$ for $K_{a1:2}$. Again the general picture of a major 1:1 binding accompanied by a minor 1:2 complex formation was confirmed for bis-sulfonamide based acyclic receptors.

3.5 Binding studies on receptor **88** with halides

In order to investigate the affinity of this type of receptors towards other anions, binding studies were carried out on macrocycle **88** with the TBA salts of three halides, chloride, bromide and fluoride. For the titrations with chloride and bromide, both amidic and sulfonamidic protons were followed and reasonably high $\Delta\delta_{\max}$ were found ($\sim 1 \text{ ppm}$ for Cl^- and $\sim 0.8 \text{ ppm}$ for Br^-) (**Figure 3.8**).

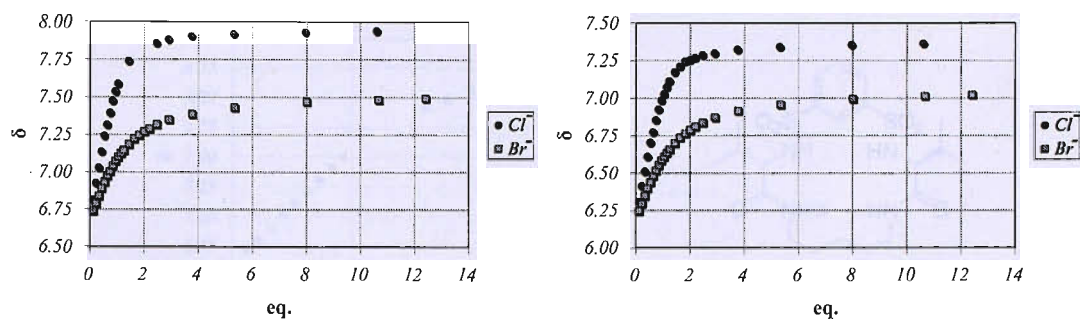


Figure 3.8 Binding titration curves for amidic (left) and sulfonamidic (right) protons of receptor **88** upon addition of chloride and bromide TBA salts in MeCN-d_3 .

In contrast with the binding studies carried out with acetate, all curves showed an excellent fit with the 1:1 titrating program and the constants were calculated as the average of the values obtained from each different proton (**Table 3.1**).

Host	Guest	$K_a (M^{-1})$	Error	Solvent
88	TBACl	4260	< 1%	MeCN-d_3
88	TBABr	1065	2%	MeCN-d_3

Table 3.1

The constants calculated were relatively high. A 4:1 selectivity in favour of chloride was found.

In the case of TBA fluoride, sulfonamidic protons showed intense broadening. Amidic protons, instead, could be followed, although only few equivalents of guest could be added before broadening occurred. For this reason, the constant could not be reliably calculated. Almost a straight line resulted from the titration (**Figure 3.9**).

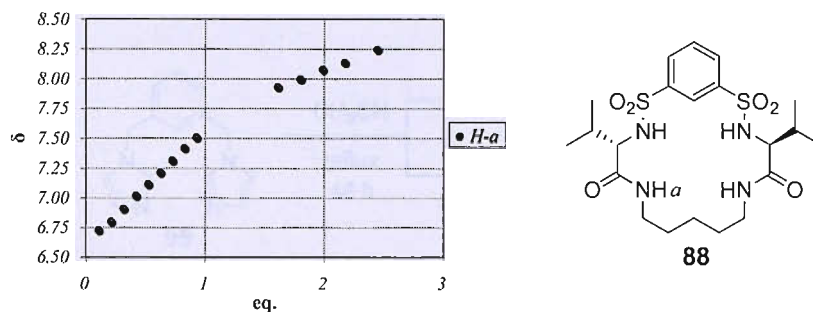
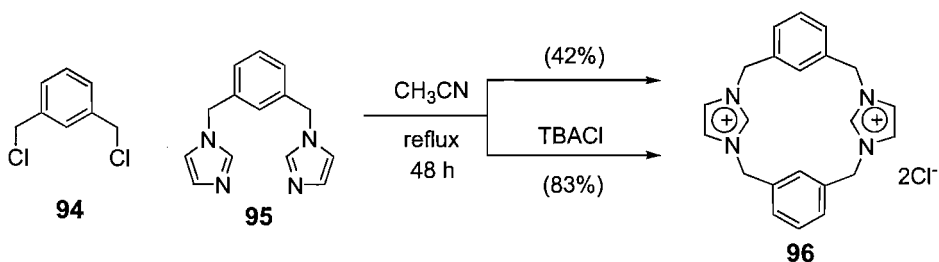


Figure 3.9 Titration curve for H-a protons of receptor **88** upon addition of fluoride TBA salt.

The unclear result of this last titration may result from the fact that the relatively acidic sulfonamidic NH protons can undergo deprotonation in presence of fluoride. The ability of the fluoride anion to deprotonate hydrogen bonding donor groups has been reported by Gale and co-workers.^[116,117]

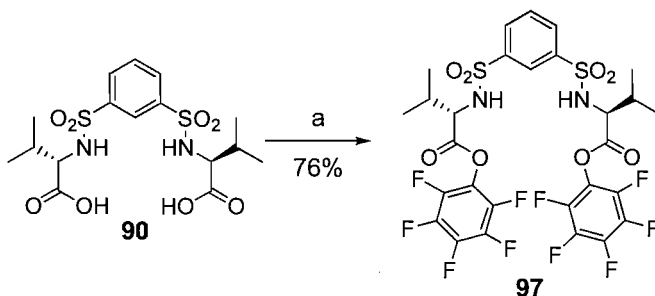
3.6 Anion templated synthesis of bis-sulfonamide based macrocycles

Receptors **87** and **88** showed very interesting results with TBA acetate and, thus, it was decided to carry on studying the binding properties of this class of macrocycles. From this point of view, the yields obtained with CDI mediated couplings, especially in the case of receptor **87**, were inadequate. In fact, in order to synthesise a family of macrocycles with different functionalities and in a scale large enough to allow extensive investigation, an efficient and reliable methodology was needed. For this reason, in analogy with the synthesis of crown ethers, whose formation is dramatically accelerated by the presence of cations,^[118] it was decided to investigate the opportunity of an anion templated synthesis. Anion templating has started to be studied only recently, compared to cation templating, and, besides, it is involved mostly in the formation of complex supramolecular assemblies rather than been used in the development of synthetic methodologies.^[119] Nevertheless, an example of anion templated bimolecular macrocyclisation was found in the literature. Alcalde and co-workers synthesised a dicationic imidazoliophane. They found that, in the presence of stoichiometric amounts of TBA chloride, the yield of macrocycle **96** was doubled (Scheme 3.4).^[120]



Scheme 3.4

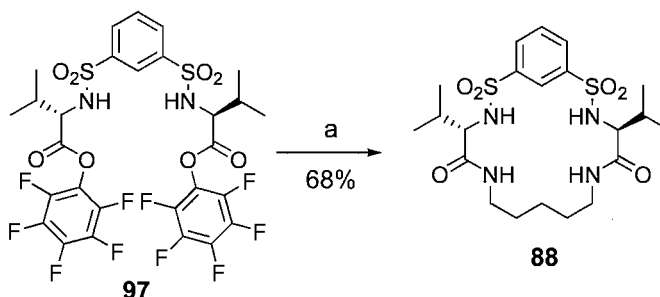
Following this encouraging example, it was decided to test if the presence of TBA chloride could induce a yield improvement for the preparation of bis-sulfonamide based macrocycles. Besides, the good affinity showed by receptor **88** towards the chloride anion (see § 3.5) and the fact that the presence of TBA chloride greatly enhanced the solubility of macrocycle **88** in DCM were favourable indications. In order to increase the chances of a significant interaction with the anion, it was decided to perform the reaction in a non-polar solvent, such as DCM. For this reason, pentafluorophenol ester of bis-acid **90** was prepared in good yield from a modified literature procedure (Scheme 3.5).^[121]



Scheme 3.5 Reagents and conditions: a) PFP, EDC, DCM.

Pentafluorophenol esters usually display good solubility in non-polar media and that was the case of **97**. Besides, for a macrocyclisation process, the isolation of the reactive intermediates is a benefit, because the number of possibly interfering additives and side-products is sensibly reduced. In addition, an example of successful macrocyclisation involving the coupling between a bis-pentafluorophenol ester and a bis-amine was known from the literature.^[108]

The macrocyclisation reaction was then carried out on activated ester **97** with 1,5-diaminopentane in presence of one equivalent of TBA chloride. Macrocycle **88** was successfully obtained in good yield (Scheme 3.6).



Scheme 3.6 Reagents and conditions: a) 1,5-diaminopentane, TBACl, Et₃N, DCM.

The reaction was performed in high dilution ($C \sim 10^{-2}$ M) and with slow addition. No indication for the presence of [2+2] macrocycle **92** was found. In order to ascertain whether the improved yield was to be ascribed to the effect of TBA chloride or simply due to the different coupling conditions, a control experiment was undertaken. Four different reactions were performed under the same conditions described in Scheme 3.6, varying exclusively the number of TBACl equivalents. From this experiment, the effect of the chloride anion on the yields emerged clearly. The results are summarised in Table 3.2.

TBACl equivalents	Yield (%)	
	88	92
0	28	26
1	65	—
2	79	—
4	79	—

Table 3.2

The presence of TBA chloride also improved the selectivity towards the [1+1] macrocycle **88**, since no appreciable amount of the [2+2] macrocycle **92** was recovered in presence of the templating agent. The yield of the reaction performed with one equivalent is in agreement with the reaction described in Scheme 3.6. Using two equivalents resulted in a three-fold increase of the yield for [1+1] macrocycle **88**. Adding more than two equivalents did not produce further improvement.

The conformation assumed by a plausible acyclic intermediate may explain the improved yields. A *syn-syn* conformation of the side ‘arms’ can be stabilised by the presence of chloride^[68] and the intramolecular attack of the amine to the activated carbonyl would have a better chance to occur than the intermolecular coupling (**Figure 3.10**).

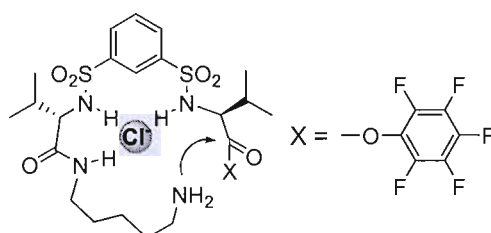
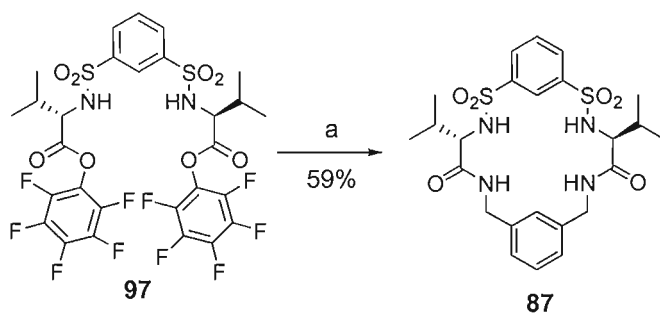


Figure 3.10 Proposed mechanism for chloride mediated templating effect.

The fact that a very similar model was validated, after extensive kinetic studies, for macrocycle **96**,^[122] which is similar in size to macrocycle **88**, gives some support to the mechanism proposed in **Figure 3.10**. Further investigations, however, are to be done in order to understand the real effect of chloride in this particular reaction and the study of the effects of other anions is particularly desirable.

The same conditions were applied successfully to the synthesis of macrocycle **87** (**Scheme 3.7**).



Scheme 3.7 Reagents and conditions: a) *m*-xylylenediamine, TBACl, Et₃N, DCM.

With this method, macrocycle **87** was obtained with a 45% overall yield from bis-acid **90**, resulting in a seven-fold increase compared to the method previously used.

3.7 Binding studies on receptor **88** with simple anions in MeCN- d_3 /2% H₂O

Macrocycle **88** showed a strong affinity towards acetate (see § 3.4). However, this affinity could not be assessed properly because of the probable presence of minor 1:2 complexation. In order to solve this problem, titrations were conducted in presence of a small amount of water. This choice was made with the intent to limit secondary interactions, allowing a more accurate measure of the binding, possibly using the 1:1 model. Addition of water is current practice in NMR titrations and is normally used in order to standardise the moisture in polar solvents or to reduce the values of binding constants otherwise exceeding the maximum measurable limit.^[56,75,76]

During the titrations, only amidic protons could be followed. A water content of 1% v/v produced an improvement of the fit compared to the neat MeCN- d_3 , but several points resulted still untouched by the trajectory of the curve calculated with the 1:1 treating program. Conversely, an excellent fit was obtained with a water content of 2% (**Figure 3.11**).

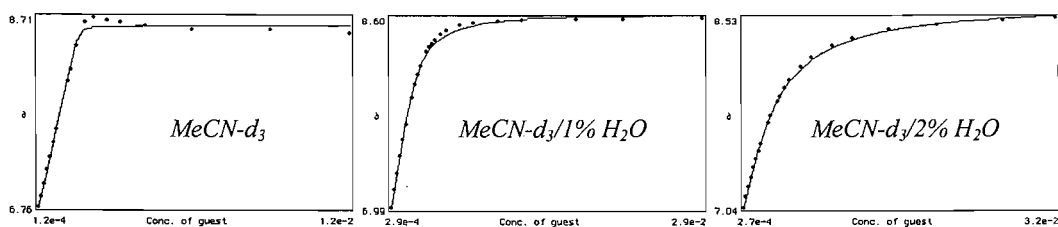


Figure 3.11 Effect of the water content on the titration curve for the amidic protons of receptor **88** upon addition of acetate TBA salt in MeCN- d_3 . Curves calculated with the 1:1 treating program.

A binding constant, thus, could be accurately measured in this competitive solvent and the value obtained was $K_a = 540 \text{ M}^{-1}$. Binding studies were then performed on receptor **88** with other anions in the same solvent mixture (**Figure 3.12**).

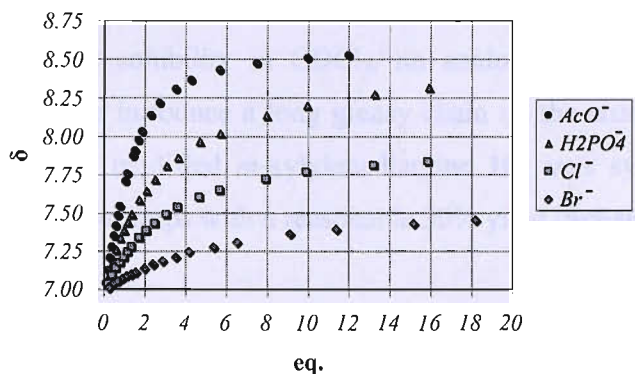


Figure 3.12 Binding titration curves for amidic protons of receptor **88** upon addition of the TBA salts of different anions in MeCN- d_3 /2% H_2O .

All curves obtained showed excellent fit with the 1:1 treating program. With the dihydrogen phosphate anion, as in the case of acetate, sulfonamidic protons underwent intense broadening and only amidic protons could be followed. Conversely, with chloride and bromide, both signals could be followed and thus the binding constants resulted from the average of two values. From **Figure 3.12**, the preference of receptor **88** for the acetate anion is clear, as confirmed by the values calculated for the binding constants (**Table 3.3**).

Host	Guest	K_a (M^{-1})	Error	Solvent
88	TBAOAc	540	< 5%	MeCN- d_3 /2% H_2O
88	TBAH ₂ PO ₄	281	< 5%	MeCN- d_3 /2% H_2O
88	TBACl	183	2%	MeCN- d_3 /2% H_2O
88	TBABr	111	2%	MeCN- d_3 /2% H_2O

Table 3.3

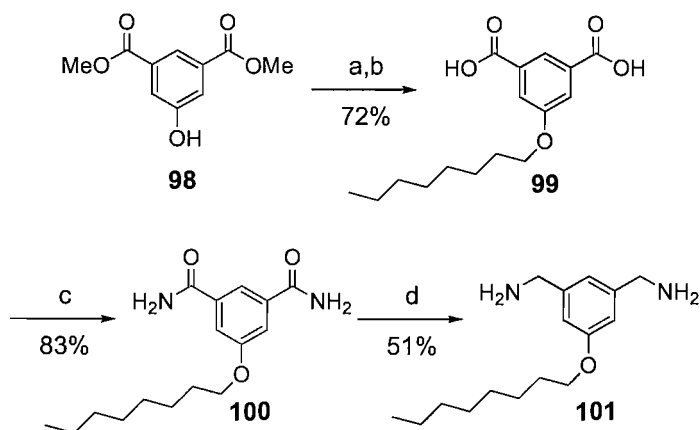
A preference for the oxyanions was found. Acetate was preferred over dihydrogen phosphate with a 2:1 selectivity. For the halides, chloride was still preferred over bromide, although the selectivity was attenuated by the presence of water (see § 3.5).

In conclusion, macrocycle **88** was found to be a good selector for acetate in the solvent mixture MeCN- d_3 /2% H_2O .

3.8 Synthesis of macrocycle 102

Receptor **87** displayed interesting binding properties towards acetate in MeCN- d_3 . However, the solubility in this solvent was poor, resulting in a laborious preparation of

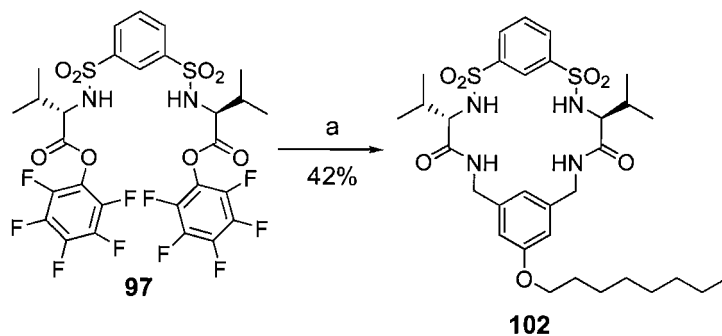
the solutions for the binding studies. In order to overcome this problem, along with the purpose of improving the solubility in CDCl_3 , an analogue of macrocycle **87** was designed. It was decided to introduce a long greasy chain on the aromatic spacer at the 'southern' end. Therefore, modified *m*-xylylenediamine **101** was synthesised from 5-hydroxyisophthalate **98** in four steps with a reasonable 30% yield (**Scheme 3.8**).



Scheme 3.8 Reagents and conditions: a) 1-iodooctane, K_2CO_3 , acetone; b) 50:50 1,4-dioxane/1.5 M LiOH ; c) PCl_5 ; NH_3 sat. DCM; d) LiAlH_4 , THF.

5-Hydroxyisophthalate was alkylated with 1-iodooctane following a procedure by Slater and co-workers.^[123] The resulting bis-ester was not purified and hydrolysis followed to give bis-acid **99** in good overall yield. Bis-amide **100** was then prepared in high yield modifying a literature procedure.^[124] Bis-amine **101** was finally obtained in acceptable yield after reduction with LiAlH_4 .^[125]

Macrocycle **102** was synthesised by coupling bis-amine **101** with pentafluorophenol ester **97** in presence of TBA chloride (**Scheme 3.9**).



Scheme 3.9 Reagents and conditions: a) **101**, TBACl , Et_3N , DCM.

The yield was lower than in the case of macrocycle **88**, but still good for a macrocyclisation reaction.

3.9 Binding studies on receptor **102** in CDCl_3

Receptor **102** showed good solubility in $\text{MeCN-}d_3$. In CDCl_3 the solubility was limited to low concentrations of macrocycle. The spectrum recorded in this solvent showed a bad resolution of the peaks. Nevertheless, a NMR titration of receptor **102** with TBA acetate in CDCl_3 was made, hoping that the effect of the anion might contribute to obtain a better resolution. Upon addition of guest solution, the NMR spectrum was undergoing significant changes, but the signals could not be followed due to bad resolution and merging of the peaks (**Figure 3.13**).

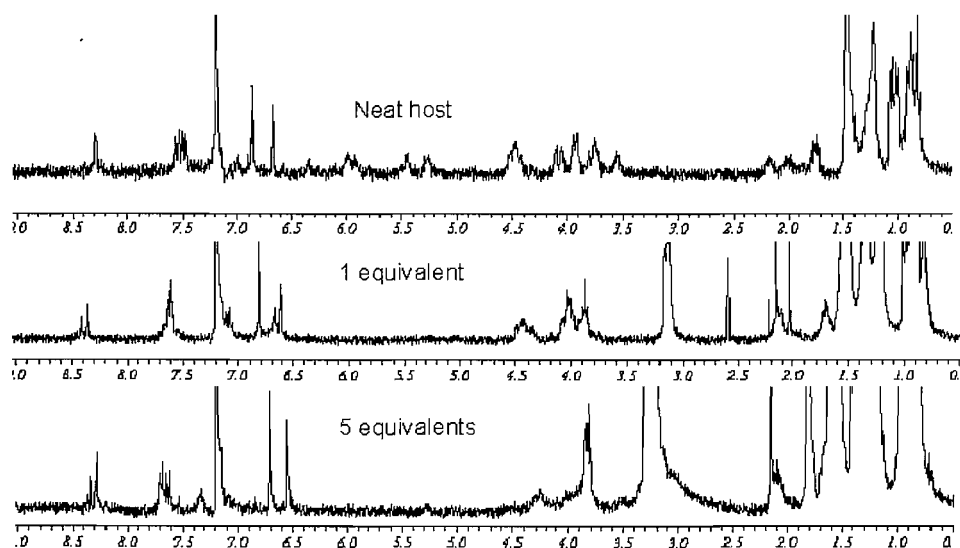


Figure 3.13 ^1H NMR spectrum of neat receptor **102** and after addition of one and five equivalents of acetate TBA salt. Spectra recorded in CDCl_3 .

A better resolution was obtained recording a spectrum of macrocycle **102** in $\text{CDCl}_3/2\%$ MeOH (**Figure 3.14**).

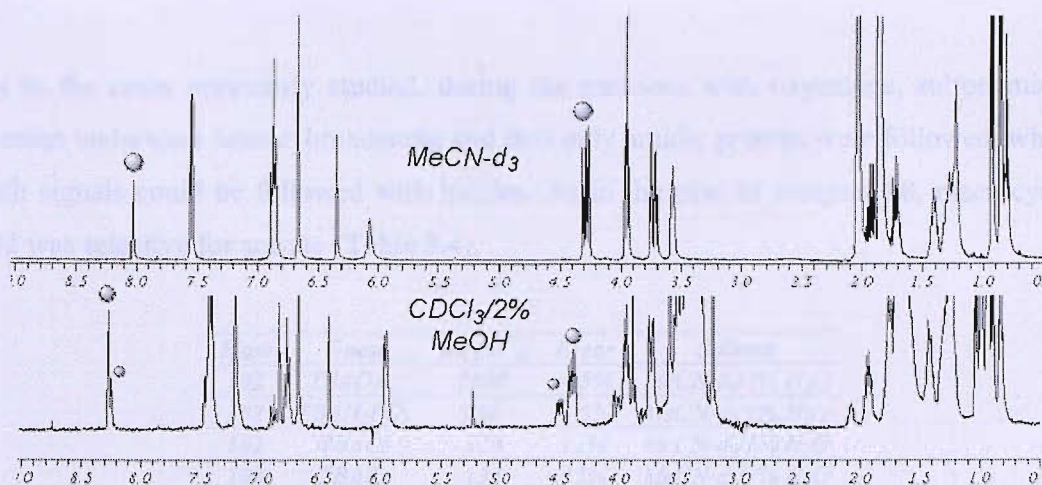


Figure 3.14 Comparison between the ^1H NMR spectra of receptor **102** recorded in $\text{MeCN-}d_3$ and in $\text{CDCl}_3/2\% \text{ MeOH}$.

In comparison with the spectrum recorded in $\text{MeCN-}d_3$, some peaks appeared clearly to be split into a major and a minor component (**Figure 3.14**). This fact is consistent with the presence in solution of a major and a minor conformation, whose interconversion is slow in the NMR time-scale. No further studies were carried out in this solvent.

3.10 Binding studies on receptor **102** in wet $\text{MeCN-}d_3$

Binding studies with different anions were carried out on macrocycle **102**. In contrast with receptor **88**, an excellent fit was found with acetate in $\text{MeCN-}d_3/1\% \text{ H}_2\text{O}$. A series of binding studies were thus performed in this solvent mixture.

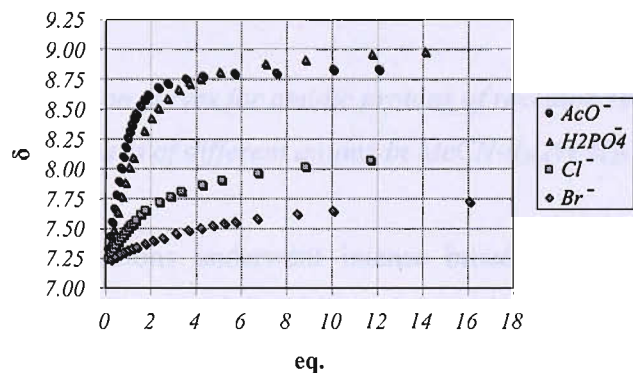


Figure 3.15 Binding titration curves for amidic protons of receptor **102** upon addition of the TBA salts of different anions in $\text{MeCN-}d_3/1\% \text{ H}_2\text{O}$.

As in the cases previously studied, during the titrations with oxyanions, sulfonamidic protons underwent intense broadening and thus only amidic protons were followed, while both signals could be followed with halides. As in the case of receptor **88**, macrocycle **102** was selective for acetate (Table 3.4).

Host	Guest	$K_a (M^{-1})$	Error	Solvent
102	TBAOAc	2690	< 5%	MeCN- d_3 /1% H ₂ O
102	TBAH ₂ PO ₄	866	< 5%	MeCN- d_3 /1% H ₂ O
102	TBACl	328	11%	MeCN- d_3 /1% H ₂ O
102	TBABr	134	13%	MeCN- d_3 /1% H ₂ O

Table 3.4

Again oxyanions were preferred over halides. The selectivity in favour of acetate over dihydrogen phosphate was ~ 3:1. A sensible error was found for the halides.

In order to compare receptors **102** and **88** and to assess the effect of increasing the water content of the solvent, titrations with the same guests were performed in MeCN- d_3 /2% H₂O (Figure 3.16).

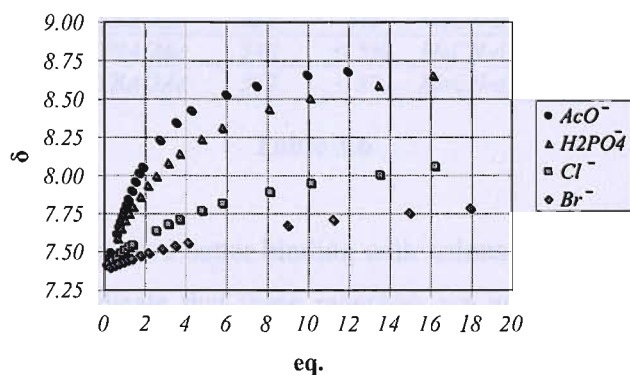


Figure 3.16 Binding titration curves for amidic protons of receptor **102** upon addition of the TBA salts of different anions in MeCN- d_3 /2% H₂O.

As usual, sulfonamidic protons underwent intense broadening with oxyanions. For bromide only amidic protons could be followed because of the superimposition of sulfonamidic protons with other signals. For binding studies with halides, the accuracy was affected by low percentage of saturation. All binding constants resulted considerably reduced by the increased water content (Table 3.5).

<i>Host</i>	<i>Guest</i>	<i>K_a (M⁻¹)</i>	<i>Error</i>	<i>Solvent</i>
102	TBAOAc	372	< 5%	MeCN-d ₃ /2% H ₂ O
102	TBAH ₂ PO ₄	201	< 5%	MeCN-d ₃ /2% H ₂ O
102	TBACl	104	*	MeCN-d ₃ /2% H ₂ O
102	TBABr	55	*	MeCN-d ₃ /2% H ₂ O

(* low percentage of saturation)

Table 3.5

Compared to the values obtained in MeCN-d₃/1% H₂O, a seven-fold decrease resulted for the affinity towards acetate. Selectivity was also affected. It was registered a decrease from ~ 3:1 to ~ 2:1 for the preference for acetate over dihydrogen phosphate and a ~ 9:1 to ~ 3:1 drop for the selectivity over the chloride anion.

A control experiment was performed on receptor **87** with acetate in order to check if the greasy chain at the ‘southern’ end of macrocycle **102** was somehow affecting the binding. A good fit resulted with the 1:1 treating program and a very similar constant was found ($K_a = 351 \text{ M}^{-1}$). In **Table 3.6** are reported the values found for receptors **87**, **88** and **102**.

<i>Host</i>	<i>Guest</i>	<i>K_a (M⁻¹)</i>	<i>Error</i>	<i>Solvent</i>
87	TBAOAc	351	5%	MeCN-d ₃ /2% H ₂ O
88	TBAOAc	540	< 5%	MeCN-d ₃ /2% H ₂ O
102	TBAOAc	372	< 5%	MeCN-d ₃ /2% H ₂ O

Table 3.6

Flexible macrocycle **88** displayed better binding with anions than more rigid receptors **87** and **102**. This fact may indicate that these receptors are not well preorganised to bind anions. In fact, flexibility can help receptor **88** to reorganise into a conformation more suitable for binding, while for receptors **87** and **102** this process can be more expensive in terms of free energy. Further corroboration to this hypothesis was provided by the crystal structures of receptors **87** and **88**. Macrocycle **87** crystallised with two molecules of water (**Figure 3.17**).

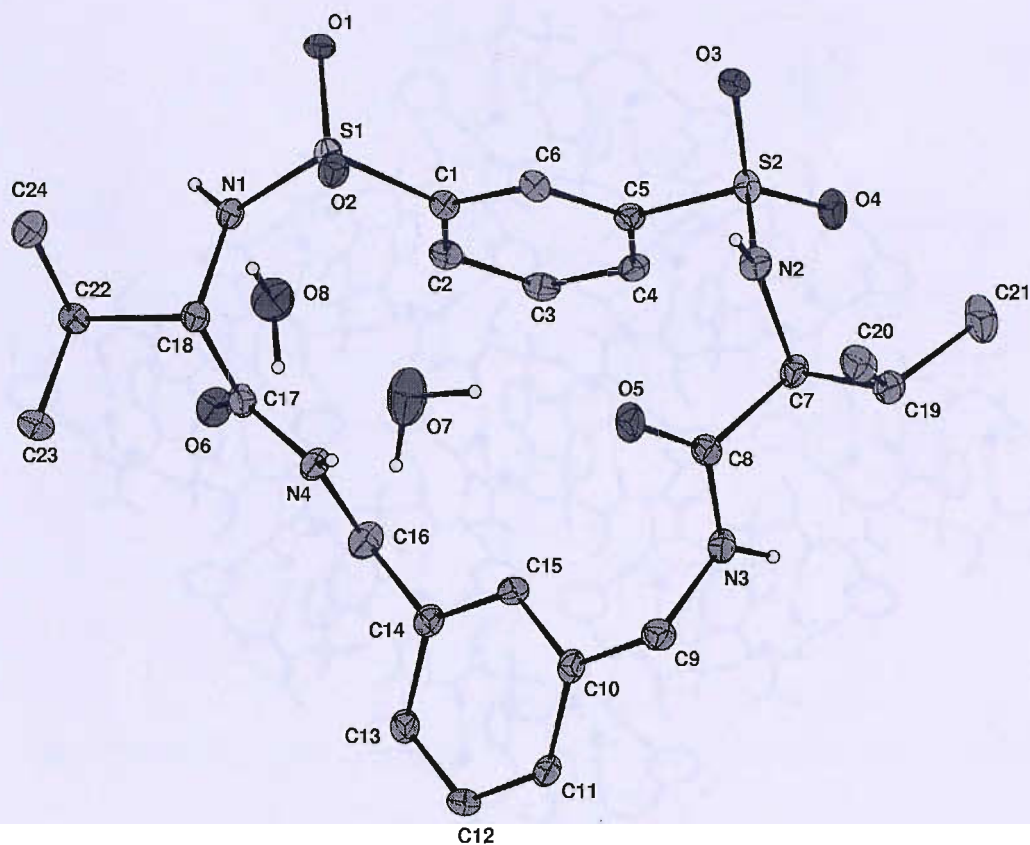


Figure 3.17 Crystal structure of macrocycle **87**. Thermal ellipsoids drawn at the 35% probability level, non acidic hydrogens omitted for clarity.

The crystal structure showed clearly that the *NH* bonds were pointing alternatively in opposite directions.

The extended structure revealed an interesting hydrogen bonding network constituted by dimers in which the sulfonamide units on adjacent molecules are linked together by four intermolecular hydrogen bonds ($N_1H \cdots O_3$ [$N_1 \cdots O_3$ 2.881(4) Å] and $N_2H \cdots O_1$ [$N_2 \cdots O_1$ 2.945(4) Å] for each unit). Amidic *NH* bonds are contributing to the network with the $N_3H \cdots O_6$ [$N_3 \cdots O_6$ 2.849(4) Å] interaction and by coordinating the molecules of the solvent (**Figure 3.18**).

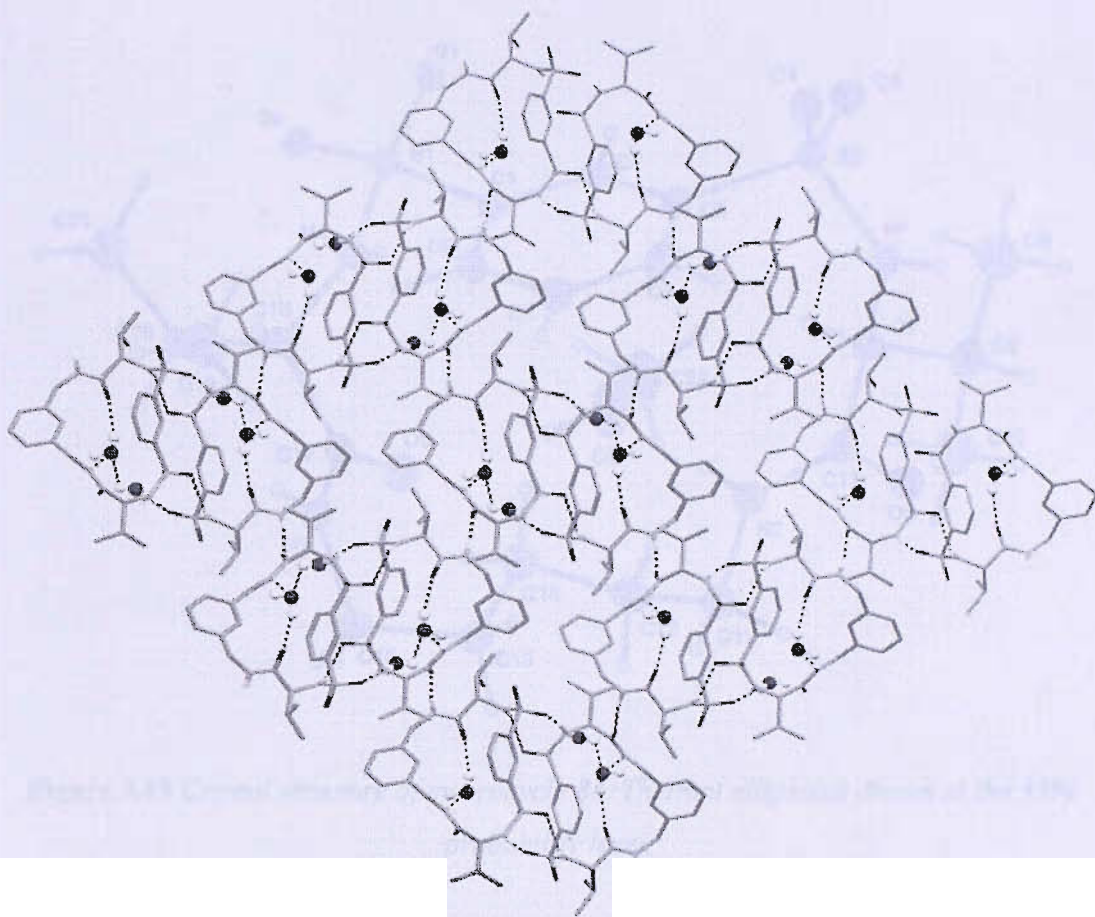


Figure 3.18 *Extended structure of macrocycle 87 showing the hydrogen bonding network.*

Although macrocycle **88** crystallised with one molecule of MeOH, the crystal structure showed many similarities with macrocycle **87** (**Figure 3.19**).

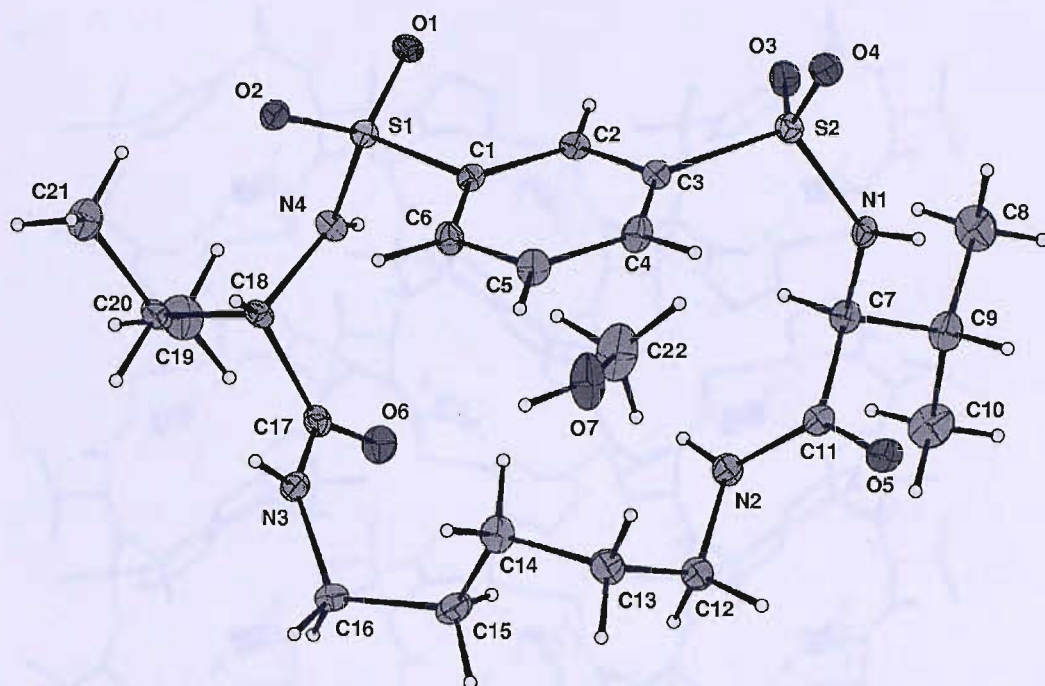


Figure 3.19 Crystal structure of macrocycle **88**. Thermal ellipsoids drawn at the 35% probability level.

Again, the crystal structure showed clearly that the *NH* bonds were pointing alternatively in opposite directions. Also in this case, the extended structure showed an interesting hydrogen bonding network, with the sulfonamide units of two adjacent molecules embedded together by four hydrogen bonds ($N_1H \cdots O_1$ [$N_1 \cdots O_1$ 2.904(2) Å] and $N_4H \cdots O_4$ [$N_4 \cdots O_4$ 3.012(2) Å] for each unit). Amidic *NH* bonds are contributing to the network with the $N_3H \cdots O_5$ [$N_3 \cdots O_5$ 2.912(2) Å] interaction and by coordinating the molecule of the solvent (**Figure 3.20**).

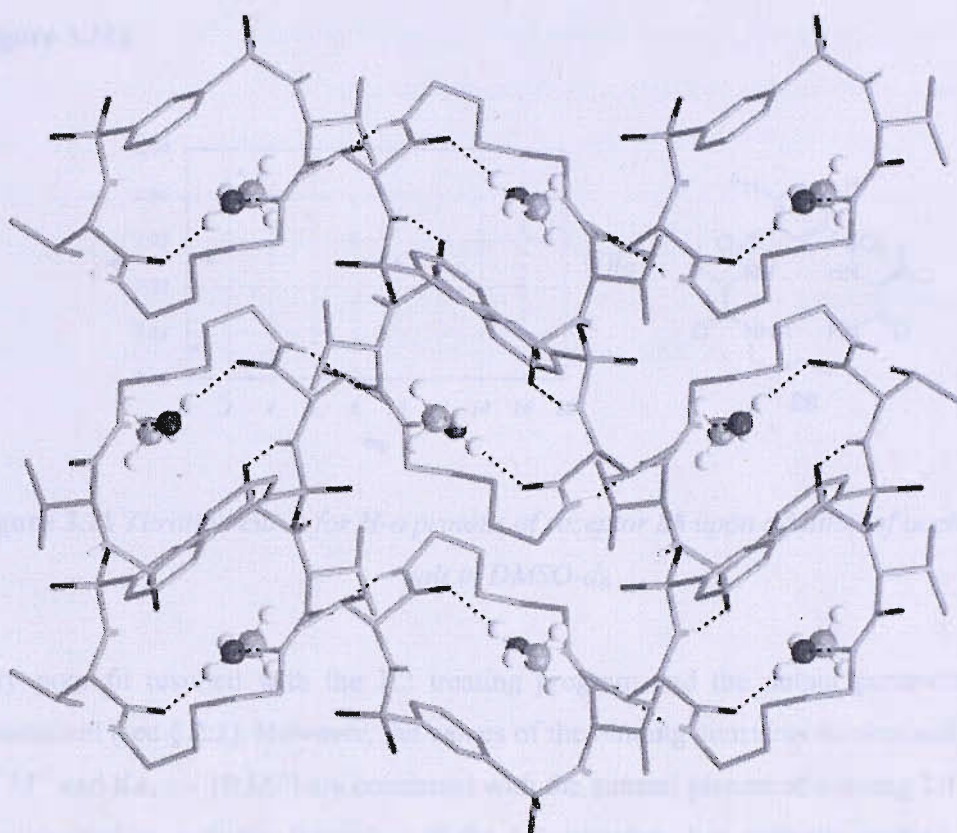


Figure 3.20 *Extended structure of macrocycle 88 showing the hydrogen bonding network.*

Crystal structures of macrocycles **87** and **88** showed again an ‘alternate’ conformation, similar to that found for receptors **85** and **86**. Receptors **87** and **88**, however, did not suffer from the severe conformational restrictions induced by the cyclohexane rings present in macrocycles **84-86**. For this reason, they are likely allowed to rearrange in order to display efficacious binding with carboxylates.

Despite several attempts, a crystal structure of a complex of receptor **87** or **88** with acetate or other anions had not been obtained, preventing the attainment of a conclusive picture of the binding mode between receptors **87**, **88** and **102** and their anionic guests.

3.11 Binding studies on receptor **88** in DMSO- d_6

Binding studies on receptor **88** were carried out in DMSO- d_6 with TBA acetate. Sulfonamidic protons underwent intense broadening, while amidic protons showed a modest, although appreciable, change in the chemical shift. An unusual pattern was found

for the curve, similar to those described in § 3.4 for macrocycles **87** and **88** in MeCN- d_3 (Figure 3.21).

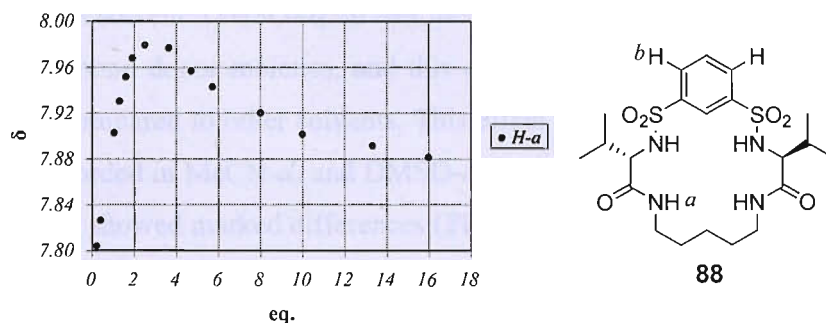


Figure 3.21 Titration curve for H-a protons of receptor **88** upon addition of acetate TBA salt in DMSO- d_6 .

Very poor fit resulted with the 1:2 treating program and the output parameters were nonsensical (see § 2.2). However, the values of the binding constants so obtained ($K_{a1:1} \sim 10^3 \text{ M}^{-1}$ and $K_{a1:2} \sim 10 \text{ M}^{-1}$) are consistent with the general picture of a strong 1:1 binding accompanied by a minor formation of the 1:2 complex. For aromatic protons H-b, an unusually large upfield $\Delta\delta_{\text{max}}$ was registered ($\sim 0.35 \text{ ppm}$) (Figure 3.22).

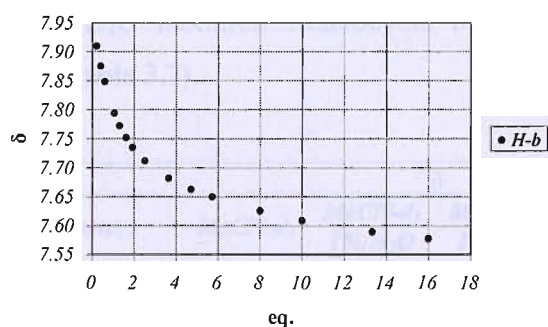


Figure 3.22 Titration curve for H-b protons of receptor **88** upon addition of acetate TBA salt in DMSO- d_6 .

This fact corroborates the hypothesis that receptor **88** undergoes an important conformational rearrangement in order to bind acetate. The titration curve of H-b protons showed an excellent fit with the 1:2 treating program, although the low percentage of

saturation affected the accuracy of the calculation. The values obtained were $K_{a1:1} = 928 \text{ M}^{-1}$ and $K_{a1:2} = 6 \text{ M}^{-1}$, consistent with those calculated from the amidic protons.

The 1:2 binding in DMSO- d_6 may be the result of a different conformation assumed by receptor **88** in this solvent. DMSO- d_6 , in fact, is responsible of a high degree of solvation of the hydrogen bond donor moieties, and this can produce a different conformation of the macrocycle compared to other solvents. This effect can be seen by comparing the ^1H NMR spectra recorded in MeCN- d_3 and DMSO- d_6 . Some signals, especially those related to the NH groups, showed marked differences (Figure 3.23).

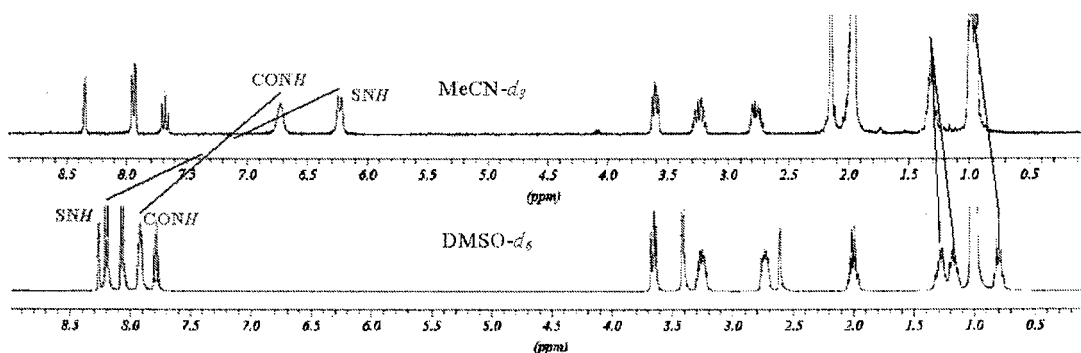


Figure 3.23 ^1H NMR spectra of macrocycle **88** in MeCN- d_3 and DMSO- d_6 .

The strong interaction between the solvent molecules and the NH protons of receptor **88** is reflected by the substantial difference in chemical shift recorded in DMSO- d_6 in comparison with MeCN- d_3 /H $_2$ O mixtures. Macrocycle **87** also displayed this large variation in chemical shift (Table 3.7).

Receptor	Protons	δ			
		MeCN- d_3	MeCN- d_3 1% H $_2$ O	MeCN- d_3 2% H $_2$ O	DMSO- d_6
87	Amidic NH	6.96	—	7.45	8.42
	Sulfonamidic NH	6.13	—	6.36	8.13
88	Amidic NH	6.68	6.86	6.98	7.81
	Sulfonamidic NH	6.18	6.29	6.39	8.10

Table 3.7

3.12 Binding studies with *N*-Boc-phenylalanine

In order to test if receptors **88** and **102** were suitable for chiral recognition, binding studies were carried out with the TBA salts of the two enantiomers of *N*-Boc-phenylalanine. ^1H NMR titrations on receptor **88** were performed in MeCN- d_3 /2% H $_2$ O.

As usual, sulfonamidic protons showed intense broadening, while amidic protons could be followed. The curves could be fitted in the 1:1 treating program with an excellent fit. The constants obtained for the two enantiomers were very similar ($K_a = 264 \text{ M}^{-1}$ for Boc-L-Phe and $K_a = 241 \text{ M}^{-1}$ for Boc-D-Phe), with a very low preference for the L enantiomer. A more marked, although still low, selectivity for the L enantiomer was found for receptor **102** in MeCN- d_3 /1% H₂O ($K_a = 742 \text{ M}^{-1}$ for Boc-L-Phe and $K_a = 582 \text{ M}^{-1}$ for Boc-D-Phe). The results for receptors **88** and **102** are summarised in **Table 3.8**.

Host	Guest	$K_a \text{ (M}^{-1}\text{)}$	Error	Solvent	Selectivity (L/D)
88	<i>N</i> -Boc-L-Phe-OTBA	264	< 5%	MeCN- d_3 /2% H ₂ O	1.1:1
88	<i>N</i> -Boc-D-Phe-OTBA	241	< 5%	MeCN- d_3 /2% H ₂ O	
102	<i>N</i> -Boc-L-Phe-OTBA	742	< 5%	MeCN- d_3 /1% H ₂ O	1.3:1
102	<i>N</i> -Boc-D-Phe-OTBA	582	< 5%	MeCN- d_3 /1% H ₂ O	

Table 3.8

An explanation of the low enantioselectivity may be found in a possible binding mode of receptors **88** and **102** with the carboxylate anion. In fact, it is possible that the macrocycle is able to bind only one oxygen atom of the carboxylate, in a manner that the amino acid side chain is far from the chirophore isopropyl groups of the receptor, reducing the chances of selective steric repulsion (**Figure 3.24**).

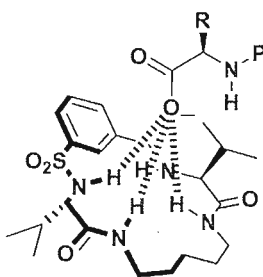


Figure 3.24 Possible binding mode between receptor **88** and an amino acid carboxylate.

A binding mode with a carboxylate anion involving only one oxygen atom was well illustrated by the crystal structure of a complex between a tetralactam macrocycle and TBA acetate obtained by Jurczak and co-workers (**Figure 3.25**).^[126]

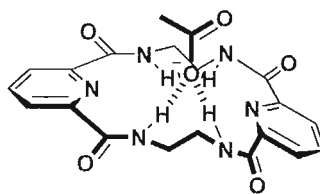
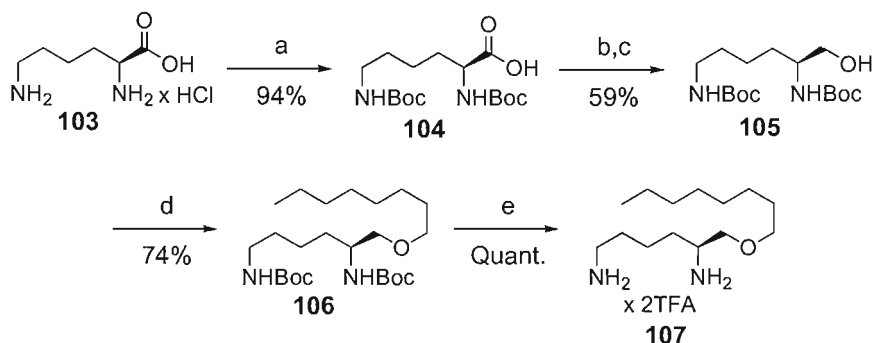


Figure 3.25 Complex between TBA acetate and Jurczak's tetralactam macrocycle.

Another example of this particular binding mode was provided by Sessler and co-workers, with the crystal structure of a calix[4]pyrrole carboxylate dimer.^[127]

3.13 Synthesis of macrocycle **108**

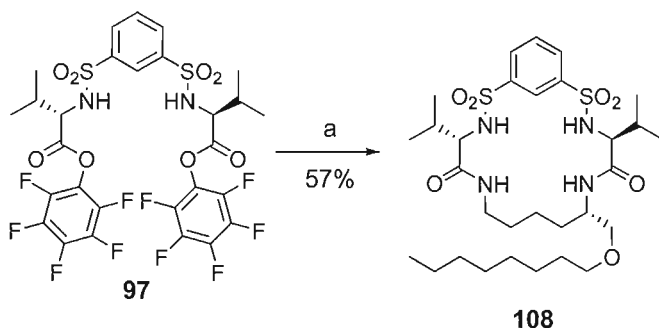
Macrocycle **88** displayed better binding with acetate compared to macrocycles **87** and **102**. However, receptor **88** was insoluble in CDCl_3 and, for this reason, it could not be tested in this solvent. Therefore, it was decided to synthesise a more soluble macrocycle with a flexible chain at the 'southern end'. Lipophilic bis-aminoether **107**, derived from lysine, was chosen to replace the 1,5-diaminopentane moiety in macrocycle **88** (Scheme 3.10).



Scheme 3.10 Reagents and conditions: a) Boc_2O , 2 M NaOH, 50:50 1,4-dioxane/ H_2O ; b) *N*-hydroxysuccinimide, EDC, DCM; c) LiAlH_4 , THF; d) 1-iodooctane, TBAHSO₄ cat., 50% NaOH/ H_2O , Toluene; e) 80:20 DCM/TFA.

L-Lysine monochloride **103** was protected with excellent yield following a procedure by Rudkevich and co-workers.^[128] Acid **104** was activated with *N*-hydroxysuccinimide^[129] and then reduced in presence of LiAlH_4 with reasonable yield.^[130] Protected lysinol **105** was alkylated with 1-iodooctane in good yield under phase-transfer catalysis conditions modifying a literature procedure.^[131] Deprotection in standard conditions yielded finally bis-aminoether **107**, which was readily coupled with pentafluorophenol ester **97** to give

receptor **108** in good yield under the anion-templating conditions previously used (Scheme 3.11).



Scheme 3.11 Reagents and conditions: a) **107**, TBACl, Et₃N, DCM.

3.14 Binding studies with acetate

Receptor **108** resulted to be soluble in CDCl₃ and thus binding studies could be carried out in this solvent. Following the different protons had proven to be more difficult than for other receptors because of the desymmetrisation induced by the substituted spacer at the ‘southern’ end. In fact, the number of NH signals was doubled, while their intensities were halved. Amidic peaks were assigned on the basis of C-H long range correlation 2D NMR. Sulfonamidic peaks could not be distinguished by this technique. A NMR titration was carried out on receptor **108** with TBA acetate as guest. Amidic proton *H-a* and one unassigned sulfonamidic proton were followed (Figure 3.26).

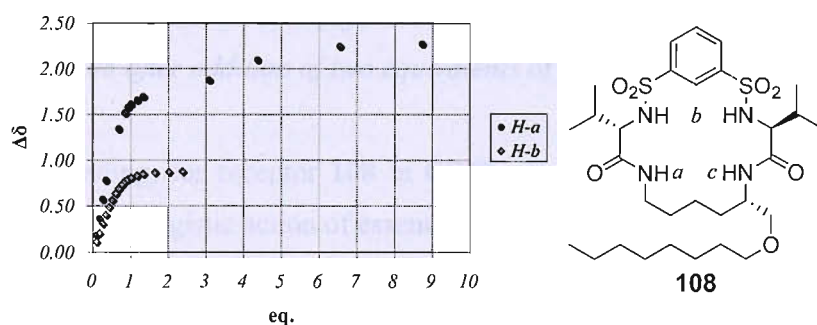


Figure 3.26 Binding titration curves for amidic proton *H-a* and a sulfonamidic proton (*H-b*) of receptor **108** upon addition of acetate TBA salt in CDCl₃.

An appropriate number of data points could not be obtained for amidic *H-c* due to superimposition with various signals. Amidic proton *H-a* displayed a high $\Delta\delta_{\max}$ (~ 2

ppm) and the curve profile seemed to indicate the presence of a 1:2 complex. The curve could be fitted with the 1:2 treating program, although poor fit and low percentage of saturation undermined the accuracy of the results. The indicative values obtained for the two constants were $K_{A1:1} \sim 5 \cdot 10^4 \text{ M}^{-1}$ and $K_{A1:2} \sim 20 \text{ M}^{-1}$. Again the picture of a strong 1:1 binding accompanied by a minor formation of a 1:2 complex was confirmed. A sulfonamidic proton showed extensive superimposition with various signals and, eventually, intense broadening. The curve obtained by following the other sulfonamidic proton could neither be fitted in the 1:1 nor in the 1:2 treating program, due to the early broadening of signal (**Figure 3.26**).

The two amidic protons showed comparable changes in chemical shift upon addition of acetate, indicating similar participation in hydrogen bonding with the guest. Sulfonamidic protons, conversely, showed a markedly different $\Delta\delta$ ($\sim 0.9 \text{ ppm}$ vs. $\sim 2.5 \text{ ppm}$) after addition of two equivalents of guest. This fact indicated that one sulfonamidic proton was less involved than the other one in hydrogen bonding with acetate (**Figure 3.27**).

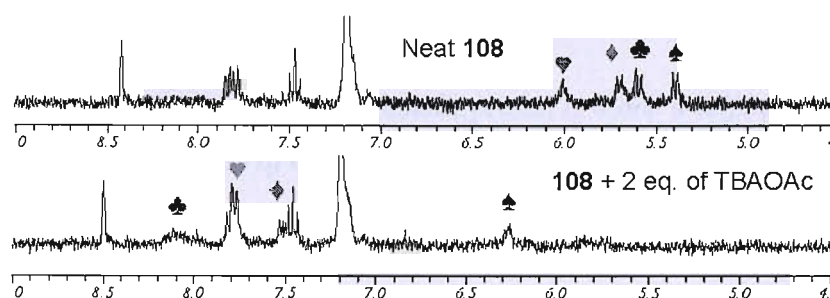


Figure 3.27 Changes in chemical shift for amidic (♥, ♦) and sulfonamidic (♣, ♠) protons of receptor **108** after addition of two equivalents of acetate TBA salt in CDCl_3 .

From the latter finding, for receptor **108** in CDCl_3 , it is possible to assume a binding mode involving the synergistic action of essentially three *NH* protons, two amidic and one sulfonamidic.

In order to assess the influence of the introduction of a 'greasy' chain at the 'southern' end, a NMR titration was performed on receptor **108** with acetate in $\text{MeCN-}d_3/2\% \text{ H}_2\text{O}$. In this case, only *H-a* was followed, due to superimposition with various signals of *H-c* and the intense broadening of sulfonamidic peaks. In comparison with receptor **88**, a lower binding constant was obtained ($K_a = 303 \text{ M}^{-1}$, error < 5%). Therefore, in contrast

with the case of receptor **102**, the aliphatic chain attached to the ‘southern’ end of macrocycle **108** affected negatively the binding with acetate.

3.15 Binding studies with halides

Binding studies were carried out on receptor **108** with TBA chloride and TBA bromide in CDCl_3 . In both cases, appropriate sets of data points could be taken only for the amidic proton *H-a* (Figure 3.26) and for one of the sulfonamidic protons. In all cases, the curves showed a clear 1:1 profile (Figure 3.28).

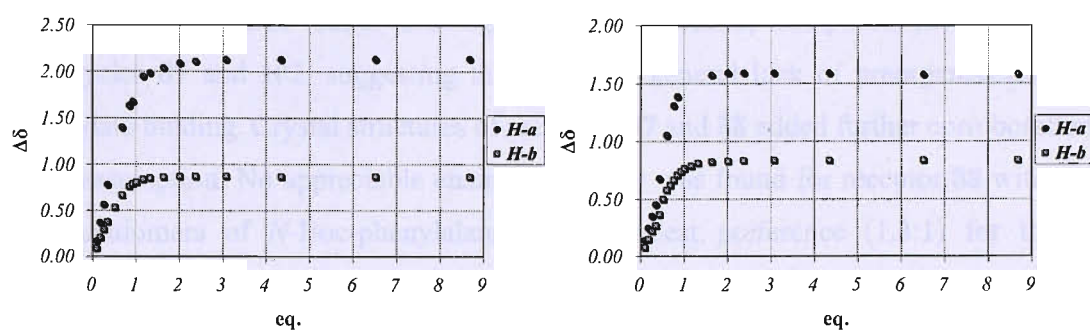


Figure 3.28 Binding titration curves for amidic proton *H-a* and a sulfonamidic proton of receptor **108** upon addition of chloride TBA salt (left) and bromide TBA salt (right).

Again, as in the case of acetate, a low $\Delta\delta_{\text{max}}$ resulted from a sulfonamidic proton. The other one could not be followed due to intense broadening. This result is consistent with a binding mode involving chiefly three *NH* protons, as described in the previous paragraph. With both halides, the binding was too tight to obtain accurate constants. For all curves, values exceeding 10^5 M^{-1} were calculated, with the exception of the titration curve of the *H-a* proton with chloride, which gave a calculated constant of $2.1 \cdot 10^4 \text{ M}^{-1}$. According to the literature on the limits of applicability of traditional NMR titrations in order to measure association constants,^[96,97] for chloride and bromide binding constants were estimated to be $> 10^4 \text{ M}^{-1}$.

A connection is likely to exist between the very high affinity of receptor **108** for halides in CDCl_3 and the high yields for the formation of macrocycles **87**, **88**, **102** and **108** in presence of TBA chloride in the similar solvent DCM. Due to time constraints, this aspect could not be investigated further. Therefore, a more profound study on the relationship between anion complexation and anion-templating effect is highly desirable.

3.16 Conclusions

In this chapter, the synthesis of a new family of sulfonamide-based macrocycles has been described. Macrocycles **87**, **88**, **102** and **108** were prepared via a relatively efficient anion-templated process. Stronger affinity towards carboxylates was found, in comparison with macrocycles reported in the previous chapter. By measuring the binding constants in MeCN-*d*₃ in presence of a known amount of water, accurate values for 1:1 complexes were obtained allowing comparisons among different anions and different receptors. Receptors **88** and **102** had proven to be selective for acetate. Flexible macrocycle **88** showed better binding with TBA acetate, compared to more rigid macrocycles **87** and **102**, suggesting the idea of a general lack of preorganisation for carboxylate binding. Crystal structures of receptors **87** and **88** added further corroboration to this assumption. No appreciable enantioselectivity was found for receptor **88** with the two enantiomers of *N*-Boc-phenylalanine and modest preference (1.3:1) for the L enantiomer was showed by receptor **102**. Soluble receptor **108** showed strong affinity towards halides in CDCl₃. This fact is likely to be connected with the anion-templating effect displayed by TBA chloride in the synthesis of macrocycles **87**, **88**, **102** and **108**. The most relevant results obtained from the binding studies described in this chapter are summarised in **Table 3.9**.

Host	Guest	$K_a (M^{-1})$	Error	Solvent
87	TBAOAc	351	5%	MeCN- d_3 /2% H_2O
88	TBACl	4260	< 1%	MeCN- d_3
	TBABr	1065	2%	
	TBAOAc	540	< 5%	MeCN- d_3 /2% H_2O
	TBAH ₂ PO ₄	281	< 5%	
	TBACl	183	2%	
	TBABr	111	2%	
	N-Boc-L-Phe-OTBA	264	< 5%	
N-Boc-D-PheOTBA	241	< 5%		
102	TBAOAc	2690	< 5%	MeCN- d_3 /1% H_2O
	TBAH ₂ PO ₄	866	< 5%	
	TBACl	328	11%	
	TBABr	134	13%	
	TBAOAc	372	< 5%	MeCN- d_3 /2% H_2O
	TBAH ₂ PO ₄	201	< 5%	
	TBACl	104	*	
	TBABr	55	*	MeCN- d_3 /1% H_2O
	N-Boc-L-Phe-OTBA	742	< 5%	
N-Boc-D-PheOTBA	582	< 5%		
108	TBACl	>10 ⁴	—	CDCl ₃
	TBABr	>10 ⁴	—	

(* low percentage of saturation)

Table 3.9

Chapter IV

Bis-Sulfonamide Based Macrocycles Bearing Polar Groups

4.1 Introduction

Macrocycles **88** and **102** displayed good binding and selectivity for carboxylate anions. However, poor enantioselectivity was found in binding studies with the two enantiomers of *N*-Boc-phenylalanine. This result was explained assuming a binding mode in which the chirophore groups of host and guest are at considerable distance from each other (see § 3.12). On the basis of this assumption, it was decided to derivatise the macrocyclic scaffold with polar groups, with the purpose of introducing additional interactions with the guest. In this manner, closer proximity between host and guest can be favoured, enhancing the chances of enantioselectivity (**Figure 4.1**).

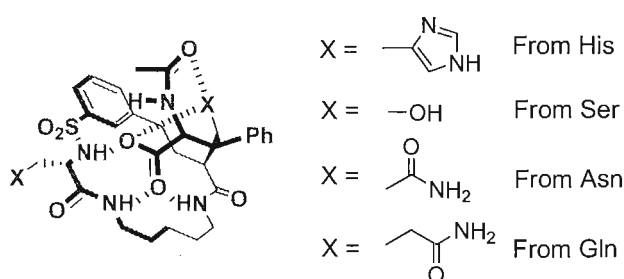
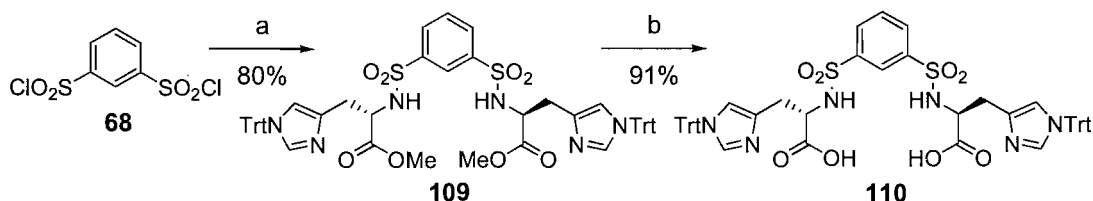


Figure 4.1 Possible effect of introducing polar groups in bis-sulfonamide based macrocycles.

Polar groups can be introduced easily by varying the side chain of the amino acid precursor. It was, therefore, decided to incorporate an imidazole moiety starting from a histidine derivative, a hydroxyl group from a serine derivative and a primary amide moiety with two different spacers from asparagine and glutamine derivatives (**Figure 4.1**). Because of the better binding found for flexible receptor **88**, compared to more rigid **87** and **102**, it was decided to incorporate the flexible 1,5-diaminopentane spacer at the 'southern' end.

4.2 Synthesis of macrocycle 112

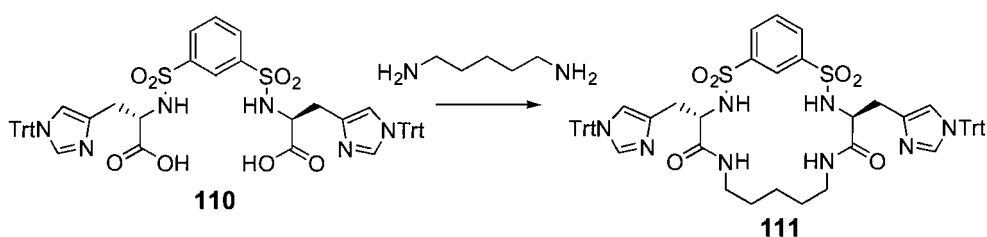
In order to incorporate two imidazole groups in a bis-sulfonamide based macrocyclic scaffold, bis-acid **110** was obtained easily in two steps from bis-sulfonyl chloride **68** (Scheme 4.1).



Scheme 4.1 Reagents and conditions: a) *H*-His(τ -Trt)-OMe-HCl, Et_3N , DCM; b) 60:40 1,4-dioxane/1 M LiOH.

Bis-sulfonyl chloride **68** was coupled with trityl-protected histidine methyl ester to give bis-ester intermediate **109** in good yield. Bis-acid **110** was obtained after hydrolysis in excellent yield.

Disappointingly, all attempts to obtain the pentafluorophenol ester of bis-acid **110** failed. It was thus decided to try a variety of different coupling procedures^[132] in order to synthesise protected macrocycle **111** (Scheme 4.2).



Scheme 4.2

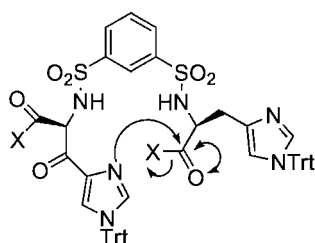
Only CDI coupling, among the various methods, gave access to macrocycle **111**, with a very low yield. Table 4.1 summarises the different coupling conditions which had been tested.

Coupling reagent	Activating group	Solvent	Base	Yield
DCC	PFP	DCM	Et ₃ N	—
PyBOP	—	DCM	DMAP	—
EDC	HOSu	DCM	Et ₃ N	—
EDC	HOSu	DME	Et ₃ N	—
EDC	HOBt	DCM	DIPEA	—
CDI	—	THF	Et ₃ N	3%

Table 4.1

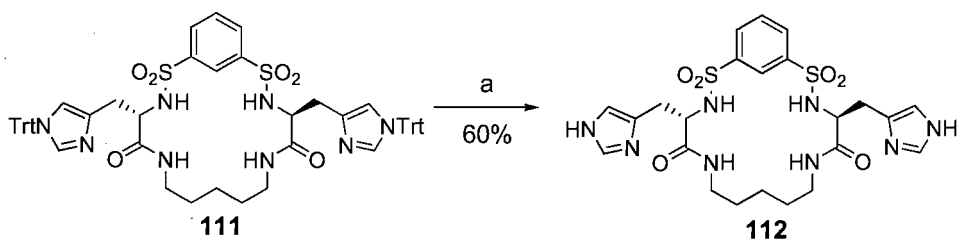
CDI coupling had proven to be scale-sensitive. Several reactions on small scale, hence, were performed in order to accumulate a viable amount of macrocycle **111**.

A possible explanation of the reluctance to cyclise showed by bis-acid **110** can be found in the presence of two imidazoles in the molecule. It has been proven that trityl-protected imidazoles can act as nucleophiles.^[133] Therefore, the hydrolysis of the activated ester can be initiated by intramolecular nucleophilic attack from the neighbouring imidazole group (Figure 4.2).

Figure 4.2 Proposed mechanism for the hydrolysis of the activated ester of bis-acid **110**.

In another plausible mechanism, the imidazole group can hydrolyse the activated ester acting as a neighbouring base.^[134]

Macrocycle **111** was finally deprotected^[135] to give receptor **112** (Scheme 4.3).



Scheme 4.3 Reagents and conditions: a) TFA.

The harsh conditions used for the deprotection might have caused the relatively low efficiency of this transformation.

4.3 Binding studies

Macrocycle **112** was insoluble in the most commonly used solvents, with the exception of MeOH and DMSO. For this reason, binding studies were carried out in DMSO- d_6 with TBA acetate. Sulfonamidic protons could not be followed due to intense broadening, while the amidic protons did not show significant changes in the chemical shift. Conversely, a considerable $\Delta\delta_{\max}$ towards upfield was registered for the CH protons on the imidazole groups (**Figure 4.3**).

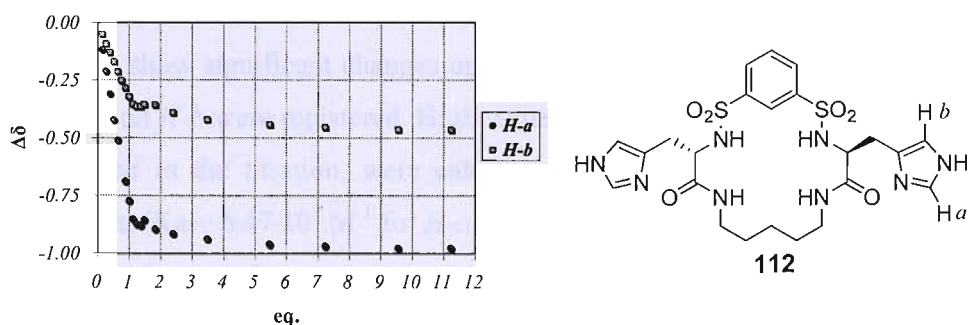


Figure 4.3 Titration curves for *H-a* and *H-b* protons of receptor **112** upon addition of acetate TBA salt in DMSO- d_6 .

The curves seem to indicate a tight 1:1 binding, although, in the range between one and two equivalents of guest added, a deviation from the 1:1 pattern seems to occur. The curve obtained from following *H-a* protons could be reasonably fitted in the 1:1 treating program and a considerably high constant was obtained ($K_a > 10^4 \text{ M}^{-1}$). The curve obtained from *H-b* protons resulted poorly fitted in the 1:1 treating program and gave the indicative value of $K_a \sim 6 \cdot 10^3 \text{ M}^{-1}$. Binding studies were repeated in the more competitive solvent mixture DMSO- d_6 /5% H_2O (**Figure 4.4**).

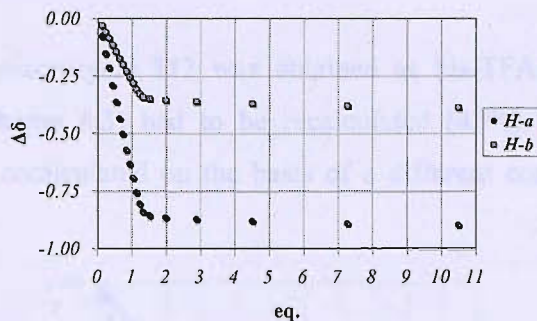


Figure 4.4 Titration curves for *H-a* and *H-b* protons of receptor **112** upon addition of acetate TBA salt in DMSO- d_6 /5% H_2O .

A part from the fact that the deviation from the 1:1 pattern had disappeared, no other change from the titration conducted in neat DMSO- d_6 was registered. Again, amidic protons did not show significant changes upon addition of the guest solution and similar $\Delta\delta_{\max}$ for *H-a* and *H-b* were registered. High values for the binding constants, considering the solvent used in the titration, were calculated from an acceptable fit with the 1:1 treating program ($K_a = 6.47 \cdot 10^3 \text{ M}^{-1}$ for *H-a* and $K_a = 4.45 \cdot 10^3 \text{ M}^{-1}$ for *H-b*).

The fact that the increased water content had very little influence on titration curves and the negligible $\Delta\delta_{\max}$ observed for amidic protons were in contrast with the general pattern of anion binding showed by bis-sulfonamide based macrocycles previously described. At this regard, the possibility that one or both imidazole groups might remain protonated after purification was considered. In that case, macrocycle **112** would be present in solution as a TFA salt. Therefore, upon addition of guest aliquots, acetate would replace the non-basic TFA anion as counterion of the protonated imidazole groups. According to this hypothesis, the upfield shift would be caused by the formation of a new ionic couple between macrocycle **112** and the more basic acetate anion.

Evidence that macrocycle **112** was obtained as a TFA salt arose from ^{19}F NMR, which indicated the presence of trifluoroacetate. The elemental analysis, moreover, indicated the bis-protonated species as the more likely (**Table 4.2**).

	C (%)	H (%)	N (%)
112	47.74	5.23	19.36
112·TFA	43.35	4.51	16.18
112·2TFA	40.20	4.00	13.89
Found	39.91	4.19	13.10

Table 4.2

Due to the fact that macrocycle **112** was obtained as bis-TFA salt, the yield of the deprotection step (**Scheme 4.3**) had to be recalculated (42%). The curves shown in **Figure 4.4** were also recalculated on the basis of a different concentration of the host (**Figure 4.5**).

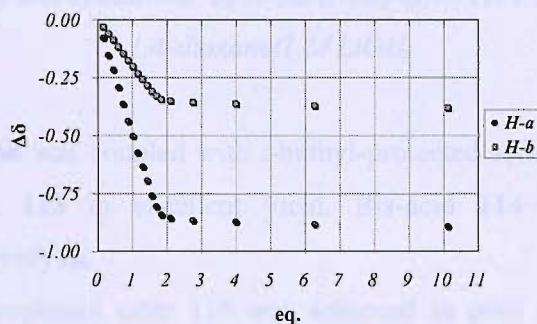


Figure 4.5 Recalculated titration curves for H-a and H-b protons of receptor **112** upon addition of acetate TBA salt in DMSO- d_6 /5% H_2O .

Taking into account the new formula weight, the equivalency point was reached, for both protons, at 2 equivalents of guest added. This fact corroborated the above mentioned observations.

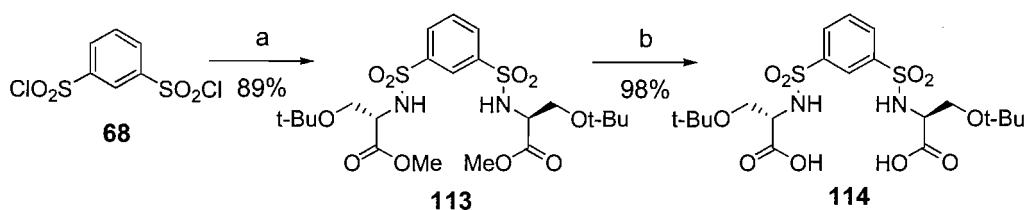
All attempts to obtain a crystal structure of **112** as conclusive evidence unfortunately failed.

Because of the inefficient synthesis of protected macrocycle **111** and because of the difficulty to obtain receptor **112** in a neutral form, no further studies on bis-sulfonamide macrocycles bearing imidazole groups were conducted.

4.4 Synthesis of macrocycle **117**

After the problems encountered with the incorporation of imidazole units, it was decided to introduce hydroxyl groups in the general macrocyclic structure shown in **Figure 3.1**.

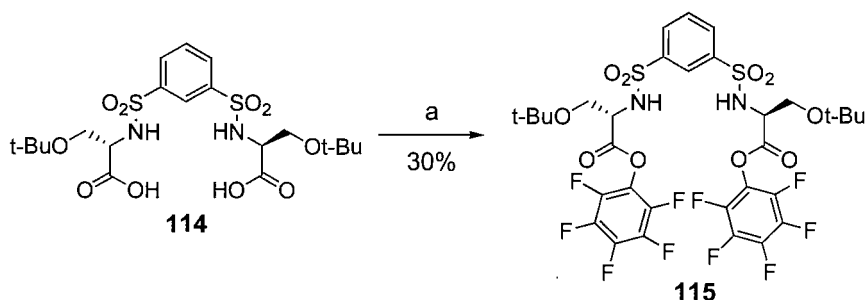
Bis-acid **114** was easily prepared in two steps from bis-sulfonyl chloride **68** by following the general synthetic route which led successfully to macrocycles **87**, **88**, **102**, and **108** (**Scheme 4.4**).



Scheme 4.4 Reagents and conditions: a) *H*-Ser(*t*-Bu)-OMe·HCl, Et₃N, DCM; b) 50:50 1,4-dioxane/1 M LiOH.

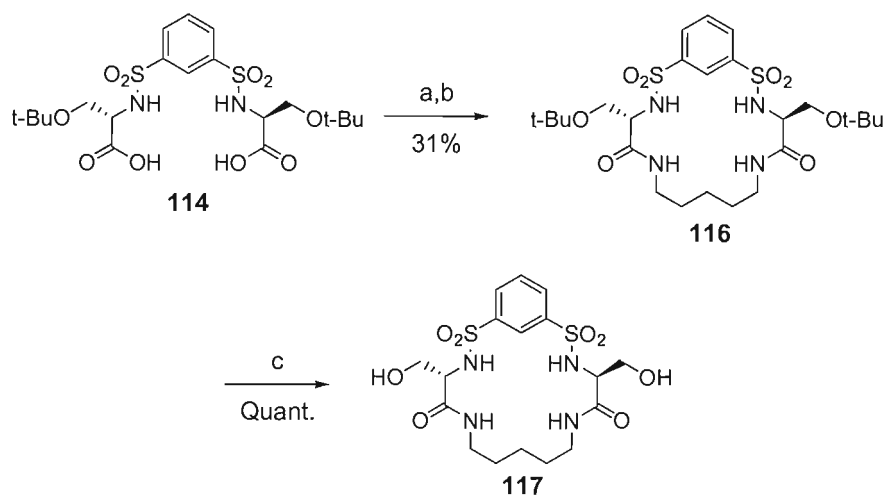
Bis-sulfonyl chloride **68** was coupled with *t*-buthyl-protected serine methyl ester to give bis-ester intermediate **113** in excellent yield. Bis-acid **114** was obtained almost quantitatively after hydrolysis.

Isolation of pentafluorophenol ester **115** was achieved in poor yield. The reason was probably due to decomposition of the product on silica (**Scheme 4.5**).



Scheme 4.5 Reagents and conditions: a) PFP, EDC, DCM.

The reaction was thus repeated and purification consisted exclusively of a simple aqueous work up. Crude pentafluorophenol ester **115** was then coupled with 1,5-diaminopentane under anion-templating conditions to give macrocycle **116**. Receptor **117** was finally obtained after quantitative deprotection carried out under standard conditions (**Scheme 4.6**).



Scheme 4.6 Reagents and conditions: a) PFP, EDC, DCM; b) 1,5-diaminopentane, TBACl, Et₃N, DCM; c) 80:20 DCM/TFA.

Macrocycle **117** was synthesised with an acceptable 31% overall yield from bis-acid **114**. A crystal structure was obtained. Receptor **117** crystallised with three molecules of water (Figure 4.6).

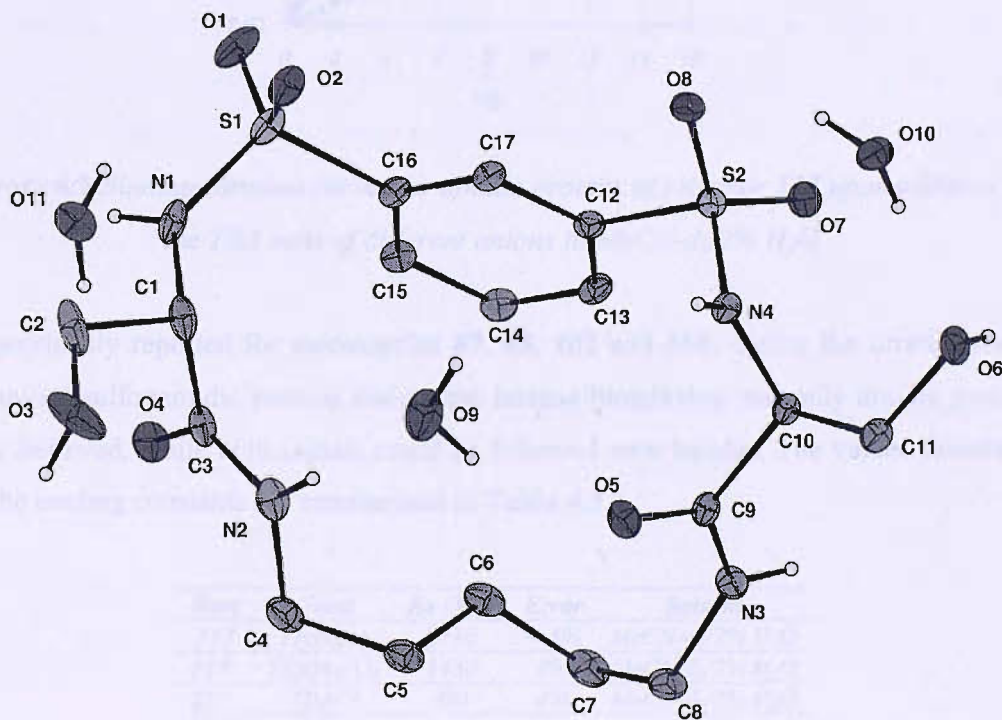


Figure 4.6 Crystal structure of macrocycle **117**. Thermal ellipsoids drawn at the 35% probability level, non acidic hydrogens omitted for clarity.

Again, as in the case of receptors **87** and **88**, the crystal structure presented an ‘alternate’ motif. N_4H was interacting with an amidic carbonyl of an adjacent molecule [$N_4 \cdots O_4$ 2.926(3) Å], while the other NH bonds were mainly involved in interactions with the molecules of water.

4.5 Binding studies with simple anions in MeCN- d_3 /2% H₂O

Receptor **117** proved to be soluble in MeCN- d_3 . For this reason, in order to make a comparison with receptors **88** and **102**, binding studies were carried out with simple anions in MeCN- d_3 /2% H₂O.

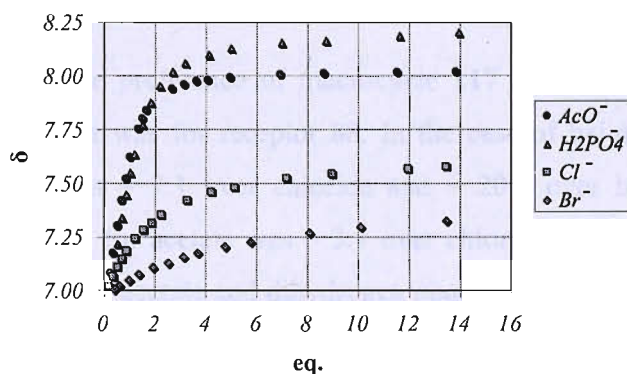


Figure 4.7 Binding titration curves for amidic protons of receptor **117** upon addition of the TBA salts of different anions in MeCN- d_3 /2% H₂O.

As previously reported for macrocycles **87**, **88**, **102** and **108**, during the titrations with oxyanions sulfonamidic protons underwent intense broadening and only amidic protons were followed, while both signals could be followed with halides. The values calculated for the binding constants are summarised in **Table 4.3**.

Host	Guest	K_a (M^{-1})	Error	Solvent
117	TBAOAc	2730	< 5%	MeCN- d_3 /2% H ₂ O
117	TBAH ₂ PO ₄	1430	8%	MeCN- d_3 /2% H ₂ O
117	TBACl	391	4%	MeCN- d_3 /2% H ₂ O
117	TBABr	137	5%	MeCN- d_3 /2% H ₂ O

Table 4.3

In this series of experiments, receptor **117** showed strong affinity for oxyanions. The binding constants obtained with TBA acetate and dihydrogen phosphate were considerably higher than those obtained with macrocycles built from valine. The ratio between the values obtained from macrocycles **117** and **88** was $\sim 5:1$ in favour of **117** for both acetate and dihydrogen phosphate. Between **117** and **102** the ratio was $\sim 7:1$ (Table 4.4).

<i>Host</i>	<i>Guest</i>	<i>K_a (M⁻¹)</i>	<i>Error</i>	<i>Solvent</i>
117	TBAOAc	2730	< 5%	MeCN- <i>d</i> ₃ /2% H ₂ O
88	TBAOAc	540	< 5%	MeCN- <i>d</i> ₃ /2% H ₂ O
102	TBAOAc	372	< 5%	MeCN- <i>d</i> ₃ /2% H ₂ O
117	TBAH ₂ PO ₄	1430	8%	MeCN- <i>d</i> ₃ /2% H ₂ O
88	TBAH ₂ PO ₄	281	< 5%	MeCN- <i>d</i> ₃ /2% H ₂ O
102	TBAH ₂ PO ₄	201	< 5%	MeCN- <i>d</i> ₃ /2% H ₂ O

Table 4.4

In terms of selectivity, the preference of macrocycle **117** for acetate over dihydrogen phosphate was $\sim 2:1$, as it was for receptor **88**. In the case of halides, conversely, the preference for acetate was $\sim 7:1$ over chloride and $\sim 20:1$ over bromide, whilst for receptor **88** the preference for acetate was $\sim 3:1$ over chloride and $\sim 5:1$ over bromide. The increased selectivity for acetate and dihydrogen phosphate can be certainly related to the presence of the hydroxyl groups on receptor **117**.^[136] At this regard, it is plausible to assume the presence of a favourable three-centred hydrogen bonding interaction involving the hydroxyl groups of receptor **117** and the negatively charged oxygen of the guest (see § 1.7.4).

4.6 Binding studies with various amino acids in MeCN-*d*₃/2% H₂O

After the encouraging results obtained with TBA acetate, macrocycle **117** was tested for enantioselectivity with the two enantiomers of *N*-Ac-phenylalanine.

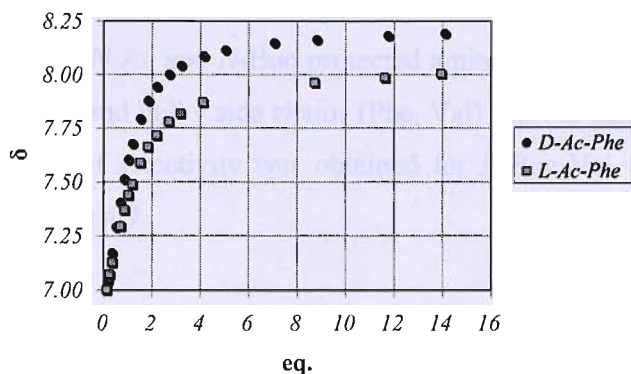


Figure 4.8 Binding titration curves for amidic protons of receptor **117** upon addition of the TBA salts of the two enantiomers of *N*-Ac-Phe in MeCN- d_3 /2% H_2O .

Again sulfonamidic protons underwent intense broadening and thus only amidic protons could be followed. Although the profile of the curves shown in **Figure 4.8** is similar, the addition of the D enantiomer to a solution of macrocycle **117** provoked higher changes in chemical shift and a more pronounced curvature compared to the L enantiomer. The result was a higher binding constant ($K_a = 1490 \text{ M}^{-1}$ for Ac-D-Phe and $K_a = 934 \text{ M}^{-1}$ for Ac-L-Phe). Other TBA salts of *N*-protected amino acids were investigated. The TBA salts of the two enantiomer of α -hydroxy-acid mandelic acid were studied as well. The results are summarised in **Table 4.5**.

Host	Guest	$K_a \text{ (M}^{-1}\text{)}$	Error	Solvent	Selectivity (D/L)
117	<i>N</i> -Ac-D-Ala-OTBA	1240	< 5%	MeCN- d_3 /2% H_2O	1.5:1
117	<i>N</i> -Ac-L-Ala-OTBA	838	< 5%	MeCN- d_3 /2% H_2O	
117	<i>N</i> -Boc-D-Phe-OTBA	1180	< 5%	MeCN- d_3 /2% H_2O	1.4:1
117	<i>N</i> -Boc-L-Phe-OTBA	858	< 5%	MeCN- d_3 /2% H_2O	
117	<i>N</i> -Ac-D-Phe-OTBA	1490	< 5%	MeCN- d_3 /2% H_2O	1.6:1
117	<i>N</i> -Ac-L-Phe-OTBA	934	< 5%	MeCN- d_3 /2% H_2O	
117	<i>N</i> -Boc-D-Val-OTBA	1640	< 5%	MeCN- d_3 /2% H_2O	1.7:1
117	<i>N</i> -Boc-L-Val-OTBA	976	< 5%	MeCN- d_3 /2% H_2O	
117	<i>N</i> -Boc-D-Ser-OTBA	469	< 5%	MeCN- d_3 /2% H_2O	1.1:1
117	<i>N</i> -Boc-L-Ser-OTBA	426	< 5%	MeCN- d_3 /2% H_2O	
117	<i>N</i> -Boc-D-Gln-OTBA	679	< 5%	MeCN- d_3 /2% H_2O	1:1
117	<i>N</i> -Boc-L-Gln-OTBA	670	< 5%	MeCN- d_3 /2% H_2O	
117	<i>R</i> -Mand-OTBA	489	< 5%	MeCN- d_3 /2% H_2O	1.3:1
117	<i>S</i> -Mand-OTBA	369	< 5%	MeCN- d_3 /2% H_2O	

Table 4.5

In all cases only amidic protons could be followed, due to intense broadening of sulfonamidic protons. All curves showed an excellent fit in the 1:1 treating program. For

amino acids with non-polar side chains the moderate enantioselectivity found for *N*-Ac-Phe proved to be general. *N*-Ac and *N*-Boc protected amino acids showed similar values of selectivity. Small (Ala) and bulky side chains (Phe, Val) showed similar values as well. The best result in terms of selectivity was obtained for *N*-Boc-Val. The profile of the curves is showed in **Figure 4.9**.

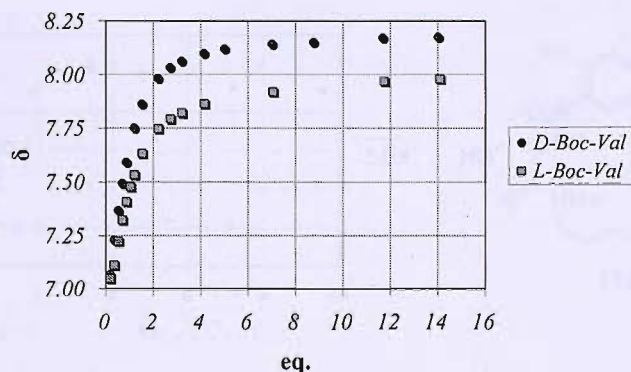


Figure 4.9 Binding titration curves for amidic protons of receptor **117** upon addition of the TBA salts of the two enantiomers of *N*-Boc-Val in MeCN- d_3 /2% H_2O .

Surprisingly, amino acids with polar side chains such as *N*-Boc-Ser and *N*-Boc-Gln showed sensibly lower binding constants and practically no selectivity. Due to the presence of several hydrogen bonding donors and acceptors on both host and guest, a strong and selective binding was expected. Probably the presence of *inter*- or *intra*-molecular interactions between the polar side chain of the amino acid and the carboxylate moiety somehow affected the binding with macrocycle **117**. This explanation can also account for the low binding constants obtained from the two enantiomers of mandelic acid, although some enantioselectivity was found in this case.

The fact that all constants obtained with amino acids were lower than the one obtained with acetate seems to suggest that, a part from the binding between the carboxylate anion and the hydrogen bonding donors of the receptor, no other significant dipolar attractive interactions between host and guest were present. For this reason, the enantioselectivity displayed by receptor **117** may depend largely on steric repulsion. In absence of crystal structures of the complexes, however, this conclusion remains speculative.

4.7 Binding studies with TBA acetate in DMSO- d_6

Binding studies were carried out on macrocycle **117** in DMSO- d_6 . When TBA acetate was used as guest, the results were very similar to those obtained with receptor **88** (see § 3.11). Again the curve resulting from following the amidic protons showed an unusual profile indicating the presence of a 1:2 complex (**Figure 4.10**).

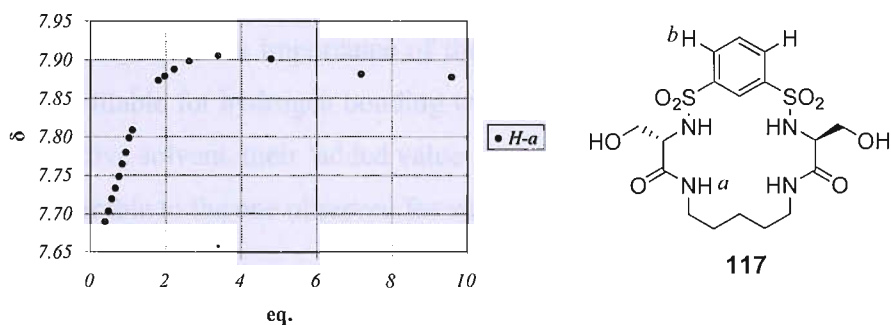


Figure 4.10 Titration curve for *H-a* protons of receptor **117** upon addition of acetate TBA salt in DMSO- d_6 .

Poor fit resulted with the 1:2 treating program and the output parameters were nonsensical (see § 2.2). As for receptor **88**, the indicative values of the binding constants so obtained ($K_{a1:1} \sim 10^3 \text{ M}^{-1}$ and $K_{a1:2} \sim 3 \text{ M}^{-1}$) were consistent with the general picture of a strong 1:1 binding accompanied by a minor formation of the 1:2 complex. Also in this case, for aromatic protons *H-b* an unusually large upfield $\Delta\delta_{\text{max}}$ was registered (~ 0.30 ppm) (**Figure 4.11**).

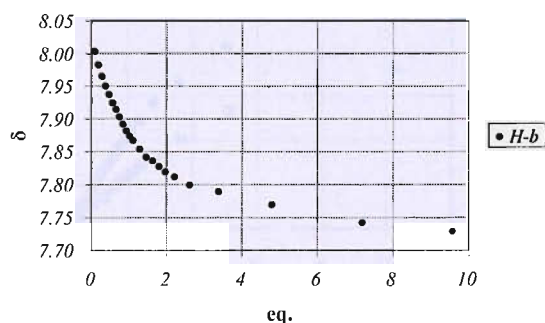


Figure 4.11 Titration curve for *H-b* protons of receptor **117** upon addition of acetate TBA salt in DMSO- d_6 .

The titration curve of *H-b* protons produced an excellent fit with the 1:2 treating program, although the low percentage of saturation affected the accuracy of the calculation. The binding constants observed were $K_{a_{1:1}} = 1408 \text{ M}^{-1}$ and $K_{a_{1:2}} = 5 \text{ M}^{-1}$. They were consistent with those obtained from amidic protons *H-a*. By comparing these figures with the constants obtained with receptor **88** (Table 4.6), the stronger affinity of macrocycle **117** for acetate was confirmed. In the more competitive DMSO- d_6 , however, the selectivity in favour of macrocycle **117** dropped from 5:1 (Table 4.4) to 1.5:1 (Table 4.6). This fact illustrates the importance of the hydroxyl groups on receptor **117**. When they are less available for hydrogen bonding with acetate, because of the interaction with a more competitive solvent, their ‘added value’ is depleted and the strength of the binding becomes comparable to the one observed for valine based receptor **88**.

Host	Guest	$K_{a_{1:1}} (\text{M}^{-1})$	$K_{a_{1:2}} (\text{M}^{-1})$	Error	Solvent
88	TBAOAc	928	6	*	DMSO- d_6
117	TBAOAc	1408	5	*	DMSO- d_6

(* low percentage of saturation)

Table 4.6

4.8 Binding studies with *N*-Ac-phenylalanine in DMSO- d_6

Binding studies were carried out on macrocycle **117** with *N*-Ac-Phe in DMSO- d_6 in order to make a comparison with the positive results obtained in MeCN- d_3 /2% H₂O.

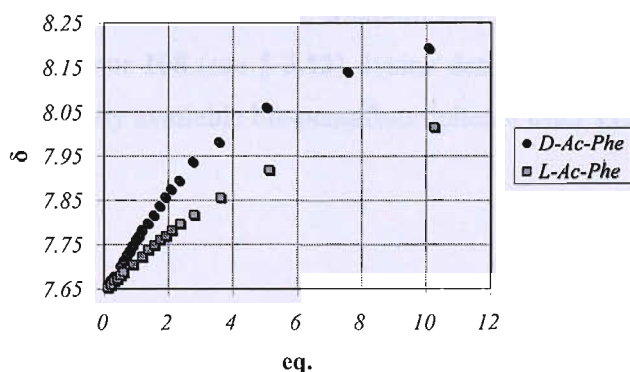


Figure 4.12 Binding titration curves for amidic protons of receptor **117** upon addition of the TBA salts of the two enantiomers of *N*-Ac-Phe in DMSO- d_6 .

In this case, the curves could be fitted with the 1:1 treating program. The values of the association constants were affected by a low percentage of saturation. However, although the absolute values were considerably lower, they indicated quite clearly that the enantioselectivity found in MeCN- d_3 was maintained (Table 4.7).

<i>Host</i>	<i>Guest</i>	<i>K_a (M⁻¹)</i>	<i>Error</i>	<i>Solvent</i>	<i>Selectivity (D/L)</i>
117	<i>N-Ac-D-Phe-OTBA</i>	111	*	DMSO- d_6	1.5:1
117	<i>N-Ac-L-Phe-OTBA</i>	75	*	DMSO- d_6	

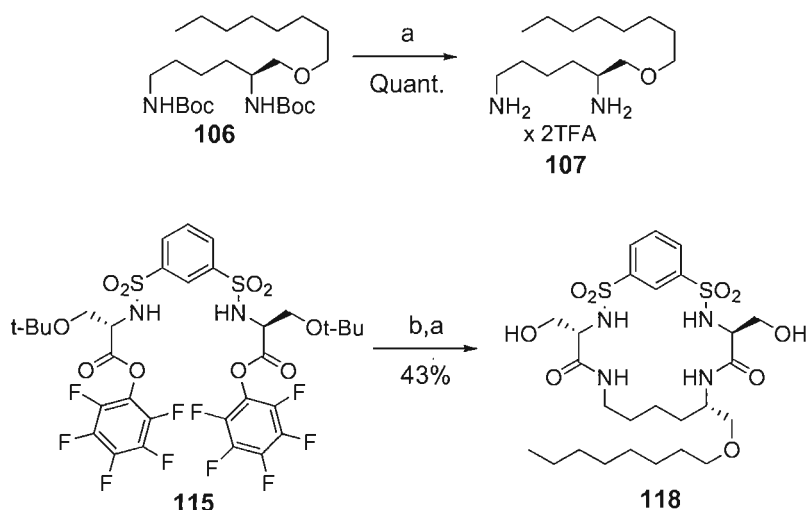
(* low percentage of saturation)

Table 4.7

The fact that a very similar value of enantioselectivity was found in solvents with different polarity, such as DMSO- d_6 and MeCN- d_3 /2% H₂O, seems to indicate, as already suggested in § 4.6, that secondary dipolar interactions between host and guest play a small role in the enantioselectivity, which is probably originated by steric repulsion.

4.9 Synthesis of receptor 118

Macrocycle **117** showed interesting binding properties towards the TBA salts of various amino acids. Binding studies were carried out in MeCN- d_3 /2% H₂O and, in minor extent, in DMSO- d_6 . Binding studies in CDCl₃ were not carried out, because macrocycle **117** was not soluble in this solvent. In order to investigate the influence on binding and enantioselectivity by using a less polar solvent, macrocycle **117** was modified by introducing a flexible aliphatic chain at the 'southern end'. For this purpose, in analogy with the synthesis of receptor **108** (see § 3.13), lysine derivative **106** was coupled, after deprotection, with the already available bis-pentafluorophenol ester **115** (Scheme 4.7).



Scheme 4.7 Reagents and conditions: a) 80:20 DCM/TFA; b) **107**, TBACl, Et_3N , DCM.

The macrocyclisation step was carried out, as previously described, under anion-templating conditions. Receptor **118** was finally obtained in good overall yield after deprotection.

4.10 Binding studies with *N*-Ac-phenylalanine in CDCl_3

Macrocycle **118** proved to be soluble in CDCl_3 . Binding studies, thus, could be carried out in this solvent. *N*-Ac-Phe was chosen in order to test enantioselectivity. During the titration, amidic proton *H-a* (Figure 4.13) and one unassigned sulfonamidic proton were followed. Amidic proton *H-c* could not be followed because of superimposition with other signals, while the other unassigned sulfonamidic proton showed intense broadening.

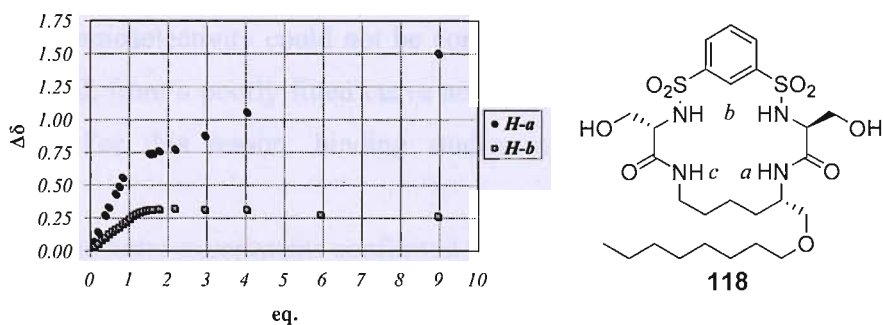


Figure 4.13 Binding titration curves for amidic proton *H-a* and a sulfonamidic proton (*H-b*) of receptor **118** upon addition of *N*-Ac-D-Phe TBA salt in CDCl_3 .

In **Figure 4.13** are showed the results for *N*-Ac-D-Phe. Very similar results were obtained with *N*-Ac-L-Phe (**Figure 4.14**).

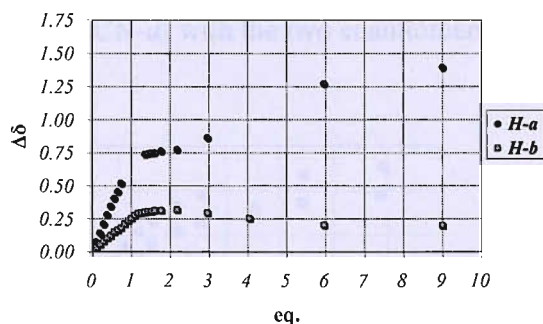


Figure 4.14 Binding titration curves for amidic proton *H*-a and a sulfonamidic proton (*H*-b) of receptor **118** upon addition of *N*-Ac-L-Phe TBA salt in CDCl_3 .

Because of their change in slope after the addition of one equivalent of guest, all curve profiles seemed to indicate the formation of a 1:1 complex accompanied by a 1:2 adduct. The small $\Delta\delta_{\text{max}}$ of a sulfonamidic proton (*H*-b in **Figure 4.14**) associated with the intense broadening of the other one can be ascribed, again, to a binding mode involving mainly three *NH* bonds, one amidic and one sulfonamidic (see § 3.14).

For both enantiomers, the curves obtained from following amidic *H*-a proton gave no fit with any treating program. The curves obtained from following *H*-b gave poor fit with the 1:2 treating program and were characterised by nonsensical output parameters. For this reason, the values obtained have to be taken only as a rough indication. For *N*-Ac-D-Phe $K_{a1:1} \sim 3000 \text{ M}^{-1}$ and $K_{a1:2} \sim 70 \text{ M}^{-1}$, while for *N*-Ac-L-Phe $K_{a1:1} \sim 3000 \text{ M}^{-1}$ and $K_{a1:2} \sim 140 \text{ M}^{-1}$. Although $K_{a1:2}$ for *N*-Ac-L-Phe was twice bigger than for *N*-Ac-D-Phe, the presence of enantioselectivity could not be concluded from these data. The values were obtained, indeed, from a poorly fitted curve and, moreover, $K_{a1:1}$ was the same for both enantiomers. For this reason, binding studies with amino acids in CDCl_3 were abandoned.

The results of the latter experiments confirmed the general tendency of sulfonamide based macrocycles to give complex association modes with oxyanions in non-polar CDCl_3 . Binding studies in this solvent were characterised by the difficulty to quantify with accuracy the association constants and the binding, when it could be assessed, was generally poorer than in $\text{MeCN-}d_3$.

4.11 Binding studies with *N*-Boc-phenylalanine in MeCN-*d*₃

In order to compare macrocycles **117** and **118** in terms of enantioselectivity, binding studies were carried out in MeCN-*d*₃ with the two enantiomers of *N*-Boc-phenylalanine.

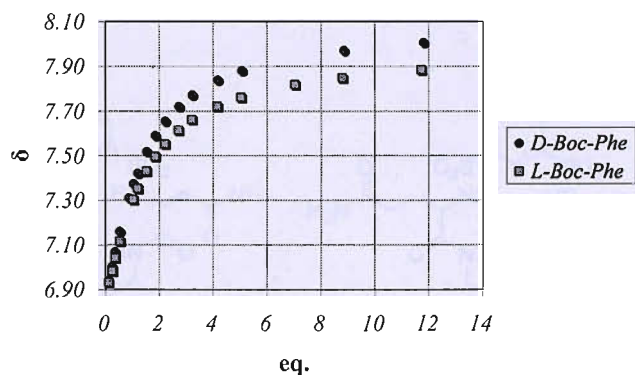


Figure 4.15 Binding titration curves for *H*-*a* amidic proton of receptor **118** upon addition of the TBA salts of the two enantiomers of *N*-Boc-Phe in MeCN-*d*₃/2% H₂O.

H-*a* amidic proton (Figure 4.13) was followed. The curve profiles were similar for the two enantiomers and, hence, only a small preference was found for *N*-Boc-D-Phe (Table 4.8).

Host	Guest	K_a (M^{-1})	Error	Solvent	Selectivity (D/L)
118	<i>N</i> -Boc-D-Phe-OTBA	690	< 5%	MeCN- <i>d</i> ₃ /2% H ₂ O	1.1:1
118	<i>N</i> -Boc-L-Phe-OTBA	644	< 5%	MeCN- <i>d</i> ₃ /2% H ₂ O	

Table 4.8

The introduction of a long aliphatic chain on the parent macrocycle **117** by ether linkage resulted in a decreased binding strength and in an almost complete loss of enantioselectivity. Contrarily to the expectations, the introduction of a long aliphatic chain to help solubility did not have a 'neutral' effect on binding, as already observed for receptor **108** with acetate (see § 3.14), and resulted detrimental in terms of enantioselectivity.

4.12 Synthesis of macrocycles **119** and **120**

The introduction of two hydroxyl groups in the general macrocyclic scaffold had a favourable effect on binding and enantioselectivity. After the extensive studies on macrocycles **117** and **118**, it was decided to explore whether the incorporation of two primary amides could promote again chiral recognition. For this purpose, two different macrocyclic receptor were conceived (**Figure 4.16**).

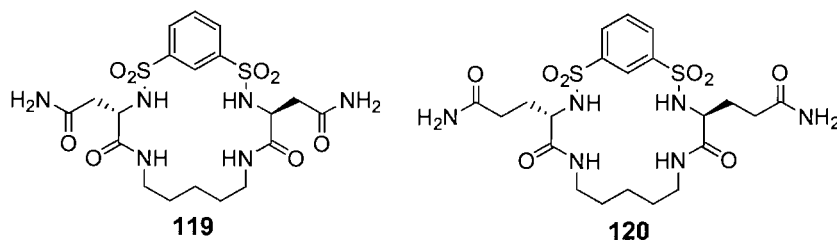
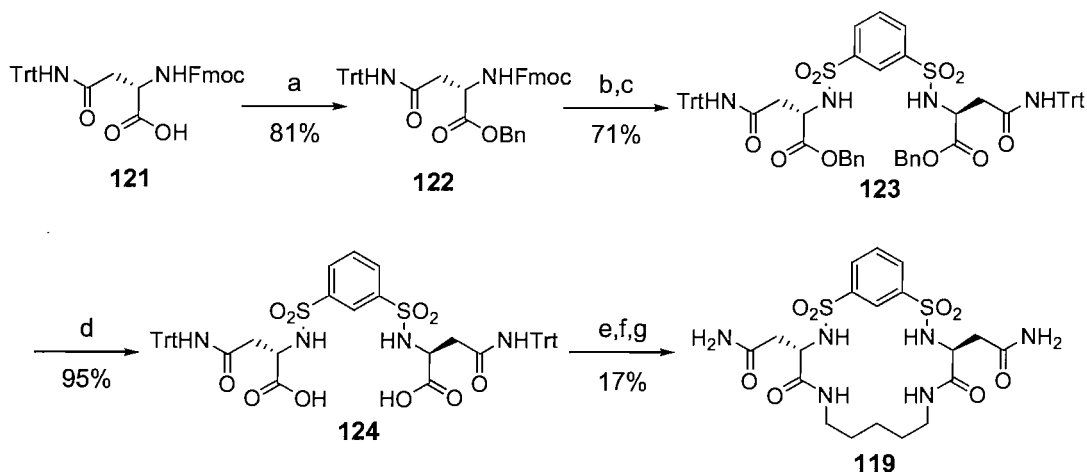


Figure 4.16 Bis-sulfonamide based receptors bearing primary amide moieties.

Macrocycles **119** and **120** are built, respectively, from asparagine and glutamine. They present spacers of different length connecting amidic groups to the macrocyclic core.

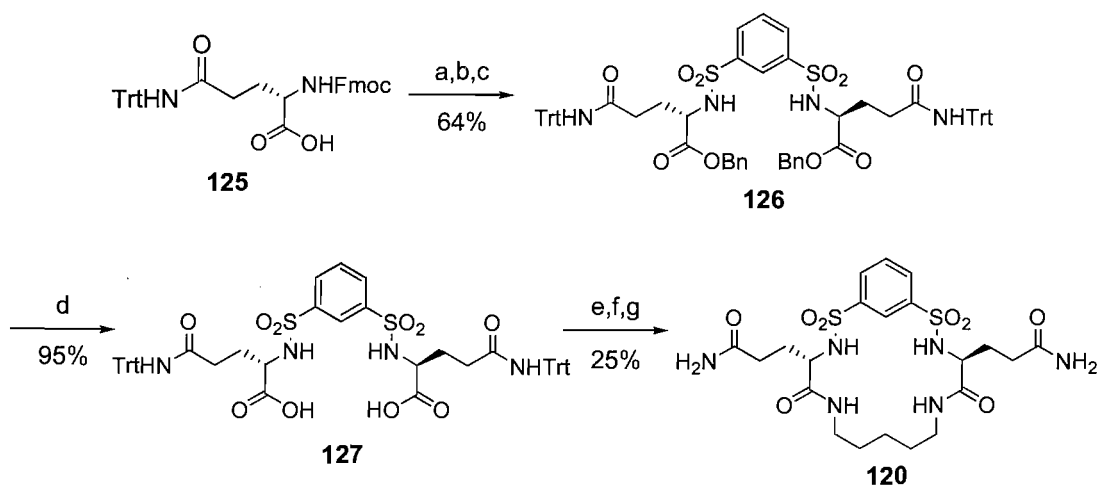
The synthesis of receptor **119** was achieved by following the general route that was used, with the sole exception of histidine based receptor **112**, for all amino acid based macrocycles presented in this work (**Scheme 4.8**).



Scheme 4.8 Reagents and conditions: a) $BnBr$, K_2CO_3 , acetone; b) 80:20 DMF/piperidine; c) benzene-1,3-disulfonyl chloride, Et_3N , DCM; d) Pd/C 10% cat., H_2 , 2:1 MeOH/THF; e) PFP, EDC, DCM; f) 1,5-diaminopentane, TBACl, Et_3N , DCM; g) TFA.

Commercial *N*-Fmoc-Asn(Trt) **121** was benzylated in good yield by following a modified literature procedure.^[123] After deprotection,^[132] bis-ester **123** was obtained by standard coupling with benzene-1,3-disulfonyl chloride **68**.^[94] Benzyl removal was achieved by catalytic hydrogenolysis.^[113] It was found that using a MeOH/THF mixture as solvent, instead of neat MeOH, insured a faster reaction rate and avoided the troublesome precipitation of the product in presence of charcoal. Bis-acid **124** was then converted into its bis-pentafluorophenol ester and coupled, after a quick work-up, with 1,5-diaminopentane under the usual anion-templating conditions. The product of the coupling was immediately deprotected to give macrocycle **119** in reasonable overall yield from bis-acid **124**.

Macrocycle **120** was synthesised using the same strategy (Scheme 4.9).



Scheme 4.9 Reagents and conditions: a) *BnBr*, K_2CO_3 , acetone; b) 80:20 DMF/piperidine; c) benzene-1,3-disulfonyl chloride, Et_3N , DCM; d) Pd/C 10% cat., H_2 , 2:1 MeOH/THF; e) PFP, EDC, DCM; f) 1,5-diaminopentane, TBACl, Et_3N , DCM; g) TFA.

Unlike the synthesis of macrocycle **119**, benzyl ester of commercial *N*-Fmoc-Gln(Trt) **125** was not isolated from the reaction solution. Once dried, indeed, it stayed as a gel and was practically insoluble in any solvent. Receptor **120** was finally obtained in acceptable overall yield from bis-acid **127**.

4.13 Binding studies with *N*-Ac-phenylalanine in DMSO-*d*₆

Macrocycles **119** and **120** proved to be insoluble in the most commonly used solvents, especially in MeCN-*d*₃ and CDCl₃. Binding studies, therefore, were not allowed in these solvents. Macrocycle **119**, moreover, showed only limited solubility in DMSO-*d*₆, although the concentration obtained was reasonably high to perform binding studies. Macrocycle **120** proved to be largely soluble in DMSO-*d*₆. For this reason, in order to have a comparison with receptor **117** (see § 4.8), binding studies were carried out for both receptors with the two enantiomers of *N*-Ac-phenylalanine in DMSO-*d*₆.

In the case of macrocycle **119**, only amidic protons *H*-*a* (**Figure 4.17**) could be followed, due to large broadening of the sulfonamidic peaks. Amidic protons on the side arms showed only small changes in chemical shift upon addition of the guest.

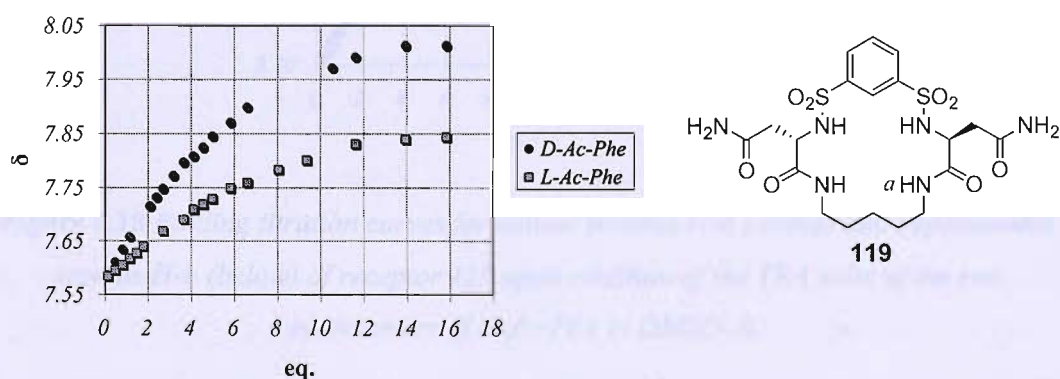


Figure 4.17 Binding titration curves for amidic protons of receptor **119** upon addition of the TBA salts of the two enantiomers of *N*-Ac-Phe in DMSO-*d*₆.

The profile of the curves seemed to indicate a large preference for the D enantiomer. The values obtained with the 1:1 titrating program, however, showed only a modest enantioselectivity with a 1.3:1 D/L ratio ($K_a = 83 \text{ M}^{-1}$ for *N*-Ac-D-Phe and $K_a = 63 \text{ M}^{-1}$ for *N*-Ac-L-Phe). The results, moreover, were affected by low percentage of saturation, and thus the values have to be taken as an indication.

A similar picture was found for receptor **120**. In this case, however, both amidic and sulfonamidic signals could be followed (**Figure 4.18**).

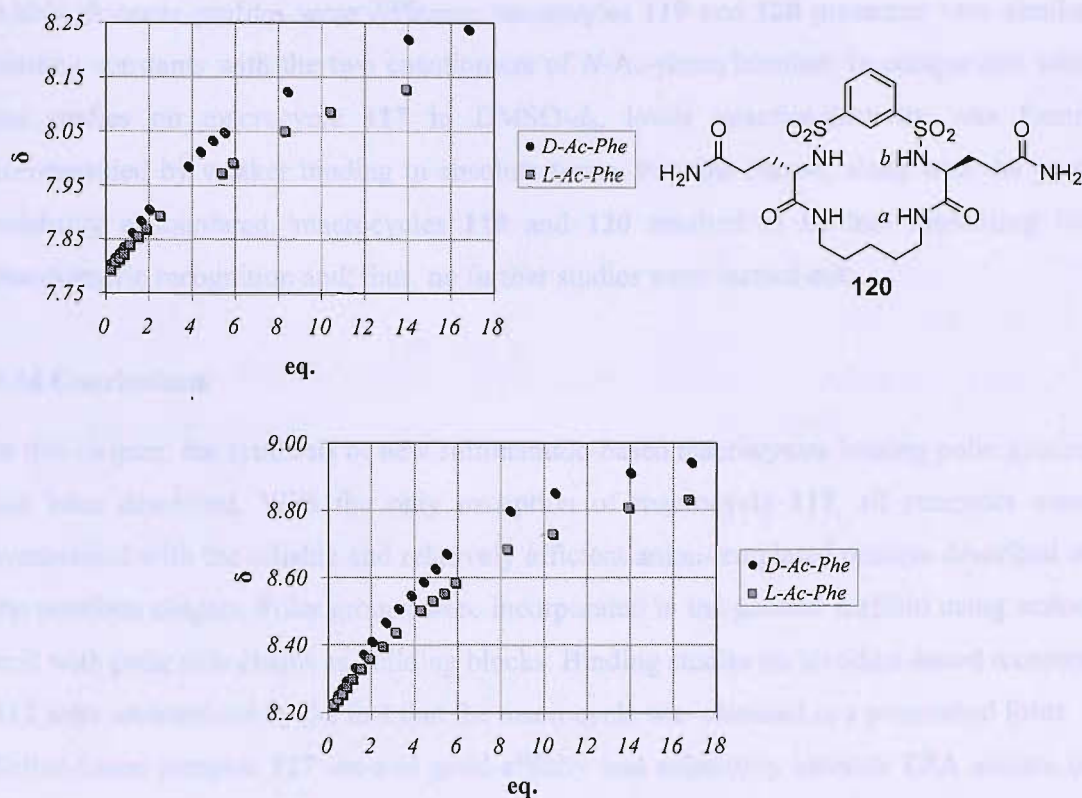


Figure 4.18 Binding titration curves for amide protons H-a (above) and sulfonamidic protons H-b (below) of receptor **120** upon addition of the TBA salts of the two enantiomers of *N*-Ac-Phe in $\text{DMSO-}d_6$.

All curves were characterised by low percentage of saturation and hence the values obtained have to be taken as an indication. The constants were calculated as the average of the values obtained from the two curves. For receptor **120**, again, a modest preference for the D enantiomer was found ($K_a = 85 \text{ M}^{-1}$ for *N*-Ac-D-Phe and $K_a = 64 \text{ M}^{-1}$ for *N*-Ac-L-Phe, enantioselectivity $\sim 1.3:1$).

The data for the two receptors are summarised in **Table 4.9**.

Host	Guest	$K_a (\text{M}^{-1})$	Error	Solvent	Selectivity (D/L)
119	<i>N</i> -Ac-D-Phe-OTBA	83	*	$\text{DMSO-}d_6$	1.3:1
119	<i>N</i> -Ac-L-Phe-OTBA	63	*	$\text{DMSO-}d_6$	
120	<i>N</i> -Ac-D-Phe-OTBA	85	*	$\text{DMSO-}d_6$	1.3:1
120	<i>N</i> -Ac-L-Phe-OTBA	64	*	$\text{DMSO-}d_6$	

(* low percentage of saturation)

Table 4.9

Although curve profiles were different, macrocycles **119** and **120** presented very similar binding constants with the two enantiomers of *N*-Ac-phenylalanine. In comparison with the studies on macrocycle **117** in DMSO-*d*₆, lower enantioselectivity was found accompanied by weaker binding in absolute terms. For this reason, along with the poor solubility encountered, macrocycles **119** and **120** resulted to be less interesting for enantiomeric recognition and, thus, no further studies were carried out.

4.14 Conclusions

In this chapter, the synthesis of new sulfonamide-based macrocycles bearing polar groups has been described. With the only exception of macrocycle **112**, all receptors were synthesised with the reliable and relatively efficient anion-templated process described in the previous chapter. Polar groups were incorporated in the general scaffold using amino acid with polar side chains as building blocks. Binding studies on histidine-based receptor **112** were undermined by the fact that the macrocycle was obtained in a protonated form. Serine-based receptor **117** showed good affinity and selectivity towards TBA acetate in the solvent mixture MeCN-*d*₃/2% H₂O. Compared to the valine-based receptor **88** described in the previous chapter, a five-time greater constant was found. The enhanced binding can be ascribed to the presence of additional hydrogen bonding deriving from the hydroxyl groups incorporated in receptor **117**. Receptor **117**, moreover, displayed moderate enantiomeric recognition with the TBA salts of protected amino acid with non-polar side chains. Although these enantioselectivities were comprised only between 1.4:1 and 1.7:1, the preference for the D enantiomer proved to be general in the case of non-polar side chains. In case of polar side chains, conversely, no significant enantioselectivity and lower binding constants in absolute terms were found. This result can be explained with the presence of *inter*- or *intra*-molecular interactions between the polar side chain of the amino acid and the negatively charged carboxylate moiety. Receptor **117** proved to be enantioselective in competitive DMSO-*d*₆ as well, although binding constants were markedly lower in this solvent.

Receptor **117** was subsequently modified into receptor **118** with the introduction of a long aliphatic chain at the 'southern' end, in order to perform binding studies in CDCl₃. Unfortunately, multiple equilibria were present and apparently no enantioselectivity was found. Binding studies on receptor **118** were then carried out in MeCN-*d*₃/2% H₂O. In comparison with the parent macrocycle **117**, enantioselectivity resulted significantly

reduced as well as the values of binding constants. The latter result demonstrated that the introduction of an apparently 'neutral' group, such as a long aliphatic chain, can have serious consequences on binding efficacy.

Macrocycles **119** and **120**, in the end, were synthesised using asparagine and glutamine as building blocks. The primary amide groups were responsible for the poor solubility of these receptors without bringing any improvement in terms of binding or enantioselectivity.

The most relevant results obtained from the binding studies described in this chapter are summarised in **Table 4.10**.

Host	Guest	K_a (M^{-1})	Error	Solvent	
117	TBAOAc	2730	< 5%	MeCN- d_3 /2% H_2O	
	TBAH ₂ PO ₄	1430	8%		
	TBACl	391	4%		
	TBABr	137	5%		
	N-Ac-D-Ala-OTBA	1240	< 5%	MeCN- d_3 /2% H_2O	
	N-Ac-L-Ala-OTBA	838	< 5%		
	N-Boc-D-Phe-OTBA	1180	< 5%		
	N-Boc-L-Phe-OTBA	858	< 5%		
	N-Ac-D-Phe-OTBA	1490	< 5%		
	N-Ac-L-Phe-OTBA	934	< 5%		
	N-Boc-D-Val-OTBA	1640	< 5%		
	N-Boc-L-Val-OTBA	976	< 5%		
	N-Boc-D-Ser-OTBA	469	< 5%		
	N-Boc-L-Ser-OTBA	426	< 5%		
	N-Boc-D-Gln-OTBA	679	< 5%		
	N-Boc-L-Gln-OTBA	670	< 5%		
	R-Mand-OTBA	489	< 5%		
	S-Mand-OTBA	369	< 5%		
	N-Ac-D-Phe-OTBA	111	*		DMSO- d_6
	N-Ac-L-Phe-OTBA	75	*		
118	N-Boc-D-Phe-OTBA	690	< 5%	MeCN- d_3 /2% H_2O	
	N-Boc-L-Phe-OTBA	644	< 5%		
119	N-Ac-D-Phe-OTBA	83	*	DMSO- d_6	
	N-Ac-L-Phe-OTBA	63	*		
120	N-Ac-D-Phe-OTBA	85	*	DMSO- d_6	
	N-Ac-L-Phe-OTBA	64	*		

(* low percentage of saturation)

Table 4.10

4.15 General conclusions and outlooks

Chapter II described synthesis and binding studies of simple, acyclic bis-sulfonamide receptors. All titrations with carboxylates in MeCN- d_3 suggested the formation of a strong 1:1 host/guest complex accompanied by a weaker 1:2 adduct. In order to obtain a

clear 1:1 stoichiometry, macrocyclic receptors were synthesised. Achiral macrocycles **73** and **74** were insoluble in MeCN-*d*₃ and, although a direct comparison with their acyclic counterparts was not possible, binding studies in DMSO-*d*₆ showed a clear-cut 1:1 behaviour for macrocycle **73** with benzoate and for macrocycle **74** with acetate. Chiral 1,2-bis-aminocyclohexane based macrocycles **84**, **85** and **86** showed small or no affinity for carboxylates in non-polar CDCl₃. Surprisingly, an improvement was found in the more competitive MeCN-*d*₃. This fact was explained with the presence, in non-polar solvents, of strong intramolecular hydrogen bonding, making these receptors unsuitable for carboxylate binding. Despite the high degree of chirality, none of the receptors showed enantioselectivity towards *N*-protected amino acids. Chapter III described the high yielding anion templated synthesis of a new class of bis-sulfonamide based macrocycles, built from valine. The different arrangement of hydrogen bonding acceptors and donors in the macrocyclic scaffold had proven to be efficacious for carboxylate binding. Macrocycles **88** and **102** showed moderately strong binding and selectivity for acetate in MeCN-*d*₃/H₂O mixtures. The extremely high binding constants of soluble macrocycle **108** with halides in CDCl₃ accounted for the anion-templating effect displayed by TBA chloride in the macrocyclisation step. The abandoning of the cyclohexane moiety also played favourably. More flexible macrocycles were allowed to rearrange from an unfavourable set up to a conformation more suitable for carboxylate binding. This conclusion was drawn from analysing the crystal structures of the receptors. All of them exhibited an internal hydrogen bonding network featuring *NH* bonds pointing alternatively above and below the plan of the ring. Binding studies on macrocycle **108** with acetate in CDCl₃ suggested a binding mode involving the synergistic action of three *NH* protons, two amidic and one sulfonamidic. This conclusion, however, is to remain purely speculative, in absence of a crystal structure of a host/guest complex. None of the valine based macrocycles showed significant enantioselectivity. Chapter IV described the incorporation of polar groups into the macrocyclic scaffold in order to improve the enantioselectivity. All macrocycles, apart from the histidine based receptor **112**, were synthesised in relatively good yields by using anion templating conditions. Macrocycle **112** proved to be difficult to synthesise, scarcely soluble and, moreover, it was obtained in a protonated form, a fact that led to ambiguous results in binding studies with acetate. Serine based macrocycle **117** showed strong affinity and selectivity for acetate in the competitive MeCN-*d*₃/2% H₂O solvent mixture. This result was attributed to the positive effect played by the hydroxyl groups. Receptor **117**, moreover, showed moderate but

general enantioselectivity towards amino acids with non-polar side chains. Enantioselectivity was confirmed also in DMSO-*d*₆. Macrocycle **117** was modified by introducing a long aliphatic chain in order to increase the solubility in less polar solvents. No enantioselectivity was found in CDCl₃ and, additionally, only negligible enantioselectivity was showed by a control experiment in MeCN-*d*₃, proving that the introduction of a long aliphatic chain was detrimental to enantiomeric recognition. Poorly soluble macrocycles **119** and **120**, finally, showed only modest enantioselectivity in DMSO-*d*₆.

From a synthetic point of view, anion templating proved to be of general applicability and permitted an expeditious access to relatively complex systems. The reliability of this method, besides, allowed the accumulation of considerable amounts of different valuable receptors. It would be interesting to extend the investigation to other anions, such as other halides or oxyanions, and to study, eventually, the correlation between templating effect and anion binding. This methodology might also be applied to other important macrocyclic targets, such as tetralactams and cyclic peptides.

Macrocycle **117** emerged as the best receptor in terms of binding strength and selectivity. It displayed also good solubility. The general enantioselectivity shown in MeCN-*d*₃/2% H₂O can make it an ideal candidate for the design of HPLC chiral columns. Diederich and co-workers designed a receptor which performed poor separations on a stationary phase, despite the fact that it displayed good enantioselectivities in solution.^[137] This result was ascribed to the different solvent mixtures used in the two different contexts. In general, however, there is a good correlation between the data obtained in solution and on a stationary phase, if a similar solvent is used.^[138] At this regard, in favour of macrocycle **117**, there is the fact that HPLC separations, as well known, are normally performed using MeCN/H₂O mixtures.

Chapter V

Experimental

5.1 General experimental

Reactions were carried out in solvents of commercial grade, unless otherwise stated. Reactions requiring a dry atmosphere were conducted in flame dried glassware, under nitrogen and with distilled solvents. THF was distilled under argon from benzophenone and sodium. DCM, Et₃N and MeCN were distilled from calcium hydride. TLC analysis was conducted on foil backed sheets coated with silica gel (0.25 mm) which contained the fluorescent indicator UV₂₅₄. Column chromatography was performed on Sorbsil C60, 40-60 mesh silica using solvents of commercial grade. For petroleum ether, the fraction boiling between 40 and 60°C was used.

5.2 Instrumentation

¹H NMR spectra were obtained at 300 MHz on a Brüker AC 300 and at 400 MHz on a Brüker DPX 400 spectrometer. ¹³C NMR spectra were recorded at 75 MHz on a Brüker AC 300 spectrometer and at 100 MHz on a Brüker DPX 400 spectrometer. Chemical shifts are reported in ppm on the δ scale relative to the signal of the solvent used. Solvent peaks were calibrated according to the measurements of Nudelman and co-workers.^[139] For ¹H NMR spectra, coupling constants (*J*) are given in Hz. Signal multiplicities and coupling constants were determined using the Lorenz-Gauss function for resolution enhancement in spectra editing. Ambiguous peaks in complex molecules were assigned, where possible, on the basis of two dimensional NMR experiments, especially H-H correlation and C-H long-range correlation. For ¹³C NMR spectra, superimposing peaks are reported once. Peaks reported with the same chemical shift are distinguishable in the spectrum. The number of adjacent protons was determined by distortionless enhancement by polarization transfer (DEPT) experiments. Infra-red spectra were recorded on BIORAD Golden Gate FTS 135. The samples were run either as neat solids or as oils. Melting points were determined in open capillary tubes using a Gallenkamp Electrothermal melting point apparatus. Optical rotations were measured on a PolAr2001 polarimeter using the solvent stated. The concentration given is in g/100 ml. Mass spectra

were obtained on a VG analytical 70-250 SE normal geometry double focusing mass spectrometer. All electrospray (ES) spectra were recorded on a Micromass Platform quadrupole mass analyser with an electrospray ion source using acetonitrile or methanol as solvent. High resolution accurate mass measurements were carried out at 10,000 resolution on a Brüker Apex III FT-ICR mass spectrometer. Microanalyses were performed by MEDAC Ltd., Surrey.

5.3 Experimental for NMR binding studies

Obtaining association constants by ^1H NMR titration experiments involves titration of a solution of host with a specific guest and recording a ^1H NMR spectrum after each addition. Upon complexation, protons in the host or guest may undergo a change in chemical shifts. In particular, protons involved in hydrogen bonding undergo a dramatic shift and, therefore, they are used to determine association constants. After the data from the titration experiment have been acquired, curve fitting software is employed to determine the association constant. Free host and guest are in equilibrium with the host-guest complex. As association and dissociation is fast on the NMR time scale, only a time averaged spectrum of the host (or guest) and the host-guest complex is observed. Therefore, any observed chemical shift (δ_{obs}) is the mole fraction weighted average of the shifts observed in the free (δ_{free}) and complexed (δ_{bound}) molecule. During the curve fitting procedure, after an initial estimate for K_a and $\Delta\delta$, the theoretical δ_{obs} is obtained for each point. The theoretical values are then compared with the experimentally observed ones and the sum of the difference between each point is determined by the following equation:

$$\text{Sum of differences} = \sum (\delta_{\text{obs (experimental)}} - \delta_{\text{obs(theoretical)}})$$

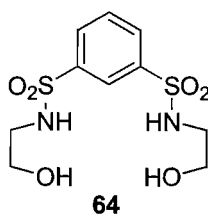
If the sum of differences is positive (or negative), the K_a is increased (or decreased) and the value $\Delta\delta$ recalculated and the whole calculation repeated until the values converge. A detailed explanation of the theoretical basis of the above discussion has been published by Wilcox.^[140] A more recent review on the determination of association constants from solution NMR data has been published by Fielding.^[96]

5.4 Method used for obtaining binding constants

All ^1H NMR titration experiments were conducted on a Brüker AM 300 spectrometer at 298 K. Deuterated solvents of commercial grade were used. Inorganic guests, such as TBA acetate, dihydrogen phosphate, fluoride, chloride and bromide were of commercial grade. TBA salts of the amino acids and mandelic acid were prepared by adding a solution of known concentration of TBA hydroxide in MeOH to a solution of the acid in MeOH and removing the solvent under reduced pressure and finally under high vacuum for several days. The correct stoichiometry was verified performing NMR experiments with long scan delays. In a typical titration experiment, a sample of host was dissolved in the appropriate solvent or preset solvent mixture. A portion of this mixture (usually 600 μl) was transferred into an NMR tube. The remainder was used to dissolve a sample of the guest to provide the guest stock solution. In this manner, the concentration of the host was set constant, avoiding concentration-dependent effects. Successive aliquots of the guest solution were added to the host solution in the NMR tube and a ^1H NMR spectrum was recorded after each addition. If significant changes on host protons signals were induced by the presence of the guest, the recorded chemical shifts were analysed with purpose-written software, kindly provided by Hunter, where a 1:1 binding mode or a 1:2 mode was assumed (see Appendix B for details).^[95] These programs fit the data to the appropriate binding model to provide the association constant, the bound chemical shift and the free chemical shift. When more than one proton could be monitored during the same titration, the error was calculated on the basis the average of all the constants calculated. When only one proton could be monitored, the errors reported were calculated with the software program EQNMR,^[106] errors calculated with EQNMR which were below the 5% threshold were reported as < 5%.

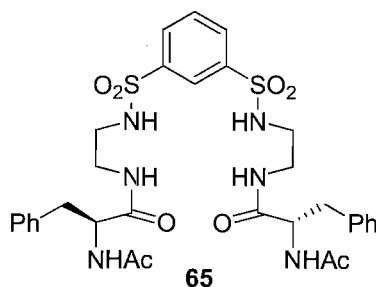
5.5 Synthesis

Benzene-1,3-disulfonic acid bis-[(2-hydroxy-ethyl)-amide] 64



A solution of bis-sulfonyl chloride **68** (320 mg, 1.16 mmol) in dry DCM (4 ml) was added dropwise to a solution of 2-aminoethanol (290 μ l, 4.82 mmol) in dry DCM (1 ml) at 0 °C. The reaction was allowed to reach room temperature and stirred for 7 h under N₂. The solvent was removed under reduced pressure and the residue was purified by flash column chromatography (SiO₂, 95:5 \rightarrow 90:10 DCM/MeOH) to give a colourless oil. Recrystallisation (MeOH/*n*-Bu₂O) yielded the desired product **64** as white crystals (268 mg, 71%). MP = 82-84 °C (MeOH/*n*-Bu₂O) (lit.^[89d] 80.5 °C); R_f = 0.29 (90:10 DCM/MeOH); FT-IR (neat): ν_{\max} = 3308 (br), 3232 (s), 1431 (m), 1300 (s), 1144 (s), 1077 (s), 949 (s), 891 (m), 798 (m) cm⁻¹; ¹H NMR (300 MHz, MeCN-*d*₃): δ = 8.26 (1 H, t, *J* = 2.0 Hz, ArH), 8.05 (2 H, dd, *J* = 8.0, 2.0 Hz, ArH), 7.76 (1 H, t, *J* = 8.0, ArH), 5.88 (2 H, br s, NH), 3.47 (4 H, t, *J* = 5.5 Hz, OCH₂), 2.98 (4 H, t, 5.5 Hz, NCH₂), 2.88 (2 H, br s, OH); ¹³C NMR (75 MHz, MeCN-*d*₃): δ = 142.7 (0), 131.5 (1), 131.4 (1), 126.1 (1), 61.2 (2), 46.3 (2); ESMS: *m/z* = 671 [2M+Na]⁺; HRMS (ES): calcd for C₁₀H₁₆N₂NaO₆S₂ ([M+Na]⁺) 347.0342, found 347.0346; calcd for C₂₀H₃₂N₄NaO₁₂S₄ ([2M+Na]⁺) 671.0792, found 671.0804. Data according to literature.^[89d]

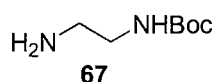
(S)-2-Acetylamino-N-(2-{3-[2-((S)-2-acetylamino-3-phenyl-propionylamino)-ethylsulfamoyl]-benzenesulfonylamino}-ethyl)-3-phenyl-propionamide **65**



A solution of *N*-Ac-L-phenylalanine (173 mg, 0.837 mmol), HOBt (233 mg, 1.72 mmol) and EDC (162 mg, 0.845 mmol) in 50:50 DCM/DMF (6 ml) was stirred at room temperature for 5 min and added to a solution of TFA salt **70** (184 mg, 0.335 mmol) and DIPEA (300 μ l, 1.72 mmol) in 50:50 DCM/DMF (6 ml). The reaction was stirred overnight at room temperature. The solvent was removed under reduced pressure and the residue was dissolved in DCM (50 ml). The mixture was washed (1 M KHSO₄, 50 ml, 1 M K₂CO₃, 50 ml, and brine, 50 ml) and dried (MgSO₄). The solvent was removed under reduced pressure and the residue was purified by flash column chromatography (SiO₂, 98:2 \rightarrow 95:5 DCM/MeOH) to yield the desired product **65** as a white solid (38 mg, 16%).

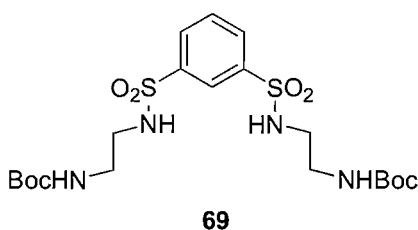
MP = 94-97 °C; R_f = 0.35 (95:5 DCM/MeOH); $[\alpha]_D^{25}$ = +5.0 (c = 0.25, MeCN); FT-IR (neat): ν_{\max} = 3271 (w), 3085 (w), 2930 (w), 1644 (s), 1531 (s), 1328 (s), 1151 (s), 1082 (m), 798 (w), 745 (m), 683 (s) cm^{-1} ; ^1H NMR (400 MHz, MeCN- d_3): δ = 8.20 (1 H, t, J = 2.0 Hz, ArH), 8.04 (2 H, dd, J = 8.0, 2.0 Hz, ArH), 7.76 (1 H, t, J = 8.0 Hz, ArH), 7.30-7.15 (10 H, m, PhH), 6.95 (2 H, t, J = 6.0 Hz, CH_2NHCO), 6.87 (2 H, d, J = 7.5 Hz, α -CHNH), 6.28 (2 H, br s, SNH), 4.39 (2 H, ddd, J = 8.5, 7.5, 6.0 Hz, α -CH), 3.19-3.08 (4 H, m, CONHCH₂), 3.04 (2 H, dd, J = 14.0, 6.0 Hz, PhCH_aH_b), 2.96-2.86 (4 H, m, SNHCH₂), 2.83 (2 H, dd, J = 14.0, 8.5 Hz, PhCH_aH_b), 1.84 (6 H, s, CH₃); ^{13}C NMR (100 MHz, MeCN- d_3): δ = 173.0 (0), 171.5 (0), 142.5 (0), 138.5 (0), 131.6 (1), 131.6 (1), 130.2 (1), 129.3 (1), 127.6 (1), 126.1 (1), 56.1 (1), 43.5, (2), 39.6 (2), 38.4 (2), 22.9 (3); ESMS: m/z = 723 $[\text{M}+\text{Na}]^+$; HRMS (ES): calcd for C₃₂H₄₀N₆NaO₈S₂ ($[\text{M}+\text{Na}]^+$) 723.2241, found 723.2257.

(2-Amino-ethyl)-carbamic acid tert-butyl ester **67**



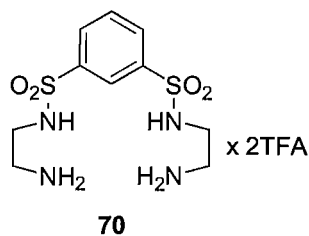
A solution of Boc₂O (8.2 g, 37.6 mmol) in DCM (800 ml) was added dropwise to a solution of 1,2-ethylene diamine **66** (11.5 ml, 172 mmol) in DCM (30 ml) at room temperature over a period of 10 h. The reaction was stirred for 48 h at room temperature. The mixture was washed (4 M Na₂CO₃, 2 x 350 ml) and the solvent was removed under reduced pressure to yield the desired product **67** as a colourless oil (6.02 g, 100%). FT-IR (neat): ν_{\max} = 3350 (br), 2977 (w), 2932 (w), 1687 (s), 1514 (m), 1268 (m), 1250 (m), 1165 (s), 773 (s) cm^{-1} ; ^1H NMR (300 MHz, CDCl₃): δ = 5.12 (1 H, br s, BocNH), 3.20 (2 H, apparent q, J = 6.0 Hz, BocNHCH₂), 2.80 (2 H, t, J = 6.0 Hz, NH₂CH₂), 1.42 (9 H, s, CH₃); ^{13}C NMR (75 MHz, CDCl₃): δ = 156.4 (0), 79.4 (0), 42.9 (2), 41.7 (2), 28.5 (3). Data according to literature.^[141]

**{2-[3-(2-tert-Butoxycarbonylamino-ethylsulfamoyl)-benzenesulfonylamino]-ethyl}-
carbamic acid tert-butyl ester **69****



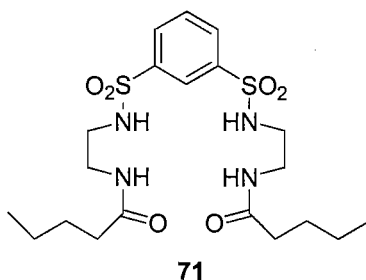
A solution of bis-sulfonyl chloride **68** (4.75 g, 17.3 mmol) in dry DCM (30 ml) was added dropwise to a solution of amine **67** (6.08 g, 38.0 mmol) and dry Et₃N (2.5 ml, 17.9 mmol) in dry DCM (80 ml) at 0 °C. The reaction was allowed to reach room temperature and stirred overnight under N₂. The mixture was diluted (DCM, 100 ml), washed (1 M KHSO₄, 100 ml, 1 M K₂CO₃, 100 ml, and brine, 100 ml) and dried (MgSO₄). The solvent was removed under reduced pressure and the residue was purified by flash column chromatography (SiO₂, 50:50 PE/EA) to yield the desired product **69** as a white solid (4.42 g, 49%). MP = 64-66 °C; R_f = 0.33 (95:5 DCM/MeOH); FT-IR (neat): ν_{max} = 3273 (w), 2980 (w), 2935 (w), 1682 (s), 1516 (m), 1331 (s), 1153 (s), 1083 (s), 793 (m) cm⁻¹; ¹H NMR (400 MHz, CDCl₃): δ = 8.34 (1 H, s, ArH), 8.06 (2 H, dd, *J* = 8.0, 2.0 Hz, ArH), 7.67 (1 H, t, *J* = 8.0 Hz, ArH), 5.61 (2 H, br s, SNH), 4.91 (2 H, br s, BocNH), 3.22 (4 H, apparent q, *J* = 5.5 Hz, BocNHCH₂), 3.12 (4 H, apparent q, *J* = 5.5 Hz, SNHCH₂), 1.43 (18 H, s, CH₃); ¹³C NMR (100 MHz, CDCl₃): δ = 156.8 (0), 141.8 (0), 130.9 (1), 130.2 (1), 125.5 (1), 80.2 (0), 43.9 (2), 40.4 (2), 28.5 (3); ESMS: *m/z* = 545 [M+Na]⁺; HRMS (ES): calcd for C₂₀H₃₅N₄O₈S₂ ([M+H]⁺) 523.1896, found 523.1892; calcd for C₂₀H₃₄N₄NaO₈S₂ ([M+Na]⁺) 545.1710, found 545.1709; Anal. Calcd for C₂₀H₃₄N₄O₈S₂: C, 45.96; H, 6.56; N, 10.72. Found: C, 45.10; H, 6.45; N, 10.22.

TFA salt **70**



A solution of bis-sulfonamide **69** (1.95 g, 3.73 mmol) in 80:20 DCM/TFA (50 ml) was stirred for 5 h at room temperature. Toluene was added and the solvent was removed under reduced pressure. The residue was triturated with MeCN and filtered off to yield the desired product **70** as a white solid (1.69 g, 82%). MP = 200-204 °C (dec.); FT-IR (neat): ν_{\max} = 3161 (w), 1668 (s), 1595 (w), 1342 (m), 1191 (m), 1138 (s), 1079 (m), 798 (s) cm^{-1} ; ^1H NMR (300 MHz, DMSO- d_6): δ = 8.40-8.10 (2 H, br s, partially obscured by ArH, SNH), 8.20 (1 H, t, J = 2.0 Hz, ArH), 8.10 (2 H, dd, J = 8.0, 2.0 Hz, ArH), 8.00 (6 H, br s, NH₃), 7.90 (1 H, t, J = 8.0 Hz, ArH), 3.01 (4 H, t, J = 6.0 Hz, NCH₂), 2.89 (4 H, t, J = 6.0 Hz, NCH₂); ^{13}C NMR (75 MHz, DMSO- d_6): δ = 158.5 (q, J = 31 Hz, COCF₃), 140.9 (0), 131.1 (1), 130.6 (1), 124.6 (1), 117.1 (q, J = 300 Hz, COCF₃), 40.0 (2), 38.6 (2).

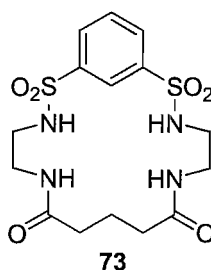
Pentanoic acid {2-[3-(2-pentanoylamino-ethylsulfamoyl)-benzenesulfonylamino]-ethyl}-amide **71**



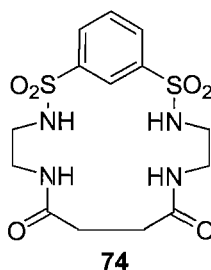
Valeryl chloride (80 μl , 0.675 mmol) was added dropwise to a solution of TFA salt **70** (175 mg, 0.318 mmol) and dry Et₃N (200 μl , 1.43 mmol) in dry MeCN (10 ml) at 0 °C. The reaction was allowed to reach room temperature and stirred overnight under N₂. The solvent was removed under reduced pressure and the residue was dissolved in DCM (50 ml). The mixture was washed (1 M KHSO₄, 50 ml, 1 M K₂CO₃, 50 ml, and brine, 50 ml) and dried (MgSO₄). The solvent was removed under reduced pressure and the residue was purified by flash column chromatography (SiO₂, DCM \rightarrow 96:4 DCM/MeOH) to yield the desired product **71** as a white solid (50 mg, 32%). MP = 64-66 °C; R_f = 0.33 (EA); FT-IR (neat): ν_{\max} = 3606 (w), 3254 (w), 2956 (w), 2931 (w), 2871 (w), 1630 (s), 1558 (s), 1431 (m), 1317 (s), 1147 (s), 1082 (s), 1073 (s), 796 (m) cm^{-1} ; ^1H NMR (400 MHz, MeCN- d_3): δ = 8.21 (1 H, t, J = 2.0 Hz, ArH), 8.03 (2 H, dd, J = 8.0, 2.0 Hz, ArH), 7.76 (1 H, t, J = 8.0 Hz, ArH), 6.57 (2 H, br s, CONH), 6.26 (2 H, br s, SNH), 3.15 (4 H, apparent q, J = 6.0 Hz, CONHCH₂), 2.96 (4 H, apparent q, J = 6.0 Hz, SNHCH₂), 2.06 (4 H, t, J = 7.5

Hz, COCH₂), 1.53-1.44 (4 H, m, COCH₂CH₂), 1.28 (4 H, apparent sext, $J = 7.0$ Hz, CH₃CH₂), 0.88 (6 H, t, 7.0 Hz, CH₃); ¹³C NMR (100 MHz, MeCN-*d*₃): $\delta = 175.0$ (0), 142.5 (0), 131.6 (1), 131.5 (1), 126.1 (1), 44.1 (2), 39.6 (2), 36.5 (2), 28.5 (2), 23.0 (2), 14.1 (3); ESMS: $m/z = 513$ [M+Na]⁺; HRMS (ES): calcd for C₂₀H₃₅N₄O₆S₂ ([M+H]⁺) 491.1993, found 491.1988.

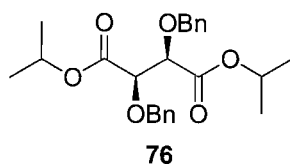
Macrocycle 73



A solution of TFA salt **70** (220 mg, 0.401 mmol) and dry Et₃N (280 μ l, 2.01 mmol) in dry MeCN (4 ml) and a solution of glutaryl dichloride (52 μ l, 0.407 mmol) in dry MeCN (4 ml) were added simultaneously, with a syringe pump, into 70 ml of dry MeCN at 60 °C over a period of 4 h. The condenser was equipped with a drying tube (CaCl₂). After the addition was completed, the reaction was stirred overnight at 60 °C. The solvent was removed under reduced pressure and the residue was purified by flash column chromatography (SiO₂, DCM \rightarrow 92.5:7.5 DCM/MeOH). After washing with MeOH, the desired product **73** was obtained as a white solid (46 mg, 27%). MP > 240 °C; $R_f = 0.30$ (90:10 DCM/MeOH); FT-IR (neat): $\nu_{\max} = 3275$ (s), 3087 (w), 2953 (w), 2874 (w), 1640 (s), 1543 (s), 1447 (m), 1331 (s), 1148 (s), 1086 (s) cm⁻¹; ¹H NMR (400 MHz, DMSO-*d*₆): $\delta = 8.21$ (1 H, t, $J = 2.0$ Hz, ArH), 8.04 (2 H, dd, $J = 8.0, 2.0$ Hz, ArH), 7.87 (1 H, t, $J = 8.0$ Hz, ArH), 7.75 (2 H, t, $J = 6.0$ Hz, SNH), 7.68 (2 H, t, $J = 6.0$ Hz, CONH), 3.00 (4 H, dt, $J = 6.0, 7.0$ Hz, CONHCH₂), 2.77 (4 H, dt, $J = 6.0, 7.0$ Hz, SNHCH₂), 1.97 (4 H, t, $J = 6.5$ Hz, COCH₂), 1.67 (2 H, quin, $J = 6.5$ Hz COCH₂CH₂); ¹³C NMR (100 MHz, DMSO-*d*₆): $\delta = 171.7$ (0), 140.9 (0), 131.0 (1), 130.3 (1), 125.0 (1), 42.2 (2), 37.7 (2), 34.0 (2), 20.0 (2); ESMS: $m/z = 419$ [M+H]⁺; HRMS (ES): calcd for C₁₅H₂₂N₄NaO₆S₂ ([M+Na]⁺) 441.0873, found 441.0866; Anal. Calcd for C₁₅H₂₂N₄O₆S₂: C, 43.05; H, 5.30; N, 13.38. Found: C, 42.21; H, 5.20; N, 12.99.

Macrocycle **74**

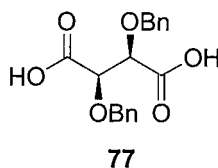
A solution of TFA salt **70** (201 mg, 0.365 mmol) and dry Et₃N (255 μ l, 1.83 mmol) in dry MeCN (4 ml) and a solution of succinyl dichloride (41 μ l, 0.372 mmol) in dry MeCN (4 ml) were added simultaneously, with a syringe pump, into 60 ml of dry MeCN at 60 °C over a period of 4 h. The condenser was equipped with a drying tube (CaCl₂). After the addition was completed, the reaction was stirred overnight at 60 °C. The solvent was removed under reduced pressure and the residue was purified by flash column chromatography (SiO₂, DCM \rightarrow 94:6 DCM/MeOH). After washing with MeOH, the desired product **74** was obtained as a white solid (21 mg, 14%). MP > 240 °C; R_f = 0.37 (90:10 DCM/MeOH); FT-IR (neat): ν_{\max} = 3301 (s), 3090 (w), 1650 (s), 1547 (s), 1434 (m), 1335 (s), 1177 (s), 1154 (s), 1106 (m), 1074 (m), 867 (m), 795 (m) cm⁻¹; ¹H NMR (400 MHz, DMSO-*d*₆): δ = 8.11 (1 H, t, *J* = 1.5 Hz, ArH), 8.04 (2 H, dd, *J* = 8.0, 1.5 Hz, ArH), 7.91 (1 H, t, *J* = 8.0 Hz, ArH), 7.87 (2 H, t, *J* = 6.0 Hz, CONH), 7.72 (2 H, br s, SNH), 3.06-2.97 (4 H, m, CONHCH₂), 2.64 (4 H, t, *J* = 7.5 Hz, SNHCH₂), 2.22 (4 H, s, COCH₂); ¹³C NMR (100 MHz, DMSO-*d*₆): δ = 171.6 (0), 140.2 (0), 131.4 (1), 130.4 (1), 125.1 (1), 41.9 (2), 38.0 (2), 31.2 (2); ESMS: *m/z* = 405 [M+H]⁺, 809 [2M+H]⁺; HRMS (ES): calcd for C₁₄H₂₁N₄O₆S₂ ([M+H]⁺) 405.0897, found 405.0902; calcd for C₁₄H₂₀N₄NaO₆S₂ ([M+Na]⁺) 427.0716, found 427.0719; Anal. Calcd for C₁₄H₂₀N₄O₆S₂: C, 41.58; H, 4.98; N, 13.85. Found: C, 40.73; H, 4.91; N, 13.29.

(2*R*,3*R*)-2,3-Bis-benzyloxy-succinic acid diisopropyl ester 76

A solution of diisopropyl L-tartrate **75** (6.46 g, 27.6 mmol) in dry THF (10 ml) was added dropwise to a suspension of NaH 60% in mineral oil (2.10 g, 52.5 mmol) in dry THF (70

ml) at 0 °C during 15 min. The mixture was allowed to reach room temperature and stirred under H₂ until bubbling ceased. TBAI (492 mg, 1.33 mmol) and 18-crown-6 (108 mg, 0.41 mmol) were added to the mixture. The temperature was brought to 0 °C and BnBr (6.24 ml, 52.5 mmol) was added dropwise over a period of 1 h. The reaction was allowed to reach room temperature and stirred overnight. Sat. NH₄Cl (50 ml) was added to the mixture and the two phases were separated. The organic layer was diluted (Et₂O, 100 ml), washed (brine, 50 ml) and dried (MgSO₄). The solvent was removed under reduced pressure and the residue was purified by flash column chromatography (SiO₂, 90:10 → 85:15 PE/Et₂O). Recrystallisation (Et₂O/PE) yielded 4.51 g of the desired product **76** as white crystals. 839 mg were recovered as a white foam after evaporation of the mother liquors (47% overall yield). MP = 68-69 °C (Et₂O/PE) (lit.^[142] 79.5-80.5 °C); R_f = 0.44 (70:30 PE/Et₂O); [α]_D²⁷ = +93.4 (*c* = 1, CHCl₃); FT-IR (neat): ν_{max} = 2987 (w), 2906 (w), 2873 (w), 1741 (s), 1451 (w), 1209 (s), 1153 (m), 1101 (s), 736 (s) cm⁻¹; ¹H NMR (400 MHz, CDCl₃): δ = 7.33-7.22 (10 H, m, PhH), 5.05 (2 H, sept, *J* = 6.0 Hz, CH₃CH), 4.83 (2 H, d, *J* = 12.0 Hz, PhCH_aH_b), 4.48 (2 H, d, *J* = 12.0 Hz, PhCH_aH_b), 4.39 (2 H, s, COCH), 1.24 (6 H, d, *J* = 6.0 Hz, CH₃), 1.16 (6 H, d, *J* = 6.0 Hz, CH₃); ¹³C NMR (100 MHz, CDCl₃): δ = 168.9 (0), 137.3 (0), 128.4 (1), 128.4 (1), 128.0 (1), 79.2 (1), 73.6 (2), 69.3 (1), 22.0 (3), 21.9 (3). Data according to literature.^[142]

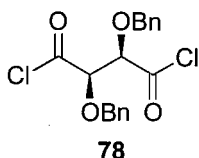
(2*R*,3*R*)-2,3-Bis-benzyloxy-succinic acid **77**



A solution of bis-ester **76** (2.11 g, 5.09 mmol) in 60:40 1,4-dioxane/1 M LiOH (100 ml) was stirred at room temperature for 5 h. 1,4-dioxane was removed under reduced pressure and the aqueous solution was washed (DCM, 2 x 50 ml), acidified (1 M HCl) and extracted (DCM, 3 x 50 ml). The combined organic layers were dried (MgSO₄) and the solvent was removed under reduced pressure to yield the desired product **77** as a white foam (1.46 g, 87%). FT-IR (DCM): ν_{max} = 2987 (w), 2906 (w), 2873 (w), 1741 (s), 1451 (w), 1209 (s), 1153 (m), 1101 (s); 736 (s); 3087 (br), 2875 (w), 1728 (s), 1265 (s), 1101 (m), 734 (s) cm⁻¹; ¹H NMR (300 MHz, CDCl₃): δ = 7.70 (2 H, br s, OH), 7.35-7.19 (10 H, m, PhH), 4.77 (2 H, d, *J* = 11.5 Hz, PhCH_aH_b), 4.50 (2 H, d, *J* = 11.5 Hz, PhCH_aH_b), 4.46

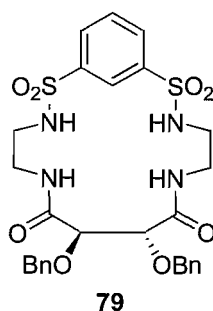
(2 H, s, COCH); ^{13}C NMR (75 MHz, CDCl_3): δ = 173.1 (0), 136.0 (0), 128.7 (1), 128.6 (1), 78.1 (1), 74.3 (2); ESMS: m/z = 329 $[\text{M}-\text{H}]^-$.

(2*R*,3*R*)-2,3-Bis-benzyloxy-butanedioyl dichloride 78



A solution of oxalyl chloride (620 μl , 7.11 mmol) in dry DCM (10 ml) was added dropwise to a solution of bis-acid **77** (467 mg, 1.41 mmol) and DMF (4 drops) in dry DCM (20 ml) at room temperature. The reaction was stirred for 5 h at room temperature under N_2 . The solvent was removed under reduced pressure, THF was added and the insoluble material was filtered off. The solvent was removed under reduced pressure to give the desired product **78** (161 mg, 91%). FT-IR (neat): ν_{max} = 3019 (w), 1747 (s), 1734 (s), 1357 (s), 1221 (s), 1081 (w), 958 (w), 865 (w) cm^{-1} .

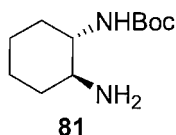
Macrocycle 79



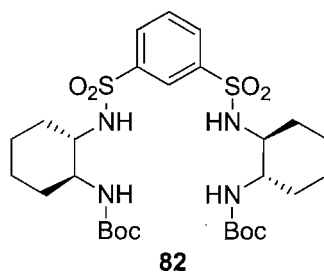
A solution of TFA salt **70** (236 mg, 0.430 mmol) and dry Et_3N (300 μl , 2.15 mmol) in dry MeCN (4.5 ml) and a solution of bis-acyl chloride **78** (161 mg, 0.438 mmol) in dry MeCN (4.5 ml) were added simultaneously, with a syringe pump, into 70 ml of dry MeCN at 60 $^\circ\text{C}$ over a period of 3.5 h. The condenser was equipped with a drying tube (CaCl_2). After the addition was completed, the reaction was stirred overnight at 60 $^\circ\text{C}$. The solvent was removed under reduced pressure and the residue was purified by flash column chromatography (SiO_2 , 70:30 \rightarrow 80:20 EA/PE). After washing with DCM, the desired product **79** was obtained as a white solid (41 mg, 15%). MP > 240 $^\circ\text{C}$; R_f = 0.29 (97.5:2.5 DCM/MeOH); $[\alpha]_{\text{D}}^{23}$ = +31.3 (c = 0.11, DMSO); FT-IR (neat): ν_{max} = 3294

(m), 1655 (s), 1554 (m), 1439 (w), 1338 (m), 1176 (m), 1107 (m), 1085 (m), 879 (w), 682 (m) cm^{-1} ; ^1H NMR (400 MHz, $\text{DMSO-}d_6$): δ = 8.23 (2 H, t, J = 6.0 Hz, CONH), 8.20 (1 H, t, J = 2.0 Hz, ArH), 8.04 (2 H, dd, J = 8.0, 2.0 Hz, ArH), 7.89 (1 H, t, J = 8.0 Hz, ArH), 7.56 (2 H, br s, SNH), 7.38-7.25 (10 H, m, PhH), 4.57 (2 H, d, J = 12.0 Hz, PhCH_aH_b), 4.42 (2 H, d, J = 12.0 Hz, PhCH_aH_b), 3.82 (2 H, s, COCH), 3.10-3.00 (2 H, m, $\text{CONHCH}_a\text{H}_b$), 2.95-2.84 (2 H, m, $\text{CONHCH}_a\text{H}_b$), 2.83-2.75 (4 H, m, SNHCH_2); ^{13}C NMR (100 MHz, $\text{DMSO-}d_6$): δ = 168.5 (0), 140.6 (0), 137.5 (0), 131.1 (1), 130.3 (1), 128.1 (1), 127.6 (1), 127.5 (1), 125.4 (1), 82.2 (1), 71.5 (2), 41.3 (2), 37.9 (2); ESMS: m/z = 639 $[\text{M}+\text{Na}]^+$; HRMS (ES): calcd for $\text{C}_{28}\text{H}_{32}\text{N}_4\text{NaO}_8\text{S}_2$ ($[\text{M}+\text{Na}]^+$) 639.1554, found 639.1551.

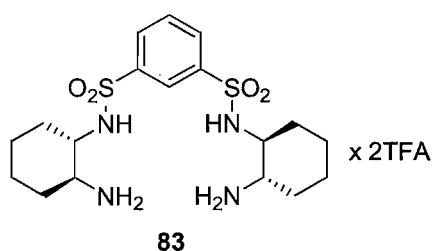
((1*S*,2*S*)-2-Amino-cyclohexyl)-carbamic acid tert-butyl ester **81**



A mixture of tartrate salt **80** (12.6 g, 47.7 mmol) and K_2CO_3 (36.8 g, 266 mmol) in 2:1 $\text{H}_2\text{O}/\text{EtOH}$ (150 ml) was vigorously stirred for 45 min at room temperature. A solution of Boc_2O (3.74 g, 17.1 mmol) in EtOH (650 ml) was added dropwise over a period of 9 h. After the addition was completed, the reaction was stirred overnight at room temperature. The reaction mixture was concentrated under reduced pressure, diluted (H_2O , 700 ml) and the insoluble material was filtered off. The aqueous solution was extracted (DCM , 2 x 300 and 2 x 100 ml), the combined organic layers were dried (MgSO_4) and the solvent was removed under reduced pressure to yield the desired product **81** as a pale yellow solid (1.55 g, 42%). MP = 94-95 $^\circ\text{C}$ ($\text{DCM}/\text{hexanes}$) (lit.^[143] 110-111 $^\circ\text{C}$); R_f = 0.29 (95:5 DCM/MeOH); $[\alpha]_D^{27} = +26.0$ (c = 0.5, CHCl_3); FT-IR (neat): ν_{max} = 3349 (w), 2927 (m), 1694 (s), 1541 (m), 1170 (s), 1013 (m), 963 (m) cm^{-1} ; ^1H NMR (300 MHz, CDCl_3): δ = 4.47 (1 H, br s, BocNH), 3.19-3.02 (1 H, m, BocNHCH), 2.31 (1 H, dt, J = 4.0, 10.0 Hz, NH_2CH), 2.03-1.89 (2 H, m, CyH), 1.73-1.63 (2 H, m, CyH), 1.48 (2 H, br s, NH_2), 1.43 (9 H, s, CH_3), 1.37-1.00 (4 H, m, CyH); ^{13}C NMR (75 MHz, CDCl_3): δ = 156.3 (0), 79.4 (0), 57.8 (1), 55.8 (1), 35.4 (2), 33.0 (2), 28.5 (3), 25.3 (2), 25.2 (2); ESMS: m/z = 215 $[\text{M}+\text{H}]^+$. Data according to literature.^[143]

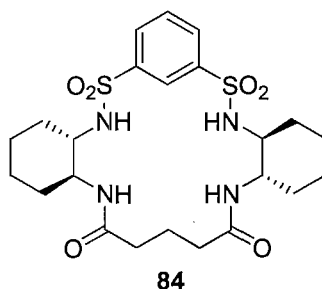
1,3-Bis-((1*S*,2*S*)-2-tert-butoxycarbonylamino-cyclohexylsulfamoyl)-benzene 82

A solution of bis-sulfonyl chloride **68** (915 mg, 3.32 mmol) in dry DCM (10 ml) was added dropwise to a solution of amine **81** (1.44 g, 6.73 mmol) and dry Et₃N (950 μl, 6.82 mmol) in dry DCM (20 ml) at 0 °C. The reaction was allowed to reach room temperature and stirred overnight under N₂. The reaction mixture was diluted (DCM, 90 ml), washed (1 M KHSO₄, 80 ml, 1 M K₂CO₃, 80 ml, and brine, 80 ml) and dried (MgSO₄). The solvent was removed under reduced pressure and the residue was purified by flash column chromatography (SiO₂, PE → 70:30 PE/EA) to yield the desired product **82** as a white solid (1.85 g, 88%). MP = 112-118 °C; R_f = 0.23 (65:35 PE/EA); [α]_D²⁷ = -76.9 (*c* = 0.5, CHCl₃); FT-IR (neat): ν_{max} = 3270 (br), 2932 (m), 2859 (w), 1681 (s), 1515 (m), 1453 (m), 1320 (s), 1256 (m), 1156 (s), 1080 (m), 964 (w), 907 (m), 792 (m) cm⁻¹; ¹H NMR (400 MHz, CDCl₃): δ = 8.35 (1 H, t, *J* = 2.0 Hz, Ar*H*), 8.01 (2 H, dd, *J* = 8.0, 2.0 Hz, Ar*H*), 7.60 (1 H, t, *J* = 8.0 Hz, Ar*H*), 5.98 (2 H, d, *J* = 5.5 Hz, SN*H*), 4.48 (2 H, d, *J* = 5.5 Hz, CON*H*), 3.39-3.26 (2 H, m, CONH*CH*), 3.04-2.92 (2 H, m, SNH*CH*), 2.05-1.89 (4 H, m, Cy*H*), 1.75-1.60 (4 H, m, Cy*H*), 1.42 (18 H, s, CH₃), 1.32-1.10 (8 H, m, Cy*H*); ¹³C NMR (100 MHz, CDCl₃): δ = 157.4 (0), 143.2 (0), 130.3 (1), 130.1 (1), 125.5 (1), 80.51 (0), 60.2 (1), 53.6 (1), 34.1 (2), 32.7 (2), 28.5 (3), 24.8 (2), 24.5 (2); ESMS: *m/z* = 631 [M+H]⁺, 653 [M+Na]⁺; HRMS (ES): calcd for C₂₈H₄₇N₄O₈S₂ ([M+H]⁺) 631.2830, found 631.2827; calcd for C₂₈H₄₆N₄NaO₈S₂ ([M+Na]⁺) 653.2649, found 653.2635.

TFA salt 83

A solution of bis-sulfonamide **82** (898 mg, 1.42 mmol) in 80:20 DCM/TFA (20 ml) was stirred for 4 h at room temperature. Toluene was added and the solvent was removed under reduced pressure. The residue was triturated with DCM and filtered off to yield the desired product **83** as a beige solid (917 mg, 98%). MP = 162-165 °C; $[\alpha]_D^{27} = -64.1$ ($c = 0.5$, MeOH); FT-IR (neat): $\nu_{\max} = 3086$ (br), 2937 (m), 2865 (m), 1666 (s), 1516 (w), 1331 (m), 1126 (s), 796 (m) cm^{-1} ; ^1H NMR (400 MHz, MeOD- d_4): $\delta = 8.42$ (1 H, t, $J = 2.0$ Hz, ArH), 8.19 (2 H, dd, $J = 8.0, 2.0$ Hz), 7.86 (1 H, t, $J = 8.0$ Hz, ArH), 3.18-3.07 (2 H, m, NCH), 2.91 (2 H, dt, $J = 4.0, 11.5$ Hz, NCH), 2.14-2.04 (2 H, m, CyH), 1.79-1.69 (2 H, m, CyH), 1.63-1.54 (2 H, m, CyH), 1.44 (2 H, apparent dq, $J = 3.5, 12.5$ Hz, CyH), 1.35-1.03 (8 H, m, CyH); ^{13}C NMR (100 MHz, MeOD- d_4): $\delta = 144.3$ (0), 132.1 (1), 132.0 (1), 126.4 (1), 56.6 (1), 55.9 (1), 32.3 (2), 30.7 (2), 25.4 (2), 24.6 (2); signals corresponding to trifluoroacetate were not detected due to the small sample size; ESMS: $m/z = 431$ $[\text{M}+\text{H}]^+$, 453 $[\text{M}+\text{Na}]^+$.

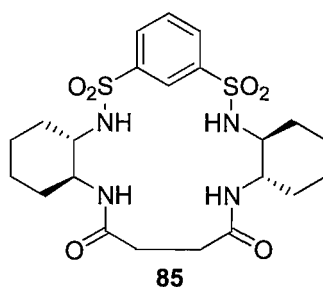
Macrocycle **84**



A solution of TFA salt **83** (212 mg, 0.322 mmol) and dry Et_3N (225 μl , 1.61 mmol) in dry MeCN (4 ml) and a solution of glutaryl dichloride (42 μl , 0.329 mmol) in dry MeCN (4 ml) were added simultaneously, with a syringe pump, into 60 ml of dry MeCN at 60 °C over a period of 3.5 h. The condenser was equipped with a drying tube (CaCl_2). After the addition was completed, the reaction was stirred overnight at 60 °C. The solvent was removed under reduced pressure and the residue was dissolved in EA (60 ml), washed (1 M KHSO_4 , 40 ml, 1 M K_2CO_3 , 30 ml, and brine, 30 ml) and dried (MgSO_4). The solvent was removed under reduced pressure and the residue was purified by flash column chromatography (SiO_2 , EA, then 97:3 \rightarrow 96:4 DCM/MeOH) to yield the desired product **84** as a white solid (48 mg, 28%). MP = 185-194 °C; $R_f = 0.24$ (95:5 DCM/MeOH); $[\alpha]_D^{22} = +45.2$ ($c = 0.3$, CHCl_3); FT-IR (neat): $\nu_{\max} = 3249$ (w), 2933 (m), 2860 (w), 1642 (s), 1532 (s), 1450 (m), 1323 (s), 1171 (s), 1152 (s), 1077 (s), 957 (w), 899 (w), 795 (w),

681 (m) cm^{-1} ; ^1H NMR (300 MHz, CDCl_3): δ = 8.27 (1 H, t, J = 1.5 Hz, ArH), 8.02 (2 H, dd, J = 8.0, 1.5 Hz, ArH), 7.63 (1H, t, J = 8.0 Hz, ArH), 6.05 (2 H, d, J = 8.0 Hz, CONH) 5.92 (2 H, d, J = 6.5 Hz, SNH), 3.74-3.70 (2 H, m, CONHCH), 3.22-3.09 (2 H, m, SNHCH), 2.50-2.40 (2 H, m, SNHCHCH_aH_b), 1.92-1.83 (2 H, m, CONHCHCH_aH_b), 1.83-1.72 (8 H, m, CyH and COCH_aH_b superimposed), 1.66-1.39 (4 H, m, partially obscured by H₂O, SNHCHCH_aH_b and COCH_aH_b superimposed), 1.38-1.24 (6 H, m, CyH, CONHCHCH_aH_b and CH₂CH₂CH₂ superimposed); ^{13}C NMR (75 MHz, CDCl_3): δ = 174.5 (0), 143.5 (0), 130.6 (1), 130.4 (1), 124.9 (1), 61.4 (1), 52.3 (1), 35.8 (2), 35.0 (2), 32.4 (2), 24.8 (2), 24.5 (2), 21.2 (2); ESMS: m/z = 527 $[\text{M}+\text{H}]^+$, 549 $[\text{M}+\text{Na}]^+$, 1053 $[2\text{M}+\text{H}]^+$; HRMS (ES): calcd for $\text{C}_{23}\text{H}_{34}\text{N}_4\text{NaO}_6\text{S}_2$ ($[\text{M}+\text{Na}]^+$) 549.1812, found 549.1815; Anal. Calcd for $\text{C}_{23}\text{H}_{34}\text{N}_4\text{O}_6\text{S}_2 \cdot 1\text{H}_2\text{O}$: C, 50.72; H, 6.66; N, 10.29. Found: C, 50.31; H, 6.33; N, 10.00.

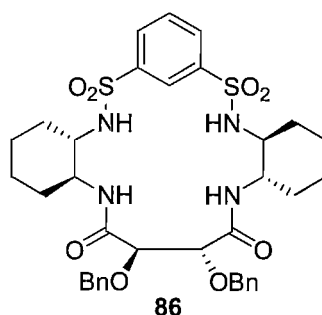
Macrocycle **85**



A solution of TFA salt **83** (216 mg, 0.328 mmol) and dry Et_3N (220 μl , 1.58 mmol) in dry MeCN (4 ml) and a solution of succinyl dichloride (37 μl , 0.336 mmol) in dry MeCN (4 ml) were added simultaneously, with a syringe pump, into 60 ml of dry MeCN at 60 °C over a period of 4 h. The condenser was equipped with a drying tube (CaCl_2). After the addition was completed, the reaction was stirred overnight at 60 °C. The solvent was removed under reduced pressure and the residue was purified by flash column chromatography (SiO_2 , DCM \rightarrow 96:4 DCM/MeOH). Recrystallisation (MeOH) yielded the desired product **85** as a crystalline powder (34 mg, 20%). MP = 185-190 °C (MeOH); R_f = 0.19 (97:3 DCM/MeOH); $[\alpha]_D^{27}$ = +31.5 (c = 0.4, CHCl_3); FT-IR (neat): ν_{max} = 3251 (w), 3076 (w), 2930 (m), 2856 (w), 1633 (s), 1537 (s), 1434 (m), 1324 (s), 1172 (s), 1152 (s), 1072 (s), 906 (m) cm^{-1} ; ^1H NMR (400 MHz, CDCl_3): δ = 8.32 (1 H, t, J = 1.5 Hz, ArH), 8.06 (2 H, dd, J = 8.0, 1.5 Hz, ArH), 7.68 (1 H, t, J = 8.0 Hz, ArH), 7.18 (2 H, d, J = 7.5 Hz, CONH), 6.10 (2 H, d, J = 5.5 Hz, SNH), 3.62-3.51 (2 H, m, CONHCH), 3.21 (2

H, apparent sept, $J = 5.5$ Hz, SNHCH), 2.43-2.32 (2 H, m, SNHCHCH_aH_b), 1.96-1.84 (4 H, m, CONHCHCH_aH_b and COCH_aH_b superimposed), 1.84-1.66 (6 H, m, partially obscured by H₂O, COCH_aH_b and CyH superimposed), 1.46 (2 H, apparent dq, $J = 3.0$, 12.5 Hz, SNHCHCH_aH_b), 1.40-1.20 (6 H, m, CONHCHCH_aH_b and CyH superimposed); ¹³C NMR (75 MHz, CDCl₃): $\delta = 174.2$ (0), 143.8 (0), 130.0 (1), 129.6(1), 124.9 (1), 61.7 (1), 51.9 (1), 36.12 (2), 32.3 (2), 31.4 (2), 24.6 (2), 24.2 (2); ESMS: $m/z = 513$ [M+H]⁺, 535 [M+Na]⁺, 1047 [2M+Na]⁺; HRMS (ES): calcd for C₂₂H₃₃N₄O₆S₂ ([M+H]⁺) 513.1836, found 513.1837; calcd for C₂₂H₃₂N₄NaO₆S₂ ([M+Na]⁺) 535.1655, found 535.1681.

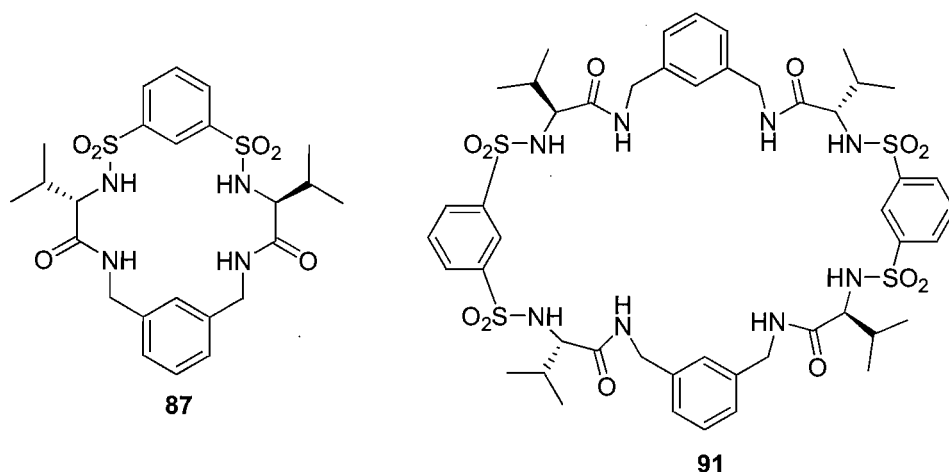
Macrocycle **86**



A solution of TFA salt **83** (187 mg, 0.284 mmol) and dry Et₃N (200 μ l, 1.43 mmol) in dry MeCN (4 ml) and a solution of bis-acyl chloride **78** (114 mg, 0.311 mmol) in dry MeCN (4 ml) were added simultaneously, with a syringe pump, into 60 ml of dry MeCN at 60 °C over a period of 4 h. The condenser was equipped with a drying tube (CaCl₂). After the addition was completed, the reaction was stirred overnight at 60 °C. The solvent was removed under reduced pressure and the residue was dissolved in DCM (50 ml), washed (1 M KHSO₄, 30 ml, 1 M K₂CO₃, 30 ml, and brine, 30 ml) and dried (MgSO₄). The solvent was removed under reduced pressure and the residue was purified by flash column chromatography (SiO₂, 50:50 \rightarrow 60:40 EA/PE) to yield the desired product **86** as a white solid (42 mg, 20%). MP > 240 °C (acetone); $R_f = 0.44$ (70:30 EA/PE); $[\alpha]_D^{27} = +45.2$ ($c = 0.25$, CHCl₃); FT-IR (neat): $\nu_{max} = 3379$ (w), 3259 (w), 2936 (w), 2857 (w), 1665 (s), 1516 (s), 1431 (m), 1318 (s), 1061 (s), 684 (m) cm⁻¹; ¹H NMR (400 MHz, CDCl₃): $\delta = 8.15$ (2 H, dd, $J = 8.0, 1.5$ Hz, ArH), 7.96 (1 H, t, $J = 1.5$ Hz, ArH), 7.72 (1 H, t, $J = 8.0$ Hz, ArH), 7.44-7.16 (10 H, m, PhH), 6.09 (2 H, d, $J = 10.0$ Hz, CONH), 5.33 (2 H, d, $J = 2.5$ Hz, SNH), 4.93 (2 H, d, $J = 12.0$ Hz, PhCH_aH_b), 4.53 (2 H, s, COCH),

4.36 (2 H, d, $J = 12.0$ Hz, PhCH_aH_b), 3.60 (2 H, apparent dq, $J = 4.0, 10.0$ Hz, CONHCH), 2.64 (2 H, apparent tt, $J = 11.0, 3.0$ Hz, SNHCH), 2.59-2.50 (2 H, m, SNHCHCH_aH_b), 1.75-1.51 (4 H, m, partially obscured by H₂O, CyH), 1.50-1.41 (2 H, m, CONHCHCH_aH_b), 1.41-1.35 (2 H, m, SNHCHCH_aH_b), 1.35-1.07 (4 H, m, CyH), 0.78 (2 H, apparent dq, $J = 4.0, 13.0$ Hz, CONHCHCH_aH_b); ¹³C NMR (100 MHz, CDCl₃): $\delta = 168.9$ (0), 141.8 (0), 135.5 (0), 132.0 (1), 130.6 (1), 129.9 (1), 129.4 (1), 129.2 (1), 122.8 (1), 81.3 (1), 77.4 (2), 58.1 (1), 51.5 (1), 33.4 (2), 32.4 (2), 24.6 (2), 24.1 (2); ESMS: $m/z = 725$ [M+H]⁺, 747 [M+Na]⁺, 1471 [2M+Na]⁺; HRMS (ES): calcd for C₃₆H₄₅N₄O₈S₂ ([M+H]⁺) 725.2673, found 725.2659; calcd for C₃₆H₄₄N₄NaO₈S₂ ([M+Na]⁺) 747.2493, found 747.2530.

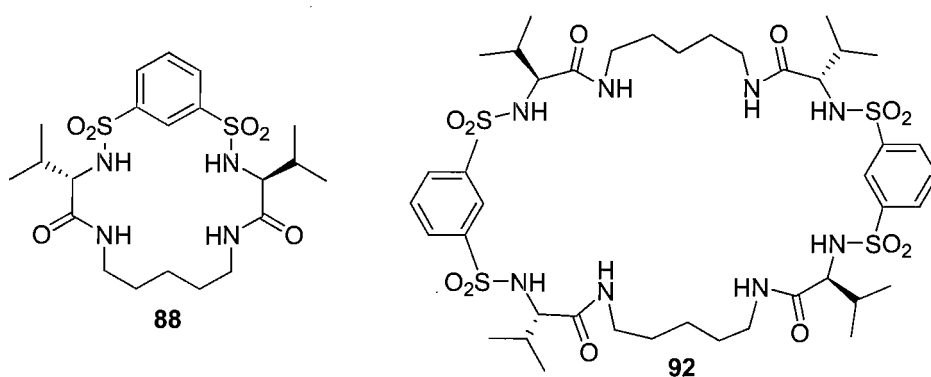
Macrocycle 87 and macrocycle 91



Method A. A solution of bis-acid **90** (416 mg, 0.953 mmol) and CDI (314 mg, 1.93 mmol) in dry THF (16 ml) was stirred for 45 min at room temperature under N₂. The mixture and a solution of *m*-xylylenediamine (125 μ l, 0.947 mmol) and dry Et₃N (80 μ l, 0.574 mmol) in dry THF (16 ml) were added simultaneously into 20 ml of dry THF in one portion. The reaction was stirred overnight at room temperature under N₂. The solvent was removed under reduced pressure and the residue was purified by flash column chromatography (SiO₂, DCM \rightarrow 98:2 DCM/MeOH) to yield the desired product **87** as a white powder (31 mg, 6%) accompanied by macrocycle **91** (white solid, 39 mg, 8%). **Method B.** A solution of pentafluorophenol ester **97** (677 mg, 0.881 mmol) and TBACl (500 mg, 1.80 mmol) in dry DCM (5 ml) and a solution of *m*-xylylenediamine (120 μ l, 0.909 mmol) and dry Et₃N (500 μ l, 3.59 mmol) in dry DCM (5 ml) were added

simultaneously, with a syringe pump, into 100 ml of dry DCM at room temperature over a period of 5 h. The reaction was stirred overnight at room temperature. The solvent was removed under reduced pressure and the residue was purified by flash column chromatography (SiO₂, 40:60 → 55:45 EA/PE) to yield the desired product **87** as a white solid (280 mg, 59%). **Macrocycle 87**: MP > 240 °C (MeOH); R_f = 0.63 (75:25 EA/PE); [α]_D²⁶ = +195 (c = 0.5, DMSO); FT-IR (neat): ν_{max} = 3599 (w), 3488 (w), 3238 (m), 3090 (w), 2968 (w), 2873 (w), 1688 (m), 1651 (s), 1548 (m), 1462 (m), 1454 (m), 1325 (s), 1269 (w), 1224 (w), 1178 (s), 1128 (m), 1089 (m), 1050 (m), 803 (m), 793 (m), 719 (w), 703 (w), 680 (m) cm⁻¹; ¹H NMR (400 MHz, DMSO-*d*₆): δ = 8.42 (2 H, dd, *J* = 7.0, 4.0 Hz, CONH), 8.13 (2 H, br s, SNH), 7.98 (1 H, s, O₂SArH), 7.62 (2 H, dd, *J* = 8.0, 1.5 Hz, O₂SArH), 7.33 (1 H, t, *J* = 7.5 Hz, ArH), 7.21 (2 H, d, *J* = 7.5 Hz, ArH), 6.77 (1 H, t, *J* = 8.0 Hz, O₂SArH), 6.75 (1 H, s, ArH), 4.34 (2 H, dd, *J* = 14.0, 7.0 Hz, NHCH_aH_b), 3.75 (2 H, dd, *J* = 14.0, 4.0 Hz, NHCH_aH_b), 3.62 (2 H, br s, α-CH), 1.92 (2 H, apparent oct, *J* = 7.0 Hz, α-CHCH), 0.95 (6 H, d, *J* = 7.0 Hz, CH₃), 0.94 (6 H, d, *J* = 7.0 Hz, CH₃); ¹³C NMR (100 MHz, DMSO-*d*₆): δ = 169.4 (0), 142.5 (0), 138.6 (0), 128.9 (1), 128.5 (1), 128.3 (1), 128.0 (1), 127.6 (1), 123.3 (1), 61.9 (1), 42.4 (2), 31.3 (1), 19.1 (3), 18.3 (3); ESMS: *m/z* = 537 [M+H]⁺, 559 [M+Na]⁺; HRMS (ES): calcd for C₂₄H₃₂N₄NaO₆S₂ ([M+Na]⁺) 559.1655, found 559.1666; Anal. Calcd for C₂₄H₃₂N₄O₆S₂·1.5H₂O: C, 51.14; H, 6.26; N, 9.94. Found: C, 51.13; H, 6.15; N, 9.53. **Macrocycle 91**: MP = 176-184 °C; R_f = 0.43 (75:25 EA/PE); [α]_D²⁶ = +65.8 (c = 0.25, DMSO); FT-IR (neat): ν_{max} = 3365 (w), 2965 (w), 1663 (s), 1538 (m), 1427 (m), 1325 (s), 1274 (w), 1156 (s), 1082 (m), 1046 (w), 923 (w), 795 (m), 681 (m) cm⁻¹; ¹H NMR (400 MHz, DMSO-*d*₆): δ = 8.34 (4 H, apparent t, *J* = 6.0 Hz, CONH), 8.21 (2 H, t, *J* = 2.0 Hz, O₂SArH), 8.08 (4 H, br s, SNH), 7.93 (4 H, dd, *J* = 8.0, 2.0 Hz, O₂SArH), 7.54 (2 H, t, *J* = 8.0 Hz, O₂SArH), 7.20 (2 H, t, *J* = 8.0 Hz, ArH), 7.01 (2 H, s, ArH), 6.92 (4 H, d, *J* = 8.0 Hz, ArH), 4.07 (4 H, dd, *J* = 15.0, 6.0 Hz, NHCH_aH_b), 4.00 (4 H, dd, *J* = 15.0, 6.0 Hz, NHCH_aH_b), 3.59 (4 H, d, *J* = 7.0 Hz, α-CH), 1.87 (4 H, apparent oct, *J* = 7.0 Hz, α-CHCH), 0.79 (24 H, d, *J* = 7.0 Hz, CH₃); ¹³C NMR (100 MHz, DMSO-*d*₆): δ = 169.8 (0), 141.9 (0), 138.7 (0), 129.9 (1), 129.4 (1), 128.3 (1), 126.3 (1), 125.4 (1), 124.7 (1), 62.0 (1), 41.9 (2), 30.7 (1), 19.0 (3), 18.2 (3); ESMS: *m/z* = 1073 [M+H]⁺, 1095 [M+Na]⁺; Anal. Calcd for C₄₈H₆₄N₈O₁₂S₄·1.5H₂O: C, 52.39; H, 6.14; N, 10.18. Found: C, 52.30; H, 5.92; N, 9.99.

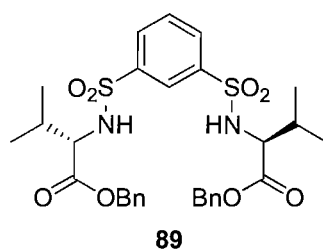
Macrocycle **88** and macrocycle **92**



Method A. A solution of bis-acid **90** (321 mg, 0.735 mmol) and CDI (245 mg, 1.51 mmol) in dry THF (15 ml) was stirred for 50 min at room temperature under N_2 . The mixture and a solution of 1,5-diaminopentane (90 μ l, 0.77 mmol) in dry THF (15 ml) were added simultaneously into 15 ml of dry THF in one portion. The reaction was stirred overnight at room temperature under N_2 . The solvent was removed under reduced pressure and the residue was purified by flash column chromatography (SiO_2 , 50:50 \rightarrow 75:25 EA/PE) to yield the desired product **88** as a white solid (85 mg, 23%) accompanied by macrocycle **92** (white solid, 42 mg, 11%). **Method B.** A solution of pentafluorophenol ester **97** (230 mg, 0.300 mmol) and TBACl (85 mg, 0.306 mmol) in dry DCM (4 ml) and a solution of 1,5-diaminopentane (35 μ l, 0.299 mmol) and dry Et_3N (250 μ l, 1.79 mmol) in dry DCM (4 ml) were added simultaneously, with a syringe pump, into 25 ml of dry DCM at room temperature over a period of 4 h. The reaction was stirred overnight at room temperature. The solvent was removed under reduced pressure and the residue was purified by flash column chromatography (SiO_2 , 50:50 \rightarrow 75:25 EA/PE) to yield the desired product **88** as a white solid (102 mg, 68%). **Method C** (anion templating effect study). Pentafluorophenol ester **97** (970 mg, 1.26 mmol) was dissolved in dry DCM (18 ml). The volume of the solution was 18.5 ml. 1,5-diaminopentane (148 μ l, 1.26 mmol) and dry Et_3N (530 μ l, 3.80 mmol) were dissolved in dry DCM (19 ml) to give 18.5 ml of solution. Successively, 0, 1 (74 mg, 0.267 mmol), 2 (149 mg, 0.534 mmol) and 4 (300 mg, 1.08 mmol) equivalents of TBACl were added to four different aliquots (4 ml) of the solution containing the pentafluorophenol ester. Each mixture so obtained and an aliquot (4 ml) of the solution containing the bis-amine were added simultaneously, with a syringe pump, into 20 ml of dry DCM at room temperature over a period of 1 h 45 min. The four reactions were stirred overnight at room temperature. For each reaction, the solvent was

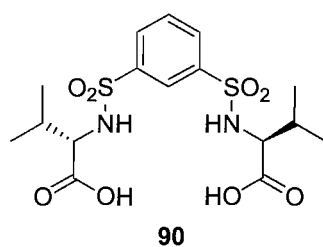
removed under reduced pressure and the residue was purified by flash column chromatography (SiO₂, 50:50 → 75:25 EA/PE). Macrocycles **88** and **92** were obtained with various yields: 0 equivalents of TBACl, **88** (38 mg, 28%) and **92** (36 mg, 26%); 1 equivalent of TBACl, exclusively **88** (90 mg, 65%); 2 equivalents of TBACl, exclusively **88** (108 mg, 79%); 4 equivalents of TBACl, exclusively **88** (108 mg, 79%). **Macrocycle 88**: MP = 160-162 °C; R_f = 0.29 (75:25 EA/PE); [α]_D²⁶ = +144 (*c* = 0.5, MeCN); FT-IR (neat): ν_{max} = 3409 (w), 3375 (w), 3271 (w), 2965 (w), 2936 (w), 1659 (s), 1538 (m), 1440 (w), 1414 (w), 1341 (s), 1329 (s), 1175 (s), 1130 (m), 1053 (m), 934 (w), 919 (w), 801 (m), 682 (m) cm⁻¹; ¹H NMR (400 MHz, DMSO-*d*₆): δ = 8.15 (1 H, t, *J* = 2.0 Hz, Ar*H*), 8.09 (2 H, d, *J* = 9.0 Hz, SN*H*), 7.96 (2 H, dd, *J* = 8.0, 2.0 Hz, Ar*H*), 7.80 (2 H, dd, *J* = 7.0, 4.5 Hz, CON*H*), 7.67 (1 H, t, *J* = 8.0 Hz, Ar*H*), 3.54 (2 H, dd, *J* = 9.0, 7.0 Hz, α-*CH*), 3.20-3.09 (2 H, m, NHCH_aH_b), 2.67-2.57 (2 H, m, NHCH_aH_b), 1.89 (2 H, apparent oct, *J* = 7.0 Hz, α-*CHCH*), 1.24-1.11 (2 H, m, NHCH₂CH_aH_b), 1.11-1.00 (2 H, m, NHCH₂CH_aH_b), 0.91 (6 H, d, *J* = 7.0 Hz, CH₃), 0.88 (6 H, d, *J* = 7.0 Hz, CH₃), 0.69 (2 H, apparent quin, *J* = 7.0 Hz, NHCH₂CH₂CH₂); ¹³C NMR (100 MHz, DMSO-*d*₆): δ = 169.5 (0), 142.7 (0), 129.7 (1), 129.2 (1), 124.4 (1), 61.7 (1), 38.1 (2), 31.1 (1), 28.1 (2), 23.3 (2), 19.1 (3), 18.2 (3); ESMS: *m/z* = 503 [M+H]⁺, 525 [M+Na]⁺, 1005 [2M+H]⁺, 1027 [2M+Na]⁺; HRMS (ES): calcd for C₂₁H₃₅N₄O₆S₂ ([M+H]⁺) 503.1993, found 503.2014; calcd for C₂₁H₃₄N₄NaO₆S₂ ([M+Na]⁺) 525.1812, found 525.1815; Anal. Calcd for C₂₁H₃₄N₄O₆S₂: C, 50.18; H, 6.82; N, 11.14. Found: C, 49.55; H, 6.78; N, 11.01. **Macrocycle 92**: MP > 240 °C; R_f = 0.11 (75:25 EA/PE); [α]_D²⁶ = +89.2 (*c* = 0.25, DMSO); FT-IR (neat): ν_{max} = 3374 (w), 3154 (w), 2962 (w), 1666 (s), 1538 (m), 1455 (m), 1320 (m), 1219 (w), 1157 (s), 1142 (s), 1078 (m), 1042 (m), 936 (m), 793 (m), 679 (m) cm⁻¹; ¹H NMR (400 MHz, DMSO-*d*₆): δ = 8.18 (2 H, s, Ar*H*), 8.03 (4 H, d, *J* = 9.0 Hz, SN*H*), 7.94 (4 H, d, *J* = 8.0 Hz, Ar*H*), 7.80 (4 H, apparent t, *J* = 5.0 Hz, CON*H*), 7.68 (2 H, t, *J* = 8.0 Hz, Ar*H*), 3.48 (4 H, apparent t, *J* = 8.0 Hz, α-*CH*), 2.88-2.76 (4 H, m, NHCH_aH_b), 2.76-2.66 (4 H, m, NHCH_aH_b), 1.88-1.74 (4 H, m, α-*CHCH*), 1.21-1.09 (8 H, m, NHCH₂CH₂), 1.09-0.99 (4 H, m, NHCH₂CH₂CH₂), 0.88 (12 H, d, *J* = 7.0 Hz, CH₃), 0.79 (12 H, d, *J* = 7.0 Hz, CH₃); ¹³C NMR (100 MHz, DMSO-*d*₆): δ = 169.4 (0), 142.0 (0), 129.8 (1), 129.3 (1), 124.8 (1), 62.0 (1), 38.2 (2), 30.7 (1), 28.2 (2), 23.6 (2), 18.9 (3), 18.3 (3); ESMS: *m/z* = 1004 [M+H]⁺, 1027 [M+Na]⁺; Anal. Calcd for C₄₂H₆₈N₈O₁₂S₄: C, 50.18; H, 6.82; N, 11.14. Found: C, 50.15; H, 6.84; N, 10.63.

(S)-2-[3-((S)-1-Benzoyloxycarbonyl-2-methyl-propylsulfamoyl)-benzenesulfonylamino]-3-methyl-butylric acid benzyl ester 89



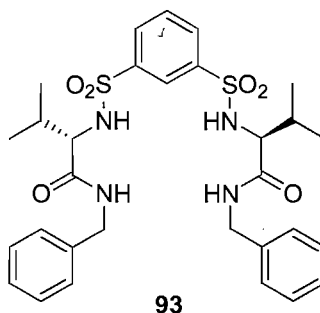
A solution of bis-sulfonyl chloride **68** (3.55 g, 12.9 mmol) in dry DCM (10 ml) was added dropwise to a solution of H-Val-OBn·TsOH (10.3 g, 27.1 mmol) and dry Et₃N (5.6 ml, 40 mmol) in dry DCM (50 ml) at 0 °C. The reaction was allowed to reach room temperature and stirred overnight under N₂. The reaction mixture was diluted (DCM, 150 ml), washed (2 M HCl, 250 ml, 1 M K₂CO₃, 2 x 200 ml, and brine, 200 ml) and dried (MgSO₄). The solvent was removed under reduced pressure and the residue was purified by flash column chromatography (SiO₂, 90:10 → 75:25 PE/EA) to yield the desired product **89** as a colourless oil (5.74 g, 72%). R_f = 0.24 (70:30 EA/PE); [α]_D²⁷ = +4.3 (c = 0.75, CHCl₃); FT-IR (neat): ν_{max} = 3272 (w), 2963 (w), 1729 (s), 1453 (m), 1334 (s), 1156 (s), 1135 (s), 913 (m), 681 (s) cm⁻¹; ¹H NMR (400 MHz, CDCl₃): δ = 8.25 (1 H, t, J = 2.0 Hz, ArH), 7.88 (2 H, dd, J = 8.0, 2.0 Hz), 7.38 (1 H, t, J = 8.0 Hz, ArH), 7.29-7.24 (6 H, m, PhH), 7.16-7.11 (4 H, m, PhH), 5.27 (2 H, d, J = 10.0 Hz, NH), 4.88 (2 H, d, J = 12.0 Hz, PhCH_aH_b), 4.84 (2 H, d, J = 12.0 Hz, PhCH_aH_b), 3.80 (2 H, dd, J = 10.0, 5.0 Hz, α-CH), 2.10-1.96 (2 H, m, α-CHCH), 0.89 (6 H, d, J = 7.0 Hz, CH₃), 0.76 (6 H, d, J = 7.0 Hz, CH₃); ¹³C NMR (100 MHz, CDCl₃): δ = 171.0 (0), 141.4 (0), 134.9 (0), 131.1 (1), 130.1 (1), 128.8 (1), 128.7 (1), 126.1 (1), 67.7 (2), 61.3 (1), 31.8 (1), 19.1 (3), 17.3 (3); ESMS: m/z = 615 [M-H].

(S)-2-[3-((S)-1-Carboxy-2-methyl-propylsulfamoyl)-benzenesulfonylamino]-3-methyl-butylric acid 90



A mixture of bis-ester **89** (5.48 g, 8.89 mmol) and Pd/C (10% wt, 976 mg, 0.917 mmol) in MeOH (60 ml) was stirred at room temperature under H₂ (atmospheric pressure) for 4 h. The mixture was filtered through a celite pad and the solvent was removed under reduced pressure to yield the desired product **90** as a white powder (3.76 g, 97%). MP = 200-203 °C; $[\alpha]_D^{27} = +23.8$ ($c = 0.5$, MeOH); FT-IR (neat): $\nu_{\max} = 3264$ (m), 2969 (w), 1713 (s), 1668 (m), 1460 (w), 1413 (m), 1347 (s), 1219 (m), 1142 (s), 1051 (s), 897 (m), 795 (s), 678 (m) cm⁻¹; ¹H NMR (400 MHz, DMSO-*d*₆): $\delta = 8.24$ (2 H, d, $J = 8.5$ Hz, *NH*), 8.16 (1 H, t, $J = 2.0$ Hz, *ArH*), 7.97 (2 H, dd, $J = 8.0, 2.0$ Hz, *ArH*), 7.74 (1 H, t, $J = 8.0$ Hz, *ArH*), 3.54 (2 H, apparent t, $J = 7.0$ Hz, α -CH), 1.95 (2 H, apparent oct, $J = 7.0$ Hz, α -CHCH), 0.80 (6 H, d, $J = 7.0$ Hz, CH₃), 0.76 (6 H, d, $J = 7.0$ Hz, CH₃); ¹³C NMR (100 MHz, DMSO-*d*₆): $\delta = 172.1$ (0), 142.0 (0), 130.0 (1), 130.0 (1), 124.5 (1), 61.4 (1), 30.3 (1), 18.9 (3), 17.8 (3); ESMS: $m/z = 435$ [M-H]⁻, 871 [2M-H]⁻.

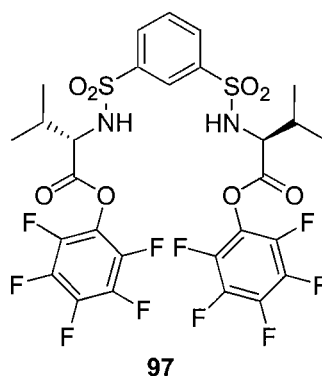
N*-Benzyl-(*S*)-2-[3-((*S*)-1-benzylcarbamoyl-2-methyl-propylsulfamoyl)-benzenesulfonylamino]-3-methyl-butylamide **93*



A solution of bis-acid **90** (97 mg, 0.22 mmol) and CDI (73 mg, 0.45 mmol) in dry THF (7 ml) was stirred for 1 h at room temperature under N₂. The mixture was added to a solution of benzylamine (62 μ l, 0.57 mmol) and dry Et₃N (50 μ l, 0.36 mmol) in dry THF (5 ml). The reaction was stirred overnight at room temperature under N₂. The solvent was removed under reduced pressure and the residue was purified by flash column chromatography (SiO₂, 70:30 \rightarrow 55:45 PE/EA) to yield the desired product **93** as a white solid (87 mg, 64%). MP = 90-92 °C; $R_f = 0.48$ (50:50 EA/PE); $[\alpha]_D^{25} = +33.2$ ($c = 0.25$, MeCN); FT-IR (neat): $\nu_{\max} = 3272$ (w), 2966 (w), 1651 (s), 1539 (w), 1455 (w), 1434 (w), 1327 (s), 1156 (s), 1142 (s), 1080 (m), 1030 (w), 915 (w), 795 (m) cm⁻¹; ¹H NMR (400 MHz, MeCN-*d*₃): $\delta = 8.26$ (1 H, t, $J = 2.0$ Hz, *ArH*), 7.99 (2 H, dd, $J = 8.0, 2.0$ Hz, *ArH*), 7.61 (1 H, t, $J = 8.0$ Hz, *ArH*), 7.32-7.21 (6 H, m, *PhH*), 7.12-7.07 (4 H, m, *PhH*),

6.92 (2 H, apparent t, $J = 6.0$ Hz, CONH), 6.11 (2 H, br s, SNH), 4.14 (2 H, dd, $J = 15.0$, 6.0 Hz, PhCH_aH_b), 4.04 (2 H, dd, $J = 15.0$, 6.0 Hz, PhCH_aH_b), 3.57 (2 H, d, $J = 6.0$ Hz, $\alpha\text{-CH}$), 1.97-1.88 (2 H, m, partially obscured by solvent peak, $\alpha\text{-CHCH}$), 0.83 (6 H, d, $J = 7.0$ Hz, CH_3), 0.82 (6 H, d, $J = 7.0$ Hz, CH_3); ^{13}C NMR (100 MHz, $\text{MeCN-}d_3$): $\delta = 170.8$ (0), 142.4 (0), 139.6 (0), 131.8 (1), 131.2 (1), 129.4 (1), 128.4 (1), 128.1 (1), 126.7 (1), 63.1 (1), 42.7 (2), 32.5 (1), 19.5 (3), 17.9 (3); ESMS: $m/z = 615$ $[\text{M}+\text{H}]^+$, 637 $[\text{M}+\text{Na}]^+$; HRMS (ES): calcd for $\text{C}_{30}\text{H}_{39}\text{N}_4\text{O}_6\text{S}_2$ ($[\text{M}+\text{H}]^+$) 615.2306, found 615.2301; calcd for $\text{C}_{30}\text{H}_{38}\text{N}_4\text{NaO}_6\text{S}_2$ ($[\text{M}+\text{Na}]^+$) 637.2125, found 637.2176.

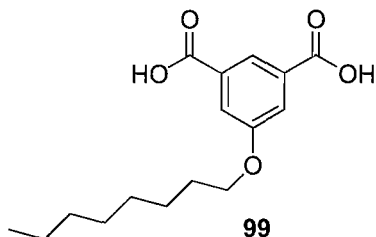
3-Methyl-(*S*)-2-[3-(2-methyl-(*S*)-1-pentafluorophenyl-oxycarbonyl-propylsulfamoyl)-benzenesulfonylamino]-butyric acid pentafluorophenyl ester **97**



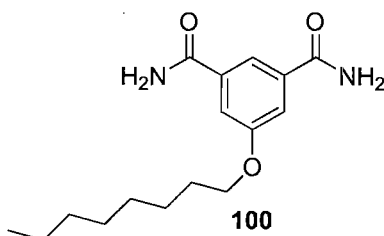
A solution of EDC (1.76 g, 9.19 mmol) in dry DCM (35 ml) was added dropwise to a solution of bis-acid **90** (1.95 g, 4.46 mmol) and pentafluorophenol (2.10 g, 11.4 mmol) in dry DCM (50 ml) during 30 min at 0 °C. The reaction was allowed to reach room temperature and stirred overnight under N_2 . The mixture was washed (5% aqueous NaHCO_3 , 2 x 150 ml), dried (MgSO_4) and the solvent was removed under reduced pressure. The residue was dissolved in EA and filtered through a small silica pad. The solvent was removed under reduced pressure to yield the desired product **97** as a white solid (2.60 g, 76%). MP = 55-61 °C; $R_f = 0.30$ (80:20 PE/EA); $[\alpha]_D^{27} = +16.2$ ($c = 0.5$, CHCl_3); FT-IR (neat): $\nu_{\text{max}} = 3285$ (w), 2972 (w), 1784 (m), 1518 (s), 1741 (w), 1338 (m), 1158 (m), 1085 (s), 992 (s), 921 (w), 893 (w), 799 (w), 682 (m) cm^{-1} ; ^1H NMR (300 MHz, CDCl_3): $\delta = 8.45$ (1 H, t, $J = 2.0$ Hz, ArH), 8.05 (2 H, dd, $J = 8.0$, 2.0 Hz, ArH), 7.66 (1 H, t, $J = 8.0$ Hz, ArH), 5.77 (2 H, d, $J = 5.0$ Hz, NH), 4.25 (2 H, dd, $J = 10.0$, 5.0 Hz, $\alpha\text{-CH}$), 2.43-2.28 (2 H, m, $\alpha\text{-CHCH}$), 1.10 (6 H, d, $J = 7.0$ Hz, CH_3), 0.97 (6 H, d, $J = 7.0$ Hz, CH_3); ^{13}C NMR (75 MHz, CDCl_3): $\delta = 167.6$ (0), 141.7 (0), 131.1 (1), 130.3 (1),

126.2 (1), 61.0 (1), 31.8 (1), 19.1 (3), 16.9 (3); signals corresponding to aromatic carbons in the pentafluorophenol groups were not detected due to the small sample size.

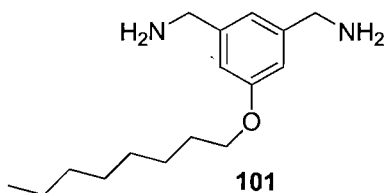
5-Octyloxy-isophthalic acid **99**



A mixture of bis ester **98** (6.20 g, 29.5 mmol), 1-iodooctane (5 ml, 27.5 mmol) and K_2CO_3 (13.9 g, 100.3 mmol) in acetone (140 ml) was refluxed overnight. After filtration, the solvent was removed under reduced pressure. DCM was added to the residue and the insoluble material was filtered off. The solvent was removed under reduced pressure and the crude material was dissolved in 50:50 1,4-dioxane/1.5 M LiOH (200 ml) and stirred overnight. The mixture was washed (Et_2O , 2 x 200 ml) and acidified (3 M $KHSO_4$). A white precipitate was formed. The solid was filtered off, washed (DCM, H_2O) and suspended in toluene. The solvent was removed under reduced pressure to yield the desired product **99** as a white solid (5.81 g, 72%). MP = 225-227 °C; FT-IR (neat): ν_{max} = 2923 (m), 2855 (m), 2566 (w), 1705 (s), 1683 (s), 1595 (m), 1643 (m), 1413 (m), 1338 (m), 1309 (m), 1271 (s), 1125 (w), 1044 (m), 929 (m), 908 (m), 759 (s), 734 (s), 685 (m) cm^{-1} ; 1H NMR (300 MHz, $DMSO-d_6$): δ = 13.20 (2 H, br s, OH), 8.06 (1 H, t, J = 1.5 Hz, ArH), 7.62 (2 H, d, J = 1.5 Hz, ArH), 4.06 (2 H, t, J = 6.5 Hz, OCH_2), 1.78-1.66 (2 H, m, OCH_2CH_2), 1.47-1.20 (10 H, m, $(CH_2)_5CH_3$), 0.85 (3 H, t, J = 7.0 Hz, CH_3); ^{13}C NMR (75 MHz, $DMSO-d_6$): δ = 166.4 (0), 158.8 (0), 132.6 (0), 122.1 (1), 119.0 (1), 68.1 (2), 31.2 (2), 28.6 (2), 28.6 (2), 28.5 (2), 25.4 (2), 22.0 (2), 13.9 (3); ESMS: m/z = 293 [M-H] $^-$, 587 [2M-H] $^-$; Anal. Calcd for $C_{16}H_{22}O_5$: C, 65.29; H, 7.53. Found: C, 65.28; H, 7.52.

5-Octyloxy-isophthalamide 100

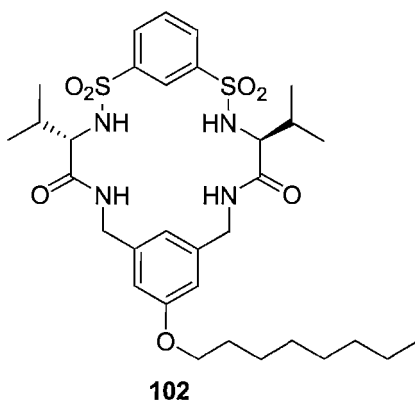
A mixture of bis-acid **99** (5.47 g, 18.6 mmol) and PCl_5 (10 g, 48 mmol) was stirred at 180 °C until a homogeneous yellow solution was formed. The mixture was allowed to cool at room temperature and carefully added into 250 ml of NH_3 saturated DCM at 0 °C. A white precipitate was formed immediately. After the addition was completed, the solid was filtered off, washed (H_2O) and suspended in toluene. The solvent was removed under reduced pressure to yield the desired product **100** as a white solid (4.53 g, 83%). MP = 200-203 °C; $R_f = 0.53$ (90:10 DCM/MeOH); FT-IR (neat): $\nu_{\text{max}} = 3400$ (m), 3323 (w), 3418 (w), 3142 (w), 2951 (w), 2918 (m), 2871 (w), 2850 (w), 1692 (s), 1652 (s), 1625 (s), 1593 (s), 1470 (w), 1432 (s), 1394 (s), 1375 (s), 1255 (m), 1090 (w), 1048 (m), 882 (m), 782 (m), 675 (m), 639 (m) cm^{-1} ; ^1H NMR (300 MHz, $\text{DMSO}-d_6$): $\delta = 7.99$ (2 H, br s, NH_aH_b), 7.96 (1 H, t, $J = 1.5$ Hz, ArH), 7.53 (2 H, d, $J = 1.5$ Hz, ArH), 7.40 (2 H, br s, NH_aH_b), 4.04 (2 H, t, $J = 6.5$ Hz, OCH_2), 1.79-1.67 (2 H, m, OCH_2CH_2), 1.48-1.22 (10 H, m, $(\text{CH}_2)_5\text{CH}_3$), 0.86 (3 H, t, $J = 7.0$ Hz, CH_3); ^{13}C NMR (75 MHz, $\text{DMSO}-d_6$): $\delta = 167.3$ (0), 158.5 (0), 135.7 (0), 119.0 (1), 116.0 (1), 67.9 (2), 31.2 (2), 28.7 (2), 28.6 (2), 28.6 (2), 25.4 (2), 22.0 (2), 13.9 (3); Anal. Calcd for $\text{C}_{16}\text{H}_{22}\text{O}_5 \cdot 0.5\text{H}_2\text{O}$: C, 63.76; H, 8.36; N, 9.30. Found: C, 63.12; H, 8.15; N, 9.87.

3-Aminomethyl-5-octyloxy-benzylamine 101

A mixture of bis-amide **100** (1.98 g, 6.77 mmol) and LiAlH_4 (1.12 g, 29.6 mmol) in dry THF (125 ml) was stirred under N_2 at room temperature for 30 min and refluxed for 2.5 h. The mixture was allowed to cool at room temperature, quenched with H_2O (100 ml), concentrated and extracted (DCM, 100 ml and 2 x 50 ml). The combined organic layers

were dried (MgSO_4) and the solvent was removed under reduced pressure. The residue was dissolved in 1 M HCl (50 ml). The aqueous solution was washed (Et_2O , 3 x 50 ml), basified (2 M NaOH, 60 ml) and extracted (DCM, 3 x 50 ml). The combined organic layers were dried (MgSO_4) and the solvent was removed under reduced pressure to yield the desired product **101** as a yellow oil (915 mg, 51%). FT-IR (neat): $\nu_{\text{max}} = 3358$ (w), 2922 (s), 2854 (s), 1673 (w), 1593 (s), 1452 (s), 1378 (m), 1326 (m), 1287 (s), 1162 (s), 1053 (m), 976 (m), 836 (s), 702 (s) cm^{-1} ; ^1H NMR (400 MHz, CDCl_3): $\delta = 6.84$ (1 H, s, ArH), 6.74 (2 H, s, ArH), 3.96 (2 H, t, $J = 6.5$ Hz, OCH_2), 3.82 (4 H, s, NCH_2), 1.81-1.72 (2 H, m, OCH_2CH_2), 1.49-1.39 (2 H, m, $\text{OCH}_2\text{CH}_2\text{CH}_2$), 1.39-1.21 (8 H, m, $(\text{CH}_2)_4\text{CH}_3$), 0.88 (3 H, t, $J = 7.0$ Hz, CH_3); ^{13}C NMR (75 MHz, CDCl_3): $\delta = 159.9$ (0), 145.3 (0), 118.0 (1), 111.7 (1), 68.2 (2), 46.7 (2), 32.0 (2), 29.5 (2), 29.4 (2), 29.4 (2), 26.2 (2), 22.8 (2), 14.2 (3); ESMS: $m/z = 265$ $[\text{M}+\text{H}]^+$, 287 $[\text{M}+\text{Na}]^+$.

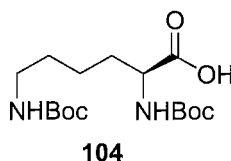
Macrocycle **102**



A solution of pentafluorophenol ester **97** (682 mg, 0.888 mmol) and TBACl (501 mg, 1.80 mmol) in dry DCM (5 ml) and a solution of bis-amine **101** (239 mg, 0.904 mmol) and dry Et_3N (500 μl , 3.59 mmol) in dry DCM (5 ml) were added simultaneously, with a syringe pump, into 100 ml of dry DCM at room temperature over a period of 5 h. The reaction was stirred overnight at room temperature. The solvent was removed under reduced pressure and the residue was purified by flash column chromatography (SiO_2 , 85:15 \rightarrow 65:35 PE/EA). Reprecipitation (EA/PE) yielded the desired product **102** as a white, flocculent solid (246 mg, 42%). MP = 130-132 $^\circ\text{C}$ (EA/PE); $R_f = 0.25$ (60:40 PE/EA); $[\alpha]_D^{26} = +185$ ($c = 0.25$, MeCN); FT-IR (neat): $\nu_{\text{max}} = 3361$ (w), 2929 (m), 1661 (s), 1598 (m), 1539 (m), 1456 (s), 1325 (s), 1297 (s), 1219 (w), 1174 (s), 1156 (s), 1125 (s), 1082 (s), 919 (m), 860 (m), 794 (s), 720 (m), 681 (m) cm^{-1} ; ^1H NMR (400 MHz,

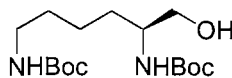
MeCN- d_3): δ = 8.11 (1 H, t, J = 2.0 Hz, O₂SArH), 7.64 (2 H, dd, J = 8.0, 2.0 Hz, O₂SArH), 6.98-6.91 (2 H, m, partially obscured by O₂SArH, CONH), 6.95 (1 H, t, J = 8.0 Hz, O₂SArH), 6.75 (2 H, d, J = 1.5 Hz, ArH), 6.42 (1 H, t, J = 1.5 Hz, ArH), 6.15 (2 H, br s, SNH), 4.37 (2 H, dd, J = 14.0, 8.0 Hz, NHCH_aH_b), 4.03 (2 H, t, J = 6.5 Hz, OCH₂), 3.81 (2 H, dd, J = 14.0, 4.5 Hz, NHCH_aH_b), 3.65 (2 H, br s, α -CH), 2.05-1.96 (2 H, m, α -CHCH), 1.85-1.76 (2 H, m, OCH₂CH₂), 1.54-1.44 (2 H, m, OCH₂CH₂CH₂), 1.43-1.24 (8 H, m, (CH₂)₄CH₃), 1.01 (6 H, d, J = 7.0 Hz, CHCH₃), 0.94 (6 H, d, J = 7.0 Hz, CHCH₃), 0.89 (3 H, t, J = 7.0 Hz, CH₂CH₃); ¹³C NMR (100 MHz, MeCN- d_3): δ = 170.6 (0), 160.1 (0), 143.1 (0), 141.2 (0), 130.6 (1), 130.2 (1), 125.7 (1), 121.4 (1), 114.6 (1), 68.9 (2), 62.9 (1), 43.9 (2), 33.1 (1), 32.6 (2), 30.1 (2), 30.0 (2), 26.8 (2), 23.4 (2), 19.6 (3), 17.9 (3), 14.4 (3); ESMS: m/z = 687 [M+Na]⁺; HRMS (ES): calcd for C₃₂H₄₈N₄NaO₇S₂ ([M+Na]⁺) 687.2857, found 687.2862; Anal. Calcd for C₃₂H₄₈N₄O₇S₂·1H₂O: C, 56.28; H, 7.38; N, 8.20. Found: C, 56.76; H, 7.20; N, 8.22.

(2S)-2,6-Bis-tert-butoxycarbonylamino-hexanoic acid 104



2 M NaOH (40 ml) was added at room temperature to a solution of L-Lysine monochloride **103** (3.40 g, 18.6 mmol) and Boc₂O (9.0 g, 41 mmol) in 50:50 1,4-dioxane/H₂O (60 ml). The reaction was stirred overnight at room temperature. The mixture was concentrated, acidified (1 M KHSO₄, 100 ml) and extracted (EA, 3 x 150 ml). The combined organic layers were dried (MgSO₄) and the solvent was removed under reduced pressure to yield the desired product **104** as a white foam (6.05 g, 94%). $[\alpha]_D^{27} = +13.8$ (c = 0.25, CHCl₃); FT-IR (neat): ν_{\max} = 3341 (w), 2977 (w), 2933 (w), 1686 (s), 1518 (m), 1455 (w), 1392 (w), 1366 (m), 1248 (m), 1159 (s), 1046 (w), 1020 (w), 860 (w), 779 (w), 648 (w) cm⁻¹; ¹H NMR (400 MHz, CDCl₃): δ = 5.24 (1 H, br s, α -CHNH), 4.67 (1 H, br s, CH₂NH), 4.29 (1 H, br s, α -CH), 3.17-3.01 (2 H, m, NHCH₂), 1.55-1.37 (6 H, m, α -CH(CH₂)₃), 1.44 (18 H, s, CH₃); ¹³C NMR (75 MHz, CDCl₃): δ = 176.1 (0), 156.4 (0), 155.8 (0), 80.0 (0), 79.4 (0), 53.3 (1), 40.2 (2), 32.2 (2), 29.5 (2), 28.5 (3), 28.4 (3), 22.5 (2); ESMS: m/z = 345 [M-H]⁻, 691 [2M-H]⁻. Data according to literature.^[128]

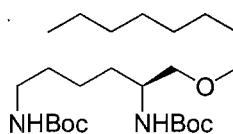
((S)-5-tert-Butoxycarbonylamino-6-hydroxy-hexyl)-carbamic acid tert-butyl ester
105



105

A solution of acid **104** (6.00 g, 17.3 mmol), *N*-hydroxysuccinimide (2.12 g, 18.4 mmol) and EDC (3.7 g, 19 mmol) in dry DCM (85 ml) was stirred overnight at room temperature. The mixture was washed (sat. NH₄Cl, 2 x 150 ml), dried (MgSO₄) and the solvent was removed under reduced pressure. The residue was dissolved in dry THF (150 ml). LiAlH₄ (965 mg, 25.4 mmol) was carefully added to the solution at room temperature. The slurry was stirred for 30 min at room temperature under N₂. The mixture was diluted (DCM, 300 ml) and washed (10% NaOH). The two phases were separated and the aqueous layer was extracted (DCM, 2 x 150 ml). The combined organic layers were dried (MgSO₄) and the solvent was removed under reduced pressure. The residue was purified by flash column chromatography (SiO₂, 60:40 PE/EA) to yield the desired product **105** as a colourless oil (3.37 g, 59%). *R*_f = 0.41 (50:50 PE/EA); [α]_D²⁷ = -14.8 (*c* = 0.25, CHCl₃); FT-IR (neat): *v*_{max} = 3337 (w), 2976 (w), 2932 (w), 1682 (s), 1518 (m), 1456 (w), 1391 (w), 1365 (m), 1247 (m), 1164 (s), 1048 (m), 864 (w), 780 (w), 736 (w) cm⁻¹; ¹H NMR (400 MHz, DMSO-*d*₆): δ = 6.70 (1 H, br s, CH₂NH), 6.37 (1 H, d, *J* = 8.0 Hz, α-CHNH), 4.50 (1 H, apparent t, *J* = 5.0 Hz, OH), 3.37-3.24 (2 H, m, partially obscured by H₂O, α-CH and OCH_aH_b superimposed), 3.24-3.15 (1 H, m, OCH_aH_b), 2.88 (2 H, apparent q, *J* = 6.0 Hz, NHCH₂), 1.54-1.11 (6 H, m, α-CH(CH₂)₃), 1.37 (9 H, s, CH₃), 1.37 (9 H, s, CH₃); ¹³C NMR (75 MHz, DMSO-*d*₆): δ = 155.5 (0), 155.4 (0), 77.3 (0), 77.3 (0), 63.6 (2), 52.2 (1), 39.5 (2), 30.6 (2), 29.5 (2), 28.2 (3), 22.8 (2); ESMS: *m/z* = 333 [M+H]⁺, 355 [M+Na]⁺.

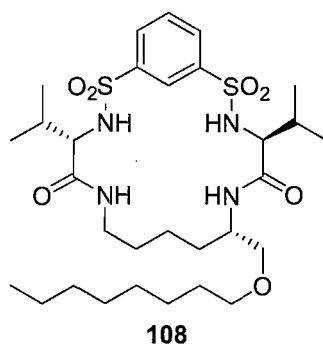
(5-tert-Butoxycarbonylamino-(S)-1-octyloxymethyl-pentyl)-carbamic acid tert-butyl ester
106



106

A mixture of alcohol **105** (2.92 g, 8.79 mmol), 1-iodooctane (8.0 ml, 44 mmol) and TBAHSO₄ (319 mg, 0.940 mmol) in 50% aqueous NaOH (50 g) and toluene (15 ml) was stirred overnight at 70 °C. The two phases were separated and the organic layer was washed (brine, 2 x 50 ml), dried (MgSO₄) and the solvent was removed under reduced pressure. The residue was purified by flash column chromatography (SiO₂, PE → 85:15 PE/EA) to yield the desired product **106** as a colourless oil (2.88 g, 74%). *R_f* = 0.57 (80:20 PE/EA); [α]_D²⁷ = -15.3 (*c* = 1, CHCl₃); FT-IR (neat): ν_{\max} = 3349 (w), 2928 (m), 2857 (m), 1689 (s), 1506 (m), 1456 (m), 1390 (w), 1364 (m), 1246 (m), 1169 (s), 1119 (m), 1023 (w), 866 (w), 779 (w), 737 (w) cm⁻¹; ¹H NMR (400 MHz, CDCl₃): δ = 4.69 (1 H, br s, α -CHNH), 4.58 (1 H, br s, CH₂NH), 3.71-3.60 (1 H, m, α -CH), 3.44-3.32 (4 H, m, α -CHCH₂O and OCH₂CH₂ superimposed), 3.09 (2 H, apparent q, *J* = 6.0 Hz, NHCH₂), 1.59-1.21 (18 H, m, α -CH(CH₂)₃ and CH₃(CH₂)₆ superimposed), 1.43 (18 H, s, CCH₃), 0.87 (3 H, t, *J* = 7.0 Hz, CH₂CH₃); ¹³C NMR (75 MHz, CDCl₃): δ = 156.2 (0), 155.9 (0), 79.2 (0), 79.2 (0), 72.6 (2), 71.6 (2), 50.3 (1), 40.6 (2), 32.1 (2), 32.0 (2), 30.0 (2), 29.7 (2), 29.6 (2), 29.4 (2), 28.6 (3), 26.3 (2), 23.3 (2), 22.8 (2), 14.2 (3); ESMS: *m/z* = 445 [M+H]⁺, 467 [M+Na]⁺; HRMS (ES): calcd for C₂₄H₄₈N₂NaO₅ ([M+Na]⁺) 467.3455, found 467.3450.

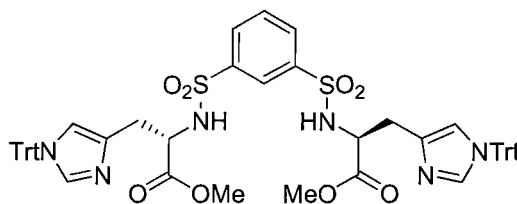
Macrocycle **108**



A solution of ether **106** (357 mg, 0.803 mmol) in 80:20 DCM/TFA (15 ml) was stirred for 4.5 h at room temperature. Toluene was added and the solvent was removed under reduced pressure. The residue was dissolved in dry DCM (5 ml) and dry Et₃N (600 μ l, 4.30 mmol) was added. The mixture and a solution of pentafluorophenol ester **97** (609 mg, 0.753 mmol) and TBACl (420 mg, 1.51 mmol) in dry DCM (5 ml) were added simultaneously, with a syringe pump, into 100 ml of dry DCM at room temperature over a period of 5 h. The reaction was stirred overnight at room temperature. The mixture was

washed (1 M KHSO₄, 2 x 100 ml, 1 M K₂CO₃, 2 x 100 ml, and brine, 100 ml) and dried (MgSO₄). The solvent was removed under reduced pressure and the residue was purified by flash column chromatography (SiO₂, 70:30 → 50:50 PE/EA) to yield the desired product **108** as a white solid (292 mg, 57%). MP = 98-103 °C; R_f = 0.29 (50:50 PE/EA); [α]_D²⁶ = +118 (*c* = 0.5, MeCN); FT-IR (neat): ν_{max} = 3290 (w), 2929 (m), 2857 (m), 1651 (s), 1548 (m), 1435 (m), 1326 (s), 1226 (w), 1177 (s), 1158 (s), 1111 (s), 1083 (s), 1048 (m), 998 (w), 917 (m), 796 (m), 681 (m) cm⁻¹; ¹H NMR (400 MHz, CDCl₃): δ = 8.50 (1 H, apparent t, *J* = 2.0 Hz, ArH), 7.93 (1 H, d, *J* = 8.0 Hz, ArH), 7.89 (1 H, d, *J* = 8.0 Hz, ArH), 7.55 (1 H, apparent t, *J* = 8.0 Hz, ArH), 6.46 (1 H, dd, *J* = 7.0, 5.0 Hz, CH₂NH), 6.05 (1 H, d, *J* = 9.0 Hz, CH₂CHNH), 5.94 (1 H, d, *J* = 9.0 Hz, SNH), 5.91 (1 H, d, *J* = 8.0 Hz, SNH), 3.90-3.82 (1 H, m, NHCHCH₂), 3.74 (1 H, dd, *J* = 8.0, 5.0 Hz, SNHCH), 3.42 (1 H, dd, *J* = 9.0, 6.0 Hz, SNHCH), 3.39-3.25 (3 H, m, CHCH₂O and NHCH_aH_b superimposed), 3.36 (2 H, t, *J* = 6.5 Hz, CH₂CH₂O), 2.87-2.77 (1 H, m, NHCH_aH_b), 2.05-1.89 (2 H, m, partially obscured by H₂O, CH₃CH), 1.55-1.44 (4 H, m, OCH₂CH₂ and NHCHCH₂ superimposed), 1.36-1.22 (12 H, m, NHCH₂CH₂ and CH₃(CH₂)₅ superimposed), 1.06 (3 H, d, *J* = 7.0 Hz, CHCH₃), 1.03-0.75 (2 H, m, NHCH₂CH₂CH₂), 0.97 (3 H, d, *J* = 7.0 Hz, CHCH₃), 0.96 (3 H, d, *J* = 7.0 Hz, CHCH₃), 0.95 (3 H, d, *J* = 7.0 Hz, CHCH₃), 0.88 (3 H, t, *J* = 7.0 Hz, CH₂CH₃); ¹³C NMR (100 MHz, CDCl₃): δ = 170.6 (0), 170.2 (0), 142.2 (0), 141.4 (0), 130.2 (1), 130.2 (1), 130.0 (1), 127.3 (1), 73.1 (2), 71.7 (2), 62.2 (1), 62.1 (1), 50.0 (1), 38.7 (2), 32.9 (1), 32.6 (1), 32.0 (2), 31.7 (2), 29.7 (2), 29.5 (2), 29.4 (2), 28.9 (2), 26.3 (2), 22.8 (2), 22.3 (2), 19.3 (3), 19.2 (3), 18.0 (3), 17.8 (3), 14.2 (3); ESMS: *m/z* = 667 [M+Na]⁺; HRMS (ES): calcd for C₃₀H₅₂N₄NaO₇S₂ ([M+Na]⁺) 667.3170, found 667.3186; Anal. Calcd for C₃₀H₅₂N₄O₇S₂: C, 55.88; H, 8.13; N, 8.68. Found: C, 55.19; H, 8.03; N, 8.41.

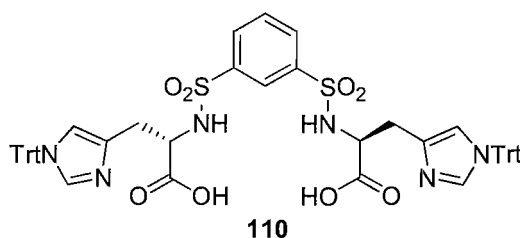
(S)-2-{3-[1-Methoxycarbonyl-(S)-2-(1-trityl-1H-imidazol-4-yl)-ethylsulfamoyl]-benzenesulfonylamino}-3-(1-trityl-1H-imidazol-4-yl)-propionic acid methyl ester **109**



109

A solution of bis-sulfonyl chloride **68** (1.29 g, 4.68 mmol) in dry DCM (20 ml) was added dropwise to a solution of H-His(τ -Trt)-OMe-HCl (4.31 g, 9.62 mmol) and dry Et₃N (2.7 ml, 19 mmol) in dry DCM (40 ml) at 0 °C. The reaction was allowed to reach room temperature and stirred overnight under N₂. The reaction mixture was diluted (DCM, 40 ml), washed (1 M KHSO₄, 100 ml, 1 M K₂CO₃, 100 ml, and brine, 100 ml) and dried (MgSO₄). The solvent was removed under reduced pressure and the residue was purified by flash column chromatography (SiO₂, 50:50 \rightarrow 85:15 EA/PE) to yield the desired product **109** as a white solid (3.84 g, 80%). MP = 90-96 °C; R_f = 0.31 (80:20 EA/PE); FT-IR (neat): ν_{\max} = 3507 (w), 1738 (m), 1598 (w), 1494 (m), 1445 (m), 1338 (s), 1238 (m), 1152 (s), 1130 (s), 1085 (s), 1036 (m), 1001 (m), 848 (w), 799 (w), 747 (s), 699 (s), 683 (s), 659 (m) cm⁻¹; ¹H NMR (400 MHz, CDCl₃): δ = 8.37 (1 H, t, J = 2.0 Hz, ArH), 8.01 (2 H, dd, J = 8.0, 2.0 Hz, ArH), 7.54 (1 H, t, J = 8.0 Hz, ArH), 7.36 (2 H, s, NCHN), 7.34-7.29 (18 H, m, PhH), 7.11-7.05 (12 H, m, PhH), 6.88 (2 H, br s, NH), 6.51 (2 H, s, TrtNCHC), 4.32 (2 H, apparent t, J = 5.0 Hz, α -CH), 3.44 (6 H, s, CH₃), 2.96 (2 H, dd, J = 14.0, 5.0 Hz, α -CHCH_aH_b), 2.90 (2 H, dd, J = 14.0, 5.0 Hz, α -CHCH_aH_b); ¹³C NMR (75 MHz, CDCl₃): δ = 171.1 (0), 142.3 (0), 142.3 (0), 138.9 (1), 135.7 (0), 130.7 (1), 129.9 (1), 129.8 (1), 128.2 (1), 125.9 (1), 119.9 (1), 75.5 (0), 56.2 (1), 52.4 (3), 31.0 (2); ESMS: m/z = 1025 [M+H]⁺, 1047 [M+Na]⁺.

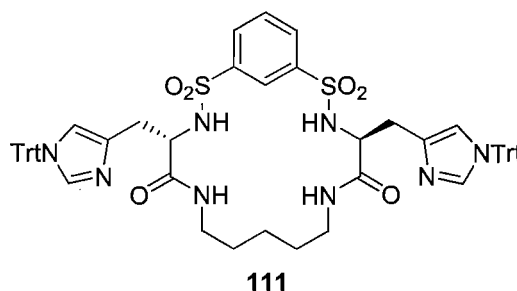
(S)-2-{3-[1-Carboxy-(S)-2-(1-trityl-1H-imidazol-4-yl)-ethylsulfamoyl]-benzenesulfonylamino}-3-(1-trityl-1H-imidazol-4-yl)-propionic acid 110



A solution of bis-ester **109** (1.70 g, 1.66 mmol) in 60:40 1,4-dioxane/1 M LiOH (50 ml) was stirred at room temperature for 5 h. The mixture was diluted (H₂O, 40 ml), washed (Et₂O, 70 + 100 ml) and acidified (2 M KHSO₄). A white precipitate was formed. The solid was filtered off and dissolved in DCM. The solution was dried (MgSO₄) and the solvent was removed under reduced pressure to yield the desired product **110** as a white solid (1.51 g, 91%). MP = 182-187 °C; FT-IR (neat): ν_{\max} = 2853 (w), 1731 (w), 1622 (w), 1494 (w), 1445 (m), 1330 (m), 1175 (m), 1152 (s), 1117 (s), 1082 (s), 1000 (w), 931

(W), 871 (m), 797 (w), 746 (m), 700 (s), 666 (m) cm^{-1} ; ^1H NMR (400 MHz, CDCl_3): δ = 8.31 (2 H, s, NCHN), 8.27 (1 H, t, J = 1.5 Hz, ArH), 7.86 (2 H, dd, J = 8.0, 1.5 Hz, ArH), 7.48 (1 H, t, J = 8.0 Hz, ArH), 7.41-7.19 (18 H, m, PhH), 7.18-7.02 (12 H, m, PhH), 6.81 (2 H, s, TrtNCHC), 4.03 (2 H, dd, J = 11.0, 3.0 Hz, α -CH), 3.20 (2 H, dd, J = 14.0, 3.0 Hz, α -CHCH_aH_b), 2.92 (2 H, dd, J = 14.0, 11.0 Hz, α -CHCH_aH_b); ^{13}C NMR (75 MHz, CDCl_3): δ = 172.5 (0), 141.0 (0), 140.2 (0), 135.9 (1), 131.7 (0), 130.5 (1), 130.0 (1), 129.8 (1), 129.0 (1), 128.8 (1), 127.3 (1), 121.7 (1), 78.4 (0), 56.4 (1), 29.2 (2); ESMS: m/z = 995 [M-H].

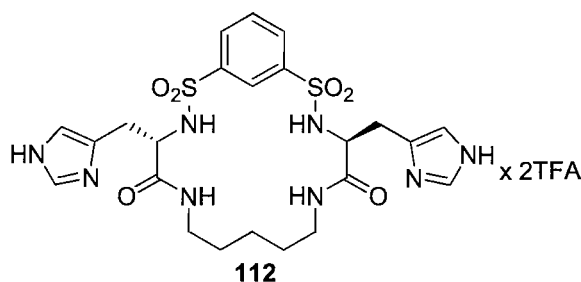
Macrocycle 111



Three solutions of bis-acid **110** (504, 501, 508 mg, 0.505, 0.502, 0.508 mmol), CDI (166, 165, 169 mg, 1.02, 1.02, 1.04 mmol) and dry Et_3N (3 x 145 μl , 1.04 mmol) in dry THF (3 x 7 ml) were stirred for 30 min at room temperature under N_2 . Each solution was added simultaneously with a solution of 1,5-diaminopentane (120, 120, 123 μl , 1.02, 1.02, 1.04 mmol) in dry THF (3 x 7 ml), with a syringe pump, into 20 mmol of dry THF at room temperature over a period of 3.5 h. The reactions were stirred overnight at room temperature under N_2 . The three batches were combined and the solvent was removed under reduced pressure. The residue was dissolved in DCM (200 ml), washed (1 M K_2CO_3 , 150 ml, 1 M KHSO_4 , 150 ml, and brine, 100 ml) and dried (MgSO_4). The solvent was removed under reduced pressure and the residue was purified by flash column chromatography (SiO_2 , 98:2 \rightarrow 97:3 DCM/MeOH) to yield the desired product **111** as a pale yellow solid (52 mg, 3%). MP = 149-157 $^\circ\text{C}$; R_f = 0.63 (95:5 DCM/MeOH); FT-IR (neat): ν_{max} = 3061 (w), 2929 (w), 1651 (m), 1557 (w), 1489 (w), 1444 (m), 1325 (m), 1238 (w), 1175 (m), 1152 (s), 1130 (m), 1084 (m), 1036 (w), 1000 (w), 935 (w), 797 (w), 746 (s), 699 (s), 659 (m) cm^{-1} ; ^1H NMR (400 MHz, CDCl_3): δ = 8.46 (1 H, t, J = 2.0 Hz, ArH), 7.92 (2 H, dd, J = 8.0, 2.0 Hz, ArH), 7.51 (1 H, t, J = 8.0 Hz, ArH), 7.45-7.39 (2 H, m, partially obscured by NCHN, CONH), 7.42 (2 H, d, J = 1.5 Hz, NCHN), 7.36-7.27 (18

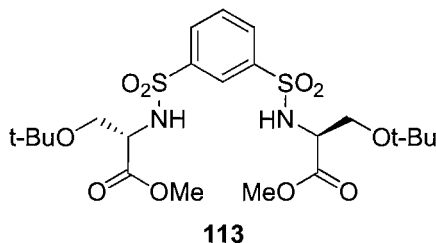
H, m, PhH), 7.14-7.08 (12 H, m, PhH), 6.66 (2 H, d, $J = 1.5$ Hz, TrtNCHC), 4.26 (2 H, apparent t, $J = 6.0$ Hz, α -CH), 3.24-3.14 (2 H, m, NHCH_aH_b), 3.00 (2 H, dd, $J = 15.0$ Hz, 6.0 Hz, α -CHCH_aH_b), 2.95 (2 H, dd, $J = 15.0$ Hz, 6.0 Hz, α -CHCH_aH_b), 2.95-2.85 (2 H, m, partially obscured by α -CHCH_aH_b, NHCH_aH_b), 1.38-1.25 (4 H, m, NHCH₂CH₂), 1.01 (2 H, quin, $J = 7.0$ Hz, NHCH₂CH₂CH₂); ¹³C NMR (75 MHz, CDCl₃): $\delta = 170.7$ (0), 142.3 (0), 141.6 (0), 138.6 (1), 136.1 (0), 130.3 (1), 129.9 (1), 128.3 (1), 127.3 (1), 120.3 (1), 75.7 (0), 56.7 (1), 39.1 (2), 33.1 (2), 28.3 (2), 23.8 (2); ESMS: $m/z = 1063$ [M+H]⁺.

TFA salt **112**



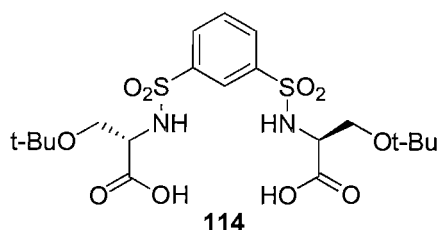
A solution of macrocycle **111** (26 mg, 0.025 mmol) in TFA (3 ml) was stirred for 1 h at room temperature. Toluene was added and the solvent was removed under reduced pressure. The residue was purified by flash column chromatography (SiO₂, 95:5 DCM/MeOH \rightarrow 90:10 DCM/NH₃ sat. MeOH) to yield TFA salt **112** as a yellowish solid (8.5 mg, 42%). MP = 132-138 °C; R_f = 0.47 (90:10 DCM/NH₃ sat. MeOH); [α]_D²⁴ = +70.4 ($c = 0.25$, DMSO); FT-IR (neat): $\nu_{\max} = 3140$ (w), 2861 (w), 1660 (s), 1651 (s), 1568 (w), 1557 (w), 1434 (m), 1329 (m), 1174 (s), 1128 (s), 954 (m), 834 (m), 797 (s), 721 (m), 681 (m) cm⁻¹; ¹H NMR (400 MHz, MeOD-*d*₄): $\delta = 8.35$ (1 H, t, $J = 2.0$ Hz, ArH), 8.30 (2 H, s, NCHN), 7.99 (2 H, dd, $J = 8.0, 2.0$ Hz, ArH), 7.67 (1 H, t, $J = 8.0$ Hz, ArH), 7.18 (2 H, s, NCCHN), 4.15 (2 H, dd, $J = 7.5, 6.0$ Hz, α -CH), 3.17 (2 H, dt, $J = 14.0, 6.0$ Hz, NHCH_aH_b), 3.14 (2 H, dd, $J = 15.0, 6.0$ Hz, α -CHCH_aH_b), 3.06 (2 H, dd, $J = 15.0, 7.5$ Hz, α -CHCH_aH_b), 2.78 (2 H, dt, $J = 14.0, 6.0$ Hz, NHCH_aH_b), 1.34-1.25 (4 H, m, NHCH₂CH₂), 0.99 (2 H, quin, $J = 6.0$ Hz, NHCH₂CH₂CH₂); ¹³C NMR (75 MHz, MeOD-*d*₄): $\delta = 171.4$ (0), 143.3 (0), 135.4 (0), 132.2 (1), 131.4 (1), 127.6 (1), 118.5 (1), 57.5 (1), 40.0 (2), 31.5 (2), 29.2 (2), 24.9 (2); signals corresponding to trifluoroacetate were not detected due to the small sample size; Anal. Calcd for C₂₇H₃₂F₆N₈O₁₀S₂: C, 40.20; H, 4.00; N, 13.89. Found: C, 39.91; H, 4.19; N, 13.10.

3-tert-Butoxy-(S)-2-[3-(2-tert-butoxy-(S)-1-methoxycarbonyl-ethylsulfamoyl)-benzenesulfonylamino]-propionic acid methyl ester **113**



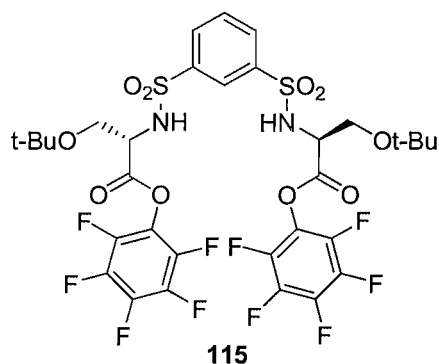
A solution of bis-sulfonyl chloride **68** (2.40 g, 8.71 mmol) in dry DCM (30 ml) was added dropwise to a solution of H-Ser(*t*-Bu)-OMe·HCl (4.05 g, 19.1 mmol) and dry Et₃N (6.4 ml, 46 mmol) in dry DCM (90 ml) at 0 °C. The reaction was allowed to reach room temperature and stirred overnight under N₂. The reaction mixture was diluted (DCM, 50 ml), washed (1 M KHSO₄, 150 ml, 1 M K₂CO₃, 150 ml, and brine, 100 ml) and dried (MgSO₄). The solvent was removed under reduced pressure and the residue was purified by flash column chromatography (SiO₂, 70:30 PE/EA) to yield the desired product **113** as a white solid (4.27 g, 89%). MP = 86-88 °C; R_f = 0.47 (65:35 PE/EA); [α]_D²⁷ = -16.1 (*c* = 0.5, CHCl₃); FT-IR (neat): ν_{max} = 3257 (w), 2977 (w), 1748 (s), 1422 (w), 1346 (m), 1332 (m), 1305 (w), 1284 (w), 1197 (m), 1177 (s), 1156 (s), 1117 (m), 1084 (s), 1050 (m), 1021 (m), 957 (m), 880 (w), 853 (w), 803 (m), 733 (m), 684 (m) cm⁻¹; ¹H NMR (400 MHz, CDCl₃): δ = 8.32 (1 H, t, *J* = 2.0 Hz, Ar*H*), 8.05 (2 H, dd, *J* = 8.0, 2.0 Hz, Ar*H*), 7.65 (1 H, t, *J* = 8.0 Hz, Ar*H*), 5.56 (2 H, d, *J* = 9.5 Hz, NH), 4.17 (2 H, apparent dt, *J* = 9.5, 3.0 Hz, α-CH), 3.74 (2 H, dd, *J* = 9.0, 3.0 Hz, α-CHCH_aH_b), 3.57 (6 H, s, OCH₃), 3.55 (2 H, dd, *J* = 9.0, 3.0 Hz, α-CHCH_aH_b), 1.09 (18 H, s, CCH₃); ¹³C NMR (75 MHz, CDCl₃): δ = 170.0 (0), 142.1 (0), 131.0 (1), 130.1 (1), 125.9 (1), 73.9 (0), 63.0 (2), 56.6 (1), 52.7 (3), 27.3 (3); ESMS: *m/z* = 575 [M+Na]⁺; HRMS (ES): calcd for C₂₂H₃₆N₂NaO₁₀ ([M+Na]⁺) 575.1704, found 575.1712.

3-tert-Butoxy-(*S*)-2-[3-(2-tert-butoxy-(*S*)-1-carboxy-ethylsulfamoyl)-benzenesulfonylamino]-propionic acid **114**



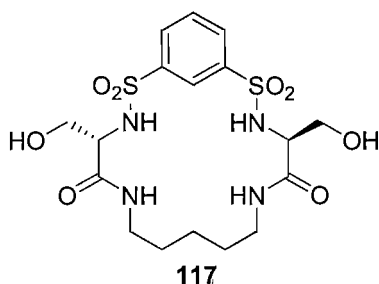
A solution of bis-ester **113** (5.22 g, 9.45 mmol) in 50:50 1,4-dioxane/1 M LiOH (140 ml) was stirred at room temperature for 5 h. The mixture was washed (Et₂O, 3 x 100 ml), acidified (1 M KHSO₄) and extracted (DCM, 3 x 100 ml). The solution was dried (MgSO₄) and the solvent was removed under reduced pressure to yield the desired product **114** as a colourless oil which solidified on standing (4.89 g, 91%). MP = 132-134 °C; $[\alpha]_D^{27} = +36.6$ ($c = 0.5$, CHCl₃); FT-IR (neat): $\nu_{\max} = 3234$ (m), 2971 (w), 1754 (m), 1732 (m), 1699 (m), 1463 (w), 1415 (w), 1391 (w), 1367 (w), 1338 (s), 1299 (w), 1181 (s), 1153 (s), 1120 (s), 1076 (s), 1022 (m), 949 (m), 842 (w), 799 (m), 680 (m) cm⁻¹; ¹H NMR (400 MHz, CDCl₃): $\delta = 8.32$ (1 H, t, $J = 2.0$ Hz, ArH), 8.06 (2 H, dd, $J = 8.0, 2.0$ Hz, ArH), 7.67 (1 H, t, $J = 8.0$ Hz, ArH), 5.63 (2 H, d, $J = 9.0$ Hz, NH), 4.17 (2 H, ddd, $J = 9.0, 6.0, 4.0$ Hz, α -CH), 3.86 (2 H, dd, $J = 9.0, 4.0$ Hz, α -CHCH₂H_b), 3.64 (2 H, dd, $J = 9.0, 6.0$ Hz, α -CHCH_aH_b), 1.19 (18 H, s, CCH₃); ¹³C NMR (100 MHz, CDCl₃): $\delta = 172.8$ (0), 141.5 (0), 131.2 (1), 130.3 (1), 126.2 (1), 75.1 (0), 62.9 (2), 56.0 (1), 27.4 (3); ESMS: $m/z = 523$ [M-H]⁻, 1047 [2M-H]⁻.

3-tert-Butoxy-(*S*)-2-[3-(2-tert-butoxy-(*S*)-1-pentafluorophenylloxycarbonyl-ethylsulfamoyl)-benzenesulfonylamino]-propionic acid pentafluorophenyl ester **115**



A solution of EDC (1.22 g, 6.34 mmol) in dry DCM (25 ml) was added dropwise to a solution of bis-acid **114** (1.50 g, 2.86 mmol) and pentafluorophenol (1.40 g, 7.63 mmol) in dry DCM (20 ml) during 30 min at 0 °C. The reaction was allowed to reach room temperature and stirred overnight under N₂. The solvent was removed under reduced pressure and the residue was purified by flash column chromatography (SiO₂, 95:5 → 85:15 PE/EA) to yield the desired product **115** as a white solid (728 mg, 30%). MP = 57-60 °C; R_f = 0.62 (80:20 PE/EA); FT-IR (neat): ν_{\max} = 3285 (w), 2977 (w), 1797 (m), 1518 (s), 1472 (w), 1418 (w), 1343 (m), 1234 (w), 1181 (m), 1158 (m), 1084 (s), 1043 (m), 989 (s), 867 (m), 808 (m), 741 (w), 682 (m) cm⁻¹; ¹H NMR (400 MHz, CDCl₃): δ = 8.43 (1 H, t, *J* = 2.0 Hz, ArH), 8.06 (2 H, dd, *J* = 8.0, 2.0 Hz, ArH), 7.66 (1 H, t, *J* = 8.0 Hz, ArH), 5.72 (2 H, d, *J* = 10.0 Hz, NH), 4.57 (2 H, apparent dt, *J* = 10.0, 3.0 Hz, α -CH), 3.95 (2 H, dd, *J* = 9.0, 3.0 Hz, α -CHCH_aH_b), 3.68 (2 H, dd, *J* = 9.0, 3.0 Hz, α -CHCH_aH_b), 1.15 (18 H, s, CCH₃); ¹³C NMR (75 MHz, CDCl₃): δ = 166.2 (0), 142.0 (0), 131.1 (1), 130.3 (1), 126.0 (1), 74.4 (0), 63.0 (2), 56.5 (1), 27.2 (3); signals corresponding to aromatic carbons in the pentafluorophenol groups were not detected due to the small sample size.

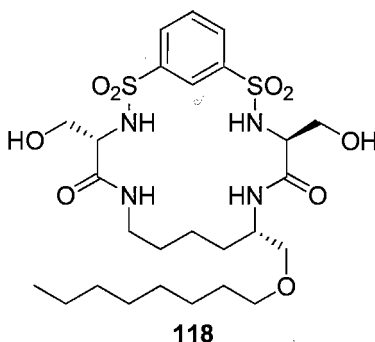
Macrocycle **117**



A solution of EDC (793 mg, 4.14 mmol) in dry DCM (60 ml) was added dropwise to a solution of bis-acid **114** (1.03 g, 1.97 mmol) and pentafluorophenol (1.69 g, 9.19 mmol) in dry DCM (50 ml) during 30 min at 0 °C. The reaction was allowed to reach room temperature and stirred overnight under N₂. The mixture was washed (5% aqueous NaHCO₃, 3 x 150 ml), dried (MgSO₄) and the solvent was removed under reduced pressure yielding the crude pentafluorophenol ester (1.40 g, 83%), which was dissolved in dry DCM (10 ml). TBACl (925 mg, 3.33 mmol) was added. The mixture and a solution of 1,5-diaminopentane (192 μ l, 1.64 mmol) and dry Et₃N (920 μ l, 6.60 mmol) in dry DCM (10 ml) were added simultaneously, with a syringe pump, into 180 ml of dry DCM at room temperature over a period of 5 h. The reaction was stirred overnight at room

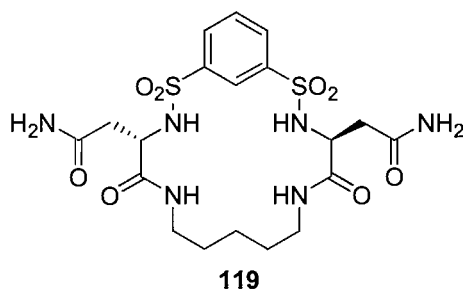
temperature. The mixture was washed (1 M KHSO₄, 150 ml, 1 M K₂CO₃, 150 ml, and brine, 100 ml) and dried (MgSO₄). The solvent was removed under reduced pressure and the residue was purified by flash column chromatography (SiO₂, 30:70 → 55:45 EA/PE) to give the protected macrocycle (360 mg, 37%). The white solid was dissolved in 80:20 DCM/TFA (15 ml) and the solution was stirred for 4 h. Toluene was added and the solvent was removed under reduced pressure. The residue was purified by flash column chromatography (SiO₂, EA, then 92:8 DCM/MeOH) to yield the desired product **117** as a slightly pink solid (289 mg, 31% from **114**). MP = 96-98 °C (acetone); R_f = 0.16 (98:2 DCM/MeOH); [α]_D²⁶ = +111 (*c* = 0.25, MeCN); FT-IR (neat): ν_{\max} = 3271 (w), 2938 (w), 1651 (s), 1548 (m), 1435 (m), 1325 (s), 1175 (s), 1154 (s), 1110 (s), 1060 (s), 999 (w), 964 (m), 799 (s), 681 (s) cm⁻¹; ¹H NMR (400 MHz, DMSO-*d*₆): δ = 8.19 (1 H, t, *J* = 2.0 Hz, ArH), 8.02 (4 H, dd, *J* = 8.0, 2.0 Hz and d, *J* = 8.0 Hz, ArH and SNH superimposed), 7.71 (1 H, t, *J* = 8.0 Hz, ArH), 7.66 (2 H, dd, *J* = 6.5, 6.0 Hz, CONH), 5.04 (2 H, t, *J* = 5.5 Hz, OH), 3.81-3.74 (2 H, m, α -CH), 3.62-3.52 (4 H, m, α -CHCH₂), 3.12-3.02 (2 H, m, NHCH_aH_b), 2.76-2.65 (2 H, m, NHCH_aH_b), 1.20-1.08 (4 H, m, NHCH₂CH₂), 0.76 (2 H, quin, *J* = 7.0 Hz, NHCH₂CH₂CH₂); ¹³C NMR (100 MHz, DMSO-*d*₆): δ = 168.4 (0), 141.8 (0), 130.1 (1), 129.8 (1), 125.1 (1), 62.9 (2), 58.1 (1), 38.3 (2), 28.0 (2), 23.3 (2); ESMS: *m/z* = 501 [M+Na]⁺, 979 [2M+Na]⁺; HRMS (ES): calcd for C₁₇H₂₆N₄NaO₈S₂ ([M+Na]⁺) 501.1084, found 501.1081; Anal. Calcd for C₁₇H₂₆N₄O₈S₂·1H₂O: C, 41.12; H, 5.68; N, 11.28. Found: C, 41.03; H, 5.28; N, 10.80.

Macrocycle **118**



A solution of ether **106** (227 mg, 0.511 mmol) in 80:20 DCM/TFA (10 ml) was stirred for 4 h at room temperature. Toluene was added and the solvent was removed under reduced pressure to give the deprotected TFA salt (240 mg, quant.). 100 mg (0.212 mmol) of the residue were dissolved in dry DCM (4 ml) and dry Et₃N (180 μ l, 1.29 mmol) was added.

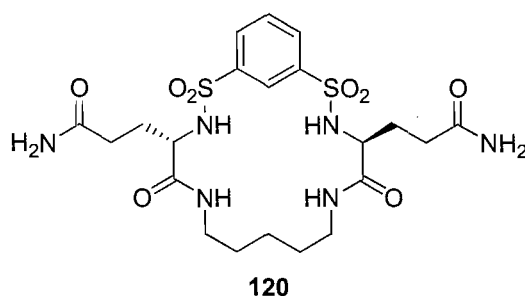
The mixture and a solution of pentafluorophenol ester **115** (183 mg, 0.213 mmol) and TBACl (59 mg, 0.21 mmol) in dry DCM (4 ml) were added simultaneously, with a syringe pump, into 20 ml of dry DCM at room temperature over a period of 5 h. The reaction was stirred overnight at room temperature. The mixture was diluted (DCM, 20 ml), washed (1 M K₂CO₃, 40 ml, 1 M KHSO₄, 40 ml, and brine, 40 ml) and dried (MgSO₄). The solvent was removed under reduced pressure and the residue was purified by flash column chromatography (SiO₂, 90:10 → 60:40 PE/EA) to give the protected macrocycle (88 mg, 56%). 62 mg (0.085 mmol) of the white solid were dissolved in 80:20 DCM/TFA (10 ml) and the solution was stirred for 5 h. Toluene was added and the solvent was removed under reduced pressure. The residue was purified by flash column chromatography (SiO₂, EA) to yield the desired product **118** as a white solid (40 mg, 43% from **115**). MP = 87-93 °C; R_f = 0.26 (EA); [α]_D²⁶ = +96.8 (c = 0.5, MeCN); FT-IR (neat): ν_{max} = 3273 (w), 2927 (w), 2856 (w), 1652 (s), 1556 (m), 1345 (m), 1328 (s), 1177 (s), 1155 (s), 1110 (s), 1082 (s), 963 (m), 798 (m), 681 (m) cm⁻¹; ¹H NMR (400 MHz, MeCN-*d*₃): δ = 8.38 (1 H, apparent t, *J* = 2.0 Hz, ArH), 8.03 (1 H, dd, *J* = 8.0, 2.0 Hz, ArH), 8.02 (1 H, dd, *J* = 8.0, 2.0 Hz, ArH), 7.71 (1 H, apparent t, *J* = 8.0 Hz, ArH), 6.76 (1 H, apparent t, *J* = 6.0 Hz, CH₂NH), 6.72 (1 H, d, *J* = 9.0 Hz, CH₂CHNH), 6.56 (1 H, d, *J* = 8.0 Hz, SNH), 6.54 (1 H, d, *J* = 7.0 Hz, SNH), 3.90-3.62 (7 H, m, NHCHCH₂, SNHCH and HOCH₂ superimposed), 3.36 (1 H, apparent quin, *J* = 6.5 Hz, CH₂CH_aH_bO), 3.35 (1 H, apparent quin, *J* = 6.5 Hz, CH₂CH_aH_bO), 3.27-3.16 (1 H, m, partially obscured by NHCHCH₂OCH₂, NHCH_aH_b), 3.25 (2 H, d, *J* = 6.0 Hz, NHCHCH₂OCH₂), 2.89-2.80 (1 H, m, NHCH_aH_b), 1.48 (2 H, apparent quin, *J* = 6.5 Hz, OCH₂CH₂), 1.37-1.19 (14 H, m, OCH₂CH₂(CH₂)₅, CONHCH₂CH₂ and CONHCHCH₂ superimposed), 1.05-0.83 (2 H, m, partially obscured by CH₃, NHCH₂CH₂CH₂), 0.88 (3 H, t, *J* = 7.0 Hz, CH₃); ¹³C NMR (100 MHz, MeCN-*d*₃): δ = 169.7 (0), 142.1 (0), 142.0 (0), 131.6 (1), 131.5 (1), 131.5 (1), 127.5 (1), 73.7 (2), 71.9 (2), 65.3 (2), 64.6 (2), 58.7 (1), 58.3 (1), 50.7 (1), 39.3 (2), 32.6 (2), 31.1 (2), 30.3 (2), 30.1 (2), 30.0 (2), 29.3 (2), 26.8 (2), 23.3 (2), 23.2 (2), 14.4 (3); ESMS: *m/z* = 643 [M+Na]⁺, 1263 [2M+Na]⁺; HRMS (ES): calcd for C₂₆H₄₄N₄NaO₉S₂ ([M+Na]⁺) 643.2442, found 643.2425; Anal. Calcd for C₂₆H₄₄N₄O₉S₂·1H₂O: C, 48.89; H, 7.26; N, 8.77. Found: C, 48.88; H, 6.96; N, 8.60.

Macrocycle **119**

A solution of EDC (374 mg, 1.95 mmol) in dry DCM (20 ml) was added dropwise to a solution of bis-acid **124** (836 mg, 0.879 mmol) and pentafluorophenol (768 mg, 4.17 mmol) in dry DCM (20 ml) during 30 min at 0 °C. The reaction was allowed to reach room temperature and stirred overnight under N₂. The mixture was washed (5% aqueous NaHCO₃, 2 x 100 ml), dried (MgSO₄) and the solvent was removed under reduced pressure yielding the crude pentafluorophenol ester (779 mg, 69%), which was dissolved in dry DCM (5 ml). TBACl (436 mg, 1.57 mmol) was added. The mixture and a solution of 1,5-diaminopentane (95 µl, 0.811 mmol) and dry Et₃N (450 µl, 3.23 mmol) in dry DCM (5 ml) were added simultaneously, with a syringe pump, into 90 ml of dry DCM at room temperature over a period of 5 h. The reaction was stirred overnight at room temperature. The mixture was washed (1 M KHSO₄, 100 ml, 1 M K₂CO₃, 100 ml, and brine, 100 ml) and dried (MgSO₄). The solvent was removed under reduced pressure and the residue was purified by flash column chromatography (SiO₂, 50:50 → 65:35 EA/PE) to give the protected macrocycle (289 mg, 47%). The white solid was dissolved in TFA (5 ml) and the solution was stirred for 40 min. Toluene was added and the solvent was removed under reduced pressure. The residue was suspended in a MeOH/DCM mixture. The insoluble material was filtered off and washed with MeOH (40 mg of desired product were recovered). The filtrate was concentrated and purified by flash column chromatography (SiO₂, 98:2 → 93:7 DCM/MeOH) to yield a further 40 mg of desired product. In total, 80 mg of the desired product **119** were obtained (17% from **124**). MP = 239-240 °C (dec.); R_f = 0.09 (90:10 DCM/MeOH); [α]_D²⁴ = +63.0 (c = 0.25, DMSO); FT-IR (neat): ν_{max} = 3301 (w), 3239 (w), 2945 (w), 1650 (s), 1549 (m), 1438 (m), 1406 (m), 1332 (m), 1320 (m), 1204 (w), 1173 (s), 1156 (s), 1094 (s), 959 (m), 875 (w), 792 (m), 680 (m) cm⁻¹; ¹H NMR (400 MHz, DMSO-*d*₆): δ = 8.21 (1 H, t, *J* = 2.0 Hz, ArH), 8.09 (2 H, br s, SNH), 8.06 (2 H, dd, *J* = 8.0, 2.0 Hz, ArH), 7.70 (1 H, t, *J* = 8.0 Hz, ArH), 7.58 (2 H, apparent t, *J* = 6.5 Hz, α-CHCONH), 7.35 (2 H, s, NH_aH_b), 6.90 (2 H, s,

NH_aH_b), 4.11 (2 H, apparent t, $J = 6.5$ Hz, α -CH), 2.97 (2 H, apparent sext, $J = 6.5$ Hz, NHCH_aH_b), 2.70 (2 H, apparent sext, $J = 6.5$ Hz, NHCH_aH_b), 2.55 (2 H, dd, $J = 15.0, 7.0$ Hz, α -CHCH_aH_b), 2.50 (2 H, dd, $J = 15.0, 6.0$ Hz, α -CHCH_aH_b), 1.17-1.05 (4 H, m, NHCH₂CH₂), 0.75 (2 H, quin, NHCH₂CH₂CH₂); ¹³C NMR (100 MHz, DMSO-*d*₆): $\delta = 170.9$ (0), 169.0 (0), 141.7 (0), 130.0 (1), 129.9 (1), 125.3 (1), 53.4 (1), 39.3 (2), 38.4 (2), 27.8 (2), 23.3 (2); ESMS: $m/z = 555$ [M+Na]⁺, 1087 [2M+Na]⁺.

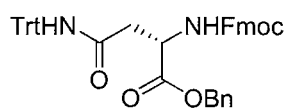
Macrocycle **120**



A solution of EDC (263 mg, 1.37 mmol) in dry DCM (20 ml) was added dropwise to a solution of bis-acid **127** (568 mg, 0.58 mmol) and pentafluorophenol (640 mg, 3.48 mmol) in dry DCM (20 ml) during 30 min at 0 °C. The reaction was allowed to reach room temperature and stirred overnight under N₂. The mixture was washed (5% aqueous NaHCO₃, 2 x 70 ml), dried (MgSO₄) and the solvent was removed under reduced pressure yielding the crude pentafluorophenol ester (707 mg, 93%), which was dissolved in dry DCM (5 ml). TBACl (299 mg, 1.08 mmol) was added. The mixture and a solution of 1,5-diaminopentane (65 μ l, 0.555 mmol) and dry Et₃N (290 μ l, 2.08 mmol) in dry DCM (5 ml) were added simultaneously, with a syringe pump, into 60 ml of dry DCM at room temperature over a period of 5 h. The reaction was stirred overnight at room temperature. The mixture was washed (1 M KHSO₄, 2 x 50 ml, 1 M K₂CO₃, 2 x 50 ml, and brine, 50 ml) and dried (MgSO₄). The solvent was removed under reduced pressure and the residue was purified by flash column chromatography (SiO₂, 50:50 \rightarrow 70:30 EA/PE) to give the protected macrocycle (208 mg, 37%). The white solid was dissolved in TFA (6 ml) and the solution was stirred for 1 h. Toluene was added and the solvent was removed under reduced pressure. The residue was purified by flash column chromatography (SiO₂, EA, then 98:2 \rightarrow 90:10 DCM/MeOH) to yield the desired product **120** as a white solid (80 mg, 25% from **127**). MP = 130-135 °C; R_f = 0.26 (90:10 DCM/MeOH); [α]_D²⁴ = +132 ($c = 0.25$, DMSO); FT-IR (neat): $\nu_{\max} = 3206$ (w), 2930 (w), 1651 (s), 1556 (m), 1414 (m),

1320 (m), 1173 (s), 1152 (s), 1107 (m), 1082 (m), 981 (w), 906 (w), 797 (m), 681 (m) cm^{-1} ; ^1H NMR (400 MHz, $\text{DMSO-}d_6$): δ = 8.20 (2 H, br s, SNH), 8.17 (1 H, t, J = 2.0 Hz, ArH), 7.97 (2 H, dd, J = 8.0, 2.0 Hz, ArH), 7.79 (2 H, dd, J = 7.0, 5.0 Hz, $\alpha\text{-CHCONH}$), 7.69 (1 H, t, J = 8.0 Hz, ArH), 7.32 (2 H, s, NH_aH_b), 6.75 (2 H, s, NH_aH_b), 3.76 (2 H, dd, J = 8.0, 6.0 Hz, $\alpha\text{-CH}$), 3.14-3.03 (2 H, m, NHCH_aH_b), 2.70-2.60 (2 H, m, NHCH_aH_b), 2.19 (2 H, ddd, J = 16.0, 10.0, 6.0 Hz, $\text{NH}_2\text{COCH}_a\text{H}_b$), 2.10 (2 H, ddd, J = 16.0, 10.0, 6.0 Hz, $\text{NH}_2\text{COCH}_a\text{H}_b$), 1.90-1.72 (4 H, m, $\alpha\text{-CHCH}_2$), 1.22-1.06 (4 H, m, NHCH_2CH_2), 0.77 (2 H, quin, J = 7.0 Hz, $\text{NHCH}_2\text{CH}_2\text{CH}_2$); ^{13}C NMR (100 MHz, $\text{DMSO-}d_6$): δ = 173.4 (0), 169.7 (0), 142.1 (0), 129.8 (1), 129.5 (1), 124.9 (1), 56.0 (1), 38.2 (2), 31.1 (2), 29.4 (2), 28.0 (2), 23.3 (2); ESMS: m/z = 583 $[\text{M}+\text{Na}]^+$, 1143 $[2\text{M}+\text{Na}]^+$; HRMS (ES): calcd for $\text{C}_{21}\text{H}_{32}\text{N}_6\text{NaO}_8\text{S}_2$ ($[\text{M}+\text{Na}]^+$) 583.1615, found 583.1600.

(S)-2-(9H-Fluoren-9-ylmethoxycarbonylamino)-N-trityl-succinamic acid benzyl ester
122

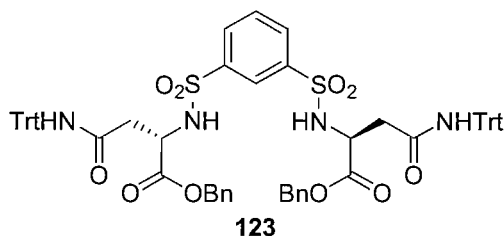


122

A mixture of Fmoc-Asn(Trt)-OH (2.98 g, 4.99 mmol), K_2CO_3 (1.40 g, 10.1 mmol) and BnBr (550 μl , 4.62 mmol) in acetone (75 ml) was refluxed for 3 h. The insoluble material was filtered off and the solvent was removed under reduced pressure. The residue was purified by flash column chromatography (SiO_2 , $\text{DCM} \rightarrow 99:1$ DCM/MeOH) to yield the desired product **122** as a white solid (2.57 g, 81%). MP = 84-87 $^\circ\text{C}$; R_f = 0.24 (75:25 PE/EA); $[\alpha]_D^{27}$ = +13.3 (c = 0.5, CHCl_3); FT-IR (neat): ν_{max} = 3324 (w), 3032 (w), 2945 (w), 1723 (m), 1715 (m), 1694 (m), 1682 (m), 1668 (m), 1597 (w), 1489 (s), 1447 (s), 1329 (w), 1187 (s), 1104 (w), 1080 (w), 1034 (m), 1002 (w), 902 (w), 738 (s), 696 (s) cm^{-1} ; ^1H NMR (300 MHz, CDCl_3): δ = 7.84 (2 H, d, J = 7.5 Hz, FluH), 7.66 (2 H, d, J = 7.5, FluH), 7.48 (2 H, t, J = 7.5 Hz, FluH), 7.41-7.32 (16 H, m, PhH and FluH superimposed), 7.30-7.21 (6 H, m, PhH), 6.81 (1 H, s, TrtNH), 6.22 (1 H, d, J = 8.5 Hz, FmocNH), 5.24 (1 H, d, J = 12.5 Hz, PhCH_aH_b), 5.19 (1 H, d, J = 12.5 Hz, PhCH_aH_b), 4.80-4.70 (1 H, m, $\alpha\text{-CH}$), 4.50 (1 H, dd, J = 10.0, 7.5 Hz, FluCH_aH_b), 4.37 (1 H, dd, J = 10.0, 7.5 Hz, FluCH_aH_b), 4.27 (1 H, apparent t, J = 7.5 Hz, FluH), 3.21 (1 H, dd, J = 16.0, 4.0 Hz, $\alpha\text{-CHCH}_a\text{H}_b$), 2.94 (1 H, dd, J = 16.0, 4.0 Hz, $\alpha\text{-CHCH}_a\text{H}_b$); ^{13}C NMR (75 MHz, CDCl_3): δ

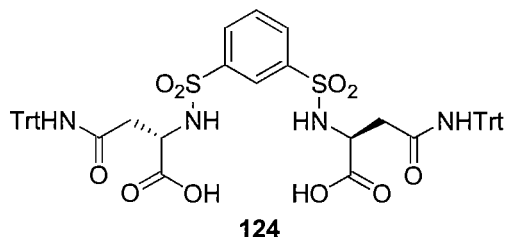
= 171.0 (0), 169.3 (0), 156.4 (0), 144.4 (0), 144.1 (0), 141.4 (0), 135.5 (0), 128.8 (1), 128.7 (1), 128.4 (1), 128.2 (1), 127.8 (1), 127.3 (1), 127.2 (1), 125.4 (1), 125.3 (1), 120.1 (1), 71.1 (0), 67.6 (2), 67.4 (2), 51.3 (1), 47.3 (1), 38.8 (2); ESMS: $m/z = 709 [M+Na]^+$.

(S)-2-{3-[(S)-1-Benzoyloxycarbonyl-2-(trityl-carbamoyl)-ethylsulfamoyl]-benzenesulfonylamino}-N-trityl-succinamic acid benzyl ester **123**



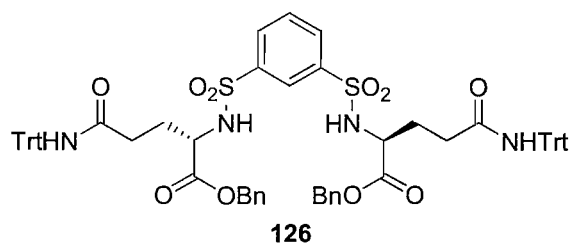
A solution of protected asparagine **122** (4.82 g, 7.23 mmol) in 80:20 DMF/piperidine (30 ml) was stirred for 1 h. Toluene was added and the solvent was removed under reduced pressure. The residue was dissolved in dry DCM (30 ml) and dry Et₃N (1.25 ml, 8.91 mmol) was added. A solution of bis-sulfonyl chloride **68** (908 mg, 3.30 mmol) in dry DCM (25 ml) was added dropwise to the mixture at room temperature during 30 min. The reaction was stirred overnight under N₂. The mixture was diluted (DCM, 45 ml), washed (1 M KHSO₄, 100 ml) and dried (MgSO₄). The solvent was removed under reduced pressure and the residue was purified by flash column chromatography (SiO₂, 95:5 → 65:35 PE/EA) to yield the desired product **123** as a white solid (2.64 g, 71%). MP = 103–107 °C; R_f = 0.19 (65:35 PE/EA); [α]_D²⁷ = +8.4 (*c* = 0.5, CHCl₃); FT-IR (neat): ν_{max} = 3296 (w), 3061 (w), 1738 (m), 1732 (m), 1681 (m), 1667 (m), 1597 (w), 1515 (m), 1494 (m), 1446 (m), 1415 (w), 1339 (m), 1274 (m), 1175 (m), 1152 (s), 1111 (m), 1083 (m), 1036 (m), 1001 (w), 947 (w), 903 (w), 825 (w), 750 (m), 696 (s), 681 (m) cm⁻¹; ¹H NMR (400 MHz, CDCl₃): δ = 8.26 (1 H, t, *J* = 2.0 Hz, Ar*H*), 7.83 (2 H, dd, *J* = 8.0, 2.0 Hz, Ar*H*), 7.30–7.19 (25 H, m, Ph*H* and Ar*H* superimposed), 7.13 (12 H, dd, *J* = 8.0, 2.0 Hz, Ph*H*), 7.05 (4 H, dd, *J* = 8.0, 2.0 Hz, Ph*H*), 6.65 (2 H, s, TrtNH), 6.08 (2 H, d, *J* = 8.5 Hz, SNH), 4.88 (2 H, d, *J* = 12.0 Hz, PhCH_aH_b), 4.81 (2 H, d, *J* = 12.0 Hz, PhCH_aH_b), 4.18 (2 H, apparent dt, *J* = 8.5, 4.0 Hz, α-CH), 3.04 (2 H, dd, *J* = 16.0, 4.0 Hz, α-CHCH_aH_b), 2.82 (2 H, dd, *J* = 16.0, 4.0 Hz, α-CHCH_aH_b); ¹³C NMR (100 MHz, CDCl₃): δ = 170.0 (0), 168.8 (0), 144.3 (0), 141.5 (0), 134.9 (0), 130.9 (1), 130.0 (1), 128.8 (1), 128.7 (1), 128.5 (1), 128.3 (1), 128.2 (1), 127.3 (1), 125.9 (1), 71.2 (0), 67.9 (2), 53.0 (1), 39.8 (2); ESMS: $m/z = 1153 [M+Na]^+$.

(S)-2-{3-[(S)-1-Carboxy-2-(trityl-carbamoyl)-ethylsulfamoyl]-benzenesulfonylamino}-N-trityl-succinamic acid **124**



A mixture of bis-ester **123** (1.66 g, 1.47 mmol) and Pd/C (10% wt, 310 mg, 0.294 mmol) in 2:1 MeOH/THF (100 ml) was stirred at room temperature under H₂ (atmospheric pressure) for 6 h. The mixture was filtered through a celite pad and the solvent was removed under reduced pressure to yield the desired product **124** as a white solid (1.33 g, 95%). MP = 125-130 °C; FT-IR (neat): ν_{\max} = 3272 (w), 3057 (w), 2874 (w), 1731 (m), 1668 (m), 1516 (m), 1491 (m), 1446 (m), 1416 (w), 1338 (m), 1117 (m), 1153 (s), 1110 (m), 1084 (w), 1050 (w), 1036 (w), 843 (w), 797 (w), 751 (m), 698 (s), 682 (m) cm⁻¹; ¹H NMR (400 MHz, CDCl₃): δ = 8.32 (1 H, t, *J* = 2.0 Hz, Ar*H*), 7.81 (2 H, dd, *J* = 8.0, 2.0 Hz, Ar*H*), 7.37-7.16 (19 H, m, Ph*H* and Ar*H* superimposed), 7.13 (12 H, dd, *J* = 8.0, 2.0 Hz, Ph*H*), 6.93 (2 H, s, TrtNH), 6.50 (2 H, d, *J* = 9.0 Hz, SNH), 4.09 (2 H, apparent quin, *J* = 4.5 Hz, α -CH), 3.13 (2 H, dd, *J* = 16.0, 4.0 Hz, α -CHCH_aH_b), 2.87 (2 H, dd, *J* = 16.0, 5.5 Hz, α -CHCH_aH_b); ¹³C NMR (100 MHz, CDCl₃): δ = 169.8 (0), 167.9 (0), 144.0 (0), 141.1 (0), 131.0 (1), 129.8 (1), 128.8 (1), 128.2 (1), 127.4 (1), 126.2 (1), 71.4 (0), 52.6 (1), 40.3 (2); ESMS: *m/z* = 949 [M-H]⁻.

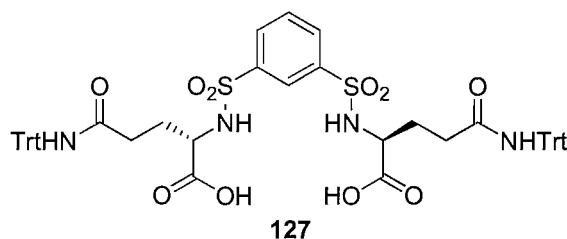
(S)-2-{3-[(S)-1-Benzoyloxycarbonyl-3-(trityl-carbamoyl)-propylsulfamoyl]-benzenesulfonylamino}-4-(trityl-carbamoyl)-butyric acid benzyl ester **126**



A mixture of Fmoc-Gln(Trt)-OH (5.08 g, 8.31 mmol), K₂CO₃ (2.40 g, 17.4 mmol) and BnBr (950 μ l, 7.99 mmol) in acetone (120 ml) was refluxed for 3.5 h. The insoluble

material was filtered off and DMF (28 ml) was added to the mixture. The solution was concentrated and piperidine (7 ml) was added. The reaction was stirred for 1 h. Toluene was added and the solvent was removed under reduced pressure. The residue was dissolved in dry DCM (60 ml) and dry Et₃N (1.0 ml, 7.2 mmol) was added. A solution of bis-sulfonyl chloride **68** (854 mg, 3.10 mmol) in dry DCM (60 ml) was added dropwise to the mixture at room temperature during 30 min. The reaction was stirred overnight under N₂. The mixture was diluted (DCM, 40 ml), washed (1 M KHSO₄, 100 ml) and dried (MgSO₄). The solvent was removed under reduced pressure and the residue was purified by flash column chromatography (SiO₂, 95:5 → 58:42 PE/EA) to yield the desired product **126** as a yellow solid (2.28 g, 64%). MP = 95-98 °C (dec.); R_f = 0.39 (55:45 PE/EA); [α]_D²⁷ = +25.2 (*c* = 1, CHCl₃); FT-IR (neat): ν_{max} = 3290 (w), 3057 (w), 1732 (m), 1668 (m), 1597 (w), 1489 (s), 1446 (m), 1338 (m), 1258 (m), 1152 (s), 1106 (m), 1082 (m), 1034 (w), 1001 (w), 902 (w), 796 (w), 749 (s), 696 (s) cm⁻¹; ¹H NMR (400 MHz, CDCl₃): δ = 8.27 (1 H, t, *J* = 2.0 Hz, Ar*H*), 7.77 (2 H, dd, *J* = 8.0, 2.0 Hz, Ar*H*), 7.30-7.11 (41 H, m, Ph*H* and Ar*H* superimposed), 6.72 (2 H, s, TrtNH), 5.87 (2 H, d, *J* = 9.0 Hz, SNH), 4.87 (4 H, s, PhCH₂), 3.74 (2 H, apparent dt, *J* = 4.0, 9.0 Hz, α-CH), 2.43-2.33 (2 H, m, α-CHCH₂CH_aH_b), 2.32-2.23 (2 H, m, α-CHCH₂CH_aH_b), 2.12-2.02 (2 H, m, α-CHCH_aH_b), 1.80-1.69 (2 H, m, α-CHCH_aH_b); ¹³C NMR (100 MHz, CDCl₃): δ = 171.0 (0), 170.6 (0), 144.7 (0), 141.4 (0), 134.9 (0), 130.9 (1), 129.9 (1), 128.8 (1), 128.8 (1), 128.7 (1), 128.6 (1), 128.1 (1), 127.2 (1), 125.9 (1), 70.8(0), 67.7 (2), 55.6 (1), 32.6 (2), 28.2 (2); ESMS: *m/z* = 1181 [M+Na]⁺.

(S)-2-{3-[(S)-1-Carboxy-3-(trityl-carbamoyl)-propylsulfamoyl]-benzenesulfonylamino}-4-(trityl-carbamoyl)-butyric acid **127**



A mixture of bis-ester **126** (1.29 g, 1.11 mmol) and Pd/C (10% wt, 257 mg, 0.244 mmol) in 2:1 MeOH/THF (75 ml) was stirred at room temperature under H₂ (atmospheric pressure) for 4.5 h. The mixture was filtered through a celite pad and the solvent was removed under reduced pressure to yield the desired product **127** as a white solid (1.04 g,

95%). MP = 144-147 °C; FT-IR (neat): ν_{\max} = 3271 (w), 3056 (w), 2928 (w), 1731 (m), 1668 (m), 1490 (s), 1446 (m), 1417 (w), 1338 (s), 1178 (m), 1152 (s), 1106 (m), 1036 (w), 1001 (w), 971 (w), 901 (w), 796 (w), 751 (m), 698 (s) cm^{-1} ; ^1H NMR (400 MHz, CDCl_3): δ = 8.25 (1 H, s, ArH), 7.83 (2 H, dd, J = 8.0, 2.0 Hz, ArH), 7.45 (1 H, t, J = 8.0 Hz, ArH), 7.30-7.10 (30 H, m, PhH), 7.07 (2 H, s, TrtNH), 6.02 (2 H, d, J = 8.5 Hz, SNH), 3.83-3.74 (2 H, m, α -CH), 2.60-2.46 (2 H, m, partially obscured by H_2O , α -CHCH $_2$ CH $_a$ H $_b$), 2.45-2.34 (2 H, m, α -CHCH $_2$ CH $_a$ H $_b$), 2.00-1.90 (2 H, m, α -CHCH $_a$ H $_b$), 1.82-1.70 (2 H, m, α -CHCH $_a$ H $_b$); ^{13}C NMR (75 MHz, CDCl_3): δ = 173.4 (0), 172.5 (0), 144.3 (0), 141.2 (0), 131.2 (1), 130.1 (1), 128.8 (1), 128.1 (1), 127.2 (1), 126.0 (1), 71.0 (0), 55.5 (1), 32.8 (2), 28.4 (2); ESMS: m/z = 977 $[\text{M}-\text{H}]^-$.

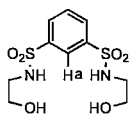
5.6 Binding studies

64 with TBAOAc in $\text{MeCN}-d_3$

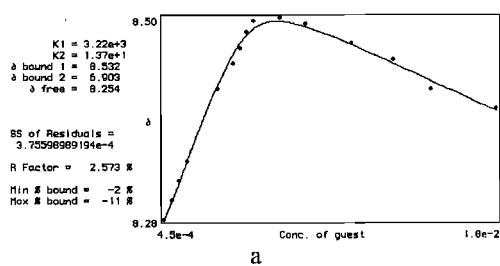
$$[\text{H}] = 5.03 \cdot 10^{-3} \text{ M}$$

$$[\text{G}] = 5.44 \cdot 10^{-2} \text{ M}$$

$$V_i = 600 \mu\text{l}$$



Volume added (μl)	δ_a
5	8.2831
10	8.3032
15	8.3233
20	8.3434
40	8.4206
50	8.447
55	8.4633
60	8.4802
65	8.4922
85	8.4959
105	8.4884
145	8.4689
185	8.4508
225	8.42
305	8.3999

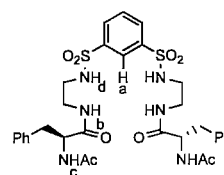


65 with *N*-Ac-L-Phe-OTBA in $\text{MeCN}-d_3$

$$[\text{H}] = 1.26 \cdot 10^{-3} \text{ M}$$

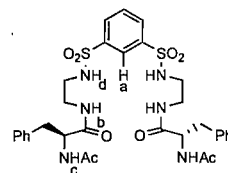
$$[\text{G}] = 4.35 \cdot 10^{-2} \text{ M}$$

$$V_i = 600 \mu\text{l}$$

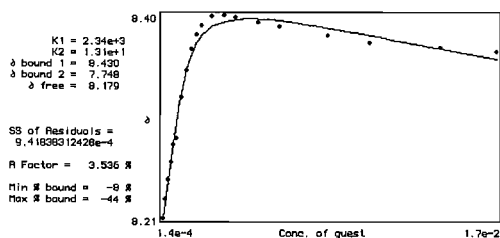


Volume added (μl)	δ_a	δ_b	δ_c	δ_d
2	8.2129	6.999	6.8998	6.3826
4	8.2304	7.0994	6.9839	6.532
6	8.2493	—	7.063	6.6751
8	8.2656	—	—	6.8157
10	8.2819	7.368	—	6.955
12	8.2882	7.4521	7.3034	7.0931
16	8.3271	7.6116	7.4471	7.3253
20	8.3522	7.7509	7.5814	7.5538
24	8.3723	7.8752	—	—
28	8.3861	7.9731	7.7936	7.8714
32	8.3949	8.0446	7.8746	7.9831

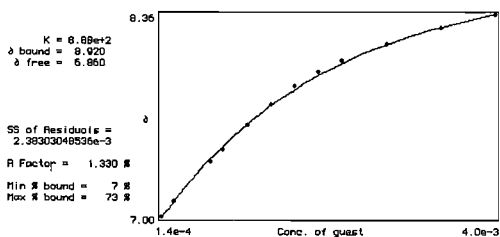
40	8.4037	8.1589	—	8.1501
50	8.4049	8.2643	8.1513	8.2882
60	8.4024	8.3604	8.2618	—
80	8.3974	—	8.4288	—
100	8.3936	—	—	—
150	8.3848	—	—	—
200	8.3786	—	—	—
300	8.3735	—	—	—
400	8.3698	—	—	—



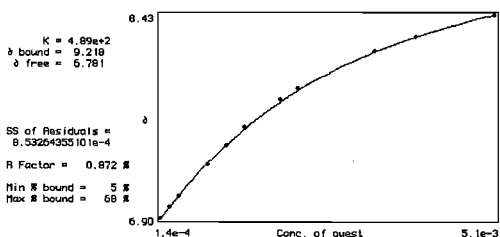
Volume added (μl)	a	b	c	d
2	8.2116	6.9651	6.8709	6.3587
4	8.2292	7.078	6.9481	6.5232
6	8.2455	—	7.0115	6.6701
8	8.2643	—	7.0893	6.8132
10	8.2819	7.3429	—	6.9701
12	8.2995	7.4371	—	—
16	8.3296	7.589	7.3617	—
20	8.356	—	7.471	7.6015
24	8.3773	—	7.5708	—
28	8.3911	—	7.653	—
32	8.4011	—	7.7258	—
40	8.4112	8.1225	7.8363	8.2179
50	8.415	8.2154	7.9417	8.3447
60	8.415	8.2819	—	—
80	8.4074	—	8.1702	8.553
100	8.4049	8.479	8.2869	8.6497
150	8.3961	8.6133	8.4752	8.8016
200	8.3936	8.6987	8.5957	8.892
300	8.3861	8.7916	8.7251	8.9861
400	8.3861	—	—	9.0502



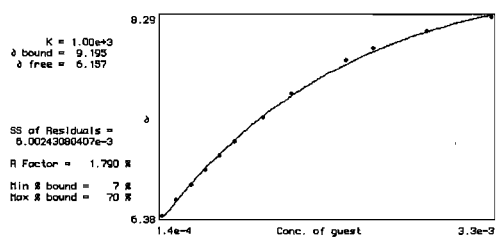
a



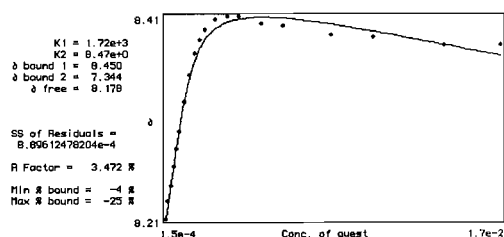
b



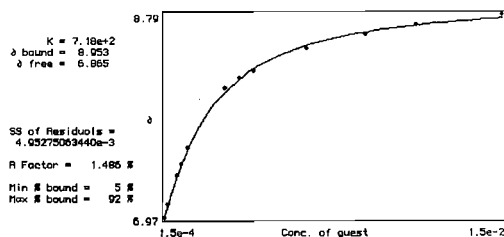
c



d



a



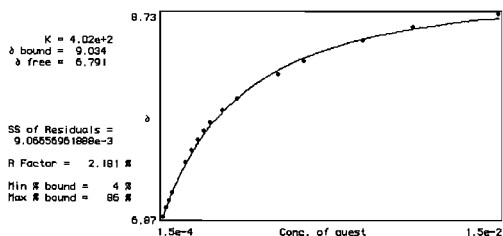
b

65 with *N*-Ac-D-Phe-OTBA in MeCN-*d*₃

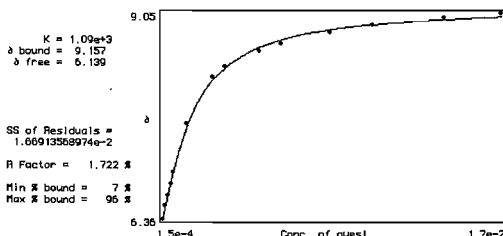
$$[H] = 1.26 \cdot 10^{-3} \text{ M}$$

$$[G] = 4.37 \cdot 10^{-2} \text{ M}$$

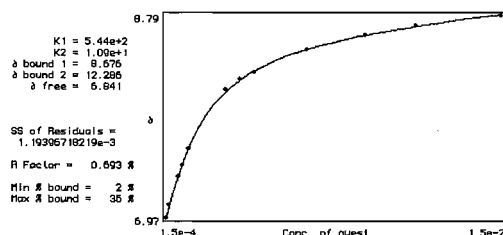
$$V_i = 600 \text{ } \mu\text{l}$$



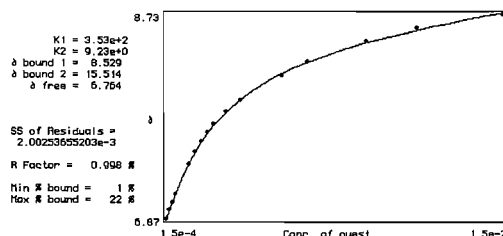
C



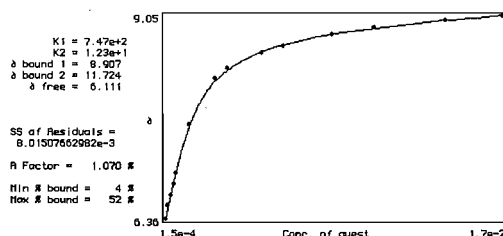
d



b



C



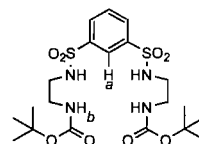
d

69 with TBAOAc in MeCN- d_3

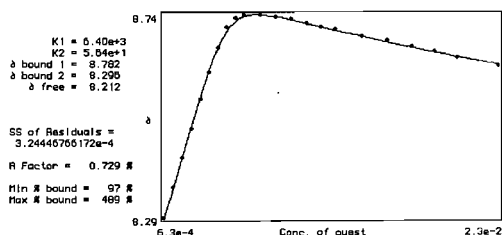
$$[H] = 4.82 \cdot 10^{-3} \text{ M}$$

$$[G] = 7.67 \cdot 10^{-2} \text{ M}$$

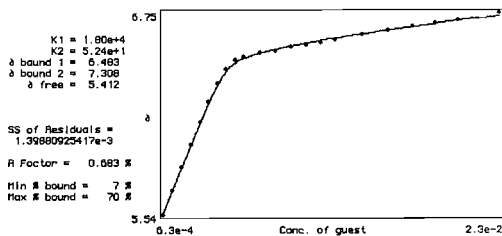
$$V_i = 600 \mu\text{l}$$



Volume added (μl)	δ_a	δ_b
5	8.2932	5.5432
10	8.3596	5.6858
15	8.4235	5.8244
20	8.4875	5.9574
25	8.551	6.2142
30	8.6106	6.0929
35	8.6634	6.3224
40	8.7087	6.4078
45	8.7286	6.463
50	8.7365	6.4841
60	8.7361	6.5075
70	8.7301	6.5206
80	8.7266	6.5437
90	8.7174	6.5564
100	8.7095	6.5703
110	8.7043	6.5866
130	8.6888	6.6164
150	8.6789	6.639
170	8.6654	6.6656
190	8.6543	6.6857
210	8.642	6.7021
250	8.6245	6.7473



a



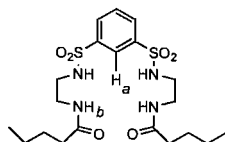
b

71 with TBAOAc in MeCN- d_3

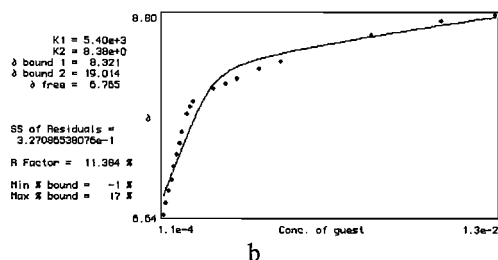
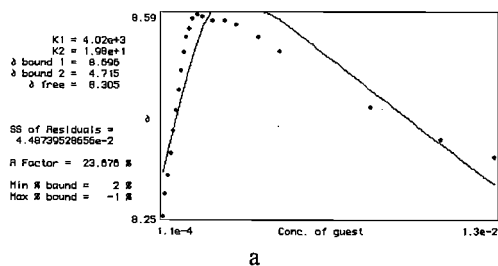
$$[H] = 2.08 \cdot 10^{-3} \text{ M}$$

$$[G] = 3.34 \cdot 10^{-2} \text{ M}$$

$$V_i = 600 \mu\text{l}$$



Volume added (μl)	δ_a	δ_b
2	8.2505	6.6362
4	8.2869	6.7667
6	8.3183	6.8923
8	8.3547	7.0128
10	8.3936	7.1559
12	8.4275	7.2852
14	8.4614	7.4044
16	8.494	7.5224
18	8.5242	—
20	8.5505	7.7296
22	8.5642	7.8024
24	8.5807	7.8526
28	8.5882	—
32	8.5844	—
40	8.5769	7.9926
50	8.5767	8.0534
60	8.5706	8.1087
80	8.5493	8.2116
100	8.5267	8.2957
200	8.4313	8.5819
300	8.3773	8.7326
394	8.3484	8.8016

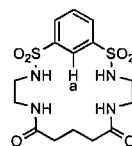


73 with TBAOAc in DMSO- d_6

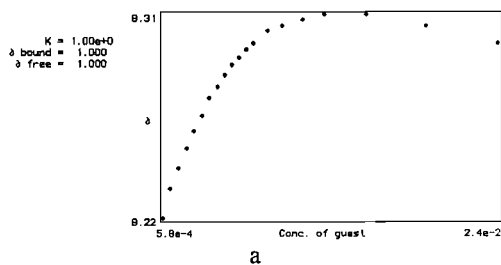
$$[H] = 5.90 \cdot 10^{-3} \text{ M}$$

$$[G] = 1.16 \cdot 10^{-1} \text{ M}$$

$$V_i = 600 \mu\text{l}$$



Volume added (μl)	δ_a
3	8.2178
6	8.2304
9	8.2392
12	8.2479
15	8.2555
18	8.2618
21	8.2693
24	8.2743
27	8.2793
30	8.2837
33	8.2869
36	8.2906
39	8.2931
45	8.2982
51	8.3007
60	8.3032
70	8.3057
90	8.3057
120	8.3007
160	8.2931

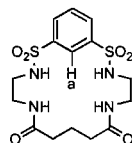


73 with TBAOAc in DMSO- d_6

$$[H] = 5.90 \cdot 10^{-3} \text{ M}$$

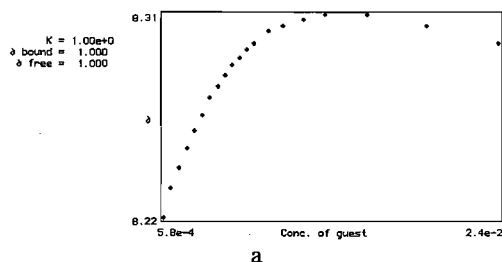
$$[G] = 1.16 \cdot 10^{-1} \text{ M}$$

$$V_i = 600 \mu\text{l}$$



Volume added (μl)	δ_a
3	8.2178
6	8.2304
9	8.2392
12	8.2479

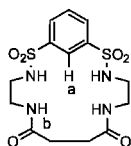
15	8.2555
18	8.2618
21	8.2693
24	8.2743
27	8.2793
30	8.2837
33	8.2869
36	8.2906
39	8.2931
45	8.2982
51	8.3007
60	8.3032
70	8.3057
90	8.3057
120	8.3007
160	8.2931

74 with TBAOAc in DMSO-*d*₆

$$[H] = 3.53 \cdot 10^{-3} \text{ M}$$

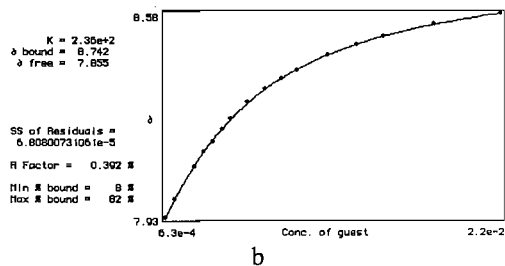
$$[G] = 7.62 \cdot 10^{-2} \text{ M}$$

$$V_i = 600 \mu\text{l}$$



Volume added (μl)	δ_a	δ_b
5	8.1075	7.9255
10	8.1176	7.982
15	8.1251	8.09
20	8.1314	8.1364
25	8.1364	8.1703
30	8.1439	8.2105
35	8.149	8.2406
40	8.1527	8.2946
50	8.159	8.3373
60	8.1653	8.3711
70	8.1703	8.3975
100	8.1778	8.449
120	8.1816	8.4816
140	8.1841	8.5067
180	8.1879	8.5456

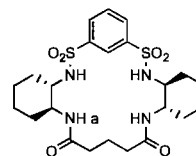
240 8.1904 8.582

84 with TBAOAc in CDCl₃

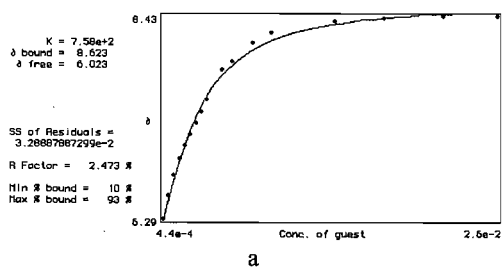
$$[H] = 3.04 \cdot 10^{-3} \text{ M}$$

$$[G] = 1.05 \cdot 10^{-1} \text{ M}$$

$$V_i = 600 \mu\text{l}$$



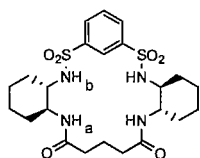
Volume added (μl)	δ_a
2.5	6.2897
5	6.5307
7.5	6.7485
10	6.923
12.5	7.0655
15	7.1797
17.5	7.2977
20	7.4219
22.5	7.5519
30	7.8632
35	7.9454
40	8.1438
45	8.2505
90	8.371
120	8.4005
160	8.4193
200	8.4294

**84** with *N*-Boc-L-Phe-OTBA in CDCl₃

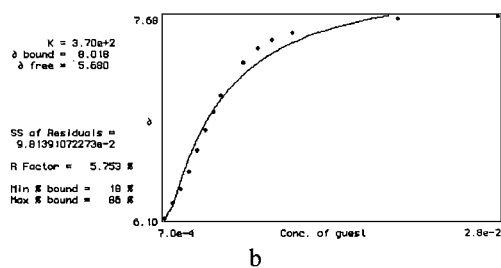
$$[H] = 2.68 \cdot 10^{-3} \text{ M}$$

$$[G] = 8.50 \cdot 10^{-2} \text{ M}$$

$$V_i = 600 \mu\text{l}$$



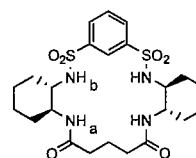
Volume added (μl)	δ_a	δ_b
5	6.5326	6.1007
10	6.7209	6.2175
15	6.9016	6.3286
20	7.0492	6.4667
25	—	6.6325
30	7.3642	6.792
35	7.469	6.9349
40	7.6121	7.0654
45	7.7082	—
55	7.8343	7.3206
65	7.9122	7.4275
75	7.9649	7.4922
90	8.0145	7.55
140	8.091	—
180	8.1186	7.6655
230	8.1362	—
290	8.1507	7.683

**84** with *N*-Boc-L-Phe-OTBA in CDCl₃

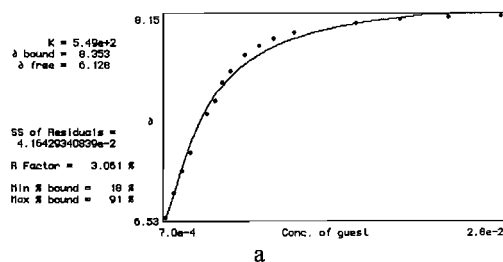
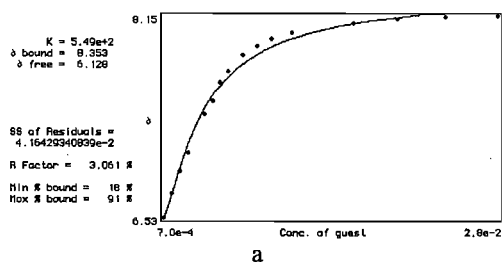
$$[H] = 2.68 \cdot 10^{-3} \text{ M}$$

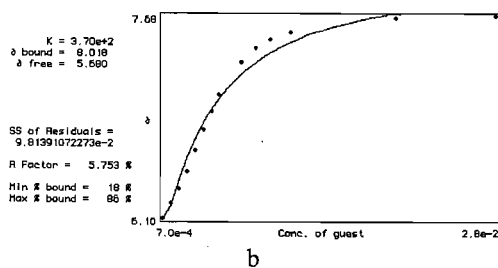
$$[G] = 8.50 \cdot 10^{-2} \text{ M}$$

$$V_i = 600 \mu\text{l}$$



Volume added (μl)	δ_a	δ_b
5	6.5326	6.1007
10	6.7209	6.2175
15	6.9016	6.3286
20	7.0492	6.4667
25	—	6.6325
30	7.3642	6.792
35	7.469	6.9349
40	7.6121	7.0654
45	7.7082	—
55	7.8343	7.3206
65	7.9122	7.4275
75	7.9649	7.4922
90	8.0145	7.55
140	8.091	—
180	8.1186	7.6655
230	8.1362	—
290	8.1507	7.683

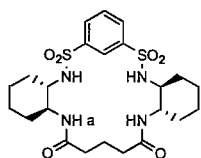


84 with TBAOAc in MeCN- d_3

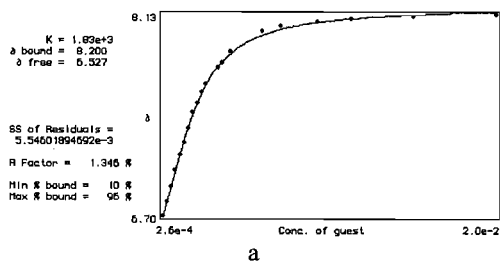
$$[H] = 2.62 \cdot 10^{-3} \text{ M}$$

$$[G] = 7.82 \cdot 10^{-2} \text{ M}$$

$$V_i = 600 \mu\text{l}$$



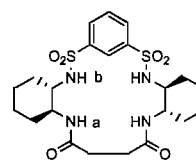
Volume added (μl)	δ_a
2	6.699
4	6.7956
6	6.908
8	7.0222
10	7.127
12	7.2174
14	7.3147
16	7.4333
18	7.4973
20	7.5789
22	7.6335
28	7.7509
30	7.7898
34	7.867
50	8.0164
60	8.0471
80	8.081
100	8.1005
140	8.1131
200	8.1325

85 with TBAOAc in CDCl_3

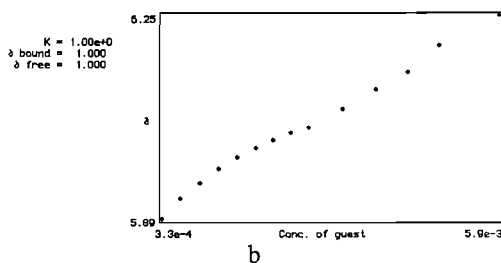
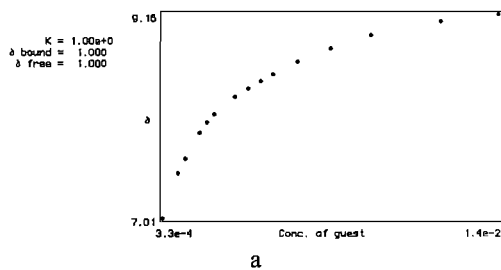
$$[H] = 2.57 \cdot 10^{-3} \text{ M}$$

$$[G] = 3.95 \cdot 10^{-2} \text{ M}$$

$$V_i = 600 \mu\text{l}$$



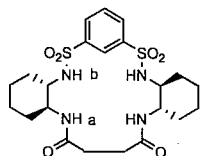
Volume added (μl)	δ_a	δ_b
5	7.0062	5.8867
10	—	5.9231
15	7.4797	5.9501
20	7.6335	5.9771
25	—	5.9965
30	7.9071	6.0135
35	8.0138	6.0279
40	8.103	6.0405
45	—	6.0505
55	8.285	6.0825
65	8.3754	6.1177
75	8.4557	6.1503
85	8.526	6.198
105	8.6522	6.252
135	8.7966	—
175	8.9371	—
255	9.0865	—
335	9.1643	—

85 with *N*-Boc-L-Phe-OTBA in CDCl_3

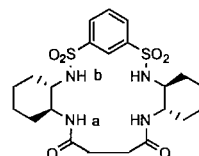
$$[H] = 2.59 \cdot 10^{-3} \text{ M}$$

$$[G] = 4.05 \cdot 10^{-2} \text{ M}$$

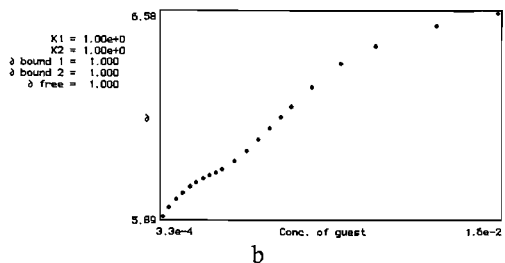
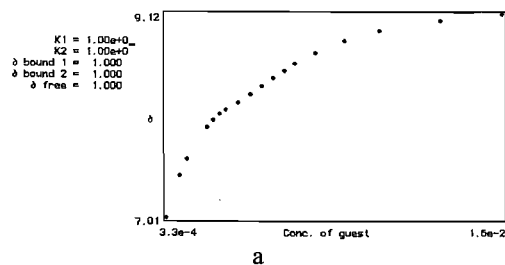
$$V_i = 600 \mu\text{l}$$



Volume added (μl)	δ_a	δ_b
5	7.0052	5.8867
10	—	5.9156
15	7.4389	5.9451
20	7.6122	5.9652
25	—	5.9871
30	—	6.0016
35	7.9348	6.0147
40	8.0159	6.0254
45	8.0812	6.0348
50	8.123	6.0467
60	8.1952	6.0731
70	8.28	6.1083
80	8.3671	6.1459
90	8.4524	6.1851
100	8.5291	6.2241
110	8.5951	6.2602
130	8.7112	6.3248
160	8.8348	6.4039
200	8.9403	6.4654
280	9.0495	6.5344
380	9.1172	6.5784



Volume added (μl)	δ_a	δ_b
5	7.0052	5.8854
10	—	5.9187
15	—	5.9457
20	7.5676	5.9633
25	7.6799	5.9815
30	—	5.9959
35	7.8858	6.0091
40	7.9687	6.0191
45	8.0383	6.0285
50	8.0898	6.0405
60	—	6.0719
80	8.3471	6.1503
120	8.6509	6.3204
200	8.939	6.5169
280	9.0501	6.5997
380	9.1191	6.6462

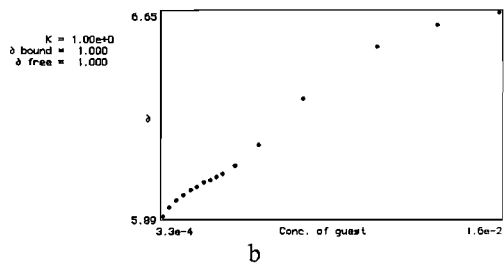


85 with *N*-Boc-D-Phe-OTBA in CDCl_3

$$[\text{H}] = 2.59 \cdot 10^{-3} \text{ M}$$

$$[\text{G}] = 4.04 \cdot 10^{-2} \text{ M}$$

$$V_i = 600 \mu\text{l}$$

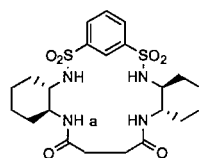


85 with TBAOAc in $\text{MeCN-}d_3$

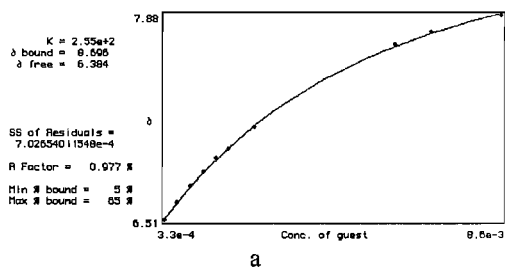
$$[\text{H}] = 2.38 \cdot 10^{-3} \text{ M}$$

$$[\text{G}] = 7.21 \cdot 10^{-2} \text{ M}$$

$$V_i = 600 \mu\text{l}$$



Volume added (μl)	δa
2	7.3153
4	7.4069
6	7.5023
8	7.6065
10	7.6931
12	7.7704
14	7.8434
16	7.904
22	8.066
30	8.2593
34	8.3509
38	8.4237
48	8.5681
58	8.6572
78	8.7489
98	8.7878
138	8.7991
238	8.7865
388	8.7351

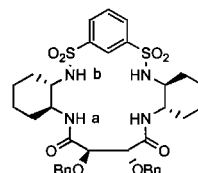


86 with *N*-Boc-L-Phe-OTBA in MeCN- d_3

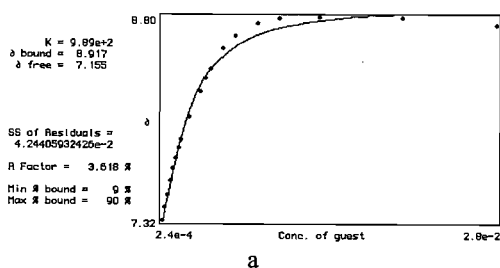
$$[H] = 1.99 \cdot 10^{-3} \text{ M}$$

$$[G] = 5.11 \cdot 10^{-2} \text{ M}$$

$$V_i = 600 \mu\text{l}$$



Volume added (μl)	δa
4	5.4574
8	5.5767
12	5.6871
16	5.7895
20	5.8779
24	5.9646
28	6.0549
32	6.1265
36	6.1993
40	6.2565
50	6.3901
60	6.5119
70	6.6023
90	6.7718
130	6.9852

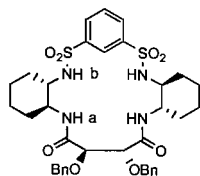


86 with TBAOAc in MeCN- d_3

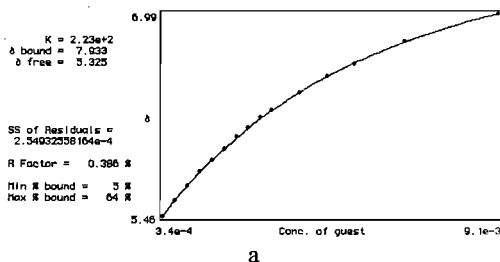
$$[H] = 1.99 \cdot 10^{-3} \text{ M}$$

$$[G] = 6.63 \cdot 10^{-2} \text{ M}$$

$$V_i = 600 \mu\text{l}$$



Volume added (μl)	δa
3	6.5069
6	6.6224
9	6.7303
12	6.8265
15	6.923
18	6.9845
24	7.1264
60	7.6794
70	7.7691
90	7.8802

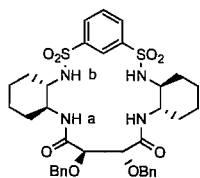


86 with *N*-Boc-D-Phe-OTBA in MeCN- d_3

$$[H] = 2.19 \cdot 10^{-3} \text{ M}$$

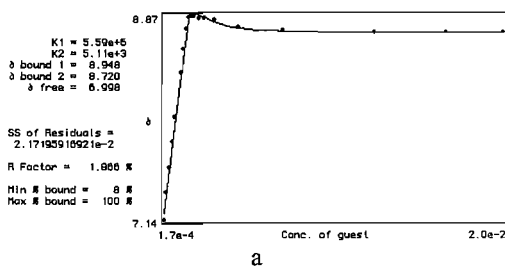
$$[G] = 5.53 \cdot 10^{-2} \text{ M}$$

$$V_i = 600 \mu\text{l}$$



Volume added (μl)	δ_a
4	5.4549
8	5.5729
12	5.6821
16	5.7813
20	5.8811
24	5.9608
28	6.0355
32	6.1152
36	6.1817
40	6.2401
45	6.306
50	6.3845
60	6.5056
80	6.6801
110	6.8935
130	6.9657

10	8.0095
14	8.3873
16	8.5907
18	8.7652
20	8.8568
22	8.8732
24	8.8694
28	8.8493
32	8.848
40	8.8342
60	8.7752
100	8.7477
200	8.7263
300	8.725
400	8.7263

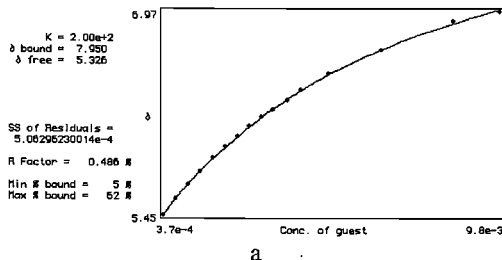
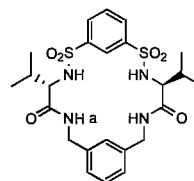


87 with TBAOAc in MeCN- d_3 /2% H₂O

$$[H] = 2.05 \cdot 10^{-3} \text{ M}$$

$$[G] = 6.18 \cdot 10^{-2} \text{ M}$$

$$V_i = 600 \mu\text{l}$$

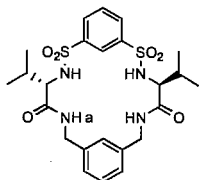


87 with TBAOAc in MeCN- d_3

$$[H] = 1.65 \cdot 10^{-3} \text{ M}$$

$$[G] = 5.00 \cdot 10^{-2} \text{ M}$$

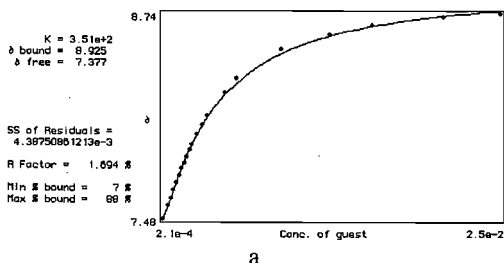
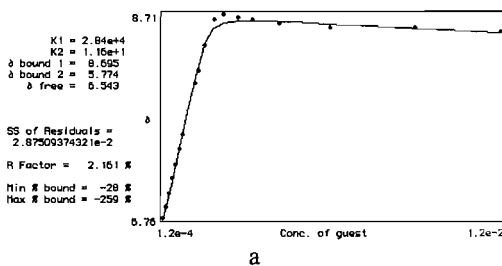
$$V_i = 600 \mu\text{l}$$



Volume added (μl)	δ_a
2	7.1383
4	7.3699
6	7.5814
8	7.7974

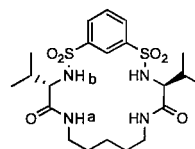
Volume added (μl)	δ_a
2	7.4798
6	7.5613
8	7.6059
10	7.6517
12	7.6982
14	7.7421
16	7.7848
18	7.8174
20	7.8592
22	7.8997
24	7.9329
28	7.9976
32	8.0545
36	8.1137

50	8.2518
60	8.3415
100	8.516
150	8.6058
200	8.6623
300	8.7125
400	8.7363



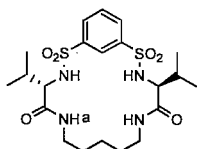
88 with TBAF in MeCN-d₃

[H] = 1.70 · 10⁻³ M
 [G] = 5.40 · 10⁻² M
 V_i = 600 μl



88 with TBAOAc in MeCN-d₃

[H] = 1.70 · 10⁻³ M
 [G] = 3.64 · 10⁻² M
 V_i = 600 μl



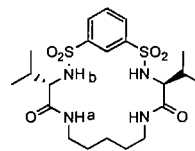
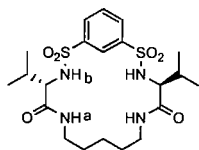
Volume added (μl)	δ _a
2	6.7278
4	6.8006
6	6.9098
8	7.0178
10	7.1164
12	7.2149
14	7.3153
16	7.4195
18	7.5083
32	7.9329
36	7.9982
40	8.0798
44	8.1375
50	8.2467

Volume added (μl)	δ _a
2	6.7554
4	6.8559
6	6.9883
8	7.1358
10	7.2638
12	7.4132
14	7.545
22	8.0459
24	8.1651
28	8.403
34	8.6497
40	8.7087
50	8.6754
60	8.6516
80	8.6171
120	8.5769
200	8.5769
300	8.5324



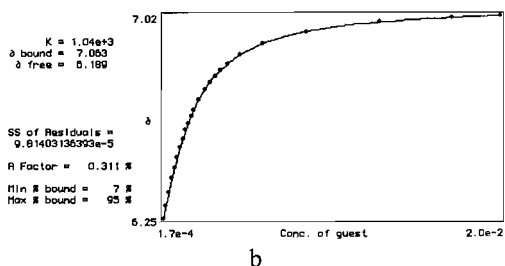
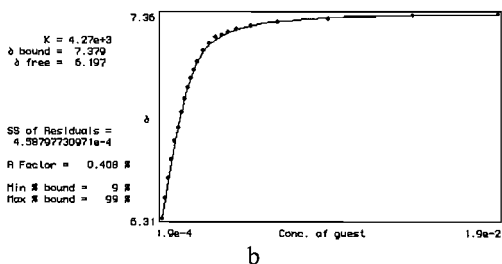
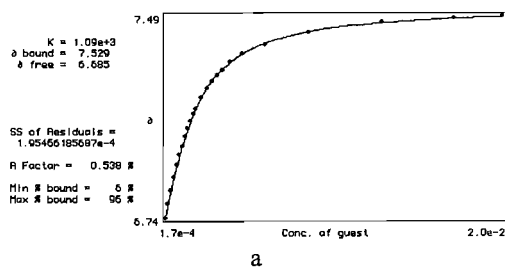
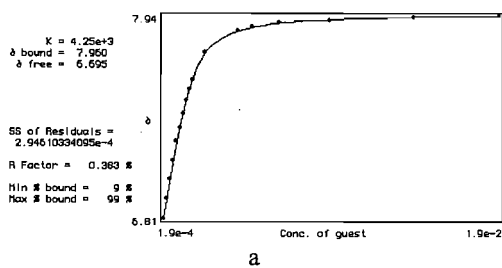
88 with TBACl in MeCN-d₃

[H] = 1.82 · 10⁻³ M
 [G] = 5.78 · 10⁻² M
 V_i = 600 μl



Volume added (μl)	δ_a	δ_b
2	6.8125	6.414
4	6.9256	6.5119
6	7.0297	6.6105
8	7.137	6.3079
10	7.2425	6.7046
12	7.3159	6.7743
14	7.3956	6.8546
16	7.4754	6.9261
18	7.5375	6.9852
20	7.589	7.0285
22	—	7.0743
24	—	7.1145
28	7.7409	7.1741
32	—	7.2124
36	—	7.2456
40	—	7.2563
44	—	7.2701
50	7.8601	7.2877
60	7.884	7.3003
80	7.9053	7.3241
120	7.9204	7.3429
200	7.9329	7.3555
300	7.9442	7.3643

Volume added (μl)	δ_a	δ_b
2	6.7391	6.2464
4	6.7893	6.2941
6	6.8395	6.3475
8	6.891	6.3996
10	6.9337	6.4397
12	6.9738	6.4812
14	7.0052	6.5175
16	7.0416	6.5521
18	7.0743	6.5859
20	7.1006	6.6104
22	7.1257	6.6349
24	7.1446	6.6594
28	7.186	6.7008
32	7.223	6.7366
36	7.2476	6.7655
40	7.2695	6.7887
44	7.2902	6.8113
50	7.3191	6.837
60	7.3504	6.8716
80	7.3868	6.9155
120	7.4308	6.9582
200	7.4697	6.9959
300	7.4835	7.0141
380	7.4936	7.0228



88 with TBABr in $\text{MeCN-}d_3$

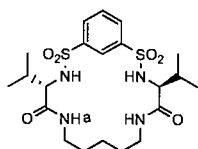
$$\begin{aligned}
 [\text{H}] &= 1.62 \cdot 10^{-3} \text{ M} \\
 [\text{G}] &= 5.18 \cdot 10^{-2} \text{ M} \\
 V_i &= 600 \mu\text{l}
 \end{aligned}$$

88 with TBAOAc in $\text{MeCN-}d_3/1\% \text{ H}_2\text{O}$

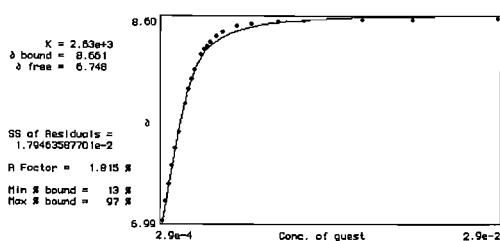
$$[\text{H}] = 2.50 \cdot 10^{-3} \text{ M}$$

$$[G] = 8.70 \cdot 10^{-2} \text{ M}$$

$$V_i = 600 \mu\text{l}$$



Volume added (μl)	δa
2	6.9927
4	7.1395
6	7.2814
8	7.4308
10	7.5661
12	7.6957
16	7.926
18	8.0346
20	8.1174
22	8.1928
26	8.3108
28	8.3522
30	8.3798
32	8.4156
36	8.4576
40	8.4941
50	8.5399
60	8.5556
80	8.5781
100	8.5838
150	8.5907
200	8.5945
300	8.6033



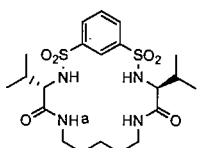
a

88 with TBAOAc in MeCN- d_3 /2% H₂O

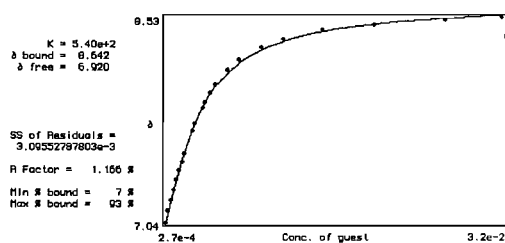
$$[H] = 2.67 \cdot 10^{-3} \text{ M}$$

$$[G] = 8.00 \cdot 10^{-2} \text{ M}$$

$$V_i = 600 \mu\text{l}$$



Volume added (μl)	δa
2	7.0398
4	7.1257
6	7.2048
8	7.2764
10	7.3492
12	7.4151
14	7.4823
16	7.5425
22	7.7057
24	7.7559
30	7.8702
32	7.9065
36	7.9743
40	8.0321
50	8.1375
60	8.216
80	8.3057
100	8.3635
140	8.43
200	8.4727
300	8.5066
400	8.5254



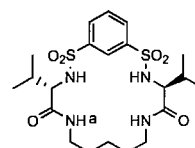
a

88 with TBAH₂PO₄ in MeCN- d_3 /2% H₂O

$$[H] = 1.65 \cdot 10^{-3} \text{ M}$$

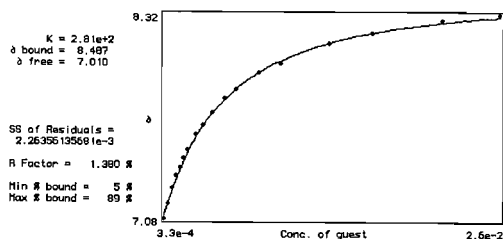
$$[G] = 6.56 \cdot 10^{-2} \text{ M}$$

$$V_i = 600 \mu\text{l}$$



Volume added (μl)	δa
3	7.0768
6	7.1684
9	7.2601
12	7.3366
15	7.3887

18	7.4408
21	7.4923
27	7.5859
33	7.6454
40	7.7195
50	7.8093
60	7.8633
80	7.9668
100	8.0208
150	8.1375
200	8.2016
300	8.2769
400	8.3183



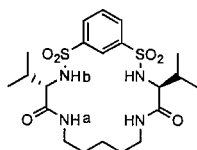
a

88 with TBACl in MeCN-*d*₃/2% H₂O

$$[H] = 2.20 \cdot 10^{-3} \text{ M}$$

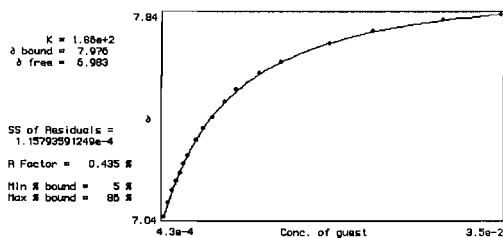
$$[G] = 8.72 \cdot 10^{-2} \text{ M}$$

$$V_i = 600 \mu\text{l}$$

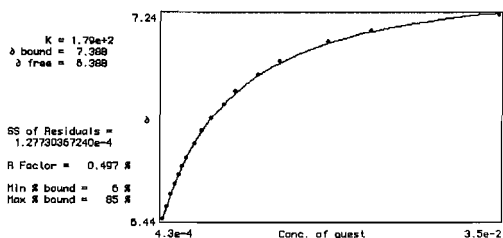


Volume added (μl)	δa	δb
3	7.0354	6.4435
6	7.0893	6.4912
9	7.1396	6.5357
12	7.1734	6.5759
15	7.2086	6.6136
18	7.245	6.6462
21	7.2776	6.6763
27	7.3373	6.7353
33	7.3843	6.7868
40	7.4308	6.832
50	7.4885	6.8872
60	7.5375	6.9362
80	7.6015	7.0015
100	7.648	7.0529
150	7.7208	7.1295
200	7.7685	7.176
300	7.8118	—

400 7.835 7.2363



a



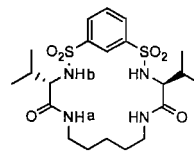
b

88 with TBABr in MeCN-*d*₃/2% H₂O

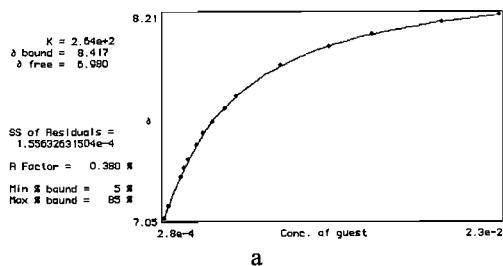
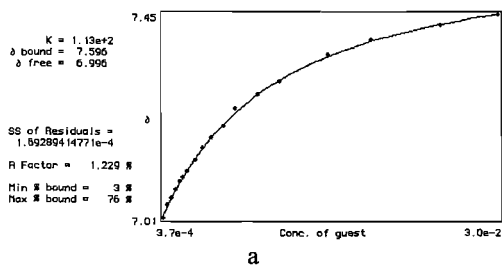
$$[H] = 1.65 \cdot 10^{-3} \text{ M}$$

$$[G] = 7.50 \cdot 10^{-2} \text{ M}$$

$$V_i = 600 \mu\text{l}$$



Volume added (μl)	δa	δb
3	7.0115	6.4165
6	7.0391	6.4403
9	7.0554	6.4579
12	7.073	6.4767
15	7.0906	6.4981
18	7.0994	6.5106
21	7.1144	6.5239
27	7.1383	6.5521
33	7.1659	6.5797
40	7.1873	6.6085
50	7.2124	6.6369
60	7.2488	6.6751
80	7.2789	6.7127
100	7.309	6.7441
150	7.3655	6.8056
200	7.3969	6.8496
300	7.4321	6.8822
400	7.4546	6.9123

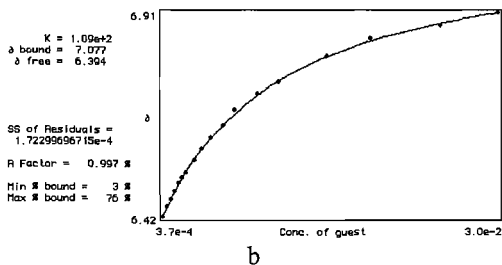
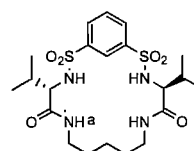


**88 with *N*-Boc-D-Phe-OTBA
in MeCN- d_3 /2% H $_2$ O**

$$[H] = 1.62 \cdot 10^{-3} \text{ M}$$

$$[G] = 5.67 \cdot 10^{-2} \text{ M}$$

$$V_i = 600 \mu\text{l}$$

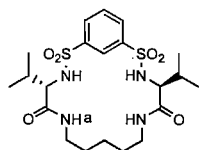


**88 with *N*-Boc-L-Phe-OTBA
in MeCN- d_3 /2% H $_2$ O**

$$[H] = 1.62 \cdot 10^{-3} \text{ M}$$

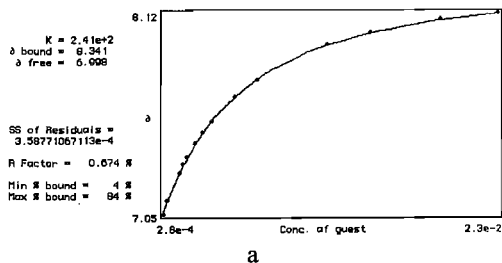
$$[G] = 5.68 \cdot 10^{-2} \text{ M}$$

$$V_i = 600 \mu\text{l}$$



Volume added (μl)	δ_a
3	7.0504
6	7.1157
15	7.2889
18	7.3385
21	7.3843
27	7.4672
33	7.5293
40	7.5977
50	7.6737
60	7.7434
100	7.9141
150	8.0214
200	8.0899
300	8.1639
400	8.2053

Volume added (μl)	δ_a
3	7.0498
6	7.1257
15	7.267
18	7.3203
21	7.358
27	7.4271
33	7.486
40	7.5463
60	7.6781
80	7.7697
150	7.9517
200	8.0158
300	8.0861
400	8.1237

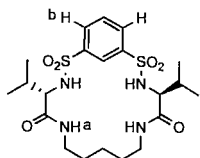


88 with TBAOAc in DMSO- d_6

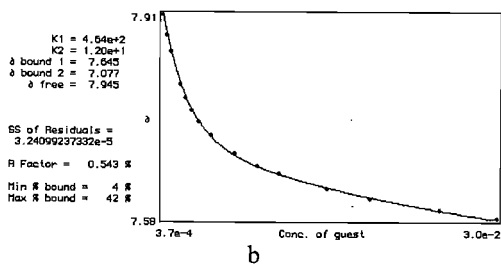
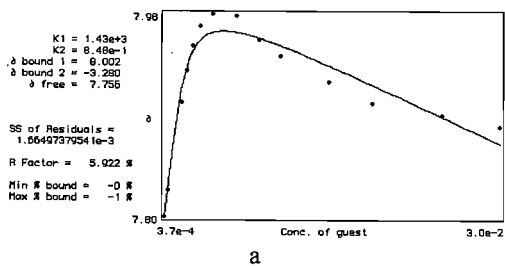
$$[H] = 1.87 \cdot 10^{-3} \text{ M}$$

$$[G] = 7.51 \cdot 10^{-2} \text{ M}$$

$$V_i = 600 \mu\text{l}$$



Volume added (μl)	δ_a	δ_b
3	7.8038	7.9098
6	7.8263	7.8753
9	—	7.8483
16	7.9029	7.7943
20	7.9305	7.773
25	7.9519	7.7523
30	7.9682	7.7354
40	7.9795	7.7121
60	7.977	7.682
80	7.9569	7.6632
100	7.9431	7.65
150	7.9205	7.6261
200	7.9017	7.6089
300	7.8916	7.5897
400	7.8816	7.5778

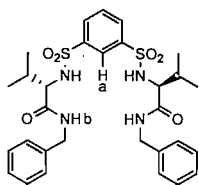


93 with TBAOAc in MeCN-d_3

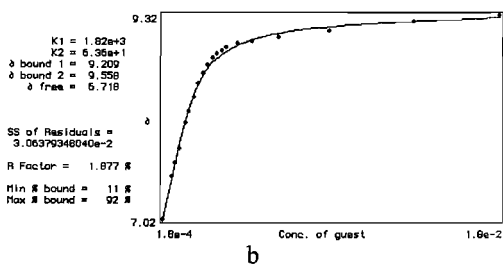
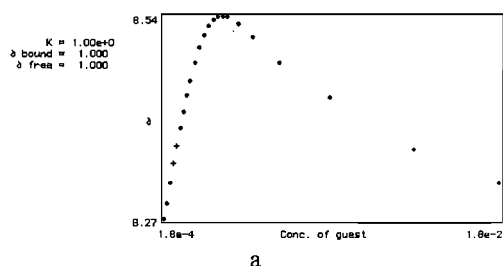
$$[\text{H}] = 1.73 \cdot 10^{-3} \text{ M}$$

$$[\text{G}] = 5.28 \cdot 10^{-2} \text{ M}$$

$$V_i = 600 \mu\text{l}$$



Volume added (μl)	δ_a	δ_b
2	8.2719	7.0203
4	8.2919	—
6	8.3183	—
8	8.3434	7.4998
10	8.3673	7.6593
12	8.3911	7.8174
14	8.4124	—
16	8.4338	8.1062
18	8.4526	8.238
21	8.4765	8.4015
24	8.4966	8.5468
27	8.5129	8.6648
30	8.5254	8.7614
33	8.533	8.8355
36	8.5367	8.887
39	8.538	8.9246
42	8.5367	8.956
50	8.5279	9.0024
60	8.5104	9.0288
80	8.4765	9.0727
120	8.4313	9.1418
200	8.3622	9.246
300	8.3183	9.3219

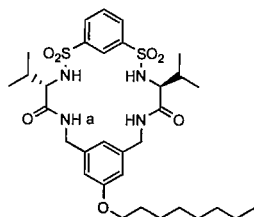


102 with TBAOAc in $\text{MeCN-d}_3/1\% \text{H}_2\text{O}$

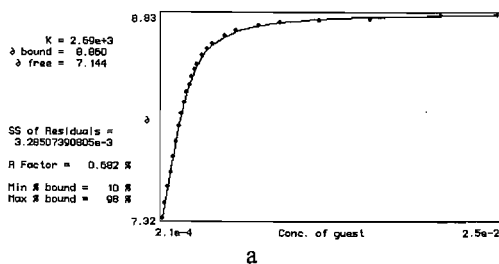
$$[\text{H}] = 2.075 \cdot 10^{-3} \text{ M}$$

$$[\text{G}] = 6.26 \cdot 10^{-2} \text{ M}$$

$$V_i = 600 \mu\text{l}$$



Volume added (μl)	δ_a
2	7.3241
4	7.4333
6	7.5526
8	7.6643
10	7.7792
12	7.8927
14	8.0039
16	8.0986
18	8.1802
20	8.258
22	8.3133
24	8.3679
26	8.4212
28	8.4589
32	8.5274
36	8.5769
40	8.6171
50	8.6767
60	8.7125
80	8.7495
100	8.7728
140	8.7935
200	8.8003
300	8.8292
400	8.8317

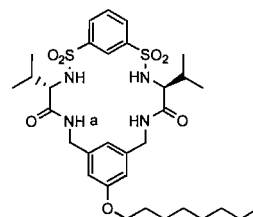


102 with TBAH_2PO_4 in $\text{MeCN-}d_3/1\%$
 H_2O

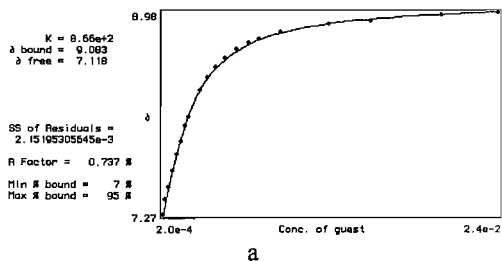
$$[\text{H}] = 1.71 \cdot 10^{-3} \text{ M}$$

$$[\text{G}] = 6.02 \cdot 10^{-2} \text{ M}$$

$$V_i = 600 \mu\text{l}$$



Volume added (μl)	δ_a
2	7.2651
4	7.3894
6	7.4923
9	7.6379
12	7.7722
15	7.8871
18	8.0157
21	8.0968
30	8.3221
36	8.4275
42	8.5104
50	8.5894
60	8.666
70	8.7162
80	8.7564
100	8.8123
150	8.8819
200	8.914
300	8.9629
400	8.9837

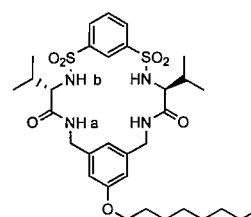


102 with TBACl in $\text{MeCN-}d_3/1\%$ H_2O

$$[\text{H}] = 2.00 \cdot 10^{-3} \text{ M}$$

$$[\text{G}] = 6.96 \cdot 10^{-2} \text{ M}$$

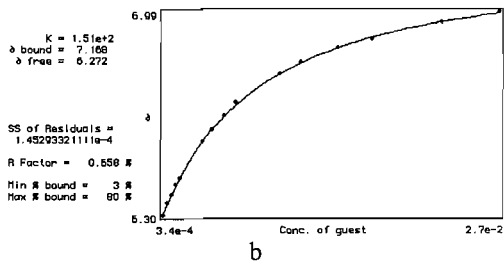
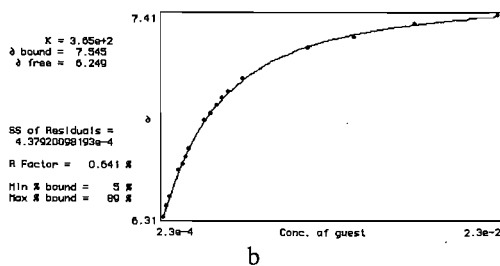
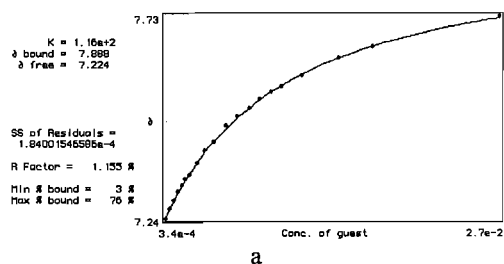
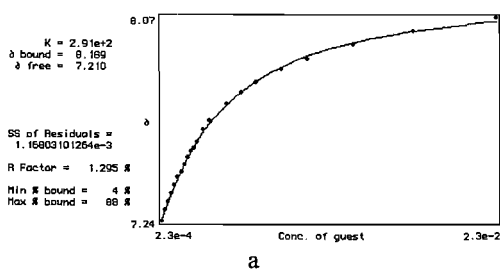
$$V_i = 600 \mu\text{l}$$



Volume added (μl) δ_a δ_b

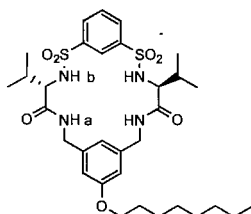
2	7.245	6.3129
4	7.2889	6.37
6	7.3241	6.4215
8	7.3555	—
10	7.3881	—
12	7.4207	6.5621
14	7.4446	6.5998
16	7.4735	6.6387
18	7.5011	6.6795
20	7.5256	—
22	7.5394	—
24	7.5664	—
28	7.6166	6.8326
32	7.6505	6.8753
44	7.7189	6.9161
54	7.7634	6.9557
64	7.8074	6.9883
84	7.8626	7.0624
104	7.9022	7.2268
144	7.9624	7.2902
204	8.0151	7.358
304	8.0723	7.4069

Volume added (μl)	δa	δb
3	7.2412	6.3035
6	7.2638	6.3418
9	7.2846	6.3713
12	7.3065	6.4046
15	7.3216	6.4272
18	7.336	—
21	7.3467	—
27	7.3756	—
33	7.4044	6.5533
40	7.4245	6.5897
50	7.4634	6.6399
60	7.4873	6.6833
70	7.5068	—
80	7.5293	—
90	7.5463	—
100	7.5588	6.7817
120	7.5852	6.8194
160	7.626	6.8703
200	7.653	6.901
300	—	6.9563
400	7.729	6.9927



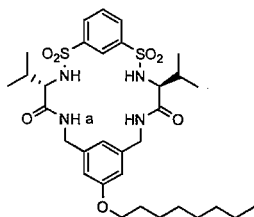
102 with TBABr in MeCN- d_3 /1% H₂O

$$\begin{aligned}
 [\text{H}] &= 1.71 \cdot 10^{-3} \text{ M} \\
 [\text{G}] &= 6.86 \cdot 10^{-2} \text{ M} \\
 V_i &= 600 \mu\text{l}
 \end{aligned}$$



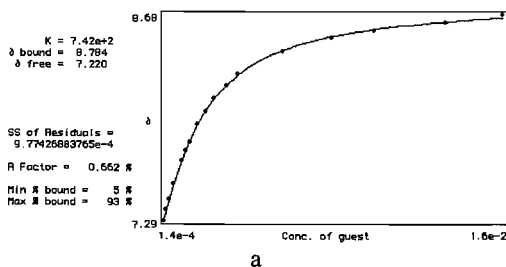
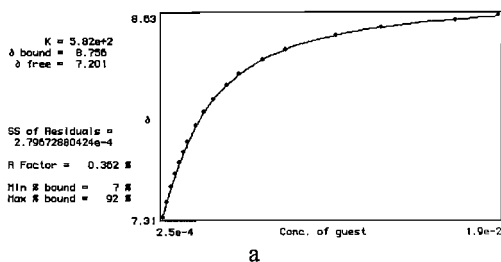
102 with *N*-Boc-L-Phe-OTBA in MeCN- d_3 /1% H₂O

$$\begin{aligned}
 [\text{H}] &= 1.37 \cdot 10^{-3} \text{ M} \\
 [\text{G}] &= 4.08 \cdot 10^{-2} \text{ M} \\
 V_i &= 600 \mu\text{l}
 \end{aligned}$$



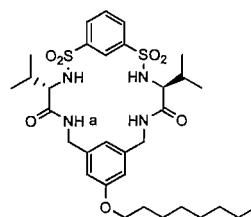
Volume added (μl)	δ _a
2	7.2914
4	7.368
6	7.433
9	7.5377
15	7.6919
18	7.7622
21	7.8212
27	7.9367
33	8.0258
40	8.1124
50	8.2016
60	8.2775
100	8.4325
150	8.5204
200	8.5719
300	8.6233
400	8.6785

9	7.5061
12	7.5902
15	7.6655
18	7.7321
21	7.7961
27	7.9028
33	7.9919
40	8.0748
50	8.1689
60	8.2367
80	8.3346
100	8.3974
150	8.494
200	8.5443
300	8.5945
370	8.6296



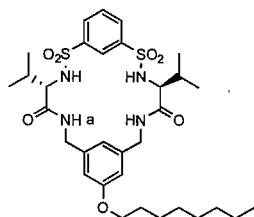
102 with TBAOAc in MeCN-d₃/2% H₂O

$[H] = 1.62 \cdot 10^{-3} \text{ M}$
 $[G] = 4.83 \cdot 10^{-2} \text{ M}$
 $V_i = 600 \mu\text{l}$



102 with *N*-Boc-D-Phe-OTBA in MeCN-d₃/1% H₂O

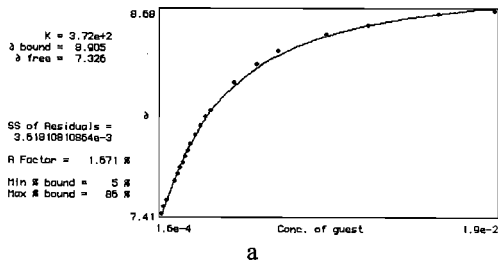
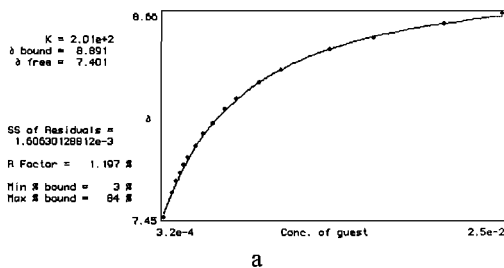
$[H] = 1.65 \cdot 10^{-3} \text{ M}$
 $[G] = 5.00 \cdot 10^{-2} \text{ M}$
 $V_i = 600 \mu\text{l}$



Volume added (μl)	δ _a
3	7.309
6	7.4082

Volume added (μl)	δ _a
2	7.4107
4	7.454
6	7.4936
12	7.6135
14	7.6605
16	7.6931
18	7.7308
20	7.7679
22	7.8049
24	7.8432
28	7.9003
32	7.9593
36	8.0145

40	8.0559
60	8.2304
80	8.3459
100	8.425
150	8.5286
200	8.5869
300	8.6585
400	8.6805

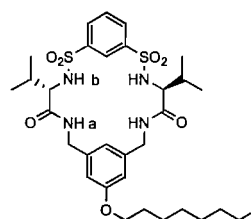


102 with TBACl in MeCN-*d*₃/2% H₂O

$$[H] = 1.58 \cdot 10^{-3} \text{ M}$$

$$[G] = 6.40 \cdot 10^{-2} \text{ M}$$

$$V_i = 600 \mu\text{l}$$

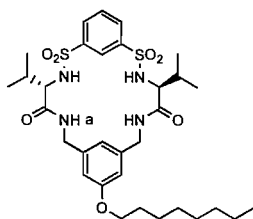


102 with TBAH₂PO₄ in MeCN-*d*₃/2% H₂O

$$[H] = 1.58 \cdot 10^{-3} \text{ M}$$

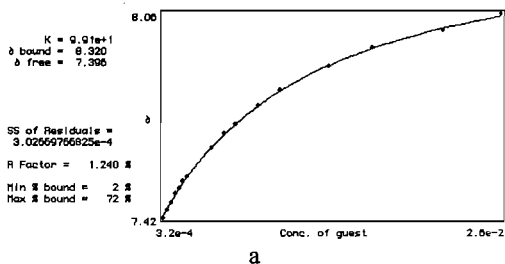
$$[G] = 6.36 \cdot 10^{-2} \text{ M}$$

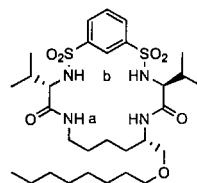
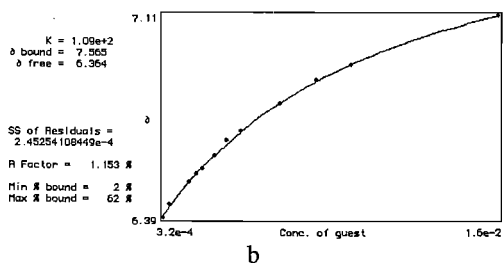
$$V_i = 600 \mu\text{l}$$



Volume added (μl)	δa	δb
3	7.4157	6.3926
6	7.4408	6.4391
9	7.4628	—
12	7.4911	—
15	7.5093	6.5188
18	7.53	6.5458
21	7.545	6.5646
27	—	6.613
33	—	6.665
40	7.6367	6.6989
50	7.6818	—
60	7.7114	6.7969
80	7.7697	6.881
100	7.8174	6.9337
150	7.8915	—
200	7.9492	7.1107
300	8.0045	—
400	8.0597	—

Volume added (μl)	δa
3	7.4484
9	7.5915
12	7.6568
15	7.7095
18	7.7547
21	7.7998
27	7.8639
33	7.9367
40	7.9989
50	8.0836
60	8.1463
80	8.2417
100	8.3145
150	8.4388
200	8.5091
300	8.5926
400	8.656



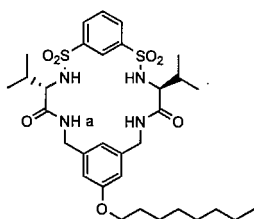


102 with TBABr in MeCN-*d*₃/2% H₂O

$$[H] = 1.85 \cdot 10^{-3} \text{ M}$$

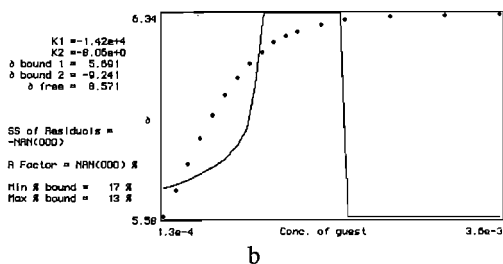
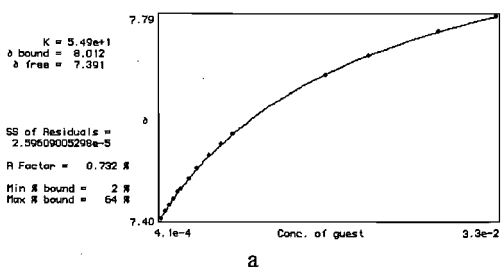
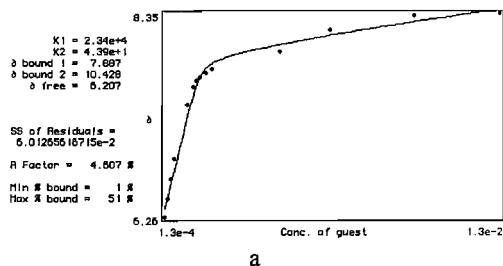
$$[G] = 8.28 \cdot 10^{-2} \text{ M}$$

$$V_i = 600 \mu\text{l}$$



Volume added (μl)	δ_a
3	7.4019
6	7.4145
9	7.4258
12	7.4371
15	7.4509
18	7.4584
24	7.4772
30	7.4961
40	7.5212
50	7.5438
60	7.5626
150	7.6762
200	7.7132
300	7.7597
400	7.7879

Volume added (μl)	δ_a	δ_b
2	6.2633	5.5766
4	6.4453	5.6752
6	6.6531	5.775
8	6.8596	5.8704
10	—	5.957
12	—	6.0336
14	—	6.1013
16	7.4213	6.1541
18	—	6.198
20	7.5964	6.2357
22	7.6579	6.2583
24	7.6931	6.2746
28	7.7358	6.2997
32	7.7734	6.3185
40	—	6.3326
50	—	6.3361
60	—	6.3411
80	7.9554	—
120	8.1776	—
200	8.3264	—
300	8.3521	—



108 with TBAOAc in CDCl₃

$$[H] = 1.51 \cdot 10^{-3} \text{ M}$$

$$[G] = 3.95 \cdot 10^{-2} \text{ M}$$

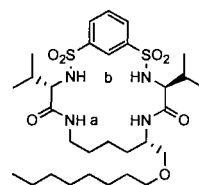
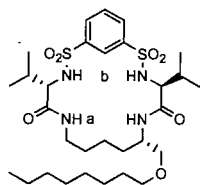
$$V_i = 600 \mu\text{l}$$

108 with TBACl in CDCl₃

$$[H] = 1.51 \cdot 10^{-3} \text{ M}$$

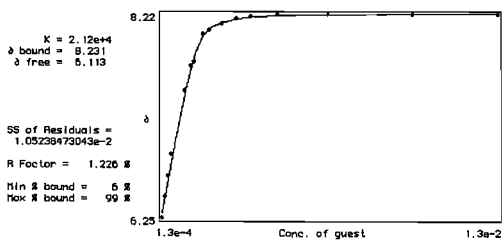
$$[G] = 3.93 \cdot 10^{-2} \text{ M}$$

$$V_i = 600 \mu\text{l}$$

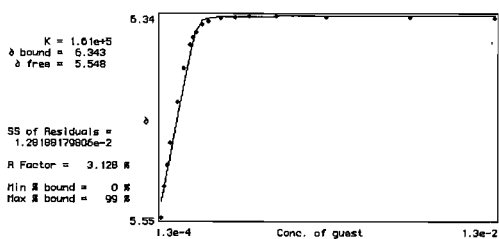


Volume added (μl)	δ_a	δ_b
2	6.2463	5.5515
4	6.4491	5.672
6	6.6461	5.7586
8	6.8608	5.8446
12	—	6.0022
16	7.4784	6.134
20	7.7107	6.2275
22	7.7559	6.2557
24	—	6.2746
28	8.027	6.3056
32	8.0622	6.321
40	8.1174	6.3298
50	8.1701	6.3361
60	8.1889	6.3374
80	8.2078	6.3411
120	8.2115	6.3336
200	8.214	6.3336
300	8.2166	6.3323

Volume added (μl)	δ_a	δ_b
2	6.2168	5.5427
4	6.3242	5.6118
6	6.4302	5.6833
8	6.5313	5.7323
10	6.7579	5.8314
12	—	5.9645
14	7.1313	6.0448
16	—	6.0863
18	7.3868	6.1315
20	7.4659	6.1741
22	—	6.2055
24	—	6.2306
28	—	6.252
32	—	6.2765
40	7.6517	6.2884
50	7.6705	6.2947
60	7.6705	6.2997
80	7.673	6.3022
120	7.6692	6.3016
200	7.6567	6.3022
300	7.6611	6.3022



a



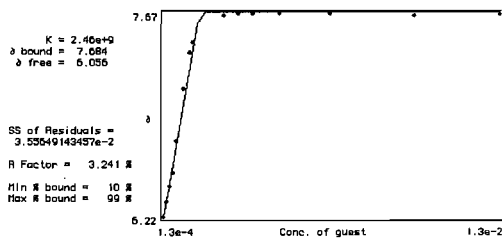
b

108 with TBABr in CDCl_3

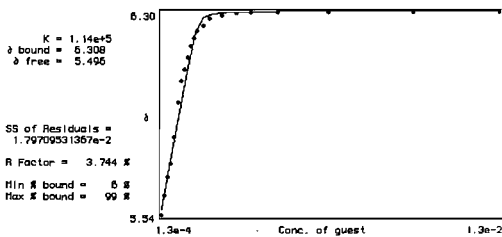
$$[\text{H}] = 1.51 \cdot 10^{-3} \text{ M}$$

$$[\text{G}] = 3.93 \cdot 10^{-2} \text{ M}$$

$$V_i = 600 \mu\text{l}$$



a



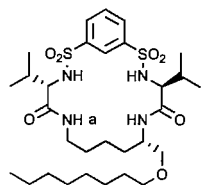
b

108 with TBAOAc in $\text{MeCN-}d_3/2\% \text{ H}_2\text{O}$

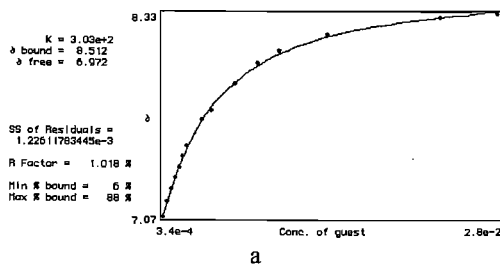
$$[\text{H}] = 1.95 \cdot 10^{-3} \text{ M}$$

$$[\text{G}] = 6.91 \cdot 10^{-2} \text{ M}$$

$$V_i = 600 \mu\text{l}$$



Volume added (μl)	δ_a
3	7.068
6	7.1609
9	7.2337
12	7.3072
15	7.3718
18	7.4396
21	7.5023
33	7.6712
40	7.7283
60	7.8915
80	8.017
100	8.0936
150	8.1965
300	8.3045
400	8.3271

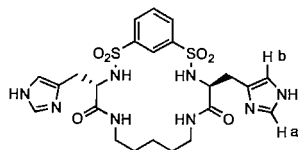


112 with TBAOAc in DMSO- d_6

$$[H] = 1.09 \cdot 10^{-3} \text{ M}^*$$

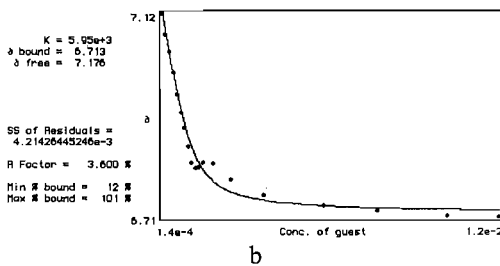
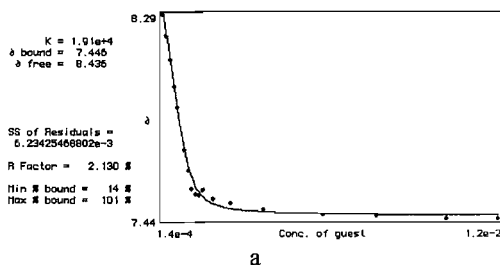
$$[G] = 4.16 \cdot 10^{-2} \text{ M}$$

$$V_i = 600 \mu\text{l}$$



Volume added (μl)	δ_a	δ_b
2	8.2933	7.121
4	8.1992	7.0782
6	8.1013	7.0418
8	7.9895	7.0003
10	7.9017	6.9577
12	—	6.92
14	7.7234	6.8874

16	7.6393	6.8497
18	7.5602	6.81705
20	7.5389	6.807
22	7.5326	6.8071
24	7.5564	6.8158
30	7.5175	6.8145
40	7.4974	6.7807
60	7.4748	6.7505
100	7.4523	6.7292
140	7.4448	6.7179
200	7.4359	6.7079
250	7.4359	6.7066

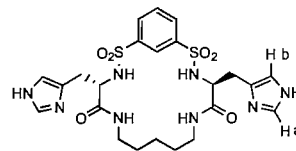


112 with TBAOAc in DMSO- d_6 /5% H_2O

$$[H] = 2.65 \cdot 10^{-3} \text{ M}^*$$

$$[G] = 8.33 \cdot 10^{-2} \text{ M}$$

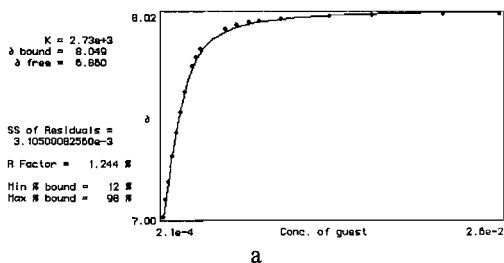
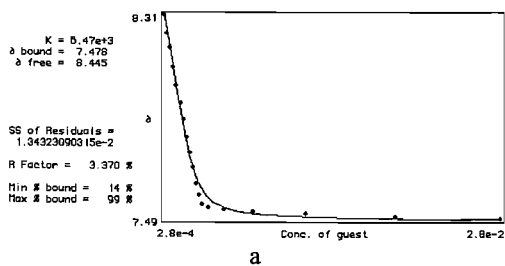
$$V_i = 600 \mu\text{l}$$



Volume added (μl)	δ_a	δ_b
2	8.3078	7.1228
4	8.2325	7.0939
6	8.171	7.0676
8	8.0944	7.0374
10	8.0216	7.0086
12	7.9488	6.9784
14	7.8835	6.9521
16	7.812	6.9219
18	7.7517	6.8968

20	7.6915	6.8717
22	7.6274	6.8441
24	7.5797	6.8253
26	7.5446	6.8102
30	7.5295	6.8039
40	7.5207	6.7977
60	7.5132	6.7914
100	7.5044	6.7826
180	7.4944	6.7726
300	7.4868	6.765

60	7.9605
70	7.9756
80	7.9806
100	7.9924
150	8.0071
200	8.0131
300	8.0168
400	8.0192

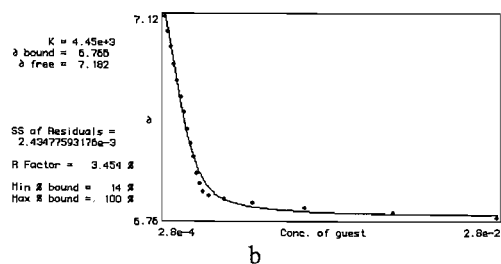
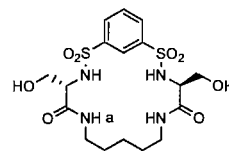


117 with TBAH₂PO₄ in MeCN-*d*₃/2% H₂O

$$[H] = 1.80 \cdot 10^{-3} \text{ M}$$

$$[G] = 6.27 \cdot 10^{-2} \text{ M}$$

$$V_i = 600 \mu\text{l}$$



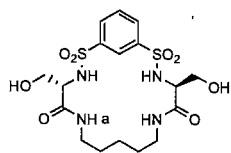
*Calculated considering 112 as free base

117 with TBAOAc in MeCN-*d*₃/2% H₂O

$$[H] = 1.85 \cdot 10^{-3} \text{ M}$$

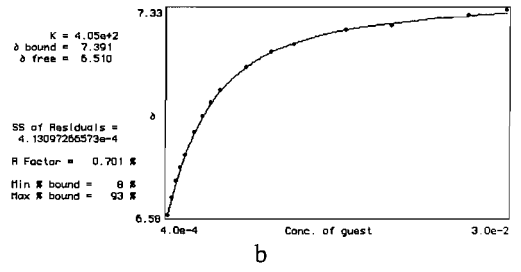
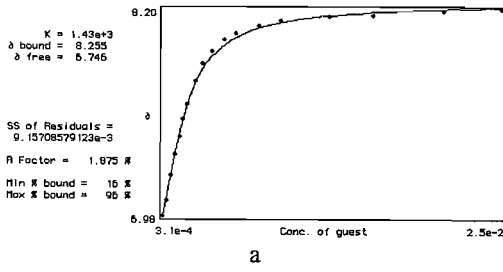
$$[G] = 6.40 \cdot 10^{-2} \text{ M}$$

$$V_i = 600 \mu\text{l}$$



Volume added (μl)	δ_a
2	6.999
4	7.0818
6	7.1741
9	7.3027
12	7.4207
15	7.5212
18	7.6229
24	7.7534
27	7.8011
30	7.84
50	7.9404

Volume added (μl)	δ_a
3	6.9833
6	7.0743
9	7.2186
12	7.3404
15	7.4484
18	7.5501
21	7.6367
27	7.7735
33	7.8765
40	7.9543
50	8.0196
60	8.0597
80	8.0986
100	8.1288
150	8.1551
200	8.1639
300	8.1865
400	8.2016

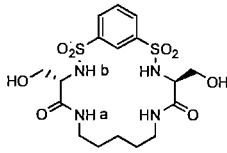


117 with TBACl in MeCN-*d*₃/2% H₂O

$$[H] = 2.23 \cdot 10^{-3} \text{ M}$$

$$[G] = 8.00 \cdot 10^{-2} \text{ M}$$

$$V_i = 600 \mu\text{l}$$

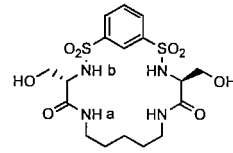


117 with TBABr in MeCN-*d*₃/2% H₂O

$$[H] = 1.74 \cdot 10^{-3} \text{ M}$$

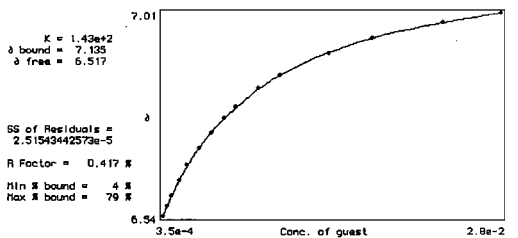
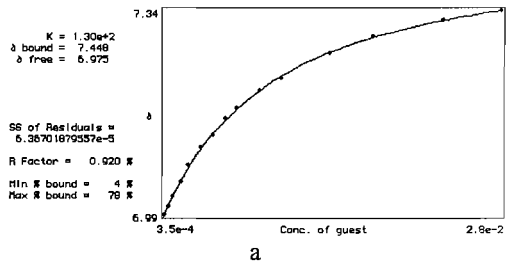
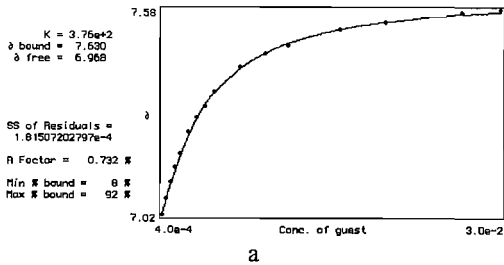
$$[G] = 7.02 \cdot 10^{-2} \text{ M}$$

$$V_i = 600 \mu\text{l}$$



Volume added (μl)	δ _a	δ _b
3	7.0178	6.5803
6	7.063	6.6424
9	7.1069	6.704
12	7.1458	6.7529
15	7.1847	6.8006
21	7.2425	6.8822
27	7.2827	6.9444
33	7.3153	6.9914
40	7.353	7.0372
60	7.4207	7.122
80	7.4597	7.1785
100	7.4823	7.2048
150	7.5237	7.2588
200	7.5438	7.2739
300	7.5676	7.3128
360	7.5789	7.3329

Volume added (μl)	δ _a	δ _b
3	6.9914	6.5389
6	7.0052	6.5621
9	7.0228	6.5847
15	7.0479	6.6211
21	7.0755	6.655
30	7.1069	6.6971
40	7.1283	6.7316
50	7.1569	6.7655
60	7.176	6.7918
80	7.2061	6.8345
100	7.2269	6.8646
150	7.2701	6.9148
200	7.2977	6.95
300	7.3266	6.9864
400	7.3429	7.0078



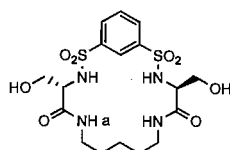
b

117 with *N*-Ac-L-Ala-OTBA
in MeCN-*d*₃/2% H₂O

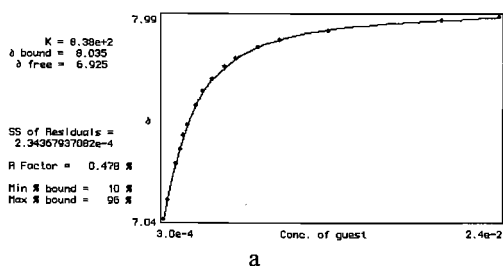
$$[H] = 1.73 \cdot 10^{-3} \text{ M}$$

$$[G] = 6.08 \cdot 10^{-2} \text{ M}$$

$$V_i = 600 \mu\text{l}$$



Volume added (μl)	δ _a
3	7.0398
6	7.1302
12	7.2977
15	7.3617
18	7.427
21	7.4772
27	7.5689
33	7.6329
40	7.6906
50	7.7471
60	7.7886
80	7.8394
100	7.8727
150	7.9173
300	7.9675
400	7.9856

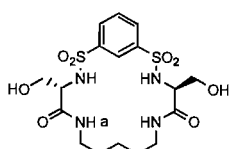


117 with *N*-Ac-D-Ala-OTBA
in MeCN-*d*₃/2% H₂O

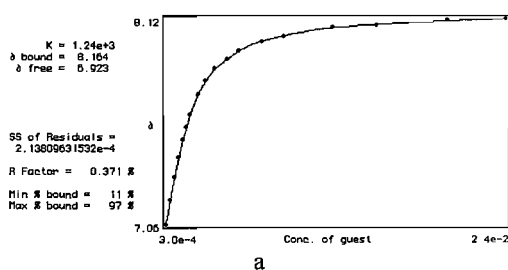
$$[H] = 1.73 \cdot 10^{-3} \text{ M}$$

$$[G] = 6.06 \cdot 10^{-2} \text{ M}$$

$$V_i = 600 \mu\text{l}$$



Volume added (μl)	δ _a
3	7.063
6	7.1885
9	7.3078
12	7.4101
15	7.4986
18	7.5645
21	7.6266
27	7.7296
33	7.7998
40	7.8626
50	7.9141
60	7.9553
80	8.0064
100	8.0315
150	8.0773
200	8.0924
300	8.1175
400	8.125

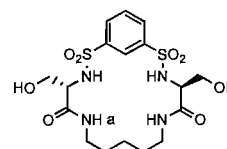


117 with *N*-Ac-L-Phe-OTBA
in MeCN-*d*₃/2% H₂O

$$[H] = 1.68 \cdot 10^{-3} \text{ M}$$

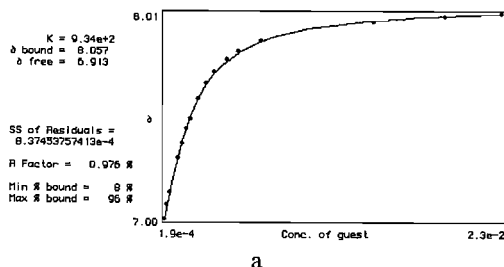
$$[G] = 5.85 \cdot 10^{-2} \text{ M}$$

$$V_i = 600 \mu\text{l}$$



Volume added (μl)	δ _a
2	7.0015
4	7.0724
6	7.1283
12	7.2959
15	7.3705
18	7.4402
21	7.4898
27	7.5892
33	7.6643
40	7.717

50	7.781
60	7.8199
80	7.8714
200	7.9643
300	7.9869
400	8.0057

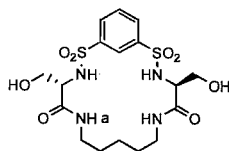


**117 with *N*-Ac-D-Phe-OTBA
in MeCN-*d*₃/2% H₂O**

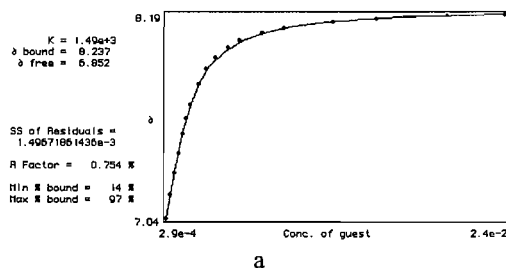
$$[H] = 1.68 \cdot 10^{-3} \text{ M}$$

$$[G] = 5.92 \cdot 10^{-2} \text{ M}$$

$$V_i = 600 \mu\text{l}$$



Volume added (μl)	δ_a
3	7.0404
6	7.1709
9	7.2914
12	7.4044
15	7.5136
18	7.604
21	7.6781
27	7.7936
33	7.8789
40	7.9442
50	8.0032
60	8.0434
80	8.0873
100	8.1149
150	8.1488
200	8.1644
300	8.1821
400	8.1928

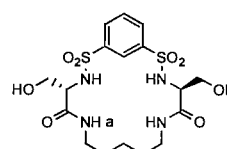


**117 with *N*-Boc-L-Gln-OTBA
in MeCN-*d*₃/2% H₂O**

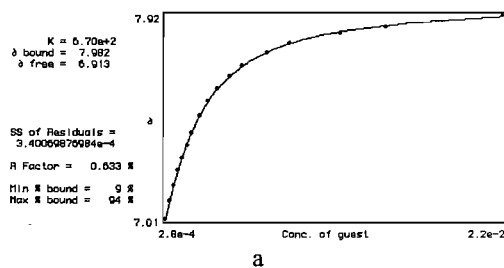
$$[H] = 1.63 \cdot 10^{-3} \text{ M}$$

$$[G] = 5.70 \cdot 10^{-2} \text{ M}$$

$$V_i = 600 \mu\text{l}$$



Volume added (μl)	δ_a
3	7.0103
6	7.0906
9	7.1596
12	7.2293
15	7.2839
18	7.3385
21	7.3919
27	7.4722
33	7.5337
40	7.5902
50	7.6461
60	7.6925
80	7.7496
100	7.7898
150	7.835
200	7.8664
367	7.9172

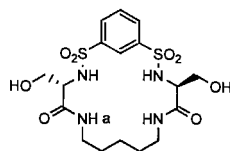


**117 with *N*-Boc-D-Gln-OTBA
in MeCN-*d*₃/2% H₂O**

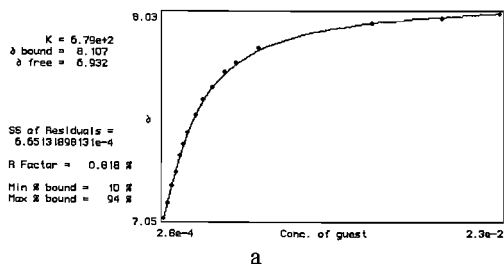
$$[H] = 1.63 \cdot 10^{-3} \text{ M}$$

$$[G] = 5.72 \cdot 10^{-2} \text{ M}$$

$$V_i = 600 \mu\text{l}$$



Volume added (μl)	δ_a
3	7.0504
6	7.1245
9	7.2086
12	7.2726
15	7.3479
18	7.4044
21	7.4571
27	7.5413
33	7.6178
40	7.6781
50	7.7509
60	7.7961
80	7.8639
200	7.9818
300	8.0107
400	8.0308

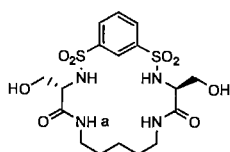


117 with *N*-Boc-L-Phe-OTBA
in MeCN- d_3 /2% H₂O

$$[H] = 1.93 \cdot 10^{-3} \text{ M}$$

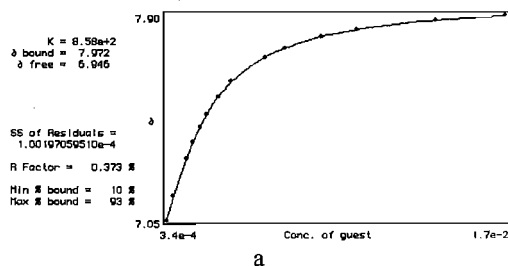
$$[G] = 6.77 \cdot 10^{-2} \text{ M}$$

$$V_i = 600 \mu\text{l}$$



Volume added (μl)	δ_a
3	7.0517
6	7.1515
12	7.3078
15	7.3756

18	7.4365
21	7.4873
27	7.5638
33	7.6254
50	7.7239
60	7.7634
80	7.8111
100	7.8413
150	7.8789
200	7.9041

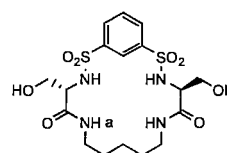


117 with *N*-Boc-D-Phe-OTBA
in MeCN- d_3 /2% H₂O

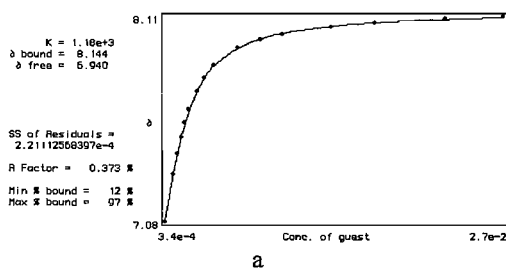
$$[H] = 1.93 \cdot 10^{-3} \text{ M}$$

$$[G] = 6.78 \cdot 10^{-2} \text{ M}$$

$$V_i = 600 \mu\text{l}$$



Volume added (μl)	δ_a
3	7.0805
9	7.3178
12	7.4195
15	7.5074
18	7.5789
21	7.6442
27	7.7321
33	7.8049
40	7.8633
60	7.9517
80	7.9944
100	8.022
150	8.0597
200	8.081
300	8.1005
400	8.1124

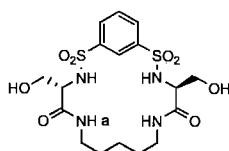


117 with *N*-Boc-L-Ser-OTBA
in MeCN- d_3 /2% H₂O

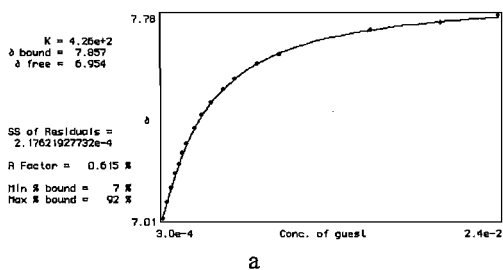
$$[H] = 1.75 \cdot 10^{-3} \text{ M}$$

$$[G] = 6.06 \cdot 10^{-2} \text{ M}$$

$$V_i = 600 \mu\text{l}$$



Volume added (μl)	δ_a
3	7.0128
6	7.073
9	7.1283
12	7.1798
15	7.2174
18	7.2582
21	7.294
27	7.3523
33	7.4019
40	7.4484
50	7.5011
60	7.5383
80	7.5952
100	7.6323
200	7.7245
300	7.7534
400	7.781

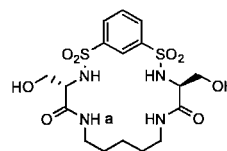


117 with *N*-Boc-D-Ser-OTBA
in MeCN- d_3 /2% H₂O

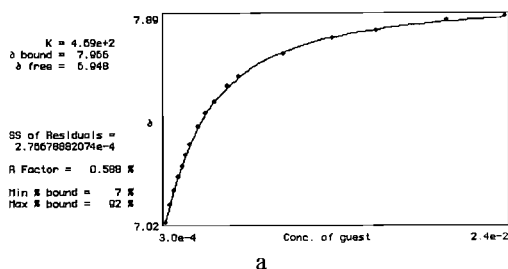
$$[H] = 1.75 \cdot 10^{-3} \text{ M}$$

$$[G] = 6.08 \cdot 10^{-2} \text{ M}$$

$$V_i = 600 \mu\text{l}$$



Volume added (μl)	δ_a
3	7.0222
6	7.0944
9	7.1559
12	7.2111
15	7.2575
18	7.3047
21	7.3467
27	7.4195
33	7.4772
40	7.5274
50	7.5902
60	7.6304
100	7.727
150	7.793
200	7.8237
300	7.8651
400	7.8865

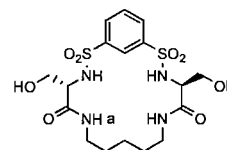


117 with *N*-Boc-L-Val-OTBA
in MeCN- d_3 /2% H₂O

$$[H] = 2.23 \cdot 10^{-3} \text{ M}$$

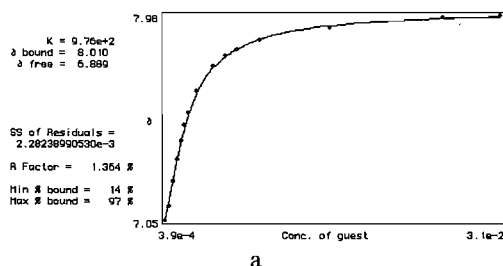
$$[G] = 7.85 \cdot 10^{-2} \text{ M}$$

$$V_i = 600 \mu\text{l}$$



Volume added (μl)	δ_a
3	7.0467
6	7.1107
9	7.2237

12	7.3228
15	7.4082
18	7.4785
21	7.5337
27	7.6341
40	7.7484
50	7.7936
60	7.8212
80	7.8639
150	7.9204
300	7.9693
400	7.9806

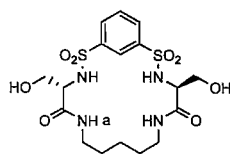


**117 with *N*-Boc-D-Val-OTBA
in MeCN-*d*₃/2% H₂O**

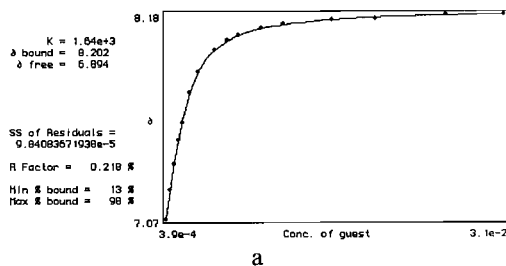
$$[H] = 2.23 \cdot 10^{-3} \text{ M}$$

$$[G] = 7.81 \cdot 10^{-2} \text{ M}$$

$$V_i = 600 \mu\text{l}$$



Volume added (μl)	δa
3	7.0667
6	7.2287
9	7.3668
12	7.4936
15	7.5927
21	7.7521
27	7.8626
40	7.9831
50	8.0346
60	8.0635
80	8.0999
100	8.1212
150	8.1438
200	8.1526
300	8.1727
400	8.1764

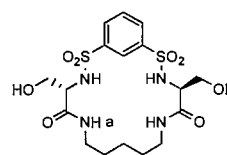


**117 with *S*-Mandelic Acid TBA salt
in MeCN-*d*₃/2% H₂O**

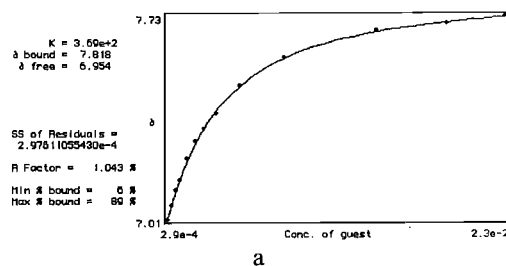
$$[H] = 1.67 \cdot 10^{-3} \text{ M}$$

$$[G] = 5.82 \cdot 10^{-2} \text{ M}$$

$$V_i = 600 \mu\text{l}$$



Volume added (μl)	δa
3	7.0052
6	7.0529
9	7.1082
12	7.1471
18	7.2218
24	7.2827
30	7.3291
40	7.3819
60	7.4797
100	7.5777
200	7.6725
300	7.7001
400	7.727

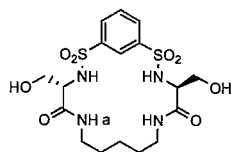


**117 with *R*-Mandelic Acid TBA salt
in MeCN-*d*₃/2% H₂O**

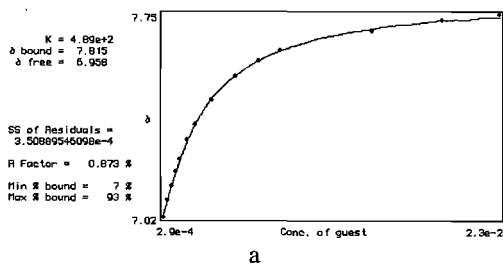
$$[H] = 1.67 \cdot 10^{-3} \text{ M}$$

$$[G] = 5.82 \cdot 10^{-2} \text{ M}$$

$$V_i = 600 \mu\text{l}$$



Volume added (μl)	δ_a
3	7.0165
6	7.078
9	7.1308
12	7.181
15	7.2262
21	7.2984
27	7.3542
40	7.4427
60	7.5274
80	7.5839
100	7.6203
200	7.6894
300	7.727
400	7.7521

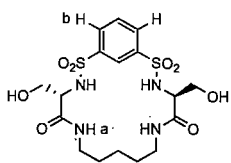


117 with TBAOAc in $\text{DMSO-}d_6$

$$[H] = 2.43 \cdot 10^{-3} \text{ M}$$

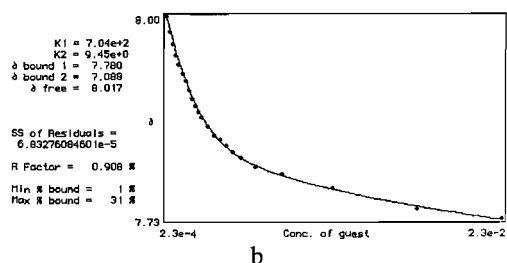
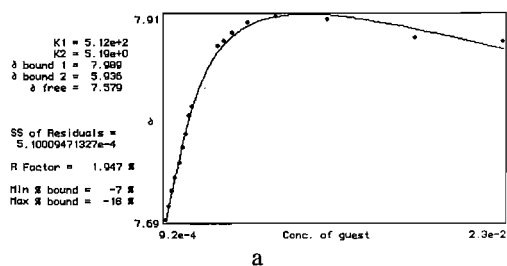
$$[G] = 6.98 \cdot 10^{-2} \text{ M}$$

$$V_i = 600 \mu\text{l}$$



Volume added (μl)	δ_a	δ_b
2	—	8.0034
4	—	7.9826
6	—	7.9657
8	7.6895	7.9506
10	7.7033	7.9375
12	7.7196	7.9249
14	7.7335	7.9149
16	7.7489	7.9036
18	7.7648	7.8923
20	7.7799	7.8822

22	7.7987	7.874
24	7.8088	7.8672
28	—	7.854
32	—	7.842
36	—	7.8364
40	7.8735	7.8276
44	7.8791	7.8195
50	7.8879	7.8119
60	7.8986	7.7994
80	7.9054	7.79
120	7.9017	7.7699
200	7.8816	7.7423
300	7.8778	7.7291

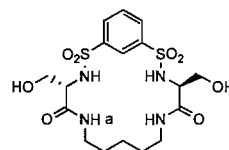


117 with *N*-Ac-L-Phe-OTBA in $\text{DMSO-}d_6$

$$[H] = 2.04 \cdot 10^{-3} \text{ M}$$

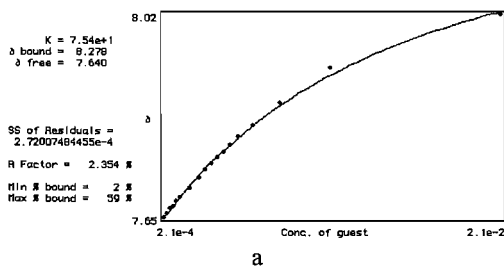
$$[G] = 6.26 \cdot 10^{-2} \text{ M}$$

$$V_i = 600 \mu\text{l}$$



Volume added (μl)	δ_a
2	7.6531
4	7.6588
6	7.6688
8	7.6732
10	7.6807
12	7.6883
18	7.7052
24	7.7228

28	7.7385
32	7.7489
36	7.7611
40	7.7698
44	7.7824
50	7.7975
60	7.817
80	7.8565
120	7.9192
300	8.0159

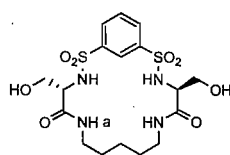


117 with *N*-Ac-D-Phe-OTBA in DMSO- d_6

$$[H] = 2.04 \cdot 10^{-3} \text{ M}$$

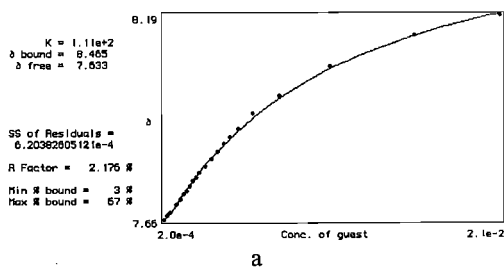
$$[G] = 6.16 \cdot 10^{-2} \text{ M}$$

$$V_i = 600 \mu\text{l}$$



Volume added (μl)	δ_a
2	7.6606
4	7.6707
6	7.6788
10	7.7008
12	7.7134
14	7.7259
16	7.736
18	7.7485
20	7.7611
22	7.7698
24	7.7837
28	7.7987
32	7.8169
36	7.8376
40	7.8577
44	7.876
50	7.8954
60	7.9381
80	7.9826

120	8.0611
200	8.1414
300	8.1941

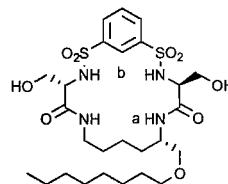


118 with *N*-Ac-L-Phe-OTBA in CDCl_3

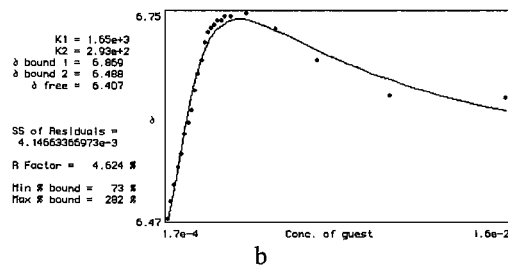
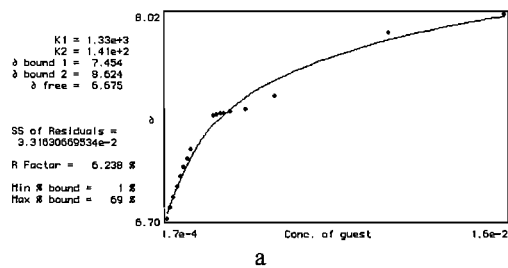
$$[H] = 1.77 \cdot 10^{-3} \text{ M}$$

$$[G] = 5.00 \cdot 10^{-2} \text{ M}$$

$$V_i = 600 \mu\text{l}$$



Volume added (μl)	δ_a	δ_b
2	6.6951	6.4666
4	6.7623	6.4905
6	6.8307	6.5131
8	6.901	6.5382
10	6.9663	6.557
12	7.0253	6.5846
14	7.0767	6.5997
16	7.1407	6.6173
18	—	6.6449
20	—	6.6688
22	—	6.6876
24	—	6.7114
26	—	6.7265
28	—	6.7315
30	7.3592	6.7365
32	7.3654	6.7416
34	7.3692	6.7422
36	7.3717	6.7478
40	7.3849	6.7478
50	7.3956	6.7528
70	7.486	6.7303
100	—	6.6876
160	7.8927	6.6374
280	8.0157	6.6348

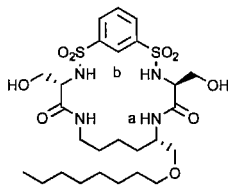


118 with *N*-Ac-D-Phe-OTBA in CDCl₃

$$[H] = 1.77 \cdot 10^{-3} \text{ M}$$

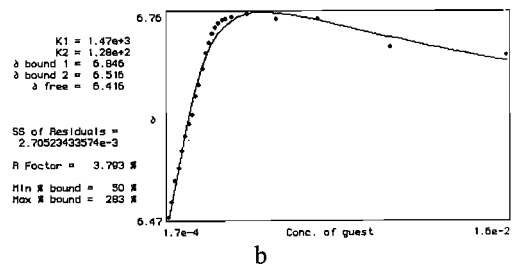
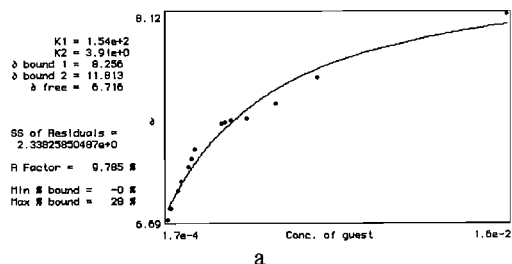
$$[G] = 4.98 \cdot 10^{-2} \text{ M}$$

$$V_i = 600 \mu\text{l}$$



Volume added (μl)	δ_a	δ_b
2	6.6913	6.4666
4	6.7641	6.488
6	—	6.5181
8	6.8934	6.5369
10	6.9537	6.562
12	—	6.5821
14	7.0554	6.5997
16	7.1122	6.6135
18	7.1816	6.6399
20	—	6.6562
22	—	6.6788
24	—	6.7014
26	—	6.7165
28	—	6.729
30	—	6.7378
32	—	6.7435
34	7.3629	6.7478
36	7.3667	6.7491
40	7.3843	6.7528
50	7.3975	6.7579
70	7.501	6.7503
100	7.6793	6.7503

160 — 6.7102
280 8.1249 6.6989

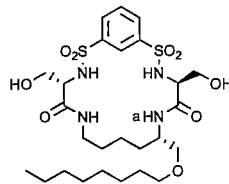


C24 with *N*-Boc-L-Phe-OTBA
in MeCN-*d*₃/2% H₂O

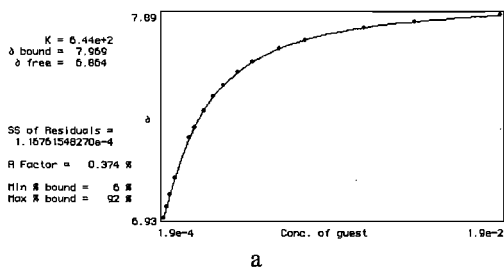
$$[H] = 1.63 \cdot 10^{-3} \text{ M}$$

$$[G] = 5.73 \cdot 10^{-2} \text{ M}$$

$$V_i = 600 \mu\text{l}$$

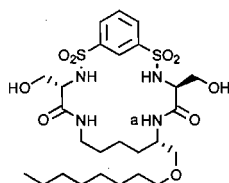


Volume added (μl)	δ_a
2	6.9324
4	6.9839
6	7.0429
9	7.117
18	7.304
21	7.353
27	7.4308
33	7.4961
40	7.5526
50	7.6141
60	7.6624
80	7.722
100	7.7622
150	7.8193
200	7.8489
300	7.8852

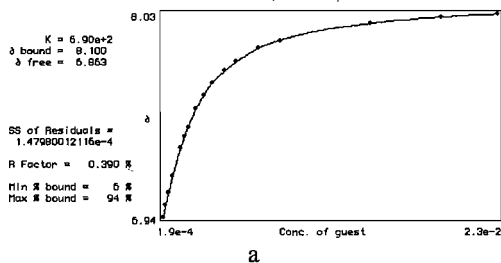


**C24 with *N*-Boc-D-Phe-OTBA
in MeCN-*d*₃/2% H₂O**

$[H] = 1.63 \cdot 10^{-3} \text{ M}$
 $[G] = 5.77 \cdot 10^{-2} \text{ M}$
 $V_i = 600 \mu\text{l}$

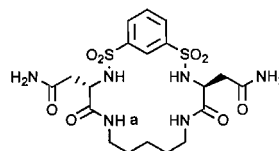


Volume added (μl)	δ_a
2	6.9425
4	7.0027
6	7.0693
9	7.1609
15	7.3109
18	7.3743
21	7.4214
27	7.5187
33	7.5903
40	7.6555
50	7.7214
60	7.7723
80	7.84
100	7.8821
200	7.9718
300	8.0083
400	8.0258

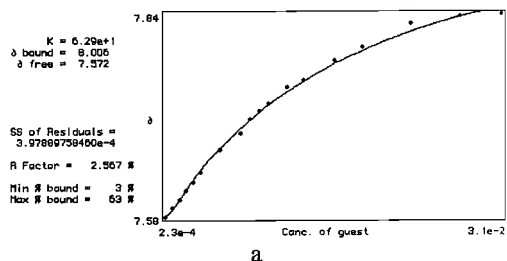


119 with *N*-Ac-L-Phe-OTBA in DMSO-*d*₆

$[H] = 1.95 \cdot 10^{-3} \text{ M}$
 $[G] = 6.79 \cdot 10^{-2} \text{ M}$
 $V_i = 600 \mu\text{l}$

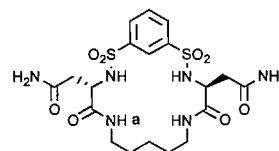


Volume added (μl)	δ_a
2	7.5841
8	7.5954
14	7.6054
20	7.618
26	7.628
32	7.6406
50	7.6694
70	7.6908
80	7.7096
90	7.7196
100	7.7297
120	7.7498
140	7.7598
180	7.7837
220	7.8012
300	7.8314
400	7.8401
500	7.8439



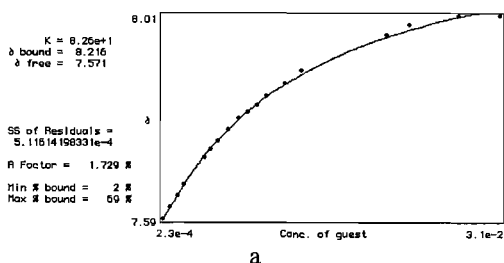
119 with *N*-Ac-D-Phe-OTBA in DMSO-*d*₆

$[H] = 1.95 \cdot 10^{-3} \text{ M}$
 $[G] = 6.79 \cdot 10^{-2} \text{ M}$
 $V_i = 600 \mu\text{l}$



Volume added (μl)	δ_a
2	7.5866

8	7.6111	148	8.051	8.685
14	7.6349	198	8.0862	8.7302
20	7.6581	298	8.1284	8.8088
38	7.7159	398	—	8.8331
44	7.7322			
50	7.7485			
60	7.7724			
70	7.7975			
80	7.8088			
90	7.8251			
100	7.8452			
120	7.8707			
140	7.8991			
260	7.972			
300	7.992			
400	8.0134			
500	8.0134			

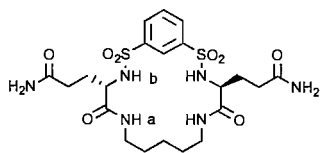


120 with *N*-Ac-L-Phe-OTBA in DMSO- d_6

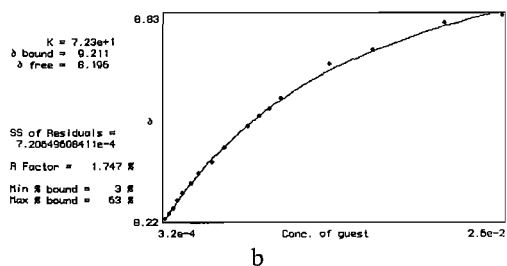
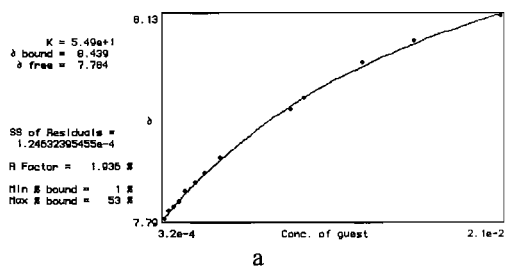
$$[H] = 1.54 \cdot 10^{-3} \text{ M}$$

$$[G] = 6.45 \cdot 10^{-2} \text{ M}$$

$$V_i = 600 \mu\text{l}$$



Volume added (μl)	δ_a	δ_b
3	7.7937	8.2218
6	7.8063	8.2368
9	7.8125	8.2525
12	7.8213	8.2745
16	7.8389	8.2984
22	7.854	8.3285
28	7.8684	8.3586
38	7.8935	8.3944
48	—	8.4364
68	—	8.5017
78	—	8.5306
88	7.9732	8.5532
98	7.992	8.5846

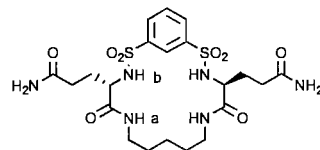


120 with *N*-Ac-D-Phe-OTBA in DMSO- d_6

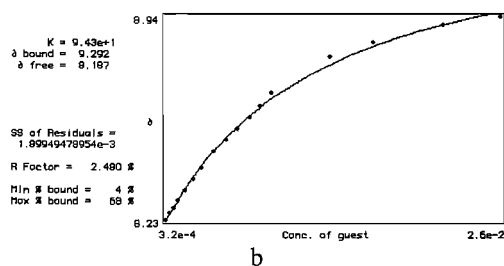
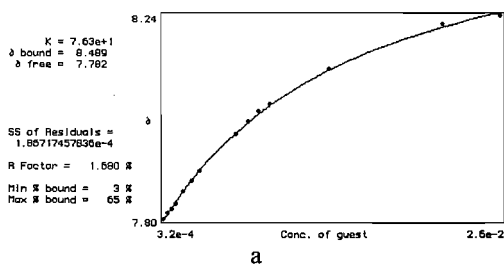
$$[H] = 1.54 \cdot 10^{-3} \text{ M}$$

$$[G] = 6.47 \cdot 10^{-2} \text{ M}$$

$$V_i = 600 \mu\text{l}$$



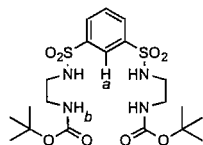
Volume added (μl)	δ_a	δ_b
3	7.8037	8.2268
6	7.815	8.2506
9	7.8238	8.2695
12	7.8351	8.2921
18	7.8615	8.331
24	7.8841	8.3711
30	7.9054	8.4101
40	—	8.4666
50	—	8.508
60	7.9858	8.5469
70	8.0121	8.5883
80	8.0335	8.6272
90	8.0485	8.6724
150	8.1239	8.7992
200	—	8.8526
300	8.2205	8.9129
400	8.2387	8.9436



Job Plot^[96] of receptor **69** with TBAOAc
in MeCN-*d*₃

Solution A: [H] = 1.00 · 10⁻² M

Solution B: [G] = 1.00 · 10⁻² M



Vol. Soln. A	Vol. Soln. B	χ_H	δ_a	δ_b	$\chi_H \cdot \Delta\delta_a$	$\chi_H \cdot \Delta\delta_b$
60	540	0.1	8.65	6.53	0.04	0.12
120	480	0.2	8.68	6.52	0.09	0.24
180	420	0.3	8.70	6.49	0.15	0.34
240	360	0.4	8.72	6.46	0.20	0.44
300	300	0.5	8.69	6.35	0.23	0.50
360	240	0.6	8.57	6.10	0.21	0.45
420	180	0.7	8.40	5.73	0.12	0.27
480	120	0.8	8.35	5.64	0.11	0.23
540	60	0.9	8.28	5.49	0.06	0.13
600	0	1	8.22	5.35	0.00	0.00

Appendices

Appendix A

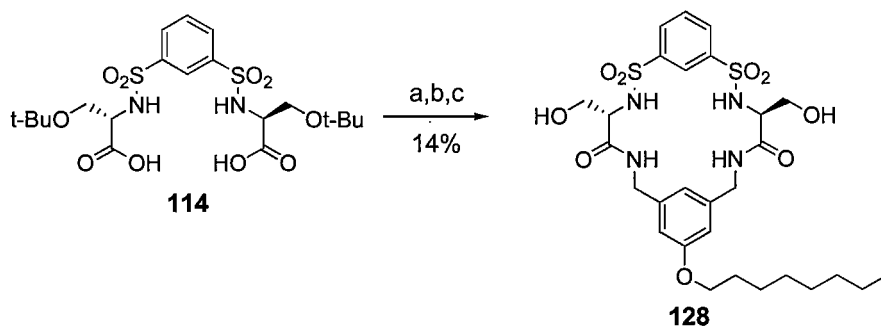
Macrocycle 128 and macrocycle 129

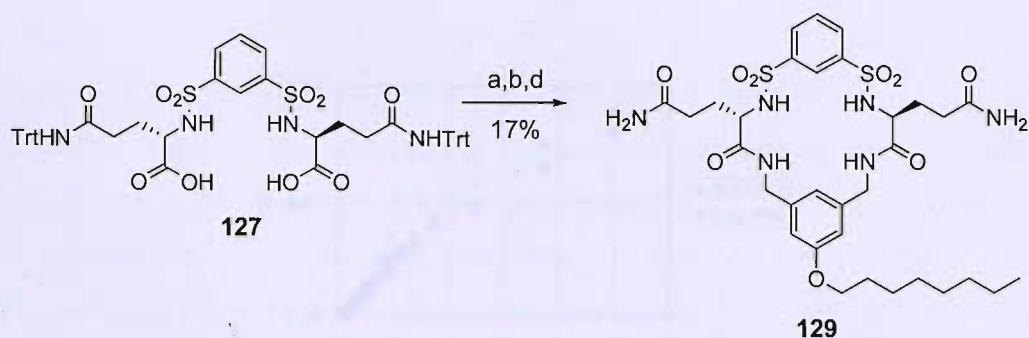
Introduction

Binding studies carried out on macrocycles **87**, **88** and **102** with acetate in MeCN- d_3 /2% H₂O showed that a flexible chain at the ‘southern end’ was more favourable, in terms of binding, than a more rigid aromatic spacer. Enantioselectivity, however, although binding studies were performed in different solvents, was slightly in favour of rigid receptor **102**. For this reason, in order to assess how rigidity and flexibility at the ‘southern’ end could influence enantioselectivity for macrocycles bearing polar groups, receptors **128** and **129** were designed.

Synthesis

The synthesis was carried out, as usual, under anion templating conditions from bis-acids **114** and **127** (Scheme A.1).





Scheme A.1 Reagents and conditions: a) PFP, EDC, DCM; b) **101**, TBACl, Et_3N , DCM; c) 80:20 DCM/TFA; d) TFA.

Binding studies

Binding studies were carried out on macrocycle **128** with the two enantiomers of *N*-Ac-phenalanine in $MeCN-d_3$ and $DMSO-d_6$. Data points collected in $MeCN-d_3$ were affected by poor fit with the 1:1 titrating program and, for this reason, they were treated with the 1:2 program. Even in this case, no reliable constants could be obtained, due to the fact that the values calculated were varying significantly depending on input values. From the plot of the two curves, nonetheless, no sensible differences seemed to emerge (**Figure A.1**).

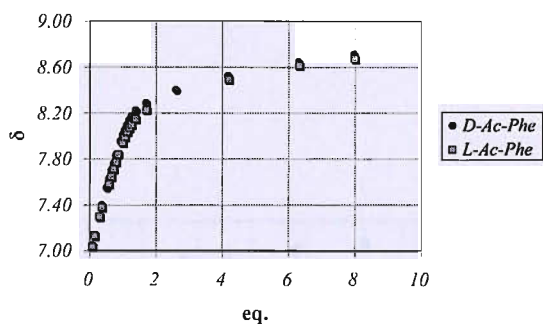


Figure A.1 Binding titration curves for amidic protons of receptor **128** upon addition of the TBA salts of the two enantiomers of *N*-Ac-Phe in $MeCN-d_3$.

In $DMSO-d_6$ it was possible to obtain a reasonable fit with the 1:1 titrating program. Binding constants, however, were affected by very low percentage of saturation at the end of the titration ($\sim 40\%$) and they were weak and very similar ($K_a = 49 M^{-1}$ for *N*-Ac-D-Phe and $K_a = 42 M^{-1}$ for *N*-Ac-L-Phe), as suggested by the plot of the two curves (**Figure A.2**).

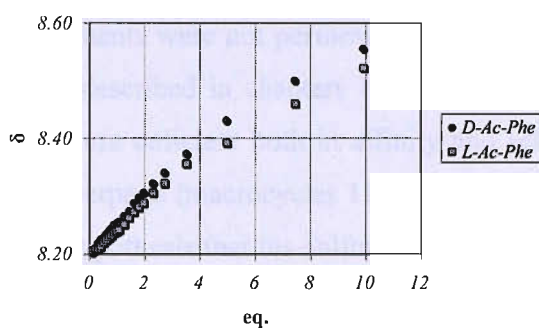


Figure A.2 Binding titration curves for amidic protons of receptor **128** upon addition of the TBA salts of the two enantiomers of *N*-Ac-Phe in $\text{DMSO-}d_6$.

The last data testified poor affinity and selectivity in comparison with those obtained from flexible macrocycle **117** (see § 4.8, $K_a = 111 \text{ M}^{-1}$ for *N*-Ac-D-Phe and $K_a = 75 \text{ M}^{-1}$ for *N*-Ac-L-Phe).

Binding studies were carried out on macrocycle **129** with the two enantiomers of *N*-Ac-phenalanine in $\text{MeCN-}d_3$. A reasonable fit was found with the 1:1 treating program. Binding constants, however, were almost identical ($K_a = 4.37 \cdot 10^3 \text{ M}^{-1}$ for *N*-Ac-D-Phe and $K_a = 4.32 \cdot 10^3 \text{ M}^{-1}$ for *N*-Ac-L-Phe), as reflected by the superimposition of the two curves (Figure A.3).

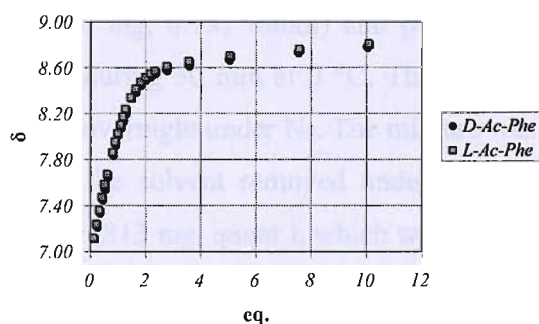


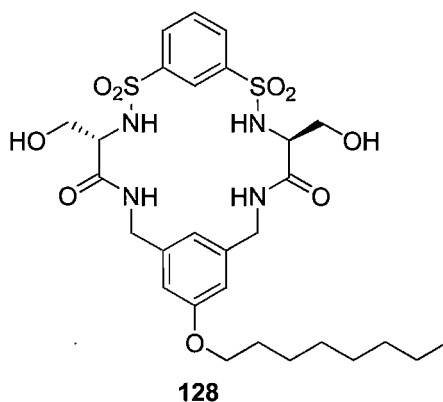
Figure A.3 Binding titration curves for amidic protons of receptor **128** upon addition of the TBA salts of the two enantiomers of *N*-Ac-Phe in $\text{MeCN-}d_3$.

Conclusions

Although a full set of experiments were not performed in order to compare macrocycles **128** and **129** with receptors described in chapters II-IV, the binding studies performed suggested clearly that they were deficient both in affinity and selectivity in comparison with their more flexible counterparts (macrocycles **117** and **120**). The latter finding added further corroboration to the hypothesis that bis-sulfonamide based macrocycles are likely suffering from a lack of preorganisation and, for this reason, they have to undergo a rearrangement in order to bind carboxylates. During this process, rigid scaffolds are to be more penalised. Experimental evidence is in agreement with this conclusion.

Experimental for synthesis

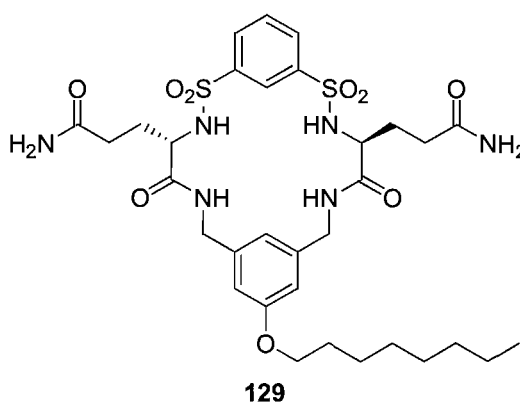
Macrocycle **128**



A solution of EDC (439 mg, 2.29 mmol) in dry DCM (20 ml) was added dropwise to a solution of bis-acid **114** (386 mg, 0.737 mmol) and pentafluorophenol (644 mg, 3.50 mmol) in dry DCM (20 ml) during 30 min at 0 °C. The reaction was allowed to reach room temperature and stirred overnight under N₂. The mixture was washed (5% NaHCO₃, 70 ml), dried (MgSO₄) and the solvent removed under reduced pressure yielding the crude pentafluorophenol ester (813 mg, quant.), which was dissolved in dry DCM (5 ml). TBACl (208 mg, 0.748 mmol) was added. The mixture and a solution of bis-amine **101** (189 mg, 0.713 mmol) and dry Et₃N (410 μl, 2.94 mmol) in dry DCM (5 ml) were added simultaneously with a syringe pump into 70 ml of dry DCM at room temperature over a period of 6 h. The reaction was stirred overnight at room temperature. The mixture was washed (1 M KHSO₄, 100 ml, 1 M K₂CO₃, 100 ml, and brine, 100 ml) and dried (MgSO₄). The solvent was removed under reduced pressure and the residue was purified

by flash column chromatography (SiO₂, 95:5 → 60:40 PE/EA) to give the protected macrocycle (180 mg, 32%). The white solid was dissolved in 80:20 DCM/TFA (15 ml) and the solution was stirred for 5 h. Toluene was added and the solvent removed under reduced pressure. The residue was purified by flash column chromatography (SiO₂, DCM → 94:6 DCM/MeOH) to yield the desired product **128** as a white solid (77 mg, 14% from **114**). MP = 123-126 °C; R_f = 0.44 (92:8 DCM/MeOH); [α]_D²⁶ = +134 (c = 0.25, MeCN); FT-IR (neat): ν_{max} = 3272 (br), 2926 (w), 1651 (s), 1598 (w), 1539 (m), 1456 (m), 1326 (m), 1295 (s), 1174 (s), 1153 (s), 1112 (m), 1055 (s), 796 (m), 680 (m) cm⁻¹; ¹H NMR (400 MHz, DMSO-*d*₆): δ = 8.20 (2 H, dd, *J* = 7.0, 5.0 Hz, CONH), 8.09 (2 H, br s, SNH), 8.03 (1 H, t, *J* = 2.0 Hz, O₂SArH), 7.80 (2 H, dd, *J* = 8.0, 2.0 Hz, O₂SArH), 7.07 (1 H, t, *J* = 2.0 Hz, O₂SArH), 6.75 (2 H, s, ArH), 6.34 (1 H, s, ArH), 5.09 (2 H, t, *J* = 6.0 Hz, α-CH), 4.22 (2 H, dd, *J* = 14.0, 7.0 Hz, NHCH_aH_b), 3.99 (2 H, t, *J* = 6.5 Hz, ArOCH₂), 3.86 (2 H, t, *J* = 6.0 Hz, OH), 3.80 (2 H, dd, *J* = 14.0, 5.0 Hz, NHCH_aH_b), 3.60 (4 H, apparent t, *J* = 6.0 Hz, α-CHCH₂), 1.79-1.70 (2 H, m, OCH₂CH₂), 1.48-1.39 (2 H, m, OCH₂CH₂CH₂), 1.38-1.20 (8 H, m, (CH₂)₄CH₃), 0.85 (3 H, t, *J* = 7.0 Hz, CH₃); ¹³C NMR (100 MHz, DMSO-*d*₆): δ = 168.4 (0), 158.3 (0), 142.0 (0), 140.0 (0), 129.3 (1), 129.1 (1), 123.7 (1), 119.8 (1), 113.5 (1), 67.3 (2), 63.1 (2), 58.3 (1), 42.6 (2), 31.2 (2), 28.7 (2), 28.6 (2), 25.5 (2), 22.0 (2), 13.9 (3); ESMS: *m/z* = 663 [M+Na]⁺; HRMS (ES): calcd for C₂₈H₄₀N₄NaO₉S₂ ([M+Na]⁺) 663.2129, found 663.2121.

Macrocycle 129



A solution of EDC (290 mg, 1.51 mmol) in dry DCM (20 ml) was added dropwise to a solution of bis-acid **127** (476 mg, 0.486 mmol) and pentafluorophenol (409 mg, 2.22 mmol) in dry DCM (10 ml) during 15 min at 0 °C. The reaction was allowed to reach room temperature and stirred overnight under N₂. The mixture was washed (5% NaHCO₃,

70 ml), dried (MgSO₄) and the solvent removed under reduced pressure yielding the crude pentafluorophenol ester (801 mg, quant.), which was dissolved in dry DCM (5 ml). TBACl (138 mg, 0.495 mmol) was added. The mixture and a solution of bis-amine **101** (126 mg, 0.477 mmol) and dry Et₃N (270 μl, 1.94 mmol) in dry DCM (5 ml) were added simultaneously with a syringe pump into 45 ml of dry DCM at room temperature over a period of 6 h. The reaction was stirred overnight at room temperature. The mixture was washed (1 M KHSO₄, 100 ml, 1 M K₂CO₃, 100 ml, and brine, 100 ml) and dried (MgSO₄). The solvent was removed under reduced pressure and the residue was purified by flash column chromatography (SiO₂, 20:80 → 55:45 EA/PE) to give the protected macrocycle (200 mg, 34%). The white solid was dissolved in TFA (10 ml) and the solution was stirred for 2 h. Toluene was added and the solvent removed under reduced pressure. The residue was purified by flash column chromatography (SiO₂, 95:5 → 93:7 DCM/MeOH) to yield the desired product **129** as a beige solid (57 mg, 17% from **127**). MP = 119-121 °C; R_f = 0.34 (90:10 DCM/MeOH); [α]_D²⁴ = +137 (*c* = 0.25, DMSO); FT-IR (neat): ν_{max} = 3273 (br), 2927 (w), 2856 (w), 1652 (s), 1597 (m), 1540 (w), 1546 (m), 1417 (m), 1322 (m), 1295 (m), 1172 (s), 1152 (s), 1108 (m), 1082 (m), 979 (w), 858 (w), 795 (m) cm⁻¹; ¹H NMR (400 MHz, DMSO-*d*₆): δ = 8.33 (2 H, dd, *J* = 7.0, 4.0 Hz, CONH), 8.27 (2 H, br s, SNH), 8.00 (1 H, t, *J* = 1.5 Hz, O₂SArH), 7.73 (2 H, dd, *J* = 8.0, 1.5 Hz, O₂SArH), 7.34 (2 H, s, NH_aH_b) 6.97 (1 H, t, *J* = 8.0 Hz, O₂SArH), 6.77 (4 H, s, NH_aH_b and ArH superimposed), 6.32 (1 H, s, ArH), 4.25 (2 H, dd, *J* = 14.0, 7.0 Hz, NHCH_aH_b), 4.00 (2 H, t, *J* = 6.0 Hz, OCH₂), 3.83 (2 H, dd, *J* = 8.0, 5.5 Hz, α-CH), 3.74 (2 H, dd, *J* = 14.0, 4.0 Hz, NHCH_aH_b), 2.23 (2 H, ddd, *J* = 16.0, 10.0, 5.5 Hz, NH₂COCH_aH_b), 2.14 (2 H, ddd, *J* = 16.0, 10.0, 6.0 Hz, NH₂COCH_aH_b), 1.95-1.83 (2 H, m, α-CHCH_aH_b), 1.83-1.70 (6 H, m, α-CHCH_aH_b and OCH₂CH₂ superimposed), 1.50-1.39 (2 H, m, OCH₂CH₂CH₂), 1.39-1.19 (8 H, m, (CH₂)₄CH₃), 0.84 (3 H, *J* = 7.0 Hz, CH₃); ¹³C NMR (100 MHz, DMSO-*d*₆): δ = 173.3 (0), 169.6 (0), 158.3 (0), 142.2 (0), 139.9 (0), 129.0 (1), 128.8 (1), 123.6 (1), 120.0 (1), 113.6 (1), 67.3 (2), 56.1 (1), 42.6 (2), 31.2 (2), 31.1 (2), 29.6 (2), 28.7 (2), 28.6 (2), 25.5 (2), 22.0 (2), 13.9 (3); ESMS: *m/z* = 745 [M+Na]⁺; HRMS (ES): calcd for C₃₂H₄₆N₆NaO₉S₂ ([M+Na]⁺) 745.2660, found 745.2651.

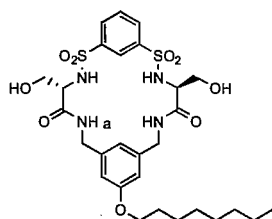
Experimental for binding studies

128 with *N*-Ac-L-Phe-OTBA
in MeCN-*d*₃

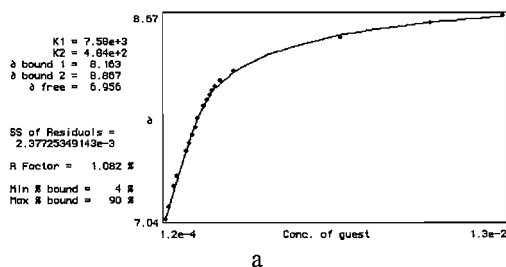
$$[H] = 1.64 \cdot 10^{-3} \text{ M}$$

$$[G] = 3.62 \cdot 10^{-2} \text{ M}$$

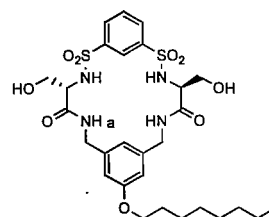
$$V_i = 600 \mu\text{l}$$



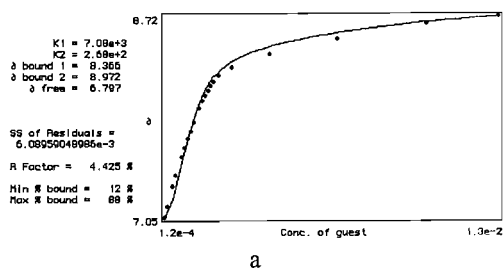
Volume added (μl)	δ_a
2	7.0373
4	7.1320
8	7.2977
10	7.3781
16	7.5821
18	7.6454
20	7.7107
22	7.7710
24	7.8394
28	7.9411
30	7.9907
32	8.0333
34	8.0685
36	8.0961
40	8.1463
50	8.2267
140	8.4935
240	8.6133
340	8.6736



$V_i = 600 \mu\text{l}$



Volume added (μl)	δ_a
2	7.0492
4	7.1395
8	7.3027
10	7.3994
14	7.5519
16	7.6266
18	7.6994
20	7.7591
22	7.8325
26	7.9556
28	8.0095
30	8.0534
32	8.0999
34	8.1388
36	8.1727
40	8.2254
50	8.2894
80	8.4037
140	8.5267
240	8.6510
340	8.7150



128 with *N*-Ac-L-Phe-OTBA
in DMSO-*d*₆

128 with *N*-Ac-D-Phe-OTBA
in MeCN-*d*₃

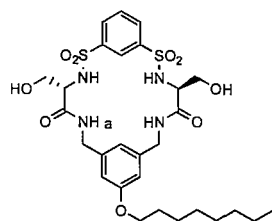
$$[H] = 1.64 \cdot 10^{-3} \text{ M}$$

$$[G] = 3.61 \cdot 10^{-2} \text{ M}$$

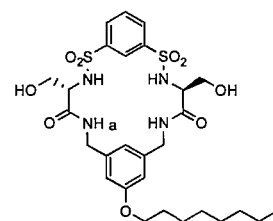
$$[H] = 1.76 \cdot 10^{-3} \text{ M}$$

$$[G] = 5.23 \cdot 10^{-2} \text{ M}$$

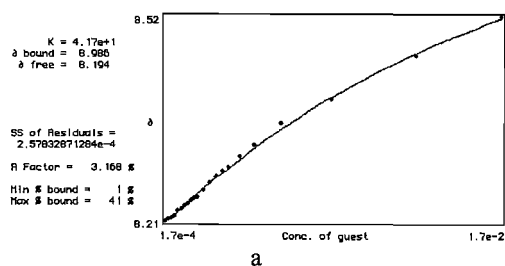
$$V_i = 600 \mu\text{l}$$



Volume added (μl)	δa
2	8.2054
4	8.2080
6	8.2092
8	8.2130
10	8.2199
12	8.2243
14	8.2281
16	8.2318
18	8.2368
20	8.2393
22	8.2419
26	8.2519
30	8.2632
34	8.2732
38	8.2808
42	8.2883
50	8.3059
60	8.3222
80	8.3561
120	8.3925
200	8.4603
300	8.5218



Volume added (μl)	δa
2	8.2029
4	8.2105
6	8.2193
8	8.2255
10	8.2280
12	8.2343
14	8.2393
16	8.2444
18	8.2506
20	8.2531
22	8.2557
26	8.2657
30	8.2745
34	8.2883
38	8.2977
42	8.3059
50	8.3222
60	8.3410
80	8.3737
120	8.4314
200	8.5004
300	8.5557

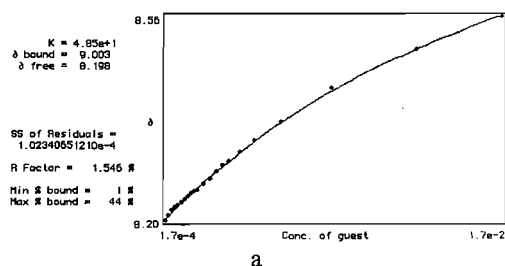


128 with *N*-Ac-D-Phe-OTBA
in DMSO-*d*₆

$$[H] = 1.76 \cdot 10^{-3} \text{ M}$$

$$[G] = 5.22 \cdot 10^{-2} \text{ M}$$

$$V_i = 600 \mu\text{l}$$

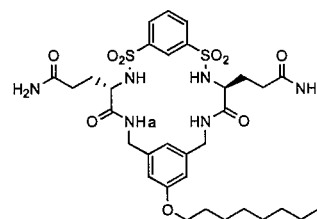
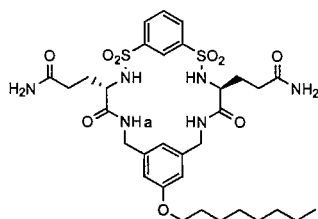


129 with *N*-Ac-L-Phe-OTBA
in MeCN-*d*₃

$$[H] = 8.21 \cdot 10^{-4} \text{ M}$$

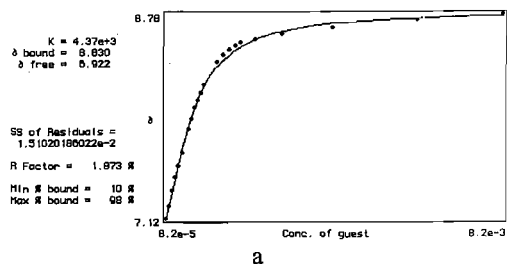
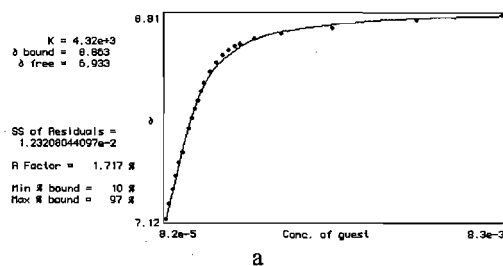
$$[G] = 2.48 \cdot 10^{-2} \text{ M}$$

$$V_i = 600 \mu\text{l}$$



Volume added (μl)	δa
2	7.1207
4	7.2406
6	7.3612
8	7.4741
10	7.5865
12	7.6743
16	7.8651
18	7.9580
20	8.0321
22	8.1024
24	8.1727
26	8.2430
30	8.3409
34	8.4175
38	8.4772
42	8.5173
46	8.5505
50	8.5719
60	8.6152
80	8.6579
120	8.7074
200	8.7665
300	8.8129

Volume added (μl)	δa
2	7.1208
4	7.2193
6	7.3404
8	7.4546
10	7.5451
12	7.6543
16	7.8450
18	7.9342
20	8.0219
22	8.0823
24	8.1401
26	8.2066
34	8.3917
38	8.4520
42	8.4979
46	8.5261
50	8.5537
60	8.5794
80	8.6208
120	8.6723
200	8.7357
300	8.7840



129 with *N*-Ac-D-Phe-OTBA
in MeCN- d_3

$$[H] = 8.21 \cdot 10^{-4} \text{ M}$$

$$[G] = 2.46 \cdot 10^{-2} \text{ M}$$

$$V_i = 600 \mu\text{l}$$

Appendix B

Software for the determination of association constants from NMR binding studies^[95]

NMRTit HG

NMRTit HG fits the data to a 1:1 binding isotherm by solving the equations (1) – (3) in which $[H]_0$ is the total concentration of host; $[G]_0$ is the total concentration of guest; $[H]$ is the concentration of unbound free host; $[HG]$ is the concentration of host + guest complex; K is the association constant for the formation of the host-guest complex; δ_f is the free chemical shift of the host; δ_b is the limiting bound chemical shift of the host-guest complex.

$$[HG] = \frac{1 + K[H]_0[G]_0 - \sqrt{(1 + [H]_0[G]_0)^2 - 4K^2[H]_0[G]_0}}{2K} \quad (1)$$

$$[H] = [H]_0 - [HG] \quad (2)$$

$$\delta_{obs} = \frac{[HG]}{[H]_0} \delta_b + \frac{[H]}{[H]_0} \delta_f \quad (3)$$

NMRTit HGG

NMRTit HGG fits the data to a 1:2 binding isotherm by an iterative procedure to solve the following simultaneous equations. The method starts by assuming the $[HGG] = 0$, so that Equation (4) can be solved exactly for $[HG]$. This value of $[HG]$ is the used to solve Equation (5) for $[HGG]$. Equation (6) gives the concentration of free host $[H]$. At this point, $[H] + [HG] + [HGG] \neq [H]_0$ so the value of $[HGG]$ from equation (5) is used in equation (4) to re-evaluate $[HG]$.

$$[HG] = \frac{1 + 2K_1[G]_0([H]_0 - [HGG]) - \sqrt{(1 + 2K_1[G]_0([H]_0 - [HGG]))^2 - 16K_1^2[G]_0([H]_0 - [HGG])}}{4K_1} \quad (4)$$

$$[HGG] = \frac{1 + 0.5K_2[G]_0([H]_0 - [HG]) - \sqrt{\{(1 + 0.5K_2[G]_0([H]_0 - [HG]))^2 - K_2[G]_0([H]_0 - [HG])\}}}{K_2} \quad (5)$$

$$[H] = [H]_0 - [HG] - [HGG] \quad (6)$$

$$\delta_{obs} = \frac{[HGG]}{[H]_0} \delta_{b2} + \frac{[HG]}{[H]_0} \delta_{b1} + \frac{[H]}{[H]_0} \delta_f \quad (7)$$

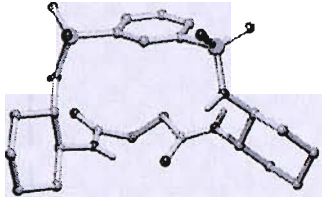
This procedure is reiterated until $[H] + [HG] + [HGG] = [H]_0$. This allows the set of simultaneous equations [Eq. (4)-(7)] to be solved for the concentrations of all species present where $[HGG]$ is the concentration of host·(guest)₂ complex; K_1 is the microscopic association constant for formation of the host·guest complex; K_2 is the microscopic association constant for formation of the host·(guest)₂ complex; δ_{b2} is the limiting bound chemical shift of the host·(guest)₂ complex. In order to calculate the macroscopic constants, the microscopic values have to be converted as follows: $K_{1mac} = 2 \cdot K_{1mic}$, $K_{2mac} = 0.5 \cdot K_{2mic}$.

Appendix C

Crystallographic data

Macrocycle 85

Table 1. Crystal data and structure refinement details for $C_{22}H_{32}N_4O_6S_2 \cdot 2CH_3OH$.

Identification code	2005sot0705	
Empirical formula	$C_{24}H_{40}N_4O_8S_2$	
Formula weight	576.72	
Temperature	120(2) K	
Wavelength	0.71073 Å	
Crystal system	Tetragonal	
Space group	$P4_32_12$	
Unit cell dimensions	$a = 9.275(5)$ Å $c = 67.73(2)$ Å	
Volume	$5826(5)$ Å ³	
Z	8	
Density (calculated)	1.315 Mg / m ³	
Absorption coefficient	0.234 mm ⁻¹	
$F(000)$	2464	
Crystal	Block; Colourless	
Crystal size	$0.10 \times 0.10 \times 0.04$ mm ³	
θ range for data collection	$3.23 - 27.48^\circ$	
Index ranges	$-12 \leq h \leq 11, -11 \leq k \leq 12, -84 \leq l \leq 86$	
Reflections collected	35210	
Independent reflections	6487 [$R_{int} = 0.2188$]	
Completeness to $\theta = 27.48^\circ$	98.0 %	
Absorption correction	Semi-empirical from equivalents	
Max. and min. transmission	0.9907 and 0.9770	
Refinement method	Full-matrix least-squares on F^2	
Data / restraints / parameters	6487 / 0 / 346	
Goodness-of-fit on F^2	1.002	
Final R indices [$F^2 > 2\sigma(F^2)$]	$RI = 0.0890, wR2 = 0.1442$	
R indices (all data)	$RI = 0.2004, wR2 = 0.1760$	
Absolute structure parameter	$-0.02(15)$	
Largest diff. peak and hole	0.347 and -0.363 e Å ⁻³	

Diffractometer: Nonius KappaCCD area detector (ϕ scans and ω scans to fill asymmetric unit). **Cell determination:** DirAx (Duisenberg, A.J.M.(1992). *J. Appl. Cryst.* 25, 92-96.) **Data collection:** Collect (Collect: Data collection software, R. Hooft, Nonius B.V., 1998). **Data reduction and cell refinement:** Denzo (Z. Otwinowski & W. Minor, *Methods in Enzymology* (1997) Vol. 276: *Macromolecular Crystallography*, part A, pp. 307-326; C. W. Carter, Jr. & R. M. Sweet, Eds., Academic Press). **Absorption correction:** Sheldrick, G. M. SADABS - Bruker Nonius area detector scaling and absorption correction - V2.10 **Structure solution:** SHELXS97 (G. M. Sheldrick, *Acta Cryst.* (1990) A46 467-473). **Structure refinement:** SHELXL97 (G. M. Sheldrick (1997), University of Göttingen, Germany). **Graphics:** Camcra - A Molecular Graphics Package. (D. M. Watkin, L. Pearce and C. K. Prout, Chemical Crystallography Laboratory, University of Oxford, 1993).

Special details: All hydrogen atoms were placed in idealised positions and refined using a riding model. Chirality: C7=S, C12=S, C17=S, C22=S

Table 2. Atomic coordinates [$\times 10^4$], equivalent isotropic displacement parameters [$\text{\AA}^2 \times 10^3$] and site occupancy factors. U_{eq} is defined as one third of the trace of the orthogonalized U^{ij} tensor.

Atom	x	y	z	U_{eq}	$S.o.f.$
S1	4452(2)	8381(2)	488(1)	26(1)	1
S2	8450(2)	10874(2)	973(1)	29(1)	1
N1	4223(5)	9349(5)	294(1)	26(1)	1
N2	5049(5)	12323(5)	203(1)	26(1)	1
N3	9145(5)	12096(5)	839(1)	27(1)	1
N4	7155(5)	14455(5)	744(1)	22(1)	1
O1	3089(4)	7718(4)	534(1)	38(1)	1
O2	5709(4)	7505(4)	454(1)	30(1)	1
O3	8450(4)	11374(4)	1175(1)	33(1)	1
O4	9137(4)	9522(4)	923(1)	42(1)	1
O5	2669(4)	12143(5)	267(1)	40(1)	1
O6	7071(4)	13860(4)	420(1)	32(1)	1
C1	4848(6)	9550(6)	689(1)	24(1)	1
C2	6291(7)	9784(6)	742(1)	25(1)	1
C3	6611(6)	10650(6)	904(1)	24(1)	1
C4	5503(7)	11250(6)	1015(1)	28(2)	1
C5	4084(7)	10971(6)	965(1)	32(2)	1
C6	3740(6)	10128(6)	803(1)	27(1)	1
C7	9413(6)	13614(5)	899(1)	21(1)	1
C8	11028(6)	13857(6)	919(1)	26(1)	1
C9	11373(6)	15420(6)	973(1)	31(2)	1
C10	10724(6)	16452(6)	826(1)	31(2)	1
C11	9101(6)	16211(6)	808(1)	28(1)	1
C12	8739(6)	14665(6)	752(1)	25(1)	1
C13	6464(6)	14097(6)	580(1)	23(1)	1
C14	4837(6)	13953(6)	607(1)	26(1)	1
C15	3968(6)	14128(6)	413(1)	27(2)	1
C16	3841(7)	12778(6)	290(1)	28(2)	1
C17	5121(6)	11159(6)	58(1)	24(1)	1
C18	6291(6)	11492(6)	-96(1)	29(1)	1
C19	6311(8)	10339(7)	-259(1)	41(2)	1
C20	6553(7)	8854(6)	-167(1)	36(2)	1
C21	5437(6)	8513(6)	-12(1)	31(1)	1
C22	5376(6)	9676(6)	151(1)	24(1)	1
C23	10495(8)	8273(7)	1360(1)	61(2)	1
O7	10546(5)	9746(5)	1408(1)	49(1)	1
C24	-490(10)	10701(12)	341(1)	120(4)	1
O8	397(6)	11364(6)	477(1)	83(2)	1

Table 3. Bond lengths [Å] and angles [°].

S1–O2	1.439(4)	O2–S1–C1	107.4(3)
S1–O1	1.441(4)	O1–S1–C1	105.9(2)
S1–N1	1.605(4)	N1–S1–C1	108.2(2)
S1–C1	1.779(5)	O4–S2–O3	119.9(2)
S2–O4	1.446(4)	O4–S2–N3	107.9(3)
S2–O3	1.446(4)	O3–S2–N3	108.1(2)
S2–N3	1.588(5)	O4–S2–C3	105.1(3)
S2–C3	1.781(6)	O3–S2–C3	106.6(3)
N1–C22	1.476(6)	N3–S2–C3	108.8(2)
N2–C16	1.335(7)	C22–N1–S1	123.9(4)
N2–C17	1.459(6)	C16–N2–C17	124.7(5)
N3–C7	1.485(6)	C7–N3–S2	126.1(4)
N4–C13	1.321(6)	C13–N4–C12	123.2(5)
N4–C12	1.484(7)	C6–C1–C2	120.3(5)
O5–C16	1.246(7)	C6–C1–S1	120.4(4)
O6–C13	1.245(6)	C2–C1–S1	119.1(4)
C1–C6	1.392(7)	C3–C2–C1	119.6(5)
C1–C2	1.401(8)	C4–C3–C2	120.0(5)
C2–C3	1.392(7)	C4–C3–S2	121.2(4)
C3–C4	1.391(7)	C2–C3–S2	118.6(5)
C4–C5	1.383(8)	C5–C4–C3	119.7(5)
C5–C6	1.387(7)	C4–C5–C6	121.3(5)
C7–C8	1.522(7)	C5–C6–C1	119.1(5)
C7–C12	1.525(7)	N3–C7–C8	109.3(4)
C8–C9	1.528(7)	N3–C7–C12	111.1(4)
C9–C10	1.505(7)	C8–C7–C12	111.6(4)
C10–C11	1.527(8)	C7–C8–C9	111.6(4)
C11–C12	1.521(7)	C10–C9–C8	111.2(4)
C13–C14	1.525(7)	C9–C10–C11	110.7(5)
C14–C15	1.549(7)	C12–C11–C10	112.0(5)
C15–C16	1.509(8)	N4–C12–C11	110.6(4)
C17–C22	1.530(7)	N4–C12–C7	110.4(4)
C17–C18	1.538(7)	C11–C12–C7	110.5(4)
C18–C19	1.535(7)	O6–C13–N4	123.8(5)
C19–C20	1.526(8)	O6–C13–C14	122.3(5)
C20–C21	1.511(7)	N4–C13–C14	113.8(5)
C21–C22	1.542(7)	C13–C14–C15	114.0(5)
C23–O7	1.407(7)	C16–C15–C14	115.0(5)
C24–O8	1.382(8)	O5–C16–N2	121.9(6)
		O5–C16–C15	121.9(5)
O2–S1–O1	120.3(2)	N2–C16–C15	116.2(5)
O2–S1–N1	106.9(2)	N2–C17–C22	113.4(4)
O1–S1–N1	107.5(2)	N2–C17–C18	109.9(4)

C22–C17–C18	110.4(5)	C20–C21–C22	112.1(5)
C19–C18–C17	110.9(5)	N1–C22–C17	110.0(4)
C20–C19–C18	109.8(4)	N1–C22–C21	110.6(4)
C21–C20–C19	111.8(5)	C17–C22–C21	110.0(4)

Table 4. Anisotropic displacement parameters [$\text{\AA}^2 \times 10^3$]. The anisotropic displacement factor exponent takes the form: $-2\pi^2[h^2a^{*2}U^{11} + \dots + 2hk a^* b^* U^{12}]$.

Atom	U^{11}	U^{22}	U^{33}	U^{23}	U^{13}	U^{12}
S1	32(1)	24(1)	23(1)	-2(1)	2(1)	-9(1)
S2	35(1)	21(1)	31(1)	-1(1)	-9(1)	1(1)
N1	23(3)	35(3)	21(3)	3(2)	-3(2)	-10(2)
N2	24(3)	26(3)	27(3)	-4(2)	-1(2)	-3(2)
N3	32(3)	29(3)	19(2)	-4(2)	6(2)	-6(2)
N4	21(3)	29(3)	16(2)	-2(2)	4(2)	-2(2)
O1	38(3)	43(3)	34(2)	-11(2)	10(2)	-29(2)
O2	46(3)	19(2)	26(2)	-5(2)	5(2)	0(2)
O3	47(3)	31(2)	20(2)	3(2)	-9(2)	-7(2)
O4	35(3)	22(2)	70(3)	-4(2)	-17(2)	10(2)
O5	27(3)	49(3)	45(3)	-14(2)	-3(2)	-10(2)
O6	28(2)	45(3)	23(2)	-13(2)	5(2)	-9(2)
C1	31(4)	21(3)	19(3)	-5(3)	2(3)	-4(3)
C2	36(4)	19(3)	20(3)	0(3)	2(3)	-1(3)
C3	31(4)	22(3)	19(3)	7(3)	-6(3)	-2(3)
C4	42(4)	23(3)	17(3)	1(3)	-5(3)	-2(3)
C5	32(4)	36(4)	29(3)	-5(3)	7(3)	9(3)
C6	24(4)	34(4)	24(3)	7(3)	3(3)	-4(3)
C7	28(3)	16(3)	18(3)	-9(2)	6(3)	-5(3)
C8	21(3)	26(4)	30(3)	-11(3)	-4(3)	2(3)
C9	23(3)	44(4)	25(3)	-5(3)	-4(3)	-1(3)
C10	35(4)	34(4)	24(3)	1(3)	3(3)	-3(3)
C11	25(4)	24(3)	35(3)	4(3)	-5(3)	1(3)
C12	29(4)	29(3)	16(3)	-1(3)	1(3)	-1(3)
C13	27(3)	22(3)	21(3)	0(3)	-1(3)	-2(3)
C14	28(4)	26(4)	24(3)	-3(3)	2(3)	-6(3)
C15	30(4)	19(3)	33(3)	-3(3)	-2(3)	8(3)
C16	25(4)	33(4)	24(3)	7(3)	-7(3)	0(3)
C17	27(3)	26(4)	20(3)	-1(3)	-4(3)	4(3)
C18	37(4)	22(3)	26(3)	4(3)	3(3)	-2(3)
C19	61(5)	47(4)	16(3)	-1(3)	4(3)	-8(4)
C20	57(4)	29(4)	22(3)	-5(3)	6(3)	3(3)
C21	30(4)	31(4)	31(3)	1(3)	4(3)	-1(3)
C22	34(4)	23(3)	15(3)	7(3)	5(3)	-3(3)
C23	76(6)	49(5)	59(5)	-14(4)	-20(4)	24(4)
O7	59(3)	45(3)	43(3)	-12(2)	-22(2)	17(2)

C24	75(7)	203(13)	82(7)	-68(8)	5(6)	-67(7)
O8	58(4)	120(5)	70(4)	-50(4)	19(3)	-30(4)

Table 5. Hydrogen coordinates [$\times 10^4$] and isotropic displacement parameters [$\text{\AA}^2 \times 10^3$].

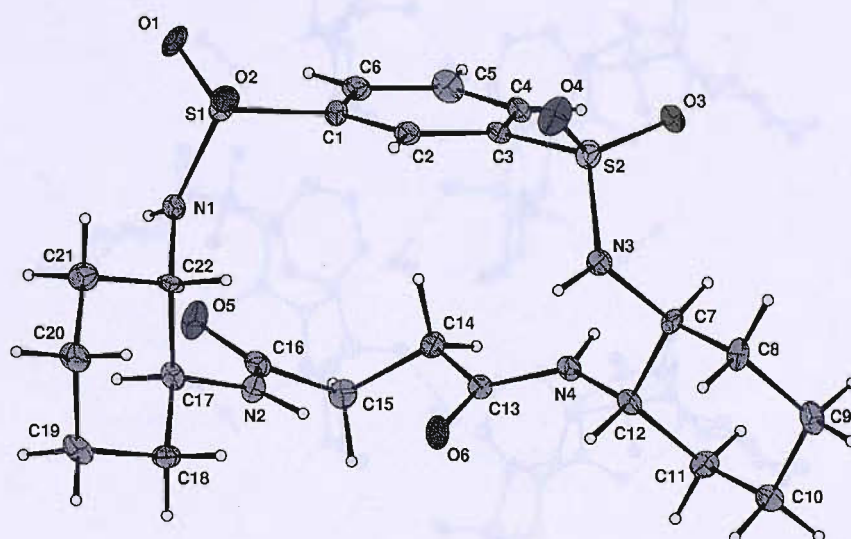
Atom	<i>x</i>	<i>y</i>	<i>z</i>	<i>U</i> _{eq}	<i>S.o.f.</i>
H1	3359	9705	272	31	1
H2	5860	12757	235	31	1
H3	9396	11851	718	32	1
H4	6651	14574	852	27	1
H2A	7045	9355	667	30	1
H4A	5720	11848	1125	33	1
H5	3331	11365	1043	39	1
H6	2761	9948	770	33	1
H7	8956	13774	1031	25	1
H8A	11509	13610	793	31	1
H8B	11414	13211	1023	31	1
H9A	10992	15634	1106	37	1
H9B	12432	15554	976	37	1
H10A	11183	16311	696	37	1
H10B	10912	17455	869	37	1
H11A	8635	16446	936	34	1
H11B	8706	16872	707	34	1
H12	9149	14466	618	30	1
H14A	4508	14691	702	31	1
H14B	4625	12994	664	31	1
H15A	2986	14465	447	33	1
H15B	4431	14887	332	33	1
H17	4173	11125	-12	29	1
H18A	6104	12448	-156	35	1
H18B	7245	11527	-31	35	1
H19A	5383	10349	-331	49	1
H19B	7092	10552	-354	49	1
H20A	6513	8113	-272	43	1
H20B	7525	8820	-107	43	1
H21A	5666	7570	49	37	1
H21B	4478	8433	-75	37	1
H22	6321	9690	222	29	1
H23A	10894	7703	1469	92	1
H23B	11063	8102	1240	92	1
H23C	9492	7986	1336	92	1
H7A	9912	10192	1344	73	1
H24A	-980	9883	403	180	1
H24B	91	10357	229	180	1
H24C	-1208	11393	293	180	1
H8	968	10755	525	124	1

Table 6. Hydrogen bonds [\AA and $^\circ$].

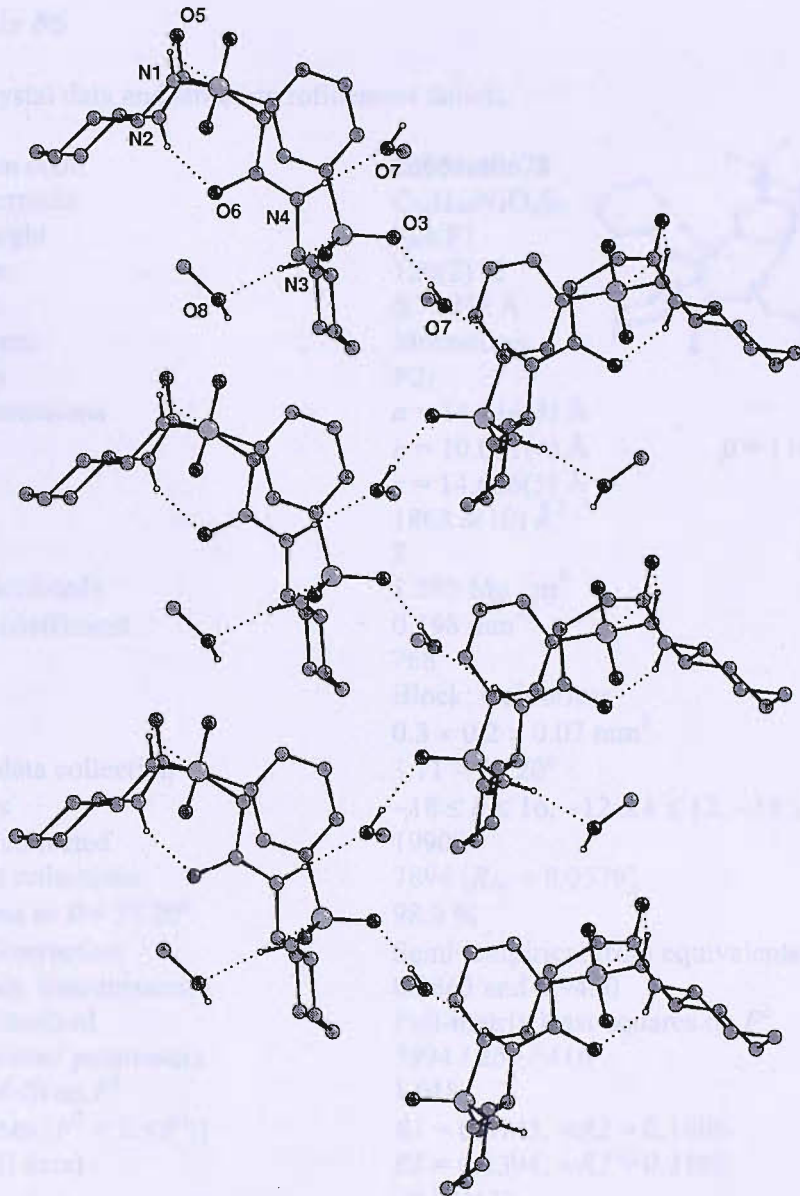
$D-H\cdots A$	$d(D-H)$	$d(H\cdots A)$	$d(D\cdots A)$	$\angle(DHA)$
N1-H1...O5	0.88	2.35	2.971(7)	127.7
N2-H2...O6	0.88	1.97	2.777(6)	151.8
N3-H3...O8 ⁱ	0.88	1.93	2.795(6)	166.6
N4-H4...O7 ⁱⁱ	0.88	2.02	2.886(6)	169.0
O7-H7A...O3	0.84	2.09	2.925(6)	176.1
O7-H7A...S2	0.84	2.93	3.684(4)	151.1

Symmetry transformations used to generate equivalent atoms:

(i) $x+1, y, z$ (ii) $x-1/2, -y+5/2, -z+1/4$



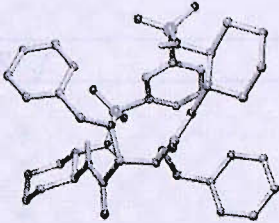
Thermal ellipsoids drawn at the 30% probability level, solvent not shown.



Part of a hydrogen bonded chain that extends along the *a* axis.

Macrocycle 86

Table 1. Crystal data and structure refinement details.

Identification code	2005sot0678		
Empirical formula	$C_{36}H_{44}N_4O_8S_2$		
Formula weight	724.87		
Temperature	120(2) K		
Wavelength	0.71073 Å		
Crystal system	Monoclinic		
Space group	$P2_1$		
Unit cell dimensions	$a = 14.114(3)$ Å $b = 10.081(4)$ Å $c = 14.606(5)$ Å		$\beta = 116.25(2)^\circ$
Volume	$1863.8(10)$ Å ³		
Z	2		
Density (calculated)	1.292 Mg / m ³		
Absorption coefficient	0.198 mm ⁻¹		
$F(000)$	768		
Crystal	Block; Colourless		
Crystal size	$0.3 \times 0.2 \times 0.07$ mm ³		
θ range for data collection	$3.11 - 27.20^\circ$		
Index ranges	$-18 \leq h \leq 16, -12 \leq k \leq 12, -18 \leq l \leq 18$		
Reflections collected	19908		
Independent reflections	7894 [$R_{int} = 0.0579$]		
Completeness to $\theta = 27.20^\circ$	98.9 %		
Absorption correction	Semi-empirical from equivalents		
Max. and min. transmission	0.9863 and 0.9430		
Refinement method	Full-matrix least-squares on F^2		
Data / restraints / parameters	7894 / 255 / 416		
Goodness-of-fit on F^2	1.018		
Final R indices [$F^2 > 2\sigma(F^2)$]	$R1 = 0.0743, wR2 = 0.1806$		
R indices (all data)	$R1 = 0.1394, wR2 = 0.2109$		
Absolute structure parameter	-0.02(11)		
Extinction coefficient	0.013(3)		
Largest diff. peak and hole	1.189 and -0.381 e Å ⁻³		

Diffraction: Nonius KappaCCD area detector (ϕ scans and ω scans to fill *asymmetric unit*). **Cell determination:** DirAx (Duisenberg, A.J.M.(1992). *J. Appl. Cryst.* 25, 92-96.) **Data collection:** Collect (Collect: Data collection software, R. Hooft, Nonius B.V., 1998). **Data reduction and cell refinement:** Denzo (Z. Otwinowski & W. Minor, *Methods in Enzymology* (1997) Vol. 276: *Macromolecular Crystallography*, part A, pp. 307-326; C. W. Carter, Jr. & R. M. Sweet, Eds., Academic Press). **Absorption correction:** Sheldrick, G. M. SADABS - Bruker Nonius area detector scaling and absorption correction - V2.10 **Structure solution:** SHELXS97 (G. M. Sheldrick, *Acta Cryst.* (1990) A46 467-473). **Structure refinement:** SHELXL97 (G. M. Sheldrick (1997), University of Göttingen, Germany). **Graphics:** Camcon - A Molecular Graphics Package. (D. M. Watkin, L. Pearce and C. K. Prout, Chemical Crystallography Laboratory, University of Oxford, 1993).

Special details: All hydrogen atoms were placed in idealised positions and refined using a riding model. One Ph group is disordered over 2 positions.

Table 2. Atomic coordinates [$\times 10^4$], equivalent isotropic displacement parameters [$\text{\AA}^2 \times 10^3$] and site occupancy factors. U_{eq} is defined as one third of the trace of the orthogonalized U^{ij} tensor.

Atom	x	y	z	U_{eq}	<i>S.o.f.</i>
C1	1192(4)	4104(5)	6234(3)	43(1)	1
C2	814(4)	5008(6)	6718(4)	53(1)	1
C3	1520(5)	5849(7)	7469(4)	63(2)	1
C4	2573(5)	5817(7)	7699(4)	58(2)	1
C5	2934(4)	4925(5)	7218(4)	47(1)	1
C6	2261(4)	4058(5)	6489(3)	41(1)	1
C7	5695(4)	3105(5)	8216(3)	42(1)	1
C8	6727(4)	3831(6)	8514(4)	52(1)	1
C9	7590(5)	2913(7)	8538(5)	66(2)	1
C10	7732(5)	1748(7)	9207(5)	72(2)	1
C11	6693(5)	989(7)	8873(5)	68(2)	1
C12	5831(4)	1904(5)	8874(4)	46(1)	1
C13	4502(4)	449(5)	9038(4)	45(1)	1
C14	3377(4)	-74(5)	8457(3)	41(1)	1
C15	3249(4)	-941(5)	6901(4)	46(1)	1
C16	3532(4)	-385(5)	6094(4)	43(1)	1
C17	2939(6)	620(7)	5461(5)	75(2)	1
C18	3165(7)	1125(8)	4698(6)	95(3)	1
C19	4014(8)	595(9)	4605(7)	106(3)	1
C20	4585(5)	-447(8)	5196(6)	75(2)	1
C21	4328(4)	-917(6)	5928(4)	57(2)	1
C22	2676(4)	680(5)	8817(4)	38(1)	1
C23	3101(4)	2865(5)	9572(4)	51(1)	1
C24A	2405(7)	2783(12)	10139(8)	66(1)	0.50
C25A	1352(8)	3175(11)	9674(6)	66(1)	0.50
C26A	746(5)	3099(10)	10206(6)	66(1)	0.50
C27A	1193(6)	2632(10)	11205(6)	66(1)	0.50
C28A	2246(7)	2241(9)	11671(5)	66(1)	0.50
C29A	2852(5)	2317(11)	11138(7)	66(1)	0.50
C24B	2319(7)	2935(12)	9996(8)	66(1)	0.50
C25B	1383(8)	3608(10)	9416(7)	66(1)	0.50
C26B	581(6)	3628(9)	9723(6)	66(1)	0.50
C27B	714(6)	2976(9)	10610(7)	66(1)	0.50
C28B	1650(7)	2304(9)	11191(6)	66(1)	0.50
C29B	2452(5)	2283(10)	10884(7)	66(1)	0.50
C30	1549(4)	159(5)	8260(3)	44(1)	1
C31	-246(4)	750(5)	6994(4)	40(1)	1
C32	-953(4)	687(6)	7536(4)	47(1)	1
C33	-2072(4)	389(6)	6805(4)	54(2)	1
C34	-2522(4)	1365(6)	5940(4)	54(1)	1
C35	-1816(4)	1487(6)	5398(4)	45(1)	1
C36	-676(4)	1781(5)	6155(4)	41(1)	1

N1	10(3)	1815(4)	5627(3)	40(1)	1
N2	4884(3)	3959(4)	8266(3)	45(1)	1
N3	4822(3)	1192(4)	8487(3)	45(1)	1
N4	844(3)	1056(4)	7685(3)	41(1)	1
O1	-642(3)	3944(3)	4734(2)	43(1)	1
O2	837(2)	2751(3)	4627(2)	40(1)	1
O3	4292(3)	4577(5)	6478(3)	70(1)	1
O4	4619(3)	6334(4)	7726(4)	84(2)	1
O5	5035(3)	203(4)	9955(3)	58(1)	1
O6	2968(3)	114(4)	7400(2)	48(1)	1
O7	2727(3)	2059(3)	8651(2)	46(1)	1
O8	1355(3)	-1020(4)	8328(3)	55(1)	1
S1	295(1)	3148(1)	5201(1)	37(1)	1
S2	4261(1)	5030(1)	7383(1)	55(1)	1

Table 3. Bond lengths [Å] and angles [°].

C1–C6	1.386(7)	C23–O7	1.456(6)
C1–C2	1.395(7)	C23–C24B	1.488(6)
C1–S1	1.766(5)	C23–C24A	1.542(6)
C2–C3	1.396(8)	C24A–C25A	1.3900
C3–C4	1.371(8)	C24A–C29A	1.3900
C4–C5	1.372(8)	C25A–C26A	1.3900
C5–C6	1.380(7)	C26A–C27A	1.3900
C5–S2	1.783(6)	C27A–C28A	1.3900
C7–N2	1.459(7)	C28A–C29A	1.3900
C7–C12	1.504(7)	C24B–C25B	1.3900
C7–C8	1.512(8)	C24B–C29B	1.3900
C8–C9	1.518(8)	C25B–C26B	1.3900
C9–C10	1.483(9)	C26B–C27B	1.3900
C10–C11	1.531(10)	C27B–C28B	1.3900
C11–C12	1.527(8)	C28B–C29B	1.3900
C12–N3	1.466(7)	C30–O8	1.233(6)
C13–O5	1.237(6)	C30–N4	1.332(6)
C13–N3	1.318(6)	C31–N4	1.452(6)
C13–C14	1.525(7)	C31–C36	1.514(7)
C14–O6	1.402(5)	C31–C32	1.524(7)
C14–C22	1.514(7)	C32–C33	1.494(7)
C15–O6	1.440(6)	C33–C34	1.503(8)
C15–C16	1.510(7)	C34–C35	1.529(7)
C16–C21	1.360(7)	C35–C36	1.524(7)
C16–C17	1.377(8)	C36–N1	1.480(6)
C17–C18	1.384(9)	N1–S1	1.605(4)
C18–C19	1.373(11)	N2–S2	1.612(4)
C19–C20	1.372(11)	O1–S1	1.435(3)
C20–C21	1.358(9)	O2–S1	1.420(3)
C22–O7	1.418(6)	O3–S2	1.417(4)
C22–C30	1.524(7)	O4–S2	1.418(4)

C6-C1-C2	120.0(5)	C27A-C26A-C25A	120.0
C6-C1-S1	119.7(4)	C26A-C27A-C28A	120.0
C2-C1-S1	119.9(4)	C27A-C28A-C29A	120.0
C1-C2-C3	119.6(5)	C28A-C29A-C24A	120.0
C4-C3-C2	119.9(6)	C25B-C24B-C29B	120.0
C3-C4-C5	119.9(6)	C25B-C24B-C23	116.7(7)
C4-C5-C6	121.7(5)	C29B-C24B-C23	123.1(7)
C4-C5-S2	119.9(4)	C26B-C25B-C24B	120.0
C6-C5-S2	117.8(4)	C27B-C26B-C25B	120.0
C5-C6-C1	118.8(5)	C26B-C27B-C28B	120.0
N2-C7-C12	109.0(4)	C29B-C28B-C27B	120.0
N2-C7-C8	112.1(4)	C28B-C29B-C24B	120.0
C12-C7-C8	111.8(4)	O8-C30-N4	125.0(5)
C7-C8-C9	111.9(5)	O8-C30-C22	120.4(4)
C10-C9-C8	111.8(5)	N4-C30-C22	114.5(5)
C9-C10-C11	110.8(5)	N4-C31-C36	109.8(4)
C12-C11-C10	110.5(6)	N4-C31-C32	112.6(4)
N3-C12-C7	108.7(4)	C36-C31-C32	109.2(4)
N3-C12-C11	110.0(5)	C33-C32-C31	111.4(4)
C7-C12-C11	111.3(4)	C32-C33-C34	112.9(4)
O5-C13-N3	124.5(5)	C33-C34-C35	111.0(4)
O5-C13-C14	121.2(4)	C36-C35-C34	111.1(4)
N3-C13-C14	114.2(4)	N1-C36-C31	108.5(4)
O6-C14-C22	107.4(4)	N1-C36-C35	110.5(4)
O6-C14-C13	112.8(4)	C31-C36-C35	111.7(4)
C22-C14-C13	108.2(4)	C36-N1-S1	123.7(3)
O6-C15-C16	110.4(4)	C7-N2-S2	121.2(3)
C21-C16-C17	118.3(5)	C13-N3-C12	125.4(4)
C21-C16-C15	121.1(5)	C30-N4-C31	124.1(4)
C17-C16-C15	120.4(5)	C14-O6-C15	112.7(4)
C16-C17-C18	121.6(6)	C22-O7-C23	114.5(4)
C19-C18-C17	117.3(7)	O2-S1-O1	120.06(19)
C20-C19-C18	122.1(7)	O2-S1-N1	106.6(2)
C21-C20-C19	118.4(6)	O1-S1-N1	108.4(2)
C20-C21-C16	122.1(6)	O2-S1-C1	106.8(2)
O7-C22-C14	110.1(4)	O1-S1-C1	105.2(2)
O7-C22-C30	111.5(4)	N1-S1-C1	109.5(2)
C14-C22-C30	109.2(4)	O3-S2-O4	118.4(3)
O7-C23-C24B	112.2(6)	O3-S2-N2	107.5(2)
O7-C23-C24A	114.2(6)	O4-S2-N2	110.8(3)
C25A-C24A-C29A	120.0	O3-S2-C5	108.6(2)
C25A-C24A-C23	121.3(7)	O4-S2-C5	106.9(3)
C29A-C24A-C23	118.7(7)	N2-S2-C5	103.7(2)
C26A-C25A-C24A	120.0		

Table 4. Anisotropic displacement parameters [$\text{\AA}^2 \times 10^3$]. The anisotropic displacement factor exponent takes the form: $-2\pi^2[h^2 a^{*2} U^{11} + \dots + 2 h k a^* b^* U^{12}]$.

Atom	U^{11}	U^{22}	U^{33}	U^{23}	U^{13}	U^{12}
C1	66(3)	29(3)	36(3)	2(2)	24(2)	-5(2)
C2	70(3)	47(3)	52(3)	-9(3)	36(3)	-8(3)
C3	88(5)	55(4)	60(4)	-19(3)	44(3)	-10(3)
C4	70(4)	53(4)	44(3)	1(3)	18(3)	-11(3)
C5	57(3)	37(3)	36(3)	10(2)	11(2)	-4(3)
C6	52(3)	30(3)	38(3)	12(2)	18(2)	2(2)
C7	66(3)	32(3)	31(2)	0(2)	26(2)	3(3)
C8	73(3)	41(3)	46(3)	-5(2)	30(3)	3(3)
C9	86(4)	65(4)	64(4)	-1(3)	50(3)	7(3)
C10	72(4)	86(5)	69(4)	11(4)	39(3)	17(4)
C11	91(5)	55(4)	78(4)	25(3)	55(4)	24(4)
C12	69(3)	43(3)	32(3)	1(2)	29(2)	13(3)
C13	60(3)	41(3)	36(3)	4(2)	24(3)	8(2)
C14	65(3)	29(3)	31(2)	15(2)	22(2)	11(2)
C15	66(3)	30(3)	42(3)	-4(2)	24(2)	4(3)
C16	56(3)	34(3)	41(3)	-2(2)	24(2)	-3(2)
C17	94(5)	67(4)	92(5)	20(4)	67(4)	30(4)
C18	153(7)	86(6)	82(5)	36(4)	84(5)	34(5)
C19	161(8)	80(6)	141(7)	27(5)	126(7)	13(6)
C20	78(4)	77(5)	90(5)	-1(4)	57(4)	8(4)
C21	65(3)	54(4)	63(4)	1(3)	38(3)	11(3)
C22	54(3)	29(3)	29(2)	4(2)	16(2)	2(2)
C23	57(3)	38(3)	52(3)	-8(2)	20(3)	-4(3)
C24A	80(2)	57(2)	70(3)	-23(2)	43(2)	-9(2)
C25A	80(2)	57(2)	70(3)	-23(2)	43(2)	-9(2)
C26A	80(2)	57(2)	70(3)	-23(2)	43(2)	-9(2)
C27A	80(2)	57(2)	70(3)	-23(2)	43(2)	-9(2)
C28A	80(2)	57(2)	70(3)	-23(2)	43(2)	-9(2)
C29A	80(2)	57(2)	70(3)	-23(2)	43(2)	-9(2)
C24B	80(2)	57(2)	70(3)	-23(2)	43(2)	-9(2)
C25B	80(2)	57(2)	70(3)	-23(2)	43(2)	-9(2)
C26B	80(2)	57(2)	70(3)	-23(2)	43(2)	-9(2)
C27B	80(2)	57(2)	70(3)	-23(2)	43(2)	-9(2)
C28B	80(2)	57(2)	70(3)	-23(2)	43(2)	-9(2)
C29B	80(2)	57(2)	70(3)	-23(2)	43(2)	-9(2)
C30	69(3)	38(3)	30(2)	2(2)	26(2)	2(3)
C31	52(3)	30(3)	38(3)	-2(2)	20(2)	-2(2)
C32	61(3)	46(3)	43(3)	1(2)	32(3)	-1(3)
C33	71(4)	48(4)	60(3)	-7(3)	45(3)	-12(3)
C34	57(3)	59(4)	54(3)	-10(3)	32(3)	-8(3)
C35	55(3)	47(3)	36(3)	0(2)	22(2)	3(3)
C36	52(3)	35(3)	40(3)	-4(2)	25(2)	-1(2)

N1	64(3)	29(2)	36(2)	4(2)	29(2)	3(2)
N2	63(3)	40(2)	33(2)	5(2)	22(2)	8(2)
N3	64(3)	40(3)	29(2)	8(2)	19(2)	3(2)
N4	63(3)	27(2)	37(2)	0(2)	25(2)	4(2)
O1	51(2)	32(2)	43(2)	10(2)	19(2)	5(2)
O2	56(2)	37(2)	36(2)	6(1)	27(2)	6(2)
O3	61(2)	109(4)	42(2)	32(2)	24(2)	5(2)
O4	61(2)	29(2)	137(4)	20(3)	22(3)	1(2)
O5	55(2)	78(3)	36(2)	26(2)	16(2)	9(2)
O6	75(2)	37(2)	34(2)	0(2)	25(2)	11(2)
O7	70(2)	32(2)	35(2)	0(2)	23(2)	4(2)
O8	84(3)	29(2)	47(2)	7(2)	24(2)	-3(2)
S1	48(1)	32(1)	33(1)	4(1)	19(1)	2(1)
S2	55(1)	45(1)	51(1)	21(1)	12(1)	-2(1)

Table 5. Hydrogen coordinates [$\times 10^4$] and isotropic displacement parameters [$\text{\AA}^2 \times 10^3$].

Atom	<i>x</i>	<i>y</i>	<i>z</i>	U_{eq}	<i>S.o.f.</i>
H2	80	5051	6537	63	1
H3	1272	6442	7820	76	1
H4	3051	6413	8191	70	1
H6	2526	3442	6167	50	1
H7	5437	2797	7495	50	1
H8A	6953	4235	9196	62	1
H8B	6619	4555	8020	62	1
H9A	7408	2603	7836	79	1
H9B	8263	3410	8787	79	1
H10A	7983	2049	9921	87	1
H10B	8275	1152	9177	87	1
H11A	6472	624	8180	82	1
H11B	6797	238	9345	82	1
H12	6030	2200	9589	55	1
H14	3362	-1040	8606	49	1
H15A	2649	-1563	6583	55	1
H15B	3859	-1438	7412	55	1
H17	2362	975	5549	90	1
H18	2750	1811	4258	114	1
H19	4212	961	4116	127	1
H20	5147	-830	5095	89	1
H21	4718	-1641	6339	69	1
H22	2936	523	9565	46	1
H23A	3138	3802	9386	61	1
H23B	3827	2581	10042	61	1
H25A	1047	3494	8991	79	0.50
H26A	27	3366	9888	79	0.50
H27A	778	2581	11569	79	0.50
H28A	2551	1922	12353	79	0.50
H29A	3571	2049	11456	79	0.50

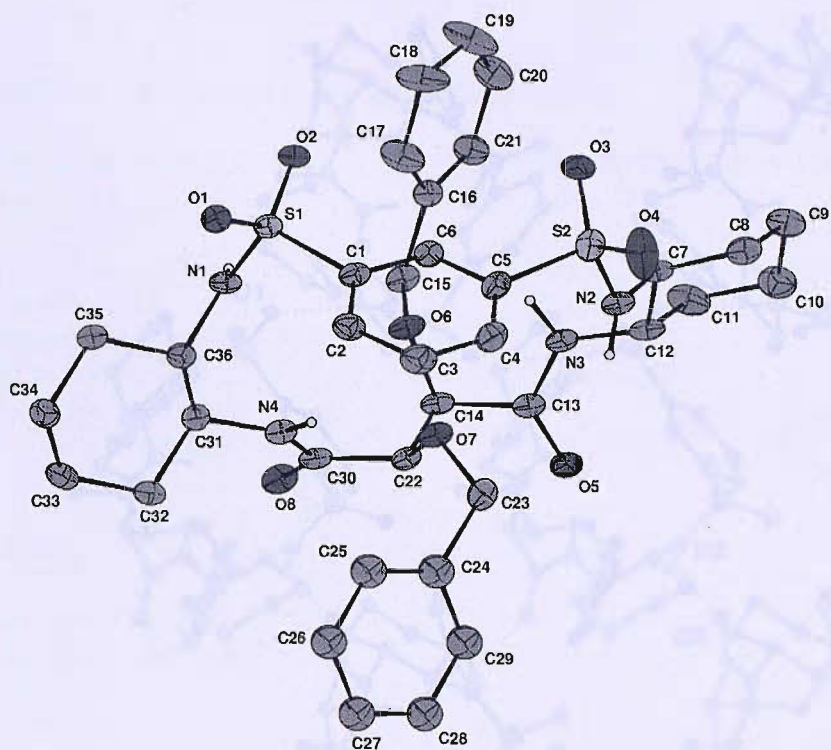
H25B	1292	4054	8809	79	0.50
H26B	-58	4088	9326	79	0.50
H27B	166	2991	10820	79	0.50
H28B	1741	1858	11797	79	0.50
H29B	3092	1823	11281	79	0.50
H31	-266	-134	6675	48	1
H32A	-688	-9	8069	56	1
H32B	-924	1547	7875	56	1
H33A	-2510	394	7179	64	1
H33B	-2108	-512	6522	64	1
H34A	-2591	2244	6208	65	1
H34B	-3236	1072	5446	65	1
H35A	-1842	650	5033	54	1
H35B	-2083	2209	4886	54	1
H36	-650	2668	6471	49	1
H1	276	1062	5543	48	1
H2A	4732	3888	8787	54	1
H3A	4396	1265	7831	54	1
H4A	1052	1886	7727	50	1

Table 6. Hydrogen bonds [\AA and $^\circ$].

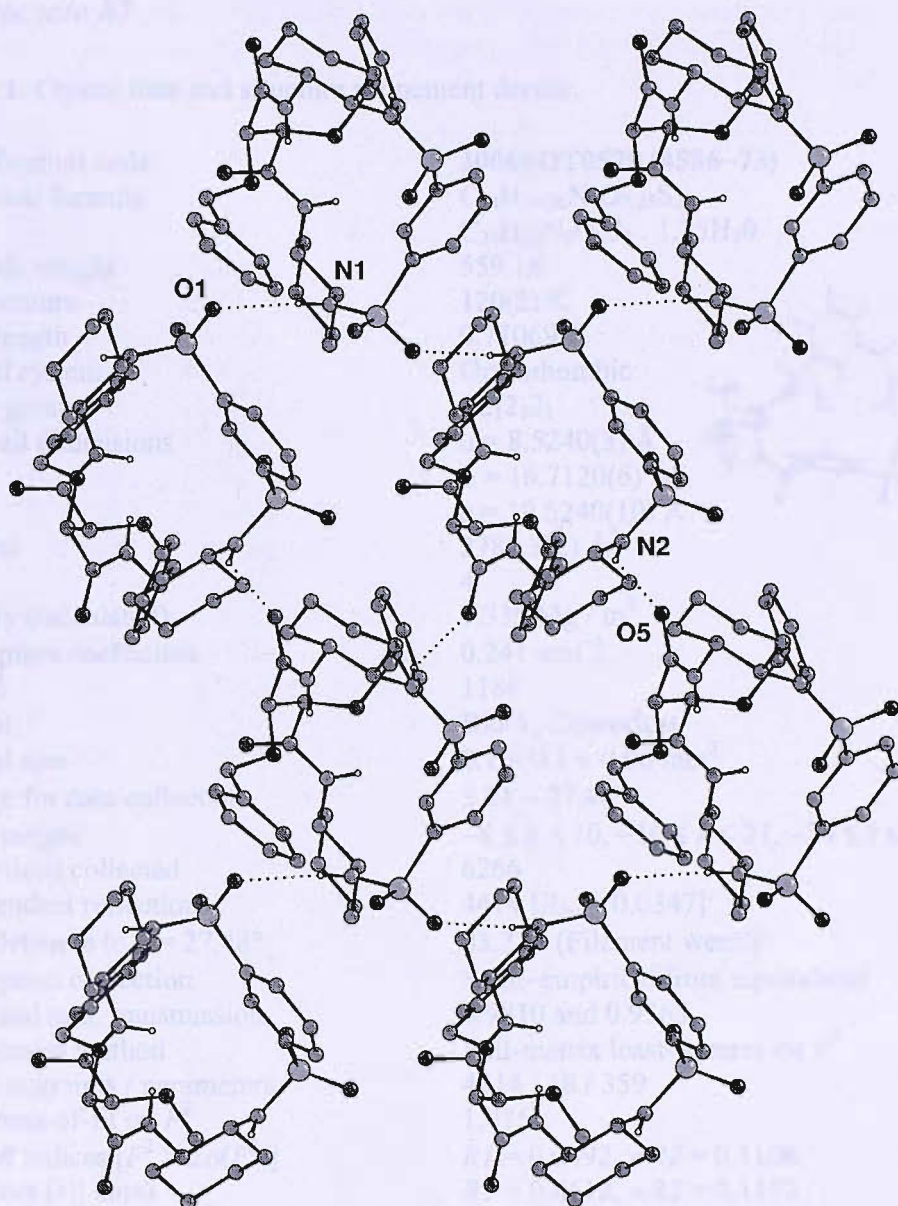
$D-H\cdots A$	$d(D-H)$	$d(H\cdots A)$	$d(D\cdots A)$	$\angle(DHA)$
N1-H1...O1 ⁱ	0.88	2.28	3.142(5)	168.4
N2-H2A...O5 ⁱⁱ	0.88	2.17	2.842(5)	132.8

Symmetry transformations used to generate equivalent atoms:

(i) $-x, y-1/2, -z+1$ (ii) $-x+1, y+1/2, -z+2$



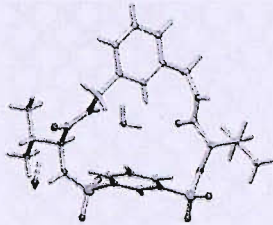
Thermal ellipsoids drawn at the 30% probability level, non acidic hydrogens omitted for clarity.



Part of one of the hydrogen bonded sheets that form in the $1\ 0\ -1$ plane.

Macrocycle 87

Table 1. Crystal data and structure refinement details.

Identification code	2006SOT0579 (4586-73)	
Empirical formula	$C_{24}H_{34.50}N_4O_{7.25}S_2$ $C_{24}H_{32}N_4O_6S_2 \cdot 1.25H_2O$	
Formula weight	559.18	
Temperature	120(2) K	
Wavelength	0.71069 Å	
Crystal system	Orthorhombic	
Space group	$P2_12_12_1$	
Unit cell dimensions	$a = 8.5240(3)$ Å $b = 16.7120(6)$ Å $c = 19.5240(10)$ Å	
Volume	$2781.3(2)$ Å ³	
Z	4	
Density (calculated)	1.335 Mg / m ³	
Absorption coefficient	0.241 mm ⁻¹	
$F(000)$	1186	
Crystal	Block; Colourless	
Crystal size	$0.1 \times 0.1 \times 0.06$ mm ³	
θ range for data collection	$3.21 - 27.48^\circ$	
Index ranges	$-8 \leq h \leq 10, -16 \leq k \leq 21, -24 \leq l \leq 9$	
Reflections collected	6266	
Independent reflections	4414 [$R_{int} = 0.0347$]	
Completeness to $\theta = 27.48^\circ$	83.2 % (Filament went!)	
Absorption correction	Semi-empirical from equivalents	
Max. and min. transmission	0.9810 and 0.9763	
Refinement method	Full-matrix least-squares on F^2	
Data / restraints / parameters	4414 / 18 / 359	
Goodness-of-fit on F^2	1.075	
Final R indices [$F^2 > 2\sigma(F^2)$]	$RI = 0.0492, wR2 = 0.1106$	
R indices (all data)	$RI = 0.0612, wR2 = 0.1192$	
Absolute structure parameter	-0.11(9)	
Largest diff. peak and hole	0.328 and -0.386 e Å ⁻³	

Diffraction: Nonius KappaCCD area detector (ϕ scans and ω scans to fill asymmetric unit). **Cell determination:** DirAx (Duisenberg, A.J.M.(1992). *J. Appl. Cryst.* 25, 92-96.) **Data collection:** Collect (Collect: Data collection software, R. Hooft, Nonius B.V., 1998). **Data reduction and cell refinement:** Denzo (Z. Otwinowski & W. Minor, *Methods in Enzymology* (1997) Vol. 276: *Macromolecular Crystallography*, part A, pp. 307-326; C. W. Carter, Jr. & R. M. Sweet, Eds., Academic Press). **Absorption correction:** Sheldrick, G. M. SADABS - Bruker Nonius area detector scaling and absorption correction - V2.10 **Structure solution:** SHELXS97 (G. M. Sheldrick, *Acta Cryst.* (1990) A46 467-473). **Structure refinement:** SHELXL97 (G. M. Sheldrick (1997), University of Göttingen, Germany). **Graphics:** Cameron - A Molecular Graphics Package. (D. M. Watkin, L. Pearce and C. K. Prout, Chemical Crystallography Laboratory, University of Oxford, 1993).

Special details: All hydrogen atoms were placed in idealised positions and refined using a riding model.

Table 2. Atomic coordinates [$\times 10^4$], equivalent isotropic displacement parameters [$\text{\AA}^2 \times 10^3$] and site occupancy factors. U_{eq} is defined as one third of the trace of the orthogonalized U^{ij} tensor.

Atom	x	y	z	U_{eq}	$S.o.f.$
C1	9636(4)	7497(2)	9323(2)	22(1)	1
C2	11008(4)	7435(2)	8950(2)	23(1)	1
C3	11493(4)	6685(2)	8720(2)	25(1)	1
C4	10631(4)	6009(2)	8875(2)	23(1)	1
C5	9249(4)	6090(2)	9251(2)	21(1)	1
C6	8730(4)	6831(2)	9481(2)	23(1)	1
C7	6492(4)	4932(2)	8342(2)	24(1)	1
C8	6094(4)	5616(2)	7844(2)	23(1)	1
C9	5921(5)	5986(2)	6637(3)	28(1)	1
C10	7082(4)	6612(2)	6390(2)	25(1)	1
C11	7132(5)	6794(2)	5703(3)	29(1)	1
C12	8117(5)	7399(2)	5463(3)	36(1)	1
C13	9038(5)	7818(2)	5926(3)	32(1)	1
C14	9014(5)	7636(2)	6619(2)	26(1)	1
C15	8036(4)	7024(2)	6851(2)	24(1)	1
N4	9209(4)	8503(2)	7645(2)	25(1)	1
C17	9970(4)	9035(2)	8036(2)	24(1)	1
C18	9064(4)	9422(2)	8621(2)	23(1)	1
C19	5264(5)	4250(2)	8278(3)	30(1)	1
C20	3652(4)	4540(2)	8496(3)	33(1)	1
C21	5737(5)	3527(2)	8704(3)	40(1)	1
C22	9197(4)	10345(2)	8606(2)	26(1)	1
C23	8573(6)	10661(2)	7932(3)	39(1)	1
C24	8361(6)	10719(2)	9222(3)	39(1)	1
N1	9721(4)	9133(2)	9266(2)	24(1)	1
N2	6556(3)	5227(2)	9045(2)	24(1)	1
N3	6466(4)	5483(2)	7198(2)	25(1)	1
C16	10070(5)	8083(2)	7112(3)	32(1)	1
O1	9738(3)	8448(1)	10357(2)	26(1)	1
O2	7331(3)	8430(1)	9644(2)	26(1)	1
O3	7692(3)	5349(1)	10187(2)	25(1)	1
O4	9052(3)	4546(1)	9303(2)	29(1)	1
O5	5400(3)	6222(1)	8060(2)	32(1)	1
O6	11367(3)	9195(1)	7943(2)	31(1)	1
S1	9013(1)	8410(1)	9698(1)	22(1)	1
S2	8146(1)	5234(1)	9485(1)	23(1)	1
O7	6193(4)	7906(2)	8203(3)	55(1)	1
O8	4816(15)	8984(7)	8895(9)	45(3)	0.25

Table 3. Bond lengths [Å] and angles [°].

C1–C2	1.381(5)	C6–C5–C4	121.7(3)
C1–C6	1.389(4)	C6–C5–S2	117.9(3)
C1–S1	1.774(4)	C4–C5–S2	120.4(3)
C2–C3	1.394(5)	C1–C6–C5	117.8(3)
C3–C4	1.382(5)	N2–C7–C8	110.6(3)
C4–C5	1.395(5)	N2–C7–C19	110.5(3)
C5–C6	1.390(5)	C8–C7–C19	110.2(3)
C5–S2	1.771(3)	O5–C8–N3	125.0(4)
C7–N2	1.458(6)	O5–C8–C7	119.7(4)
C7–C8	1.538(5)	N3–C8–C7	115.2(3)
C7–C19	1.553(5)	N3–C9–C10	115.4(3)
C8–O5	1.247(4)	C11–C10–C15	120.1(4)
C8–N3	1.319(6)	C11–C10–C9	118.8(4)
C9–N3	1.457(5)	C15–C10–C9	121.0(4)
C9–C10	1.519(5)	C10–C11–C12	120.4(4)
C10–C11	1.375(6)	C13–C12–C11	119.1(5)
C10–C15	1.395(6)	C14–C13–C12	121.2(4)
C11–C12	1.395(6)	C13–C14–C15	119.1(4)
C12–C13	1.388(7)	C13–C14–C16	120.2(4)
C13–C14	1.387(7)	C15–C14–C16	120.7(4)
C14–C15	1.394(5)	C14–C15–C10	120.1(4)
C14–C16	1.514(6)	C17–N4–C16	118.9(3)
N4–C17	1.339(5)	O6–C17–N4	121.8(4)
N4–C16	1.455(5)	O6–C17–C18	120.5(4)
C17–O6	1.234(4)	N4–C17–C18	117.6(3)
C17–C18	1.523(6)	N1–C18–C17	108.1(3)
C18–N1	1.461(5)	N1–C18–C22	108.6(3)
C18–C22	1.547(4)	C17–C18–C22	111.8(3)
C19–C20	1.518(5)	C20–C19–C21	109.9(4)
C19–C21	1.522(6)	C20–C19–C7	110.6(3)
C22–C23	1.514(6)	C21–C19–C7	111.1(4)
C22–C24	1.532(7)	C23–C22–C24	112.1(3)
N1–S1	1.591(3)	C23–C22–C18	109.9(3)
N2–S2	1.605(3)	C24–C22–C18	110.9(3)
O1–S1	1.429(3)	C18–N1–S1	124.2(2)
O2–S1	1.438(2)	C7–N2–S2	122.6(2)
O3–S2	1.436(3)	C8–N3–C9	123.0(3)
O4–S2	1.431(2)	N4–C16–C14	113.1(3)
		O1–S1–O2	119.73(19)
C2–C1–C6	121.8(3)	O1–S1–N1	106.17(17)
C2–C1–S1	122.4(2)	O2–S1–N1	108.79(17)
C6–C1–S1	115.5(3)	O1–S1–C1	106.29(17)
C1–C2–C3	119.2(3)	O2–S1–C1	106.77(16)
C4–C3–C2	120.5(4)	N1–S1–C1	108.72(18)
C3–C4–C5	119.0(3)	O4–S2–O3	119.40(17)

O4–S2–N2	108.41(17)	O3–S2–C5	106.31(18)
O3–S2–N2	106.55(17)	N2–S2–C5	108.43(17)
O4–S2–C5	107.33(16)		

Table 4. Anisotropic displacement parameters [$\text{\AA}^2 \times 10^3$]. The anisotropic displacement factor exponent takes the form: $-2\pi^2[h^2 a^{*2} U^{11} + \dots + 2 h k a^* b^* U^{12}]$.

Atom	U^{11}	U^{22}	U^{33}	U^{23}	U^{13}	U^{12}
C1	22(2)	22(2)	21(3)	2(1)	0(2)	0(1)
C2	20(2)	28(2)	21(3)	2(2)	-1(2)	-1(1)
C3	24(2)	34(2)	18(3)	2(2)	3(2)	2(2)
C4	28(2)	23(2)	18(3)	-3(1)	0(2)	3(1)
C5	21(2)	24(2)	19(3)	0(1)	-3(2)	-2(1)
C6	22(2)	23(2)	23(3)	4(2)	1(2)	0(1)
C7	27(2)	20(2)	27(3)	-4(1)	7(2)	0(1)
C8	23(2)	23(2)	24(3)	2(2)	3(2)	-3(1)
C9	29(2)	29(2)	25(3)	1(2)	-3(2)	1(2)
C10	26(2)	18(2)	30(3)	-3(2)	-4(2)	4(1)
C11	43(2)	19(2)	26(3)	-5(1)	-9(2)	5(2)
C12	63(3)	28(2)	17(3)	2(2)	3(2)	0(2)
C13	52(2)	21(2)	25(3)	-1(2)	12(2)	-1(2)
C14	32(2)	22(2)	25(3)	-4(2)	6(2)	3(2)
C15	29(2)	25(2)	19(3)	-2(1)	3(2)	2(2)
N4	29(2)	22(1)	25(2)	-6(1)	5(2)	-6(1)
C17	27(2)	18(2)	27(3)	2(2)	-2(2)	-3(1)
C18	24(2)	21(2)	23(3)	1(1)	-3(2)	-7(1)
C19	38(2)	26(2)	25(3)	-1(2)	6(2)	-14(2)
C20	29(2)	35(2)	36(3)	7(2)	-4(2)	-10(2)
C21	40(2)	26(2)	53(4)	7(2)	14(2)	-6(2)
C22	33(2)	23(2)	23(3)	2(2)	-3(2)	0(2)
C23	58(3)	34(2)	24(3)	5(2)	-9(2)	6(2)
C24	57(3)	29(2)	31(3)	-6(2)	4(2)	8(2)
N1	29(2)	20(1)	24(2)	0(1)	-5(2)	-10(1)
N2	22(1)	25(1)	27(2)	-1(1)	6(1)	3(1)
N3	28(2)	19(1)	30(3)	-1(1)	4(2)	-1(1)
C16	32(2)	31(2)	33(3)	-7(2)	3(2)	-5(2)
O1	37(1)	26(1)	16(2)	2(1)	-6(1)	-6(1)
O2	26(1)	23(1)	28(2)	-2(1)	5(1)	0(1)
O3	30(1)	24(1)	19(2)	3(1)	2(1)	1(1)
O4	30(1)	20(1)	37(2)	0(1)	5(1)	4(1)
O5	38(1)	21(1)	36(2)	-1(1)	7(1)	6(1)
O6	27(1)	32(1)	35(2)	-4(1)	9(1)	-8(1)
S1	27(1)	19(1)	19(1)	-1(1)	2(1)	-5(1)
S2	24(1)	18(1)	28(1)	1(1)	2(1)	1(1)
O7	45(2)	40(2)	80(3)	-5(2)	7(2)	-10(1)
O8	46(5)	44(4)	44(6)	-2(4)	11(4)	9(4)

Table 5. Hydrogen coordinates [$\times 10^4$] and isotropic displacement parameters [$\text{\AA}^2 \times 10^3$].

Atom	<i>x</i>	<i>y</i>	<i>z</i>	<i>U</i> _{eq}	<i>S.o.f.</i>
H2	11613	7898	8851	27	1
H3	12424	6639	8456	30	1
H4	10973	5496	8726	28	1
H6	7788	6881	9737	27	1
H7	7546	4713	8218	29	1
H9A	4951	6263	6786	33	1
H9B	5642	5637	6246	33	1
H11	6491	6506	5390	35	1
H12	8157	7522	4988	44	1
H13	9697	8236	5766	39	1
H15	8019	6888	7323	29	1
H4A	8204	8410	7710	31	1
H18	7934	9264	8591	27	1
H19	5208	4083	7786	36	1
H20A	2880	4115	8419	50	1
H20B	3364	5013	8226	50	1
H20C	3672	4680	8983	50	1
H21A	5812	3682	9187	59	1
H21B	6756	3327	8547	59	1
H21C	4946	3105	8653	59	1
H22	10334	10488	8635	32	1
H23A	7467	10512	7883	58	1
H23B	9178	10431	7553	58	1
H23C	8670	11246	7923	58	1
H24A	8512	11300	9216	59	1
H24B	8798	10498	9646	59	1
H24C	7237	10597	9199	59	1
H1	10562	9373	9427	29	1
H2A	5689	5408	9234	29	1
H3A	7070	5071	7102	30	1
H16A	10800	7698	7329	38	1
H16B	10706	8474	6852	38	1
H99	5880(50)	7398(11)	8240(20)	50	1
H98	6120(60)	7990(30)	7754(7)	50	1
H97	4460(190)	8950(100)	8470(30)	50	0.25
H96	3990(120)	9170(100)	9130(70)	50	0.25

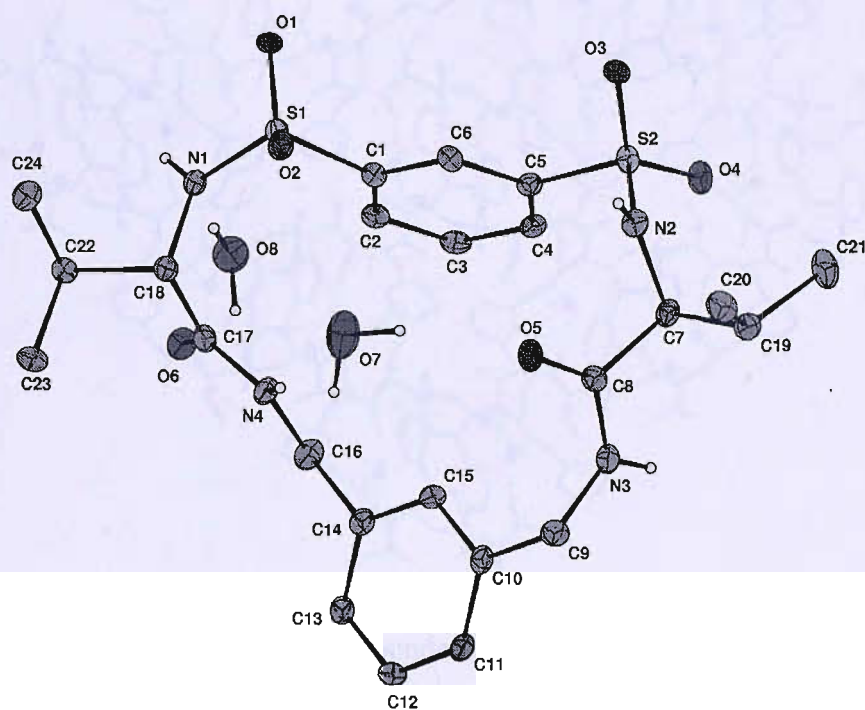
Table 6. Hydrogen bonds [\AA and $^\circ$].

<i>D</i> – <i>H</i> ⋯ <i>A</i>	<i>d</i> (<i>D</i> – <i>H</i>)	<i>d</i> (<i>H</i> ⋯ <i>A</i>)	<i>d</i> (<i>D</i> ⋯ <i>A</i>)	\angle (<i>DHA</i>)
N4–H4A⋯O7	0.88	2.14	2.965(5)	156.1
N1–H1⋯O3 ⁱ	0.88	2.02	2.881(4)	166.0
N2–H2A⋯O1 ⁱⁱ	0.88	2.22	2.945(4)	138.8

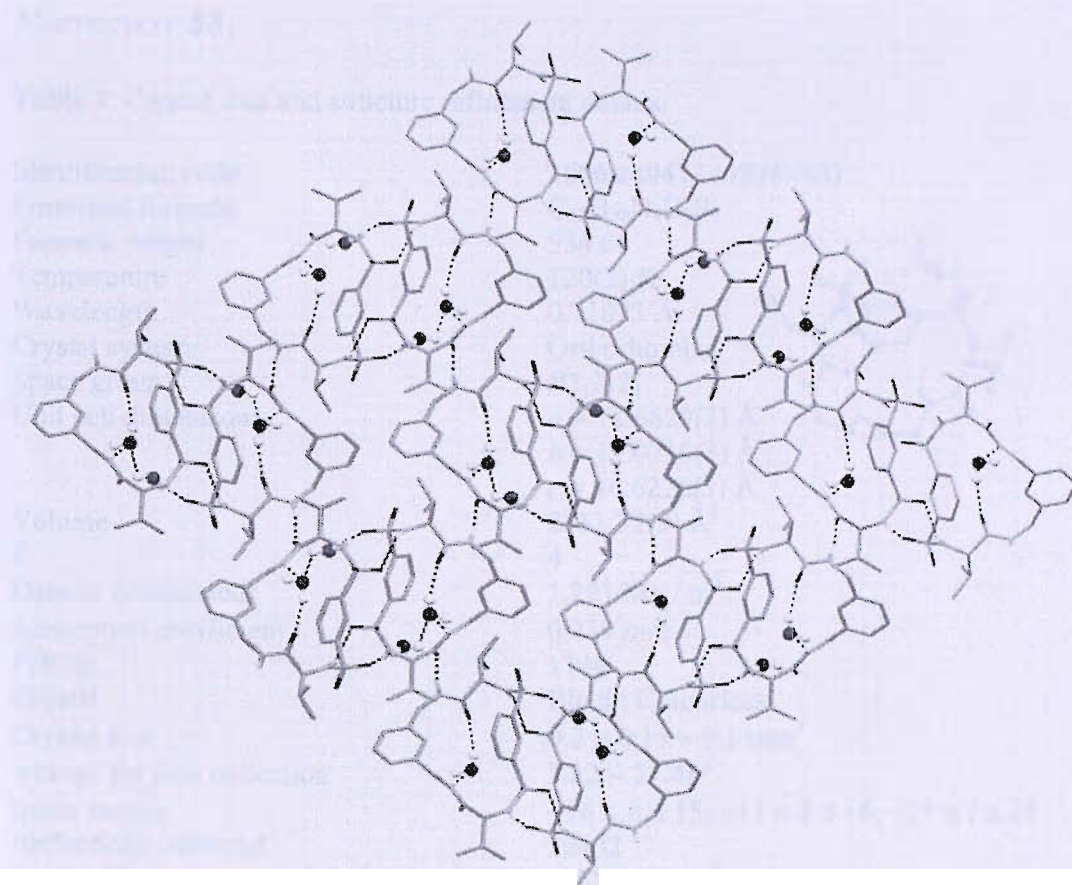
O8—H96...O3 ⁱⁱ	0.891(11)	1.92(4)	2.781(15)	163(15)
N3—H3A...O6 ⁱⁱⁱ	0.88	1.98	2.849(4)	168.7
O7—H99...O5	0.894(10)	2.039(19)	2.908(4)	164(4)

Symmetry transformations used to generate equivalent atoms:

(i) $x+1/2, -y+3/2, -z+2$ (ii) $x-1/2, -y+3/2, -z+2$ (iii) $-x+2, y-1/2, -z+3/2$



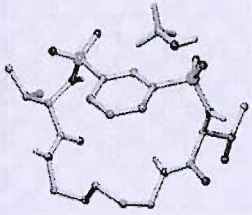
Thermal ellipsoids drawn at the 35% probability level, non-acidic hydrogens omitted for clarity



Part of the 3D hydrogen bonded network viewed down the a axis

Macrocycle 88

Table 1. Crystal data and structure refinement details.

Identification code	2006sot0477 (4586–43)	
Empirical formula	C ₂₂ H ₃₈ N ₄ O ₇ S ₂	
Formula weight	534.68	
Temperature	120(2) K	
Wavelength	0.71073 Å	
Crystal system	Orthorhombic	
Space group	P2 ₁ 2 ₁ 2 ₁	
Unit cell dimensions	<i>a</i> = 12.6629(2) Å <i>b</i> = 13.0710(3) Å <i>c</i> = 16.6226(3) Å	
Volume	2751.32(9) Å ³	
<i>Z</i>	4	
Density (calculated)	1.291 Mg / m ³	
Absorption coefficient	0.239 mm ⁻¹	
<i>F</i> (000)	1144	
Crystal	Block; Colourless	
Crystal size	0.2 × 0.15 × 0.1 mm ³	
θ range for data collection	3.22 – 27.48°	
Index ranges	–16 ≤ <i>h</i> ≤ 15, –13 ≤ <i>k</i> ≤ 16, –21 ≤ <i>l</i> ≤ 21	
Reflections collected	33432	
Independent reflections	6288 [<i>R</i> _{int} = 0.0581]	
Completeness to $\theta = 27.48^\circ$	99.7 %	
Absorption correction	Semi-empirical from equivalents	
Max. and min. transmission	0.9765 and 0.9437	
Refinement method	Full-matrix least-squares on <i>F</i> ²	
Data / restraints / parameters	6288 / 0 / 323	
Goodness-of-fit on <i>F</i> ²	1.035	
Final <i>R</i> indices [<i>F</i> ² > 2σ(<i>F</i> ²)]	<i>R</i> 1 = 0.0402, <i>wR</i> 2 = 0.0835	
<i>R</i> indices (all data)	<i>R</i> 1 = 0.0630, <i>wR</i> 2 = 0.0905	
Absolute structure parameter	–0.01(6)	
Extinction coefficient	0.0055(7)	
Largest diff. peak and hole	0.339 and –0.329 e Å ⁻³	

Diffraction: Nonius KappaCCD area detector (ϕ scans and ω scans to fill asymmetric unit). **Cell determination:** DirAx (Duisenberg, A.J.M.(1992). *J. Appl. Cryst.* 25, 92–96.) **Data collection:** Collect (Collect: Data collection software, R. Hoof, Nonius B.V., 1998). **Data reduction and cell refinement:** Denzo (Z. Otwinowski & W. Minor, *Methods in Enzymology* (1997) Vol. 276: *Macromolecular Crystallography*, part A, pp. 307–326; C. W. Carter, Jr. & R. M. Sweet, Eds., Academic Press). **Absorption correction:** Sheldrick, G. M. SADABS - Bruker Nonius area detector scaling and absorption correction - V2.10 **Structure solution:** SHELXS97 (G. M. Sheldrick, *Acta Cryst.* (1990) A46 467–473). **Structure refinement:** SHELXL97 (G. M. Sheldrick (1997), University of Göttingen, Germany). **Graphics:** Camcrn - A Molecular Graphics Package. (D. M. Watkin, L. Pearce and C. K. Prout, Chemical Crystallography Laboratory, University of Oxford, 1993).

Special details: All hydrogen atoms were placed in idealised positions and refined using a riding model.

Table 2. Atomic coordinates [$\times 10^4$], equivalent isotropic displacement parameters [$\text{\AA}^2 \times 10^3$] and site occupancy factors. U_{eq} is defined as one third of the trace of the orthogonalized U^{ij} tensor.

Atom	x	y	z	U_{eq}	<i>S.o.f.</i>
C1	5950(2)	3384(2)	8863(1)	17(1)	1
C2	5817(2)	2760(2)	9532(1)	18(1)	1
C3	6674(2)	2580(2)	10028(1)	20(1)	1
C4	7651(2)	3017(2)	9873(1)	23(1)	1
C5	7773(2)	3648(2)	9209(1)	25(1)	1
C6	6925(2)	3832(2)	8699(1)	23(1)	1
C7	6277(2)	3300(2)	11898(1)	22(1)	1
C8	5060(2)	2285(2)	12803(2)	40(1)	1
C9	5833(2)	3180(2)	12749(1)	28(1)	1
C10	5331(2)	4177(2)	13038(2)	41(1)	1
C11	7057(2)	4191(2)	11865(1)	22(1)	1
C12	7458(2)	5928(2)	11391(1)	27(1)	1
C13	8071(2)	6058(2)	10609(1)	29(1)	1
C14	7405(2)	6254(2)	9855(1)	30(1)	1
C15	6739(2)	7207(2)	9913(2)	31(1)	1
C16	6333(2)	7603(2)	9095(1)	27(1)	1
C17	5031(2)	6289(2)	8711(1)	21(1)	1
C18	4691(2)	5581(2)	8035(1)	19(1)	1
C19	2791(2)	6219(2)	7888(2)	40(1)	1
C20	3860(2)	6086(2)	7480(1)	26(1)	1
C21	3764(2)	5489(2)	6699(2)	38(1)	1
N1	6848(1)	2370(1)	11652(1)	20(1)	1
N2	6804(1)	4999(2)	11417(1)	24(1)	1
N3	5921(1)	6797(1)	8569(1)	21(1)	1
N4	4298(1)	4604(1)	8360(1)	20(1)	1
O1	4138(1)	2747(1)	8385(1)	21(1)	1
O2	5329(1)	3592(1)	7398(1)	22(1)	1
O3	5418(1)	1495(1)	10900(1)	27(1)	1
O4	7282(1)	934(1)	10778(1)	26(1)	1
O5	7877(1)	4136(1)	12268(1)	28(1)	1
O6	4504(1)	6382(1)	9333(1)	28(1)	1
S1	4879(1)	3544(1)	8186(1)	18(1)	1
S2	6519(1)	1739(1)	10858(1)	21(1)	1
O7	4835(1)	5031(2)	10558(1)	45(1)	1
C22	3818(2)	4855(3)	10887(2)	52(1)	1

Table 3. Bond lengths [\AA] and angles [$^\circ$].

C1–C2	1.388(3)	C3–C4	1.387(3)
C1–C6	1.395(3)	C3–S2	1.776(2)
C1–S1	1.774(2)	C4–C5	1.387(3)
C2–C3	1.383(3)	C5–C6	1.390(3)

C7–N1	1.472(3)	N1–C7–C9	110.59(18)
C7–C11	1.528(3)	C11–C7–C9	110.43(18)
C7–C9	1.531(3)	C8–C9–C10	111.62(19)
C8–C9	1.527(3)	C8–C9–C7	111.7(2)
C9–C10	1.528(3)	C10–C9–C7	110.9(2)
C11–O5	1.237(3)	O5–C11–N2	123.4(2)
C11–N2	1.332(3)	O5–C11–C7	118.6(2)
C12–N2	1.471(3)	N2–C11–C7	117.91(19)
C12–C13	1.522(3)	N2–C12–C13	113.9(2)
C13–C14	1.533(3)	C12–C13–C14	115.89(19)
C14–C15	1.507(3)	C15–C14–C13	113.2(2)
C15–C16	1.543(3)	C14–C15–C16	114.0(2)
C16–N3	1.466(3)	N3–C16–C15	113.83(19)
C17–O6	1.237(3)	O6–C17–N3	123.8(2)
C17–N3	1.329(3)	O6–C17–C18	121.80(19)
C17–C18	1.518(3)	N3–C17–C18	114.37(18)
C18–N4	1.474(3)	N4–C18–C17	110.56(17)
C18–C20	1.546(3)	N4–C18–C20	111.04(17)
C19–C20	1.524(3)	C17–C18–C20	112.00(17)
C20–C21	1.519(4)	C21–C20–C19	111.5(2)
N1–S2	1.6114(19)	C21–C20–C18	110.18(19)
N4–S1	1.5946(18)	C19–C20–C18	112.86(19)
O1–S1	1.4411(15)	C7–N1–S2	121.53(14)
O2–S1	1.4294(15)	C11–N2–C12	122.40(18)
O3–S2	1.4319(15)	C17–N3–C16	123.66(19)
O4–S2	1.4341(16)	C18–N4–S1	122.04(14)
O7–C22	1.418(3)	O2–S1–O1	120.05(9)
		O2–S1–N4	108.15(9)
C2–C1–C6	120.72(19)	O1–S1–N4	106.60(9)
C2–C1–S1	119.01(15)	O2–S1–C1	106.40(9)
C6–C1–S1	120.17(16)	O1–S1–C1	105.52(9)
C3–C2–C1	118.8(2)	N4–S1–C1	109.89(10)
C2–C3–C4	121.3(2)	O3–S2–O4	119.78(10)
C2–C3–S2	118.85(17)	O3–S2–N1	109.04(10)
C4–C3–S2	119.81(17)	O4–S2–N1	106.16(9)
C5–C4–C3	119.5(2)	O3–S2–C3	106.42(10)
C4–C5–C6	120.2(2)	O4–S2–C3	107.86(10)
C5–C6–C1	119.4(2)	N1–S2–C3	106.97(10)
N1–C7–C11	107.55(16)		

Table 4. Anisotropic displacement parameters [$\text{\AA}^2 \times 10^3$]. The anisotropic displacement factor exponent takes the form: $-2\pi^2[h^2 a^{*2} U^{11} + \dots + 2 h k a^* b^* U^{12}]$.

Atom	U^{11}	U^{22}	U^{33}	U^{23}	U^{13}	U^{12}
C1	13(1)	19(1)	18(1)	-2(1)	-2(1)	2(1)
C2	14(1)	19(1)	23(1)	0(1)	-1(1)	0(1)

C3	22(1)	19(1)	20(1)	1(1)	-1(1)	0(1)
C4	15(1)	33(1)	23(1)	2(1)	-4(1)	1(1)
C5	15(1)	32(1)	29(1)	3(1)	0(1)	-5(1)
C6	21(1)	26(1)	21(1)	4(1)	1(1)	-2(1)
C7	17(1)	25(1)	23(1)	0(1)	-1(1)	0(1)
C8	33(1)	49(2)	38(2)	5(1)	14(1)	-7(1)
C9	22(1)	39(2)	24(1)	2(1)	4(1)	0(1)
C10	33(1)	51(2)	37(2)	-9(1)	11(1)	2(1)
C11	19(1)	25(1)	21(1)	-4(1)	2(1)	2(1)
C12	29(1)	26(1)	27(1)	3(1)	-6(1)	-4(1)
C13	26(1)	29(1)	33(1)	5(1)	-5(1)	-3(1)
C14	31(1)	31(1)	27(1)	1(1)	0(1)	0(1)
C15	35(1)	30(1)	28(1)	-7(1)	-8(1)	-2(1)
C16	31(1)	21(1)	28(1)	-2(1)	-6(1)	-4(1)
C17	22(1)	19(1)	23(1)	4(1)	-3(1)	4(1)
C18	15(1)	16(1)	24(1)	4(1)	-1(1)	-2(1)
C19	28(1)	38(2)	54(2)	2(1)	-10(1)	12(1)
C20	28(1)	17(1)	32(1)	7(1)	-10(1)	-2(1)
C21	40(2)	41(2)	34(2)	5(1)	-13(1)	-1(1)
N1	19(1)	23(1)	18(1)	2(1)	-5(1)	3(1)
N2	21(1)	26(1)	26(1)	3(1)	-6(1)	-4(1)
N3	24(1)	23(1)	18(1)	-1(1)	0(1)	-4(1)
N4	15(1)	18(1)	27(1)	3(1)	3(1)	1(1)
O1	17(1)	19(1)	27(1)	3(1)	-3(1)	-4(1)
O2	22(1)	23(1)	19(1)	-1(1)	0(1)	-2(1)
O3	21(1)	32(1)	28(1)	7(1)	-5(1)	-9(1)
O4	28(1)	22(1)	29(1)	0(1)	-6(1)	5(1)
O5	21(1)	29(1)	34(1)	-1(1)	-8(1)	0(1)
O6	27(1)	33(1)	25(1)	-1(1)	6(1)	1(1)
S1	15(1)	18(1)	20(1)	0(1)	-2(1)	1(1)
S2	20(1)	21(1)	22(1)	3(1)	-4(1)	-1(1)
O7	22(1)	73(1)	38(1)	21(1)	-2(1)	-3(1)
C22	28(1)	85(2)	43(2)	15(2)	-1(1)	-15(2)

Table 5. Hydrogen coordinates [$\times 10^4$] and isotropic displacement parameters [$\text{\AA}^2 \times 10^3$].

Atom	x	y	z	U_{eq}	$S.o.f.$
H2	5150	2463	9647	22	1
H4	8232	2885	10220	28	1
H5	8438	3956	9103	30	1
H6	7010	4260	8241	27	1
H7	5685	3431	11513	26	1
H8A	4822	2208	13361	60	1
H8B	5413	1656	12629	60	1
H8C	4451	2419	12456	60	1
H9	6439	3025	13115	34	1
H10A	4734	4352	12689	61	1

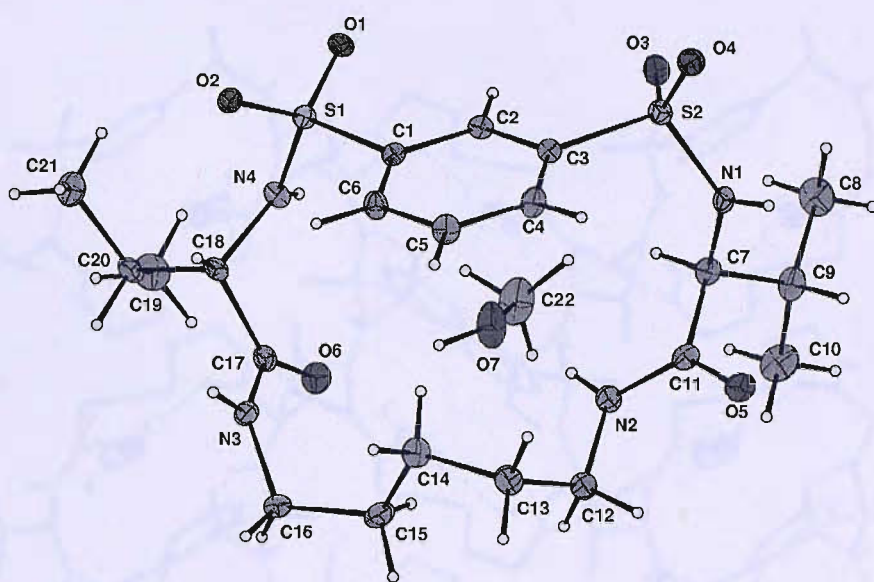
H10B	5856	4727	13019	61	1
H10C	5081	4092	13592	61	1
H12A	7965	5909	11844	33	1
H12B	6997	6531	11468	33	1
H13A	8496	5433	10519	35	1
H13B	8569	6636	10676	35	1
H14A	7881	6315	9385	35	1
H14B	6937	5659	9763	35	1
H15A	7162	7753	10172	37	1
H15B	6126	7065	10265	37	1
H16A	5766	8111	9193	32	1
H16B	6917	7958	8815	32	1
H18	5329	5429	7701	22	1
H19A	2319	6606	7533	60	1
H19B	2883	6591	8395	60	1
H19C	2484	5545	7997	60	1
H20	4126	6784	7341	31	1
H21A	3464	4812	6811	57	1
H21B	4464	5411	6456	57	1
H21C	3300	5859	6328	57	1
H1	7381	2154	11946	24	1
H2A	6224	4976	11126	29	1
H3	6283	6640	8134	26	1
H4A	3726	4605	8660	24	1
H7A	4793	5473	10193	67	1
H22A	3817	4203	11178	78	1
H22B	3297	4829	10452	78	1
H22C	3638	5411	11258	78	1

Table 6. Hydrogen bonds [\AA and $^\circ$].

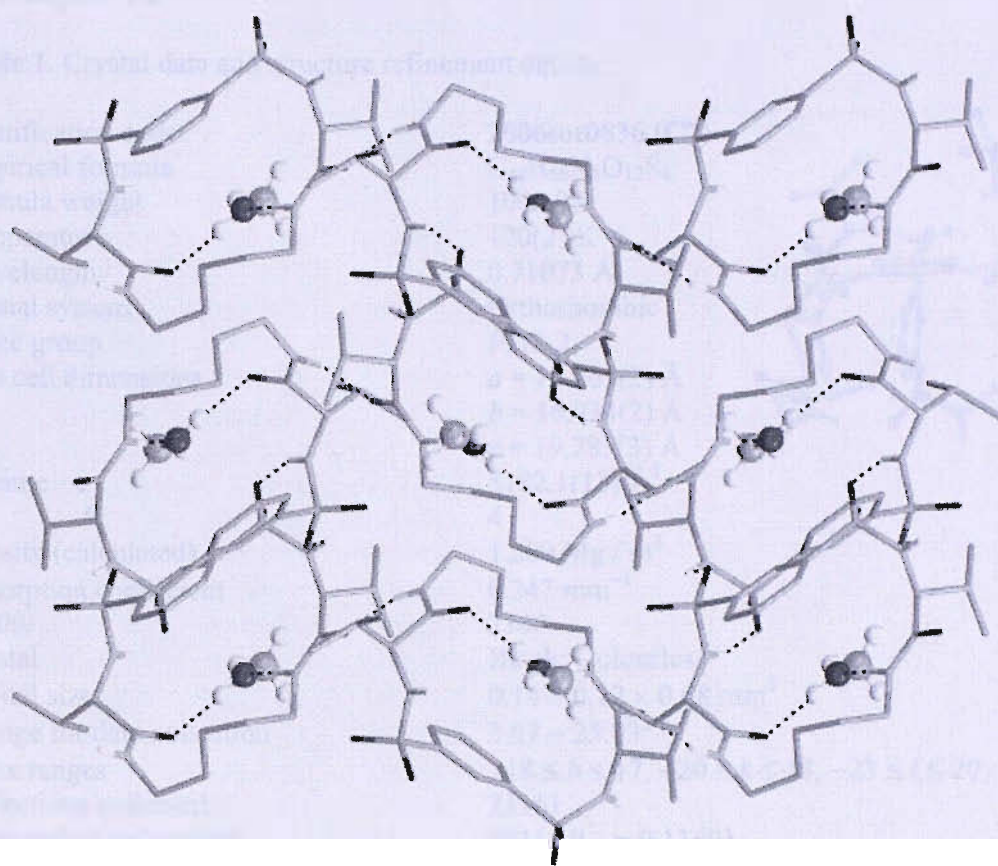
$D-H\cdots A$	$d(D-H)$	$d(H\cdots A)$	$d(D\cdots A)$	$\angle(DHA)$
N1-H1...O1 ⁱ	0.88	2.29	2.904(2)	126.3
N2-H2A...O7	0.88	2.00	2.873(2)	173.5
N3-H3...O5 ⁱⁱ	0.88	2.06	2.912(2)	163.5
N4-H4A...O4 ⁱⁱⁱ	0.88	2.17	3.012(2)	159.6
O7-H7A...O6	0.84	1.89	2.728(2)	171.6

Symmetry transformations used to generate equivalent atoms:

(i) $x+1/2, -y+1/2, -z+2$ (ii) $-x+3/2, -y+1, z-1/2$ (iii) $x-1/2, -y+1/2, -z+2$



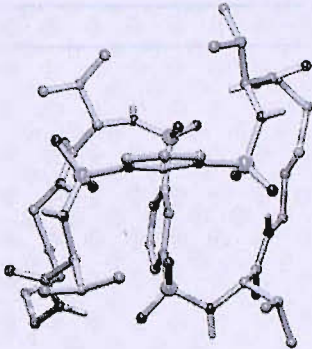
Thermal ellipsoids drawn at the 35% probability level



3D hydrogen bonded network viewed down the a axis

Macrocycle 92

Table 1. Crystal data and structure refinement details.

Identification code	2006sot0836 (C7)	
Empirical formula	C ₄₂ H ₆₈ N ₈ O ₁₂ S ₄	
Formula weight	1005.28	
Temperature	120(2) K	
Wavelength	0.71073 Å	
Crystal system	Orthorhombic	
Space group	P2 ₁ 2 ₁ 2 ₁	
Unit cell dimensions	<i>a</i> = 15.469(2) Å <i>b</i> = 16.934(2) Å <i>c</i> = 19.783(3) Å	
Volume	5182.1(13) Å ³	
Z	4	
Density (calculated)	1.289 Mg / m ³	
Absorption coefficient	0.247 mm ⁻¹	
<i>F</i> (000)	2144	
Crystal	Block; Colourless	
Crystal size	0.14 × 0.12 × 0.08 mm ³	
θ range for data collection	3.07 – 25.03°	
Index ranges	–18 ≤ <i>h</i> ≤ 17, –20 ≤ <i>k</i> ≤ 18, –23 ≤ <i>l</i> ≤ 20	
Reflections collected	23161	
Independent reflections	8911 [<i>R</i> _{int} = 0.1169]	
Completeness to $\theta = 25.03^\circ$	99.4 %	
Absorption correction	Semi-empirical from equivalents	
Max. and min. transmission	0.9805 and 0.9562	
Refinement method	Full-matrix least-squares on <i>F</i> ²	
Data / restraints / parameters	8911 / 12 / 603	
Goodness-of-fit on <i>F</i> ²	1.109	
Final <i>R</i> indices [<i>F</i> ² > 2σ(<i>F</i> ²)]	<i>R</i> 1 = 0.1251, <i>wR</i> 2 = 0.2223	
<i>R</i> indices (all data)	<i>R</i> 1 = 0.1979, <i>wR</i> 2 = 0.2492	
Absolute structure parameter	0.20(17)	
Largest diff. peak and hole	0.412 and –0.333 e Å ⁻³	

Diffractometer: Nonius KappaCCD area detector (ϕ scans and ω scans to fill asymmetric unit). **Cell determination:** DirAx (Duisenberg, A.J.M.(1992). *J. Appl. Cryst.* 25, 92-96.) **Data collection:** Collect (Collect: Data collection software, R. Hoof, Nonius B.V., 1998). **Data reduction and cell refinement:** Denzo (Z. Otwinowski & W. Minor, *Methods in Enzymology* (1997) Vol. 276: *Macromolecular Crystallography*, part A, pp. 307–326; C. W. Carter, Jr. & R. M. Sweet, Eds., Academic Press). **Absorption correction:** Sheldrick, G. M. SADABS - Bruker Nonius area detector scaling and absorption correction - V2.10 **Structure solution:** SHELXS97 (G. M. Sheldrick, *Acta Cryst.* (1990) A46 467–473). **Structure refinement:** SHELXL97 (G. M. Sheldrick (1997), University of Göttingen, Germany). **Graphics:** Camcon - A Molecular Graphics Package. (D. M. Watkin, L. Pearce and C. K. Prout, Chemical Crystallography Laboratory, University of Oxford, 1993).

Special details: All hydrogen atoms were placed in idealised positions and refined using a riding model.

Table 2. Atomic coordinates [$\times 10^4$], equivalent isotropic displacement parameters [$\text{\AA}^2 \times 10^3$] and site occupancy factors. U_{eq} is defined as one third of the trace of the orthogonalized U^{ij} tensor.

Atom	<i>x</i>	<i>y</i>	<i>z</i>	U_{eq}	S.o.f.
S1	1385(2)	4111(2)	6870(1)	42(1)	1
S2	3793(2)	6211(2)	5895(1)	40(1)	1
S3	243(2)	6352(2)	5239(1)	46(1)	1
S4	1579(2)	7039(2)	7739(1)	40(1)	1
O1	1398(4)	3777(4)	7523(3)	45(2)	1
O2	871(4)	4784(4)	6759(3)	40(2)	1
O3	4240(5)	6106(4)	5269(3)	47(2)	1
O4	3035(5)	6677(4)	5904(3)	43(2)	1
O5	4822(4)	8120(4)	6636(4)	47(2)	1
O6	1152(5)	8405(4)	4254(4)	50(2)	1
O7	777(6)	5684(4)	5372(4)	61(2)	1
O8	-627(5)	6222(5)	5108(4)	65(2)	1
O9	2105(4)	6386(5)	7536(4)	49(2)	1
O10	1995(4)	7722(5)	7963(3)	48(2)	1
O11	-875(5)	6819(5)	8187(4)	55(2)	1
O12	-437(5)	2927(5)	5674(4)	55(2)	1
N1	1148(6)	3424(6)	6351(4)	51(3)	1
N3	3675(5)	8247(6)	7336(5)	53(3)	1
N2	4471(5)	6531(5)	6429(4)	40(2)	1
N4	2067(5)	8234(5)	5116(4)	35(2)	1
N5	585(5)	6835(5)	4641(4)	41(2)	1
N6	936(5)	6765(5)	8325(4)	39(2)	1
N7	-813(6)	5801(5)	7470(4)	44(2)	1
N8	-389(6)	4186(6)	5339(5)	56(3)	1
C1	2471(7)	4385(7)	6639(5)	42(3)	1
C2	3131(8)	3830(7)	6784(6)	52(3)	1
C3	3948(8)	4008(7)	6642(6)	58(3)	1
C4	4152(7)	4716(8)	6327(6)	51(3)	1
C5	3499(7)	5254(6)	6223(5)	37(3)	1
C6	2651(7)	5110(6)	6361(5)	39(3)	1
C7	4203(7)	6927(7)	7044(5)	47(3)	1
C8	4246(7)	7832(7)	6978(6)	45(3)	1
C9	4506(8)	5816(8)	7870(6)	64(4)	1
C10	4732(7)	6644(7)	7678(5)	51(3)	1
C11	5695(8)	6727(8)	7593(7)	71(4)	1
C12	3641(8)	9090(7)	7276(6)	51(3)	1
C13	3227(7)	9368(7)	6624(6)	48(3)	1
C14	2295(8)	9097(7)	6498(6)	51(3)	1
C15	1892(7)	9407(7)	5867(6)	48(3)	1
C16	2268(8)	9051(7)	5219(6)	52(3)	1
C17	1543(6)	7985(7)	4646(5)	35(2)	1
C18	1492(7)	7081(6)	4562(5)	40(3)	1
C19	1748(7)	5946(7)	3771(6)	55(3)	1

C20	1878(7)	6801(7)	3898(6)	48(3)	1
C21	2832(7)	7028(8)	3884(6)	57(3)	1
C22	357(6)	6992(6)	5949(5)	36(3)	1
C23	-40(6)	7734(6)	5928(6)	43(3)	1
C24	32(7)	8223(7)	6464(6)	48(3)	1
C25	508(7)	7999(6)	7014(5)	37(3)	1
C26	935(6)	7306(6)	7026(5)	30(2)	1
C27	857(6)	6794(6)	6492(5)	31(2)	1
C28	1287(8)	5194(8)	8987(6)	68(4)	1
C29	373(8)	5517(6)	8822(5)	46(3)	1
C30	-20(8)	5902(7)	9442(6)	61(4)	1
C31	411(6)	6048(6)	8205(5)	41(3)	1
C32	-476(7)	6259(7)	7935(5)	41(3)	1
C33	-1670(7)	5886(7)	7197(6)	53(3)	1
C34	-1810(12)	5426(10)	6551(10)	106(6)	1
C35	-1557(13)	4705(13)	6481(12)	135(7)	1
C36	-1856(8)	4213(9)	5846(7)	68(4)	1
C37	-1330(8)	4261(8)	5244(7)	66(4)	1
C38	-15(8)	3534(7)	5576(5)	45(3)	1
C39	957(6)	3552(6)	5656(6)	42(3)	1
C40	1170(10)	3110(10)	4449(7)	88(5)	1
C41	1397(8)	2949(8)	5185(5)	60(3)	1
C42	2365(9)	2934(10)	5266(8)	87(5)	1

Table 3. Bond lengths [\AA] and angles [$^\circ$].

S1-O2	1.408(7)	N3-C12	1.434(13)
S1-O1	1.410(7)	N2-C7	1.449(13)
S1-N1	1.593(10)	N4-C17	1.305(12)
S1-C1	1.800(11)	N4-C16	1.433(13)
S2-O4	1.412(8)	N5-C18	1.471(13)
S2-O3	1.430(7)	N6-C31	1.479(12)
S2-N2	1.585(9)	N7-C32	1.311(13)
S2-C5	1.803(11)	N7-C33	1.439(13)
S3-O8	1.388(8)	N8-C38	1.332(13)
S3-O7	1.425(8)	N8-C37	1.473(14)
S3-N5	1.532(9)	C1-C6	1.374(15)
S3-C22	1.782(11)	C1-C2	1.417(15)
S4-O10	1.395(8)	C2-C3	1.329(16)
S4-O9	1.430(8)	C3-C4	1.389(16)
S4-N6	1.597(8)	C4-C5	1.376(15)
S4-C26	1.785(10)	C5-C6	1.362(14)
O5-C8	1.220(12)	C7-C8	1.539(16)
O6-C17	1.213(12)	C7-C10	1.574(14)
O11-C32	1.237(12)	C9-C10	1.495(16)
O12-C38	1.233(12)	C10-C11	1.505(15)
N1-C39	1.424(13)	C12-C13	1.514(15)
N3-C8	1.332(13)	C13-C14	1.533(15)

C14-C15	1.492(15)	O9-S4-C26	106.9(5)
C15-C16	1.530(15)	N6-S4-C26	107.4(4)
C17-C18	1.543(14)	C39-N1-S1	124.0(8)
C18-C20	1.518(14)	C8-N3-C12	120.4(10)
C19-C20	1.482(16)	C7-N2-S2	121.9(7)
C20-C21	1.526(15)	C17-N4-C16	123.2(10)
C22-C27	1.365(13)	C18-N5-S3	124.3(7)
C22-C23	1.399(14)	C31-N6-S4	117.6(7)
C23-C24	1.350(15)	C32-N7-C33	124.8(10)
C24-C25	1.367(14)	C38-N8-C37	123.1(10)
C25-C26	1.346(13)	C6-C1-C2	121.8(10)
C26-C27	1.372(13)	C6-C1-S1	121.4(9)
C28-C29	1.552(16)	C2-C1-S1	116.7(9)
C29-C30	1.515(15)	C3-C2-C1	119.6(12)
C29-C31	1.518(14)	C2-C3-C4	120.4(12)
C31-C32	1.515(14)	C5-C4-C3	118.2(11)
C33-C34	1.513(19)	C6-C5-C4	123.9(11)
C34-C35	1.29(2)	C6-C5-S2	118.4(9)
C35-C36	1.58(2)	C4-C5-S2	117.7(8)
C36-C37	1.444(17)	C5-C6-C1	115.9(11)
C38-C39	1.511(15)	N2-C7-C8	112.2(9)
C39-C41	1.541(16)	N2-C7-C10	112.3(9)
C40-C41	1.521(17)	C8-C7-C10	110.4(9)
C41-C42	1.506(17)	O5-C8-N3	124.6(11)
		O5-C8-C7	118.4(10)
O2-S1-O1	118.3(5)	N3-C8-C7	116.8(10)
O2-S1-N1	111.1(4)	C9-C10-C11	110.3(11)
O1-S1-N1	107.5(4)	C9-C10-C7	111.5(9)
O2-S1-C1	106.2(5)	C11-C10-C7	113.3(9)
O1-S1-C1	108.9(5)	N3-C12-C13	113.3(10)
N1-S1-C1	103.9(5)	C12-C13-C14	116.3(10)
O4-S2-O3	118.8(4)	C15-C14-C13	115.0(10)
O4-S2-N2	110.4(4)	C14-C15-C16	113.8(9)
O3-S2-N2	107.4(4)	N4-C16-C15	114.7(9)
O4-S2-C5	106.7(5)	O6-C17-N4	125.2(11)
O3-S2-C5	108.8(5)	O6-C17-C18	119.2(9)
N2-S2-C5	103.6(5)	N4-C17-C18	115.4(9)
O8-S3-O7	118.0(5)	N5-C18-C20	112.3(8)
O8-S3-N5	106.0(5)	N5-C18-C17	108.5(8)
O7-S3-N5	111.5(5)	C20-C18-C17	112.6(9)
O8-S3-C22	109.9(5)	C19-C20-C18	113.5(10)
O7-S3-C22	106.3(5)	C19-C20-C21	112.0(9)
N5-S3-C22	104.5(5)	C18-C20-C21	108.5(9)
O10-S4-O9	117.9(4)	C27-C22-C23	119.5(10)
O10-S4-N6	107.3(4)	C27-C22-S3	121.8(8)
O9-S4-N6	109.5(5)	C23-C22-S3	118.6(8)
O10-S4-C26	107.3(5)	C24-C23-C22	119.4(10)

C23–C24–C25	120.0(11)	N7–C33–C34	113.4(11)
C26–C25–C24	121.3(10)	C35–C34–C33	122.3(17)
C25–C26–C27	119.5(9)	C34–C35–C36	119.8(19)
C25–C26–S4	120.6(8)	C37–C36–C35	117.5(13)
C27–C26–S4	119.9(7)	C36–C37–N8	116.5(11)
C22–C27–C26	120.1(9)	O12–C38–N8	121.0(11)
C30–C29–C31	114.4(9)	O12–C38–C39	121.8(10)
C30–C29–C28	110.3(9)	N8–C38–C39	116.9(10)
C31–C29–C28	110.0(9)	N1–C39–C38	107.7(9)
N6–C31–C32	111.1(9)	N1–C39–C41	113.1(9)
N6–C31–C29	112.2(8)	C38–C39–C41	111.3(9)
C32–C31–C29	112.8(9)	C42–C41–C40	109.6(11)
O11–C32–N7	122.5(10)	C42–C41–C39	112.7(9)
O11–C32–C31	119.4(10)	C40–C41–C39	110.9(11)
N7–C32–C31	117.9(10)		

Table 4. Anisotropic displacement parameters [$\text{\AA}^2 \times 10^3$]. The anisotropic displacement factor exponent takes the form: $-2\pi^2[h^2 a^{*2} U^{11} + \dots + 2 h k a^* b^* U^{12}]$.

Atom	U^{11}	U^{22}	U^{33}	U^{23}	U^{13}	U^{12}
S1	49(2)	44(2)	32(2)	6(1)	-2(1)	-6(2)
S2	44(2)	40(2)	36(2)	4(1)	0(1)	-4(1)
S3	48(2)	51(2)	38(2)	2(2)	-2(1)	-12(2)
S4	39(2)	44(2)	36(2)	-1(1)	1(1)	-7(1)
O1	54(4)	41(4)	40(4)	-7(4)	-7(4)	-16(4)
O2	41(4)	41(5)	38(4)	5(4)	-2(3)	3(4)
O3	64(5)	48(5)	30(4)	-6(4)	6(4)	-9(4)
O4	55(5)	38(4)	35(4)	9(4)	-11(4)	-15(4)
O5	40(4)	44(5)	56(5)	-4(4)	12(4)	-13(4)
O6	59(5)	52(5)	39(4)	0(4)	-11(4)	4(4)
O7	104(7)	41(5)	38(5)	5(4)	-20(5)	-11(5)
O8	52(5)	92(7)	52(5)	3(5)	-4(4)	-28(5)
O9	38(4)	69(6)	40(4)	7(4)	2(3)	10(4)
O10	42(4)	62(6)	39(4)	8(4)	-11(3)	-15(4)
O11	72(5)	41(5)	51(5)	-4(4)	-3(4)	2(4)
O12	51(5)	51(5)	62(5)	5(4)	-12(4)	-2(4)
N1	68(6)	50(6)	35(5)	12(5)	-11(5)	-1(5)
N3	37(5)	69(8)	54(6)	-13(6)	26(5)	-3(5)
N2	35(5)	53(6)	31(5)	0(5)	8(4)	1(4)
N4	31(5)	41(6)	33(5)	-11(4)	-6(4)	-6(4)
N5	32(5)	51(6)	42(5)	9(5)	-16(4)	-3(4)
N6	49(5)	39(5)	29(5)	-12(4)	-1(4)	-11(4)
N7	60(6)	43(6)	29(5)	-4(5)	-6(4)	2(5)
N8	61(7)	44(6)	62(7)	15(6)	-5(5)	-16(5)
C1	46(7)	43(8)	36(6)	-23(6)	1(5)	-1(6)
C2	62(8)	37(7)	57(8)	6(6)	-11(6)	2(7)

C3	64(9)	49(8)	61(8)	14(7)	-25(7)	-12(7)
C4	24(6)	68(9)	60(8)	-24(7)	-3(6)	22(6)
C5	36(6)	38(7)	38(6)	-8(5)	-2(5)	-20(6)
C6	49(7)	25(6)	42(6)	-14(5)	-19(5)	-5(5)
C7	39(6)	67(9)	35(6)	4(6)	-1(5)	-13(6)
C8	28(6)	52(8)	55(8)	5(6)	-18(6)	-9(6)
C9	68(8)	78(10)	46(8)	16(7)	-1(7)	-7(7)
C10	39(6)	78(9)	35(6)	4(6)	1(5)	-13(6)
C11	75(9)	80(10)	57(9)	0(8)	-2(7)	1(8)
C12	68(8)	40(7)	46(7)	-16(6)	3(6)	18(6)
C13	47(7)	46(8)	51(7)	-8(6)	-8(6)	3(5)
C14	65(8)	49(8)	40(7)	-9(6)	10(6)	2(6)
C15	36(6)	51(8)	58(8)	11(7)	12(6)	-5(5)
C16	68(8)	55(8)	34(6)	4(6)	-1(6)	-8(7)
C17	31(5)	50(7)	25(5)	-4(6)	1(5)	5(5)
C18	54(7)	41(7)	26(6)	3(5)	-13(5)	6(6)
C19	54(7)	60(9)	53(8)	5(7)	-15(6)	1(6)
C20	59(7)	40(8)	46(7)	0(6)	8(6)	16(6)
C21	56(8)	60(9)	54(7)	-24(7)	11(6)	2(7)
C22	27(5)	43(7)	40(6)	12(6)	11(5)	8(5)
C23	40(6)	43(7)	45(7)	19(6)	1(5)	8(5)
C24	53(8)	43(7)	49(7)	14(7)	4(6)	1(6)
C25	56(7)	23(6)	33(6)	-9(5)	10(5)	4(5)
C26	38(6)	33(6)	20(5)	5(5)	10(4)	-4(5)
C27	22(5)	36(6)	36(6)	11(5)	-7(4)	19(5)
C28	86(10)	77(10)	41(7)	17(7)	-18(7)	12(8)
C29	76(9)	38(7)	24(6)	15(5)	4(6)	-14(6)
C30	73(9)	57(8)	52(8)	2(7)	-7(7)	14(7)
C31	30(6)	62(8)	30(6)	-14(6)	-4(5)	7(5)
C32	46(6)	43(7)	35(6)	-5(6)	23(5)	-21(6)
C33	57(8)	52(8)	51(7)	1(7)	-6(6)	-13(6)
C34	112(13)	69(11)	136(15)	-25(11)	-50(11)	30(10)
C35	103(13)	135(16)	166(18)	-49(15)	-17(13)	8(13)
C36	64(8)	83(10)	58(9)	-9(8)	-15(7)	11(8)
C37	50(8)	69(9)	78(10)	23(8)	-8(7)	-3(7)
C38	83(9)	34(7)	19(6)	16(5)	-9(5)	-16(7)
C39	34(6)	32(7)	61(8)	11(6)	-8(5)	4(5)
C40	94(11)	110(13)	60(9)	-27(9)	-2(8)	7(10)
C41	72(9)	76(9)	32(7)	-13(7)	-11(6)	-19(8)
C42	76(10)	110(13)	74(10)	-41(10)	-9(8)	12(9)

Table 5. Hydrogen coordinates [$\times 10^4$] and isotropic displacement parameters [$\text{\AA}^2 \times 10^3$].

Atom	x	y	z	U_{eq}	$S.o.f.$
H101	1134	2936	6504	61	1
H103	3317	8002	7610	64	1

H102	5026	6467	6350	48	1
H104	2310	7883	5384	42	1
H105	215	6974	4325	50	1
H106	895	7030	8706	47	1
H107	-491	5413	7314	53	1
H108	-59	4590	5233	67	1
H2	2991	3335	6981	62	1
H3	4395	3647	6757	70	1
H4	4727	4827	6187	61	1
H6	2212	5487	6271	46	1
H7	3585	6784	7125	57	1
H9A	4794	5679	8295	96	1
H9B	4697	5454	7513	96	1
H9C	3879	5771	7927	96	1
H10	4561	6991	8065	61	1
H11A	5890	6384	7224	106	1
H11B	5985	6573	8013	106	1
H11C	5836	7277	7486	106	1
H12A	4236	9303	7302	62	1
H12B	3310	9307	7662	62	1
H13A	3588	9184	6243	57	1
H13B	3237	9952	6619	57	1
H14A	2286	8513	6481	61	1
H14B	1935	9262	6887	61	1
H15A	1969	9988	5853	58	1
H15B	1264	9299	5880	58	1
H16A	2050	9356	4828	63	1
H16B	2905	9112	5230	63	1
H18	1832	6835	4937	49	1
H19A	2059	5640	4113	83	1
H19B	1969	5812	3321	83	1
H19C	1130	5822	3794	83	1
H20	1583	7096	3526	58	1
H21A	3076	6902	3440	85	1
H21B	3143	6732	4234	85	1
H21C	2891	7595	3970	85	1
H23	-358	7892	5540	51	1
H24	-247	8722	6460	58	1
H25	537	8338	7396	45	1
H27	1150	6302	6500	38	1
H28A	1671	5633	9103	102	1
H28B	1517	4914	8592	102	1
H28C	1251	4828	9370	102	1
H29	1	5055	8703	55	1
H30A	-633	6010	9359	91	1
H30B	282	6398	9538	91	1
H30C	36	5545	9830	91	1
H31	710	5741	7842	49	1
H33A	-1781	6452	7109	64	1
H33B	-2094	5706	7539	64	1

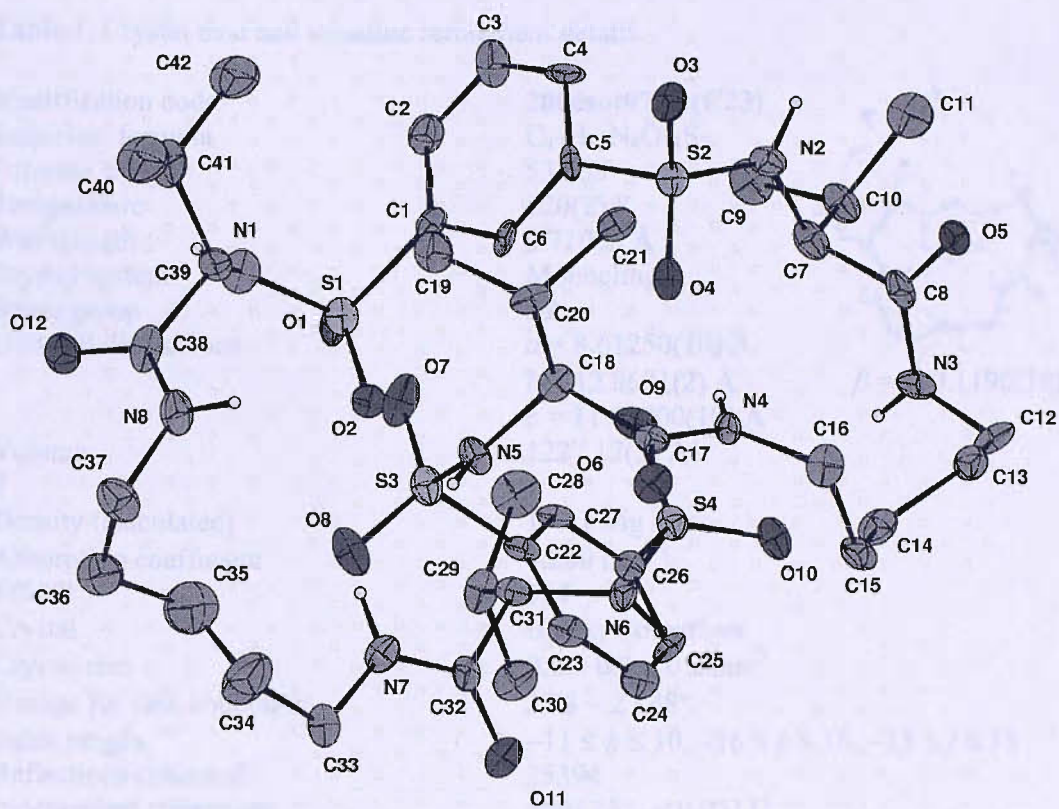
H34A	-2439	5432	6461	127	1
H34B	-1534	5734	6184	127	1
H35A	-1743	4412	6888	162	1
H35B	-917	4708	6482	162	1
H36A	-1890	3651	5982	82	1
H36B	-2449	4383	5727	82	1
H37A	-1447	4775	5024	79	1
H37B	-1521	3842	4929	79	1
H39	1165	4091	5530	51	1
H40A	1467	2728	4159	132	1
H40B	1352	3646	4329	132	1
H40C	544	3061	4387	132	1
H41	1172	2413	5303	72	1
H42A	2603	3450	5143	130	1
H42B	2610	2527	4971	130	1
H42C	2510	2815	5738	130	1

Table 6. Hydrogen bonds [\AA and $^\circ$].

$D-H\cdots A$	$d(D-H)$	$d(H\cdots A)$	$d(D\cdots A)$	$\angle(DHA)$
N3-H103...O10	0.88	2.21	3.014(11)	151.4
N4-H104...O4	0.88	2.55	3.410(11)	166.6
N7-H107...O2	0.88	2.60	3.424(11)	155.6
N8-H108...O7	0.88	2.27	3.113(12)	159.3
N8-H108...S3	0.88	3.02	3.802(10)	149.1
N1-H101...O11 ⁱ	0.88	2.03	2.898(12)	169.8
N2-H102...O6 ⁱⁱ	0.88	2.12	2.932(11)	152.7
N5-H105...O5 ⁱⁱⁱ	0.88	2.00	2.791(11)	148.3
N6-H106...O12 ^{iv}	0.88	2.08	2.897(12)	154.7

Symmetry transformations used to generate equivalent atoms:

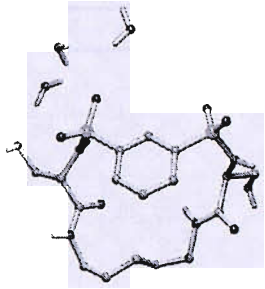
- (i) $-x, y-1/2, -z+3/2$ (ii) $x+1/2, -y+3/2, -z+1$ (iii) $x-1/2, -y+3/2, -z+1$
 (iv) $-x, y+1/2, -z+3/2$



Thermal ellipsoids drawn at the 30% probability level

Macrocycle 117

Table 1. Crystal data and structure refinement details.

Identification code	2006sot0781 (C23)		
Empirical formula	$C_{17}H_{32}N_4O_{11}S_2$		
Formula weight	532.59		
Temperature	120(2) K		
Wavelength	0.71073 Å		
Crystal system	Monoclinic		
Space group	$P2_1$		
Unit cell dimensions	$a = 8.61250(10)$ Å $b = 12.8621(2)$ Å $c = 11.79800(10)$ Å		
Volume	$1227.17(3)$ Å ³		$\beta = 110.1190(10)^\circ$
Z	2		
Density (calculated)	1.441 Mg / m ³		
Absorption coefficient	0.280 mm ⁻¹		
$F(000)$	564		
Crystal	Block; Colourless		
Crystal size	0.3 × 0.2 × 0.2 mm ³		
θ range for data collection	2.98 – 27.48°		
Index ranges	$-11 \leq h \leq 10, -16 \leq k \leq 16, -15 \leq l \leq 15$		
Reflections collected	25394		
Independent reflections	5601 [$R_{int} = 0.0511$]		
Completeness to $\theta = 27.48^\circ$	99.6 %		
Absorption correction	Semi-empirical from equivalents		
Max. and min. transmission	0.9462 and 0.9108		
Refinement method	Full-matrix least-squares on F^2		
Data / restraints / parameters	5601 / 76 / 334		
Goodness-of-fit on F^2	1.030		
Final R indices [$F^2 > 2\sigma(F^2)$]	$RI = 0.0393, wR2 = 0.0808$		
R indices (all data)	$RI = 0.0608, wR2 = 0.0892$		
Absolute structure parameter	0.02(5)		
Extinction coefficient	0.0131(16)		
Largest diff. peak and hole	0.301 and $-0.347 e \text{ \AA}^{-3}$		

Diffraction: Nonius KappaCCD area detector (ϕ scans and ω scans to fill *asymmetric unit*). **Cell determination:** DirAx (Duisenberg, A.J.M.(1992). J. Appl. Cryst. 25, 92-96.) **Data collection:** Collect (Collect: Data collection software, R. Hooft, Nonius B.V., 1998). **Data reduction and cell refinement:** Denzo (Z. Otwinowski & W. Minor, *Methods in Enzymology* (1997) Vol. 276: *Macromolecular Crystallography*, part A, pp. 307-326; C. W. Carter, Jr. & R. M. Sweet, Eds., Academic Press). **Absorption correction:** Sheldrick, G. M. SADABS - Bruker Nonius area detector scaling and absorption correction - V2.10 **Structure solution:** SHELXS97 (G. M. Sheldrick, Acta Cryst. (1990) A46 467-473). **Structure refinement:** SHELXL97 (G. M. Sheldrick (1997), University of Göttingen, Germany). **Graphics:** Camcon - A Molecular Graphics Package. (D. M. Watkin, L. Pearce and C. K. Prout, Chemical Crystallography Laboratory, University of Oxford, 1993).

Special details: All hydrogen atoms were placed in idealised positions and refined using a riding model.

Table 2. Atomic coordinates [$\times 10^4$], equivalent isotropic displacement parameters [$\text{\AA}^2 \times 10^3$] and site occupancy factors. U_{eq} is defined as one third of the trace of the orthogonalized U^{ij} tensor.

Atom	<i>x</i>	<i>y</i>	<i>z</i>	U_{eq}	<i>S.o.f.</i>
O9	9461(3)	6863(2)	5534(2)	47(1)	1
O10	15391(2)	9307(1)	9215(2)	32(1)	1
O11	11166(3)	3190(1)	1668(2)	35(1)	1
C1	9381(3)	5480(2)	2863(2)	30(1)	1
C2	7981(4)	5826(2)	1721(3)	49(1)	1
C3	8775(3)	4593(2)	3461(2)	28(1)	1
C4	7422(3)	4137(2)	4915(3)	35(1)	1
C5	7943(3)	4233(2)	6268(3)	32(1)	1
C6	9692(3)	3854(2)	6969(3)	32(1)	1
C7	9953(4)	3589(2)	8274(3)	38(1)	1
C8	9863(3)	4511(2)	9060(2)	33(1)	1
C9	11478(3)	6007(2)	8805(2)	22(1)	1
C10	13148(3)	6557(2)	9298(2)	21(1)	1
C11	13111(3)	7359(2)	10242(2)	26(1)	1
C12	14257(3)	5716(2)	6785(2)	22(1)	1
C13	14194(3)	4684(2)	7127(2)	25(1)	1
C14	13598(3)	3929(2)	6244(2)	27(1)	1
C15	13088(3)	4196(2)	5030(2)	26(1)	1
C16	13175(3)	5236(2)	4715(2)	23(1)	1
C17	13748(3)	6004(2)	5578(2)	22(1)	1
N1	10768(3)	5136(2)	2510(2)	32(1)	1
N2	8304(3)	4853(2)	4378(2)	31(1)	1
N3	11362(3)	5139(2)	9369(2)	26(1)	1
N4	13549(2)	7075(1)	8331(2)	22(1)	1
O1	13668(3)	5077(1)	2665(2)	41(1)	1
O2	12518(2)	6709(1)	3148(1)	31(1)	1
O3	6603(3)	6217(2)	1983(3)	69(1)	1
O4	8687(2)	3699(1)	3048(2)	32(1)	1
O5	10321(2)	6387(1)	7960(2)	31(1)	1
O6	14669(2)	7860(1)	10750(2)	31(1)	1
O7	16260(2)	6217(2)	8901(2)	30(1)	1
O8	15428(2)	7567(1)	7295(2)	29(1)	1
S1	12584(1)	5596(1)	3173(1)	28(1)	1
S2	15022(1)	6691(1)	7896(1)	23(1)	1

Table 3. Bond lengths [\AA] and angles [$^\circ$].

C1–N1	1.463(4)	C4–N2	1.468(3)
C1–C3	1.524(4)	C4–C5	1.508(4)
C1–C2	1.533(4)	C5–C6	1.528(4)
C2–O3	1.417(4)	C6–C7	1.516(4)
C3–O4	1.241(3)	C7–C8	1.524(4)
C3–N2	1.323(3)	C8–N3	1.459(3)

C9–O5	1.242(3)	O5–C9–C10	120.9(2)
C9–N3	1.321(3)	N3–C9–C10	115.1(2)
C9–C10	1.527(3)	N4–C10–C11	109.33(18)
C10–N4	1.461(3)	N4–C10–C9	111.01(18)
C10–C11	1.526(3)	C11–C10–C9	109.74(18)
C11–O6	1.422(3)	O6–C11–C10	111.1(2)
C12–C17	1.389(3)	C17–C12–C13	121.4(2)
C12–C13	1.394(3)	C17–C12–S2	118.49(18)
C12–S2	1.768(2)	C13–C12–S2	120.14(18)
C13–C14	1.387(4)	C14–C13–C12	119.3(2)
C14–C15	1.388(4)	C15–C14–C13	120.4(2)
C15–C16	1.398(3)	C14–C15–C16	118.9(2)
C16–C17	1.382(3)	C17–C16–C15	121.8(2)
C16–S1	1.773(2)	C17–C16–S1	118.25(17)
N1–S1	1.602(2)	C15–C16–S1	119.98(19)
N4–S2	1.601(2)	C16–C17–C12	118.2(2)
O1–S1	1.4366(18)	C1–N1–S1	120.31(17)
O2–S1	1.4330(18)	C3–N2–C4	123.0(2)
O7–S2	1.4295(17)	C9–N3–C8	123.8(2)
O8–S2	1.4379(18)	C10–N4–S2	122.34(16)
		O2–S1–O1	118.87(11)
N1–C1–C3	110.3(2)	O2–S1–N1	109.52(12)
N1–C1–C2	108.1(2)	O1–S1–N1	106.86(12)
C3–C1–C2	109.4(2)	O2–S1–C16	106.11(11)
O3–C2–C1	112.1(3)	O1–S1–C16	107.96(11)
O4–C3–N2	124.0(2)	N1–S1–C16	106.98(11)
O4–C3–C1	119.8(2)	O7–S2–O8	120.28(11)
N2–C3–C1	116.1(2)	O7–S2–N4	108.28(10)
N2–C4–C5	113.3(2)	O8–S2–N4	105.63(10)
C4–C5–C6	115.2(2)	O7–S2–C12	107.08(11)
C7–C6–C5	113.4(2)	O8–S2–C12	106.37(10)
C6–C7–C8	114.9(2)	N4–S2–C12	108.81(10)
N3–C8–C7	110.9(2)		
O5–C9–N3	123.9(2)		

Table 4. Anisotropic displacement parameters [$\text{\AA}^2 \times 10^3$]. The anisotropic displacement factor exponent takes the form: $-2\pi^2[h^2 a^{*2} U^{11} + \dots + 2 h k a^* b^* U^{12}]$.

Atom	U^{11}	U^{22}	U^{33}	U^{23}	U^{13}	U^{12}
O9	75(2)	29(1)	33(1)	-5(1)	11(1)	-11(1)
O10	44(1)	26(1)	32(1)	-6(1)	21(1)	-9(1)
O11	32(1)	26(1)	47(1)	-5(1)	12(1)	1(1)
C1	36(1)	18(1)	25(1)	-2(1)	-5(1)	2(1)
C2	57(2)	26(2)	35(2)	10(1)	-21(1)	-12(1)
C3	29(1)	23(1)	23(1)	-2(1)	-3(1)	2(1)
C4	28(1)	37(1)	42(2)	-13(1)	13(1)	-8(1)

C5	28(1)	30(1)	42(2)	-7(1)	16(1)	-2(1)
C6	28(1)	22(1)	48(2)	-8(1)	16(1)	-4(1)
C7	37(2)	24(1)	48(2)	3(1)	10(1)	-9(1)
C8	33(1)	29(1)	37(2)	5(1)	12(1)	-9(1)
C9	28(1)	19(1)	18(1)	-2(1)	8(1)	1(1)
C10	26(1)	19(1)	18(1)	0(1)	7(1)	0(1)
C11	35(1)	20(1)	24(1)	-3(1)	12(1)	-3(1)
C12	19(1)	24(1)	24(1)	2(1)	9(1)	1(1)
C13	27(1)	27(1)	23(1)	7(1)	11(1)	4(1)
C14	32(1)	19(1)	32(1)	6(1)	12(1)	2(1)
C15	29(1)	20(1)	31(1)	1(1)	13(1)	1(1)
C16	26(1)	23(1)	23(1)	2(1)	12(1)	5(1)
C17	23(1)	21(1)	24(1)	4(1)	11(1)	7(1)
N1	55(1)	23(1)	17(1)	-6(1)	10(1)	-2(1)
N2	34(1)	22(1)	32(1)	-7(1)	4(1)	0(1)
N3	27(1)	23(1)	27(1)	4(1)	5(1)	-3(1)
N4	26(1)	19(1)	21(1)	3(1)	8(1)	1(1)
O1	69(1)	31(1)	35(1)	2(1)	35(1)	8(1)
O2	50(1)	19(1)	25(1)	4(1)	14(1)	3(1)
O3	28(1)	55(1)	97(2)	49(1)	-14(1)	-11(1)
O4	40(1)	18(1)	36(1)	-6(1)	10(1)	-2(1)
O5	30(1)	25(1)	31(1)	6(1)	2(1)	-1(1)
O6	38(1)	25(1)	24(1)	-4(1)	5(1)	-9(1)
O7	23(1)	38(1)	26(1)	8(1)	3(1)	4(1)
O8	27(1)	30(1)	29(1)	4(1)	10(1)	-6(1)
S1	47(1)	19(1)	22(1)	1(1)	18(1)	4(1)
S2	21(1)	25(1)	21(1)	2(1)	6(1)	-1(1)

Table 5. Hydrogen coordinates [$\times 10^4$] and isotropic displacement parameters [$\text{\AA}^2 \times 10^3$].

Atom	<i>x</i>	<i>y</i>	<i>z</i>	<i>U</i> _{eq}	<i>S.o.f.</i>
H99	9570(50)	6540(30)	6180(20)	105(17)	1
H98	10050(40)	7403(18)	5660(30)	73(12)	1
H97	15280(40)	8813(17)	9660(20)	68(12)	1
H96	15520(40)	9080(20)	8586(19)	65(11)	1
H95	10730(30)	2746(19)	1990(30)	46(10)	1
H94	12177(15)	3090(30)	1830(30)	71(13)	1
H1	9735	6078	3437	36	1
H2A	8399	6372	1309	59	1
H2B	7624	5228	1164	59	1
H4A	7619	3414	4708	42	1
H4B	6220	4274	4556	42	1
H5A	7155	3835	6543	39	1
H5B	7857	4972	6472	39	1
H6A	9927	3231	6564	38	1
H6B	10490	4401	6948	38	1
H7A	11050	3255	8632	45	1
H7B	9109	3072	8291	45	1

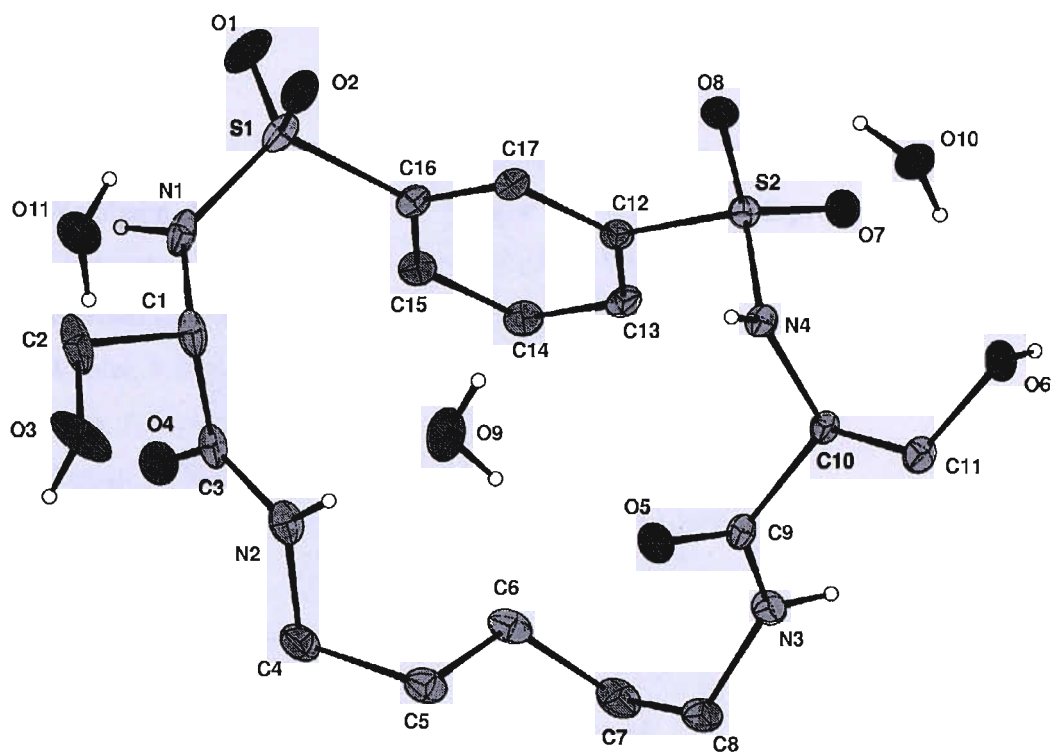
H8A	8893	4945	8623	39	1
H8B	9718	4255	9809	39	1
H10	14024	6031	9687	25	1
H11A	12251	7886	9862	31	1
H11B	12818	7011	10889	31	1
H13	14554	4499	7957	30	1
H14	13539	3226	6470	33	1
H15	12686	3679	4424	31	1
H17	13792	6709	5352	26	1
H101	10604	4673	1931	39	1
H102	8530	5482	4681	37	1
H103	12239	4928	9966	32	1
H104	12960	7618	7975	27	1
H3	5893	5745	1878	103	1
H6	15393	7416	11097	46	1

Table 6. Hydrogen bonds [\AA and $^\circ$].

$D-H\cdots A$	$d(D-H)$	$d(H\cdots A)$	$d(D\cdots A)$	$\angle(DHA)$
O9–H99...O5	0.842(10)	1.99(2)	2.767(3)	154(3)
N1–H101...O11	0.88	2.02	2.757(3)	140.9
N2–H102...O9	0.88	2.06	2.934(3)	170.2
O10–H97...O6	0.849(10)	1.976(11)	2.812(2)	168(3)
O10–H96...O8	0.839(10)	2.46(2)	3.192(2)	147(3)
O9–H98...O4 ⁱ	0.843(10)	2.27(2)	3.014(3)	148(3)
N4–H104...O4 ⁱ	0.88	2.06	2.926(3)	170.0
O10–H96...O1 ⁱⁱ	0.839(10)	2.24(2)	2.791(2)	123(3)
O3–H3...O10 ⁱⁱⁱ	0.84	2.31	3.052(3)	147.8
O11–H95...O5 ⁱⁱⁱ	0.840(10)	1.979(18)	2.756(3)	153(3)
O11–H94...O8 ^{iv}	0.835(10)	2.076(15)	2.877(3)	161(3)
O11–H94...S2 ^{iv}	0.835(10)	2.94(2)	3.688(2)	151(3)
N3–H103...O10 ^v	0.88	2.09	2.923(3)	156.9
O3–H3...O1 ^{vi}	0.84	2.55	3.254(3)	142.3
O6–H6...O3 ^{vii}	0.84	1.95	2.772(3)	165.3

Symmetry transformations used to generate equivalent atoms:

- (i) $-x+2, y+1/2, -z+1$ (ii) $-x+3, y+1/2, -z+1$ (iii) $-x+2, y-1/2, -z+1$
(iv) $-x+3, y-1/2, -z+1$ (v) $-x+3, y-1/2, -z+2$ (vi) $x-1, y, z$
(vii) $x+1, y, z+1$



Thermal ellipsoids drawn at the 35% probability level.

References

- [1] a) Lehn, J.-M. *Supramolecular Chemistry: Concepts and Perspectives*, VCH, Weinheim, **1995**. b) Beer, P. D.; Gale, P. A.; Smith, D. K. *Supramolecular Chemistry*, Oxford University Press, Oxford, **1999**. c) Steed, J. W.; Atwood, J. L. *Supramolecular Chemistry*, Wiley, Chichester **2000**.
- [2] Wöhler, F. *Poggendorfs Ann. Physik* **1828**, *12*, 252.
- [3] Lehn, J.-M. *Angew. Chem., Int. Ed. Eng.* **1988**, *27*, 89-112.
- [4] Werner, A. *Zeitschr. Anorg. Chem.* **1893**, *3*, 267-330.
- [5] Fischer, E. *Ber. Dtsch. Chem. Ges.* **1894**, *27*, 2985-2993.
- [6] Ehrlich, P. *Studies on Immunity*, Wiley, New York, **1906**.
- [7] Wolf, K. L.; Frahm, H.; Harms, H. *Z. Phys. Chem.* **1937**, *Abt. B 36*, 237.
- [8] Pedersen, C. J. *J. Am. Chem. Soc.* **1967**, *89*, 2495-2496.
- [9] Cram, D. J.; Bauer, R. H. *J. Am. Chem. Soc.* **1959**, *81*, 5971-5977.
- [10] Dietrich, B.; Lehn, J.-M.; Sauvage, J.-P. *Tetrahedron Lett.* **1969**, *10*, 2885-2888 and 2889-2892.
- [11] Lehn, J.-M. *Pure Appl. Chem.* **1978**, *50*, 871-892.
- [12] Behr, J.-P. *The Lock-and-Key Principle, Vol. 1, The State of the Art - 100 Years On*, Wiley, Chichester, **1995**.
- [13] Davis, A. M.; Teague, S. J. *Angew. Chem., Int. Ed. Eng.* **1999**, *38*, 736-749 and references therein.
- [14] Julien, L.; Lehn, J.-M. *Tetrahedron Lett.* **1988**, *29*, 3803-3806.
- [15] Pregel, M. J.; Julien, L.; Canceill, J.; Lacombe, L.; Lehn, J.-M. *J. Chem. Soc., Perkin Trans. II* **1995**, 417-426.
- [16] Horton, R. H.; Rawn, D. J.; Moran, L. A.; Ochs, R.S.; Scrimgeour, K. G.; Perry, M. D. *Principles of Biochemistry*, Prentice Hall, Upper Saddle River, NJ, **2005**.
- [17] Buchner, E. Nobel Lecture 1907, *Nobel Lectures, Chemistry 1901-1921*, Elsevier, Amsterdam, **1966**.
- [18] Sumner, J. B.; Northrop J. H.; Stanley W. M. Nobel Lectures 1946, *Nobel Lectures, Chemistry 1942-1962*, Elsevier, Amsterdam, **1966**.
- [19] Christianson, D. W.; Lipscomb, W. N. *Acc. Chem. Res.* **1989**, *22*, 62-69.
- [20] Lehn, J.-M.; Sirlin, C. *J. Chem. Soc., Chem. Commun.* **1978**, 949-951.

- [21] Kang, J.; Rebek, J. Jr *Nature* **1997**, *385*, 50-52.
- [22] a) Pohnert, G. *Chem. Biochem.* **2003**, *4*, 713-715. b) Pohnert, G. *Chem. Biochem.* **2001**, *2*, 873-875.
- [23] Werneck Guimaraes, C. R.; Udier-Blagovic, M.; Jorgensen, W. L. *J. Am. Chem. Soc.* **2005**, *127*, 3577-3588.
- [23] Werneck Guimaraes, C. R.; Udier-Blagovic, M.; Jorgensen, W. L. *J. Am. Chem. Soc.* **2005**, *127*, 3577-3588.
- [24] Chen, J.; Rebek, J. Jr *Org. Lett.* **2002**, *4*, 327-329.
- [25] a) Feynman, R. P. *Eng. Sci.* **1960**, *23*, 22-26. a) Feynman, R. P. *Saturday Rev.* **1960**, *43*, 45-47.
- [26] a) Balzani, V.; Credi, A.; Raymo, F. M.; Stoddart, J. F. *Angew. Chem., Int. Ed. Engl.* **2000**, *39*, 3348-3391. b) Kinbara, K.; Aida, T. *Chem. Rev.* **2005**, *105*, 1377-1400.
- [27] Badjic, J. D.; Balzani, V.; Credi, A.; Silvi, S.; Stoddart, J. F. *Science* **2004**, *303*, 1845-1849.
- [28] Kyba, E. P.; Helgeson, R. C.; Madan, K.; Gokel, G. W.; Tarnowski, T. L.; Moore, S. S.; Cram, D. J. *J. Am. Chem. Soc.* **1977**, *99*, 2574-2561.
- [29] Linton, B. R.; Goodman, M. S.; Fan, E.; Van Arman, S.A.; Hamilton, A. D. *J. Org. Chem.* **2001**, *66*, 7313-7319.
- [30] Wiseman, T.; Williston, S.; Brandts, J. F.; Lin, L.N. *Anal. Biochem.* **1989**, *179*, 131-137.
- [31] Cram, D. J. *Angew. Chem. Int. Ed. Engl.* **1986**, *25*, 1039-1057.
- [32] Cabiness, D. K.; Margerum, D. W. *J. Am. Chem. Soc.* **1969**, *91*, 6540-6541.
- [33] Schneider, H. J.; Blatter, T.; Palm, B.; Pflingstag, U.; Rüdiger, V.; Theis, I. *J. Am. Chem. Soc.* **1992**, *114*, 7704-7708.
- [34] Frensdorff, H. K. *J. Am. Chem. Soc.* **1971**, *93*, 600-606.
- [35] Megaw, H. D. *Nature* **1934**, *134*, 900-901.
- [36] Karle, J.; Brockway, L. O. *J. Am. Chem. Soc.* **1944**, *66*, 574-584.
- [37] Albrecht, G.; Corey, R. B. *J. Am. Chem. Soc.* **1939**, *61*, 1087-1103.
- [38] Chang, S.-K.; Hamilton, A. D. *J. Am. Chem. Soc.* **1988**, *110*, 1318-1319.
- [39] Schmuck, C.; Wienand, W. *Angew. Chem. Int. Ed. Engl.* **2001**, *40*, 4363-4369.
- [40] Murray, T. J.; Zimmerman, S.C. *J. Am. Chem. Soc.* **1992**, *114*, 4010-4011.
- [41] Saenger, W. *Principles of Nucleic Acid Structure*, Springer-Verlag, New York, **1984**, 132-140.

- [42] Desiraju, G. R.; Gavezzotti, A. *J. Chem. Soc., Chem. Commun.*, **1989**, 621-623 and references cited therein.
- [43] Hunter, C. A.; Sanders, J. K. M. *J. Am. Chem. Soc.*, **1990**, *112*, 5525-5534.
- [44] Zimmerman, S. C.; Van Zyl, C. M.; Hamilton, G. M. *J. Am. Chem. Soc.*, **1989**, *111*, 1373-1381.
- [45] Ma, J. C.; Dougherty, D. A. *Chem. Rev.* **1997**, *97*, 1303-1304.
- [46] Sunner, J.; Nishizawa, K.; Kebarle, P. *J. Phys. Chem.* **1981**, *85*, 1814-1820.
- [47] Arnecke, R.; Böhmer, V.; Cacciapaglia, R.; Dalla Cort, A.; Mandolini, L. *Tetrahedron* **1997**, *53*, 4901-4908.
- [48] Ungaro, R.; Pochini, A.; Andreotti, G. D. *J. Chem. Soc., Chem. Commun.* **1979**, 1005-1007.
- [49] Smithrud, D. B.; Sanford, E. M.; Chao, I.; Ferguson, S. B.; Carcanague, D. R.; Evanseck, J. D.; Houk, K. N.; Diederich, F. *Pure Appl. Chem.*, **1990**, *62*, 2227-2236.
- [50] Park, C. H.; Simmonds, H. E. *J. Am. Chem. Soc.* **1968**, *90*, 2431-2432.
- [51] a) Schmidtchen, F. P.; Berger, M. *Chem. Rev.* **1997**, *97*, 1609-1646. b) Beer, P. D.; Gale, P. A. *Angew. Chem. Int. Ed. Engl.* **2001**, *40*, 486-516.
- [52] Pecuh, M. W.; Hamilton, A. D. *Chem. Rev.* **2000**, *100*, 2479-2494.
- [53] Fitzmaurice, R. J.; Kyne, G. M.; Douheret, D.; Kilburn, J. D. *J. Chem. Soc., Perkin Trans. I* **2002**, 841-864.
- [54] Smith, P. J.; Reddington, M. V.; Wilcox, C. S. *Tetrahedron Lett.* **1992**, *33*, 6085-6088.
- [55] Raposo, C.; Crego, M.; Mussons, M. L.; Caballero, M. C.; Moràn, J. R. *Tetrahedron Lett.* **1994**, *35*, 3409-3410.
- [56] Brooks, S. J.; Gale, P. A.; Light, M. E. *Chem. Commun.* **2005**, 4696-4698.
- [57] Fan, E.; Van Arman, S. A.; Kincaid, S.; Hamilton, A. D. *J. Am. Chem. Soc.* **1993**, *115*, 369-370.
- [58] Sasaki, S.; Mizuno, M.; Naemura, K.; Tobe, Y. *J. Org. Chem.* **2000**, *65*, 275-283.
- [59] Müller, G.; Riede, J.; Schmidtchen, F. P. *Angew. Chem. Int. Ed. Engl.* **1988**, *27*, 1516-1518.
- [60] Linton, B.; Hamilton, A. D. *Tetrahedron* **1999**, *55*, 6027-6038.
- [61] Metzger, A.; Lynch, V. M.; Anslyn, E. V. *Angew. Chem. Int. Ed. Engl.* **1997**, *36*, 862-865.
- [62] Metzger, A.; Anslyn, E. V. *Angew. Chem. Int. Ed. Engl.* **1998**, *37*, 649-652.

- [63] Echavarren, A.; Galàn, A.; Lehn, J.-M.; de Mendoza J. *J. Am. Chem. Soc.* **1989**, *111*, 4994-4995.
- [64] Bondy, C. R.; Loeb, S. J.; *Coord. Chem. Rev.* **2003**, *240*, 77-99.
- [65] Gellman, S. H.; Dado, G. P.; Liang, G. B.; Adams, B.R. *J. Am. Chem. Soc.* **1991**, *113*, 1164-1173.
- [66] Han, S. Y.; Kim, Y. A. *Tetrahedron* **2004**, *60*, 2447-2467.
- [67] Werner, F.; Schneider, H. J. *Helv. Chim. Acta* **2000**, *83*, 465-478.
- [68] Kavallieratos, K.; Bertao, C. M.; Crabtree, R. M. *J. Org. Chem.* **1999**, *64*, 1675-1683.
- [69] Hughes, M. P.; Smith, B. D. *J. Org. Chem.* **1997**, *62*, 4492-4499.
- [70] Chmielewski, M.; Jurczak, J. *Chem. Eur. J.* **2005**, *11*, 6080-6094.
- [71] Purvis, D. H.; Hunter, C. A. *Angew. Chem. Int. Ed. Engl.* **1992**, *31*, 792-795.
- [72] Kyne, G. M.; Light, M. E.; Hursthouse, M. B.; de Mendoza, J.; Kilburn, J. D. *J. Chem. Soc., Perkin Trans. I* **2001**, 1258-1263.
- [73] Chmielewski, M.; Jurczak, J. *Tetrahedron Lett.* **2005**, *46*, 3085-3088.
- [74] Sessler, J. L.; Camiolo, S.; Gale, P. A. *Coord. Chem. Rev.* **2003**, *240*, 17-55 and references therein.
- [75] Gale, P. A.; Camiolo, S.; Tizzard, G. J.; Champman, C. P.; Light, M. E.; Coles, S. J.; Hursthouse, M. B. *J. Org. Chem.* **2001**, *66*, 7849-7853.
- [76] El Drubi Vega, I.; Camiolo, S.; Gale, P. A.; Hursthouse, M. B.; Light, M. E. *Chem. Commun.* **2003**, 1686-1687.
- [77] For a comparison of the pKa values of aliphatic and aromatic amides see Bordwell, F. G.; Harrelson, J. A.; Lynch, T. Y. *J. Org. Chem.* **1990**, *55*, 3337-3341 and Bordwell, F. G.; Ji, G. Z. *J. Am. Chem. Soc.* **1991**, *113*, 8398-8401.
- [78] Webb, T. H.; Wilcox, C. S. *Chem. Soc. Rev.* **1993**, *22*, 383-395.
- [79] Galàn, A.; Andreu, D.; Echavarren, A.; Prados, P.; de Mendoza J. *J. Am. Chem. Soc.* **1992**, *114*, 1511-1512.
- [80] Breccia, P.; Van Gool, M.; Perez-Fernandez, R.; Martin-Santamaria, S.; Gago, F.; Prados, P.; de Mendoza J. *J. Am. Chem. Soc.* **2003**, *125*, 8270-8284.
- [81] Pirkle, W. H.; Bowen, W. E. *Tetrahedron Asymm.* **1994**, *5*, 773-776.
- [82] Rossi, S.; Kyne, G. M.; Turner, D. L.; Wells, N. J.; Kilburn, J. D. *Angew. Chem. Int. Ed. Engl.* **2002**, *41*, 4233-4235.
- [83] Ragusa, A.; Rossi, S.; Hayes, J. M.; Stein, M.; Kilburn, J. D. *Chem. Eur. J.* **2005**, *11*, 5674-5688.

- [84] Lawless, L. J.; Blackburn, A. G.; Ayling, A. J.; Perez-Payan, M. N.; Davis, A. P. *J. Chem. Soc., Perkin Trans. I* **2001**, 1329-1341.
- [85] Schmuck, C. *Chem. Eur. J.* **2000**, *6*, 709-718.
- [86] Sogah, G. D. Y.; Cram, D. J. *J. Am. Chem. Soc.* **1979**, *101*, 3035-3042.
- [87] Gasparrini, F.; Misiti, D.; Pierini, M.; Villani, C. *Org. Lett.* **2002**, *4*, 3993-3996.
- [88] Fornstedt, T.; Sajonz, P.; Guiochon, G. *J. Am. Chem. Soc.* **1997**, *119*, 1254-1264.
- [89] a) Kavallieratos, K.; Moyer, B. *Chem. Commun.* **2001**, 188-189. b) Valiyaveettil, S.; Engbersen, J. F. J.; Verboom W.; Reinhoudt, D. N. *Angew. Chem. Int. Ed. Engl.* **1993**, *32*, 900-901. c) Morzherin, Y.; Rudkevich, D. M.; Verboom, W.; Reinhoudt, D. N. *J. Org. Chem.* **1993**, *58*, 7602-7605. c) Davis, A. P.; Gilmer, J. F.; Perry J. J. *J. Am. Chem. Soc.* **1997**, *119*, 1793-1794. d) Kondo, S.; Suzuki, T.; Yano, Y. *Tetrahedron Lett.* **2002**, *43*, 7059-7061.
- [90] Bordwell, F. G.; Algrim, D.; *J. Org. Chem.* **1976**, *41*, 2507-2508.
- [91] Allerhand, A.; von Ragué Schleyer, P. *J. Am. Chem. Soc.* **1963**, *85*, 1233-1237.
- [92] a) Welch, C. J. *J. Chromatogr. A.* **1994**, *666*, 3-26 and references therein. b) Gasparrini, F.; Misiti, D.; Villani, C.; Borchardt, A.; Burger, M. T.; Still, C. W. *J. Org. Chem.* **1995**, *60*, 4314-4315.
- [93] Jensen, K. B.; Braxmeier, T. M.; Demarcus, M.; Frey, J. G.; Kilburn, J. D. *Chem. Eur. J.* **2002**, *8*, 1300-1309.
- [94] Yus, M.; Ramon, D. J.; Prieto, O. *Tetrahedron Asymm.* **2002**, *13*, 1573-1579.
- [95] Bisson, A. P.; Hunter, C. A.; Morales, J. C.; Young, K. *Chem. Eur. J.* **1998**, *4*, 845-851.
- [96] Fielding, L. *Tetrahedron* **2000**, *56*, 6151-6170.
- [97] Schneider, H.-J.; Dürr, H. *Frontiers in Supramolecular Organic Chemistry and Photochemistry*, VCH, Weinheim, **1991**.
- [98] Kondo, S.; Suzuki, T.; Toyama, T.; Yano, Y. *Bull. Chem. Soc. Jpn.* **2005**, *78*, 1348-1350.
- [99] Arnaud, N.; Picard, C.; Cazaux, L.; Tisnès, P. *Tetrahedron* **1997**, *53*, 13757-13768.
- [100] a) Kalisiak, J.; Skowronek, P.; Gawronski, J.; Jurczak, J. *Chem. Eur. J.* **2006**, *12*, 4397-4406. b) Gibson, S. E.; Mainolfi, N.; Kalindjian, S. B.; Wright, P. T.; White, A. J. P. *Chem. Eur. J.* **2005**, *11*, 69-80. c) Kataoka, H.; Katagi, T. *Tetrahedron* **1987**, *43*, 4519-4530.
- [101] Nemoto, H.; Takamatsu, S.; Yamamoto, Y. *J. Org. Chem.* **1991**, *56*, 1321-1322.

- [102] Kilburn, J. D.; MacKenzie, A. R.; Still, W. C. *J. Am. Chem. Soc.* **1988**, *110*, 1307-1308.
- [103] Babudri, F.; Fiandanese, V.; Marchese, G.; Punzi A. *J. Organomet. Chem.* **2004**, 326-331.
- [104] Uray, G.; Lynder W. *Tetrahedron* **1988**, *44*, 4357-4362.
- [105] Marson, C. M.; Schwarz, I. *Tetrahedron Lett.* **2000**, *41*, 8999-9003.
- [106] Hynes, M. J. *J. Chem. Soc., Dalton Trans.* **1993**, 311-312.
- [107] Yoon, S. S.; Still, W. C. *J. Am. Chem. Soc.* **1993**, *115*, 823-824.
- [108] Chang, K.-H.; Liao, J.-H.; Chen, C.-T.; Metha, B. K.; Chou, P.-T.; Fang, J.-M. *J. Org. Chem.* **2005**, *70*, 2026-2032.
- [109] Kelly, T. R.; Kim, M. H. *J. Am. Chem. Soc.* **1994**, *116*, 7072-7080.
- [110] Camiolo, S.; Gale, P. A.; Ogden, M. I.; Skelton, B. W.; White, A. H. *J. Chem. Soc., Perkin Trans II* **2001**, 1294-1298.
- [111] Person, W. B. *J. Am. Chem. Soc.* **1965**, *87*, 167-170.
- [112] Deranleau, D. A. *J. Am. Chem. Soc.* **1969**, *91*, 4044-4049.
- [113] Cardani, S.; De Toma, C.; Gennari, C.; Scolastico, C. *Tetrahedron* **1992**, *48*, 5557-5564.
- [114] Paul, R.; Anderson, G. W. *J. Am. Chem. Soc.* **1960**, *82*, 4596-4600.
- [115] Caudle, M. T.; Stevens, R. D.; Crumbliss, A. L. *Inorg. Chem.* **1994**, *33*, 6111-6115.
- [116] Camiolo, S.; Gale, P. A.; Hursthouse, M. B.; Light, M. E.; Shi, A. *J. Chem. Commun.* **2002**, 758-759.
- [117] Camiolo, S.; Gale, P. A.; Hursthouse, M. B.; Light, M. E. *Org. Biomol. Chem.* **2003**, *1*, 741-744.
- [118] Illuminati, G.; Mandolini, L.; Masci, B. *J. Am. Chem. Soc.* **1983**, *105*, 555-563 and references therein.
- [119] Vilàr, R. *Angew. Chem. Int. Ed. Engl.* **2003**, *42*, 1460-1477.
- [120] Alcalde, E.; Ramos, S.; Perez-Garcia, L. *Org. Lett.* **1999**, *1*, 1035-1038.
- [121] Heyes, J. A.; Niculescu-Duvaz, D.; Cooper, R. G.; Springer, C. J. *J. Med. Chem.* **2002**, *45*, 99-114.
- [122] Ramos, S.; Alcalde, E.; Doddi, G.; Mencarelli, P.; Perez-Garcia, L. *J. Org. Chem.* **2002**, *67*, 8463-8468.
- [123] Bretonniere, Y.; Cann, M. J.; Parker, D.; Slater, R. *Org. Biomol. Chem.* **2004**, *2*, 1624-1632.

- [124] Romero, F. A.; Vodonick, S. M.; Criscione, K. R.; McLeish, M. J.; Grunewald, G. L. *J. Med. Chem.* **2004**, *47*, 4483-4493.
- [125] Pan, Y.; Ford, W. T. *J. Org. Chem.* **1999**, *64*, 8588-8593.
- [126] Szumna, A.; Jurczak, J. *Eur. J. Org. Chem.* **2001**, 4031-4039.
- [127] Sessler, J. L.; Andrievsky, A.; Gale, P. A.; Lynch, V. *Angew. Chem. Int. Ed. Engl.* **1996**, *35*, 2782-2785.
- [128] Xu, H.; Kinsel, G. R.; Zhang, J.; Li M.; Rudkevich, D. M. *Tetrahedron* **2003**, *59*, 5837-5848.
- [129] Liu, L.; Breslow, R. *J. Am. Chem. Soc.* **2003**, *125*, 12110-12111.
- [130] Huang, X.; Rickman, B. H.; Borhan, B.; Berova, N.; Nakanishi, K. *J. Am. Chem. Soc.* **1998**, *120*, 6185-6186.
- [131] Dumoulin, F.; Lafont, D.; Boullanger, P.; Mackenzie, G.; Mehl, G. H.; Goodby, J. W. *J. Am. Chem. Soc.* **2002**, *124*, 13737-13748.
- [132] Bodanszky, M.; Bodanszky, A. *The Practice of Peptide Synthesis*, Springer-Verlag, Berlin, **1984**.
- [133] Malanda Kimbonguila, M.; Boucida, S.; Guibé, F.; Loffet, A. *Tetrahedron* **1997**, *53*, 12525-12538.
- [134] Overberger, C. G.; Chah-Moh, S. *J. Am. Chem. Soc.* **1971**, *93*, 6992-6998.
- [135] Sieber, P.; Riniker, B. *Tetrahedron Lett.* **1987**, *28*, 6031-6034.
- [136] Albert, J. S.; Hamilton, A. D. *Tetrahedron Lett.* **1993**, *34*, 7363-7366.
- [137] Pieters, R. J.; Cuntze, J.; Bonnet, M.; Diederich, F. *J. Chem. Soc., Perkin Trans. II*, **1997**, 1891-1900.
- [138] Zimmerman, S. C.; Saionz, K. W. *J. Am. Chem. Soc.* **1995**, *117*, 1175-1176.
- [139] Gottlieb, H. E.; Kotlyar, V.; Nudelman, A. *J. Org. Chem.* **1997**, *62*, 7512-7515.
- [140] Wilcox, C. S.; Cowart, M. D. *Tetrahedron Lett.* **1986**, *27*, 5563-5566.
- [141] Kneeland, D. M.; Ariga, K.; Lynch, V. M.; Huang, C.-Y.; Anslyn, E. V. *J. Am. Chem. Soc.* **1993**, *115*, 10042-10055.
- [142] Ikemoto, N.; Schreiber, S. L. *J. Am. Chem. Soc.* **1992**, *114*, 2524-2536.
- [143] Wu, C.; Kobayashi, H.; Yoo, T. M.; Paik, C. H.; Gansow, O. A.; Carrasquillo, J. A.; Pastan, I.; Brechbiel, M. W. *Bioorg. Med. Chem.* **1997**, *5*, 1925-1934.

